Development of Biocatalytic Strategies for the Directed Oxidation of Small Molecule and Macrocyclic Substrates

by

Michael M. Gilbert

A dissertation submitted in partial fulfillment
of the requirements for the degree of
Doctor of Philosophy
(Chemistry)
In the University of Michigan
2018

Doctoral committee:
Professor John Montgomery, chair
Professor David H. Sherman
Professor Melanie Sanford
Professor John P. Wolfe

Michael M. Gilbert
mmgilbe@umich.edu
OCRID: 0000-0002-5419-7991

Dedication

This dissertation is dedicated to my parents, Christine and Wayne, my step-parents, Dave and Beth, and my siblings Rachael and Kevin.

Acknowledgements

I would like to thank my advisor Professor John Montgomery for his unwavering support, guidance, and encouragement throughout my doctoral studies. Thank you for fostering my development as an independent scientist, introducing me to the scientific community, and providing a fantastic laboratory environment. I appreciate always being able to discuss chemistry, specifically prolonged talks about NMR. I would like to thank Prof. David H. Sherman, who has been like a second advisor to me, and Prof. John P. Wolfe and Prof. Melanie Sanford for providing new ideas and perspectives during committee meetings.

I am grateful to Dr. Solymar Negretti and Professor Alison Narayan for their help with transitioning to working with PikC and demonstrating effective experimental collaboration. I would like to thank Dr. Hengbin Wang and Dr. Wanxiang (Chris) Zhao for the instruction of proper lab techniques and approaches to multi-step synthesis during my early years. I would like to thank Dr. David Todd, Jessica Stachowski, Alex Nett, Eric Wiensch, Annabel Ansel, and Hilary Kerchner for many helpful and irreverent discussions that made time in lab infinitely more enjoyable. Thank you to my cubby-mates Dr. Solymar Negretti, Dr. Wangxiang Zhao, and Amie Frank for putting up with my daily antics and terrible idle singing. Undoubtedly, this was a task of great patience and understanding. As I transitioned to a more senior student in the Montgomery group, I had the pleasure to mentor many bright colleagues: graduate students Summer Baker-Dockrey and Rosa Maria Christina Vasquez Espinoza, visiting student Emma Gendre,

and undergraduates Jake Wilson and Sara Alektiar. You have all helped me as equally as I have guided you. I would like to acknowledge the chemistry department staff Dr.Eugenio Alvarado, Dr. James Windak, Paul Lennon, and Chris Kojiro for support with instrumentation, software, and equipment.

Anyone who has met me know that I am terrible with administrative tasks. Without the support from the staff in Chemistry 1500 and fellow lab mates Jessica Stachowski and Hilary Kerchner, I would have likely missed every deadline in graduate school. Thank you all.

If the chemistry department is my home for the last five years, then the Life Sciences Institute is my home away from home. I would like to thank the Sherman lab for their help and expertise with all things biochemistry and chemical biology related. A special thanks to Matt DeMars running numerous experiments on my behalf, and Dr. Andrew Lowell, Amy Fraley, and Vikram Shende for helpful discussions.

Finally, I would like to thank my friends and family for their constant support and providing balance to my life.

Table of Contents

List of Schemes

List of Figures

List of Tables

List of Abbreviations

Ac acetyl

Bn benzyl

Boc tert-butyloxycarbonyl

brsm based on recovered starting matierial

Bz benzoate

COD 1,5-cyclooctadiene

CuAAC copper-catalyzed azide/alkyne cyclization

DAST diethylaminosulfur trifluoride

DCC *N*,*N*'-dicylohexylcarbodiimide

DCE 1,2-dichloroethane

de diasteriomeric excess

Des desosamine

Des-F desosamine fluoride

DG directing group

DIBAL-H diisobutylaluminum hydride

DMAP 4-dimethylaminopyridine

DMDO dimethyldioxirane

DME dimethoxyethane

DMF dimethylformamide

DMP Dess-Martin periodinane

dr diastereomeric ratio

dtbpy di-tert-butyl-2,2'-bipyridine

EDC 1-ethyl-3-(3-dimethylaminopropyl)carbodiimide

EDTA ethylenediaminetetraacetic acid

ee enatiomeric excess

er enantiomeric ratio

Et ethyl

FG functional group

G6P glucose-6-phosphate

G6PDH glucose-6-phosphate dehydrogenase

HPLC high pressure liquid chromatography

***i*-Pr** isopropyl

kB kilobase

KHMDS potassium bis(trimethylsilyl)amide

LCMS liquid chromatography mass spectroscopy

LDA lithium diisopropylamide

***m*CPBA** *meta*-chloroperoxybenzoic acid

Me methyl

Mes mesityl

NAD+ nicotinamide adenine dinucleotide

NADH the reduced form of NAD^+

NADP+ nicotinamide adenine dinucleotide phosphate

NADPH the reduced form of $NADP^+$

NMR nuclear magnetic resonance

NOE nuclear overhauser effect

NOESY nuclear overhauser effect spectroscopy

Pd/C palladium on carbon

Ph phenyl

phen phenanthroline

Piv pivalyl

PKS polyketide synthase

PP diphosphate

PPTS pyridinium *p*-toluenesulfonate

rr regioisomeric ratio

rt room temperature

RuAAC ruthenium-catalyzed azide/alkyne cyclization

sat'd saturated

SIPr 1,3-bis(2,6-di-*i*-propylphenyl)imidazolidine-2-ylidene

TBAF tetrabutyl ammonium fluoride

TBDPS *tert*-butyldiphenylsilyl

TBS *tert*-butyldimethylsilyl

***t*-Bu** *tert*-butyl

TE thioesterase

Tf trifluoromethanesulfonate (triflate)

TFA trifluoroacetic acid

TFDO methyl(trifluoromethyl)dioxirane

THF tetrahydrofuran

THP tetrahydropyranyl

TLC thin layer chromatography

TTN total turnover number

Abstract

The cytochrome P450 enzyme PikC has been explored as a robust biocatalyst for late-stage directed C-H hydroxylation reactions in organic synthesis. A collaborative effort between the Sherman, Houk, Podust, and Montgomery labs has resulted in the engineering of a highly active triple mutant fusion protein, PikCD$_{50N D176Q E246}$A-RhFRED. The unique mode of substrate binding to PikC allows for a substrate engineering approach to be employed whereby removable auxiliaries, termed anchors, can render compounds as suitable substrates for PikC oxidations.

Previous studies had illustrated that unnatural substrates can be designed to enable the oxidation of inert C-H bonds. However, the ability to tune and reverse the regioselectivity of oxidations was not possible in prior efforts. This dissertation describes the application of a substrate engineering approach for site-selective oxidation of small molecules with a triply mutated form of the PikC biocatalyst using synthetic anchoring groups. Oxidations performed using this approach are highly site- and diastereoselective, and the selectivities seen using PikC are orthogonal to those obtained using transition metal based approaches. Application of anchoring group technology is further streamlined though the development of triazole-based anchors. With this class of directing groups, greater anchoring group structural diversity can be sampled in a high throughput approach. This technology was applied to the site-selective oxidation of unnatural 11- and 12-membered macrocycles synthesized via regiodivergent nickel-catalyzed macrocyclization. In this study, the first example of anchoring group-promoted

differential site selectivity is demonstrated and the results are rationalized through computational investigations.

Chapter 1: Aliphatic C-H Oxidation Approaches and Their Application in the Synthesis of Complex Molecules

1.1 Introduction

The synthesis of complex, oxygen-containing molecules has a storied history in the field of organic chemistry. For decades, chemists have sought to replicate the diverse natural products effortlessly synthesized by nature using available chemical methods. Traditional target-oriented synthesis often requires extensive manipulations to incorporate oxidative complexity throughout compound assembly. Achieving the appropriate oxidation patterns while simultaneously forging necessary carbon-carbon bonds often requires numerous functional group interconversions, protecting group manipulations, as well as various oxidations and reductions. The result is often a synthetic sequence that is elegant, but ultimately inefficient.[1] This is exemplified in Nicolaou's total synthesis of taxol (Scheme 1.1A), which necessitated the use of several protective group manipulations as well as oxidation state changes prior to key C-C bond forming reactions.[2–6]

On the other hand, nature often accomplishes the synthesis of complex natural products using a fundamentally different approach. The core connectivity of the molecule is first established, then the oxidation state of the molecule is manipulated. In the context

of the biosynthesis of taxol, the all-carbon framework of the molecule is assembled from geranylgeranyl diphosphate by taxadiene synthase (Scheme 1.1B).[7] Subsequent cytochrome P450-mediated oxidations then selectively increase oxidation state of taxa-4(5), 11(12)-diene to that of taxol. A key transformation in this sequence is the selective functionalization of aliphatic C-H bonds to C-O bonds, which nature can perform with the use of enzymes.[8]

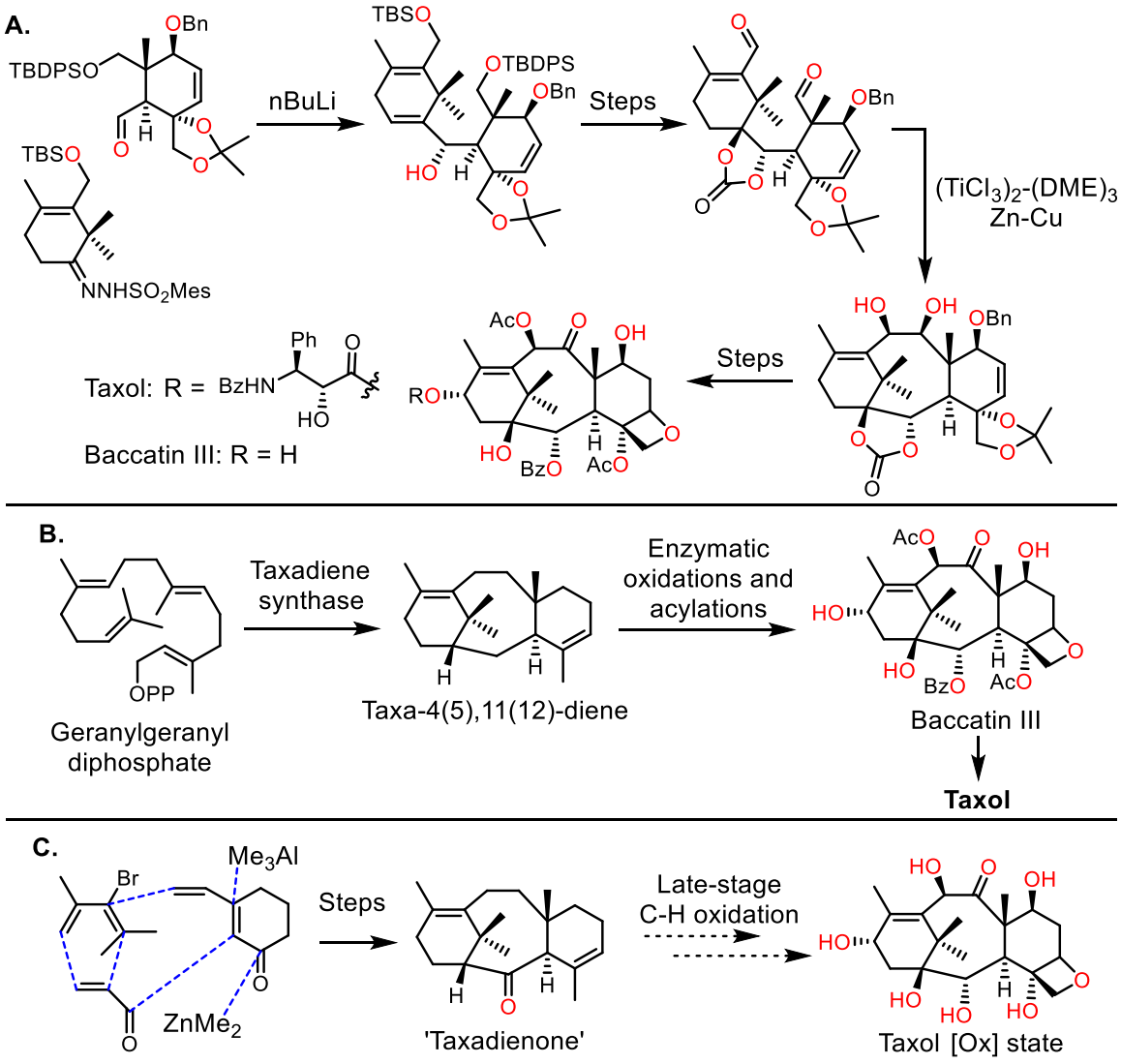

Scheme 1.1: Approaches towards the synthesis of taxol. **A**. Nicolaou's total synthesis. **B**. The biosynthesis of taxol. **C**. Baran's two-phase approach towards taxol.

With the development of numerous methods to convert C-H bonds to C-O bonds[9], chemists have begun to adopt nature's late-stage functionalization approach in the synthesis of complex molecules. These efforts represent a fundamental change in the manner in which chemists approach organic synthesis.[1,10] An important demonstration of this paradigm shift is Baran's efforts towards taxol mimicking nature's two-step process (Scheme 1.1C).[11] While the synthesis of taxol has yet to be achieved using this approach,[12] this endeavor is another demonstration of how late-stage C-H functionalization streamlines synthesis. Additionally, late-stage C-H oxidation reduces the need for protecting groups as functionalities do not need to be carried throughout an entire synthesis. For this approach to be viable, methods need to be developed that are capable of installing aliphatic oxygenation with site-, stereo-, and chemoselectivity.[1] This is complicated by the fact that numerous C-H bonds often exist in organic molecules that only possess subtle differences in steric or electronic factors.[13] This necessitates the use of a variety of approaches ranging from organometallic to biocatalytic to obtain the desired selectivity in any given system. This purpose of this chapter is to summarize approaches to aliphatic C-H oxidation employing different controlling factors for achieving selectivity as well as their application in the late-stage oxidation of complex molecules.

1.2 Transition Metal Based C-H Oxidation Strategies

Transition metals are capable of a myriad of organic transformations. Rightly so, their ability to metalate C-H bonds or form a high valent oxidizing species has been recognized by many chemists as a tool for sp^3 oxyfunctionalization. The key challenge in this area is the ubiquity of the C-H bond: achieving oxidation of the desired C-H bond

in the presence of numerous others. To achieve this goal several strategies have been leveraged for the selective oxidation of C-H bonds using a catalytic transition metal.

1.2.1 Directed C-H Functionalization

The use of a substrate-bound directing group is a powerful method for achieving site-selectivity in transition metal based aliphatic C-H oxidation reactions. By incorporating a functionality that can serve as a ligand, the metal is adjacent to C-H bonds proximal to the directing functionality (Scheme 1.2). The transition metal can then metalate proximal C-H bonds, the selectivity of which is governed by the formation of a 5- or 6-membered transition state.[14] In some instances, the metalacyclic adduct formed can be isolated under stoichiometric metal conditions and subjected to further reactions. An external oxidant then oxidizes the metal center to promote the delivery of the oxidizing functionality. The use of a removable directing group increases the utility of these reactions as many substrates do not possess the appropriate intrinsic functional groups nor are most directing groups part of the desired target.

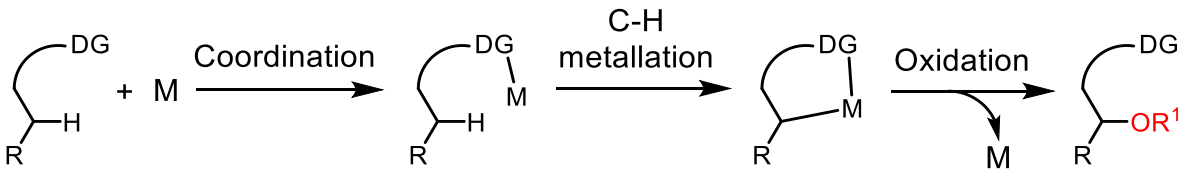

Scheme 1.2: General mechanism for directed transition metal C-H oxidation.

Early work in this area was performed by the Sames group with the development of a reaction for the C-H lactonization of amino acids using catalyst system employed in the Shilov process (Scheme 1.3).[15] The carboxylate and amino groups serve as ligands for Pt(II), which is oxidized to Pt(IV) by copper and insert into aliphatic side chain C-H

bonds. Reductive elimination affords the ɣ-lactone product and regenerated the platinum catalyst. Moderate diastereoselectivity was observed, and competing formation of cyclic amines also arose. While the substrate scope was limited, this work was an important early contribution to the field of directed C-H oxidations.

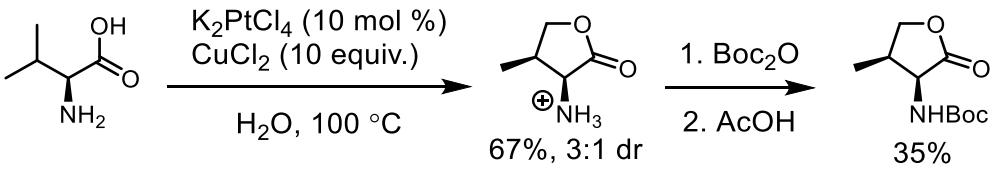

Scheme 1.3: Platinum-catalyzed lactonization of amino acids.

Palladium-catalyzed C-H oxidation reactions have also been well studied. A seminal report in this area was disclosed by Sanford whereby *O*-methyl oximes and 2-pyridyl groups were explored as competent directing functionalities for a palladium catalyzed acetoxylation.[16] Oxyfunctionalization was observed beta to both directing groups, which is consistent with the proposed 5-membered palladacyclic intermediate. Also, selectivity for the oxidation of primary carbons over secondary was observed. This was attributed to the steric preference for formation of a palladacycle incorporating a less hindered carbon. Mechanistically, the reaction occurs through a Pd(II)/Pd(IV) cycle where Pd(II) first coordinates to the directing group and inserts into a beta C-H via concerted metalation/deprotonation. The resulting palladacycle is oxidized to Pd(IV) by $PhI(OAc)_2$, and reductive elimination affords the acetoxylated product with concurrent regeneration of the Pd(II) catalyst. Similar conditions could be applied to the sp^2 acetoxylation of biaryl substrates using pyridines as a directing group.[17] This oxime directed C-H oxidation reaction has been applied towards in the synthesis of several natural products[18,19], notably Sorensen's enantiospecific total synthesis of the natural product jiadifenolide (Scheme 1.4B).[20]

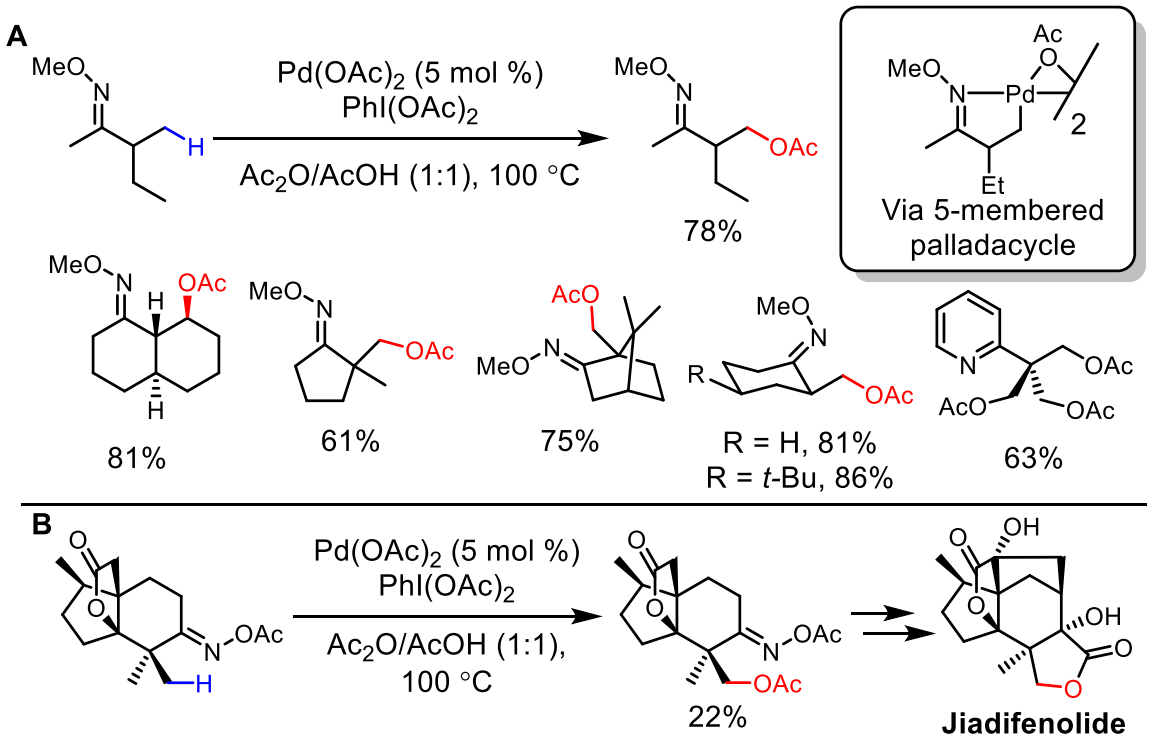

Scheme 1.4: **A**. O-Methyl oxime directed acetoxylation. **B**. Application of oxime directed acetoxylation in the total synthesis of jiadifenolide.

Using the Sanford precedent, Dong developed a modified oxime directing group for the synthesis of 1,2-diols using a Pd(II)Pd(IV) catalyst system and $PhI(OAc)_2$ as the terminal oxidant.[21] In a separate study, substrates containing a benzyl, TBS, or free hydroxyl could be used as in internal nucleophile for the formation of cyclic ethers.[22] 4-7 membered rings as well as spirocyclic ethers could effectively be synthesized followed by a Zn mediated reductive cleavage of the directing group to unmask the 1,2-diol functionality (Scheme 1.5A). Yu has leveraged the Pd(II)/Pd(IV) catalytic cycle for the acetoxylation of methylamines and alkyl groups using the Boc group and enantioenriched oxazoles respectively.[23,24] A highlight of the latter work is that the chirality of the directing group allows for diasteroselective oxidation (Scheme 1.5B).

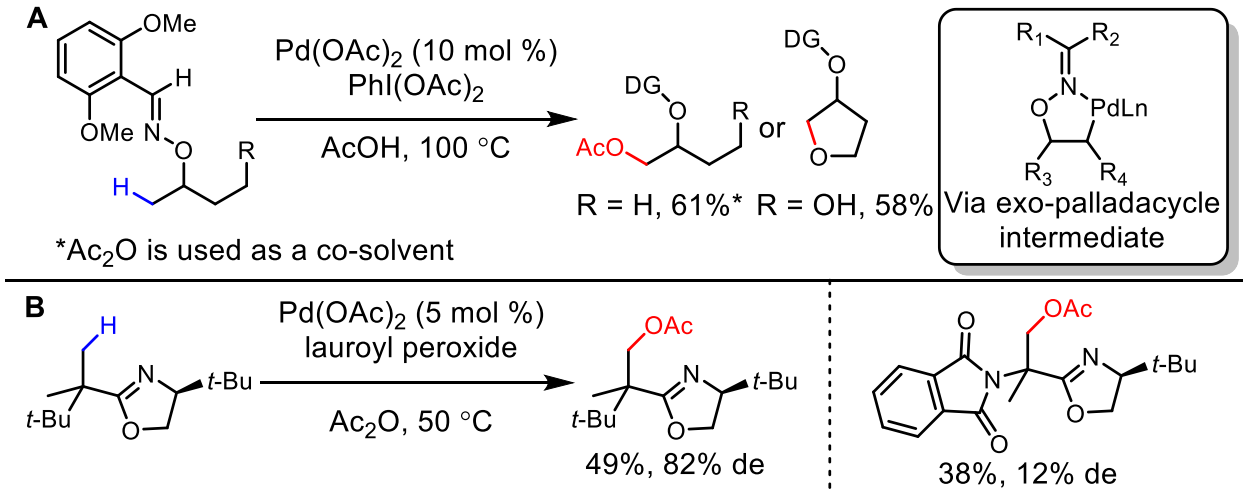

Scheme 1.5: Additional directed acetoxylation reactions. **A**. Dong's exo-oxime directed oxidation to form 1,2-diols. **B**. Yu's diastereoselective acetoxylation using a chiral directing group.

Hartwig devised a clever approach for the synthesis of 1,3-diols using a one-pot, three-step sequence.[25] In this method, diethyloxysilane serves as the directing group and can be installed by the dehydrogenative silylation of an alcohol or hydrosilylation of a ketone by the same iridium catalyst (Scheme 1.6A). Addition of more iridium precatalyst, 3,4,7,8-Me4phen, and norbornene catalyzes the dehydrogenative silylation of a ɣ C-H bond to form a 5-membered oxasilolane with norbornene as the hydrogen acceptor. Quenching the reaction with base and hydrogen peroxide oxidizes the Si-C bond to give the final diol product. Like Sanford's *O*-methyl oxime directed oxidation, Hartwig's approach is selective for the oxidation of primary carbons over secondary. Since the dehydrogenative silylation is performed under mild reducing conditions, a variety of functional groups can be tolerated such as aryl bromides and chlorides as well as silyl protected alcohols, acetals, and internal double bonds (Scheme 1.6B). However, esters, amides and other carbonyl containing functional groups were prone to hydrosilylation. Subsequent work by Hartwig focused on the development of modified conditions for the

dehydrogenative silylation of secondary alcohols by increasing the amount of iridium and ligand for the C-H silylation step as well as the reaction temperature.[26]

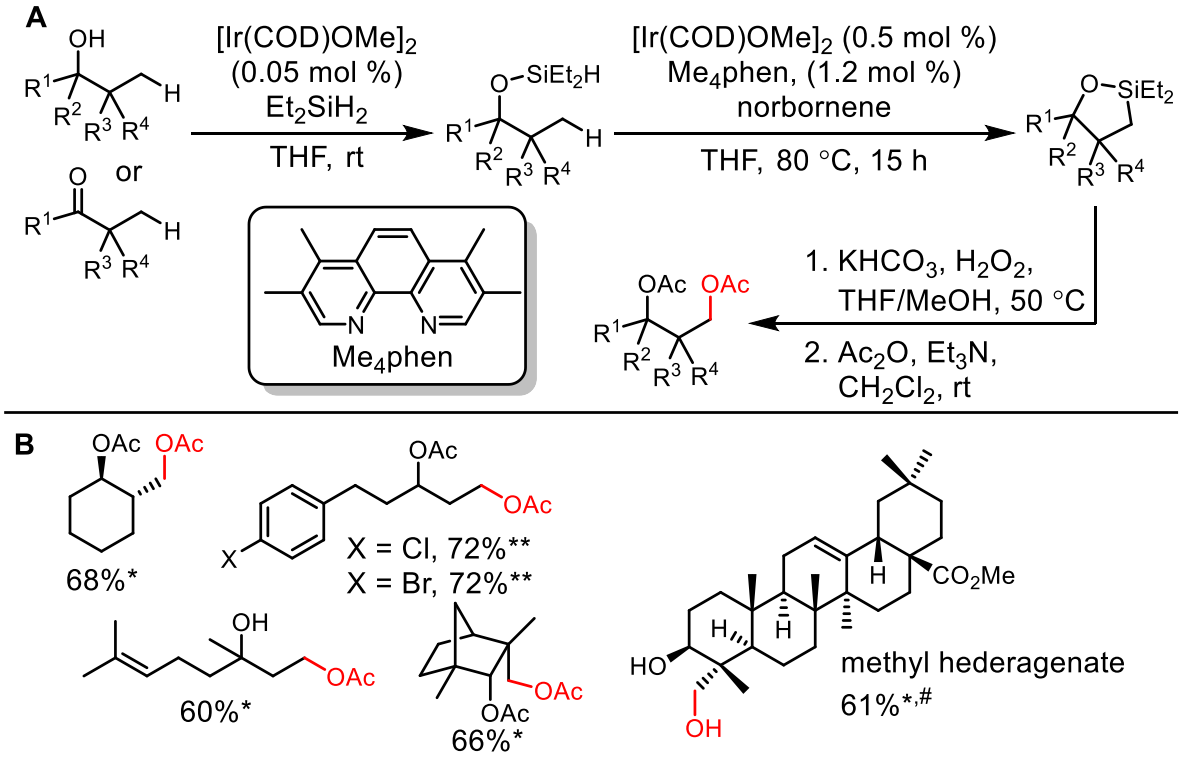

*From the alcohol starting material, **From the ketone starting material, #Acylation step ommitted.

Scheme 1.6: Iridium-catalyzed C-H silylation followed by Si-C oxidative cleavage. **A**. The one-pot, three step reaction sequence. **B**. Oxidation substrate scope.

In the examples shown, the success of the directing group strategy has relied upon the formation of a thermodynamically favorable 5- or 6-membered metallocyclic intermediate. Consequently, most strategies employing a directing group are only capable of oxidizing C-H bonds proximal to the directing functionality. Crabtree developed a ligand scaffold that enabled functionalization distal to the catalyst coordinating functionality.[27] Leveraging the propensity for carboxylic acids to form stable hydrogen bonded dimers, Crabtree developed a manganese-terpyridine dimer catalyst containing a conformationally restricted carboxylic acid functionality (Scheme 1.7). The catalyst-bound carboxylic acid forms a hydrogen bond to a substrate bound carboxylic

acid and position the substrate proximal to a transient oxidative manganese center whereupon C-H oxidation occurs. This catalyst system was used for the remote-directed oxidation of the benzylic position of ibuprofen to the corresponding ketone with high turnovers and selectivity. The authors noted that the use of a control catalyst that lacked the coordinating -COOH functionality resulted in greatly diminished selectivity. Although this system lacks broad applicability, it serves as a key example of the power of directing groups to achieve high selectivity remote from the site of catalyst binding.

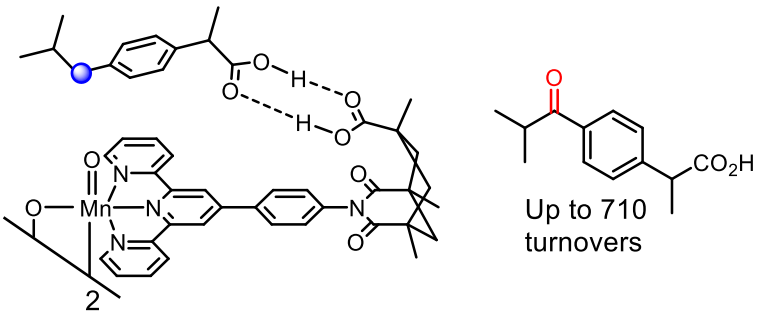

Scheme 1.7: Remote-directed oxidation of Ibuprofen using a manganese catalyst.

1.2.2 Non-Directed C-H Bond Oxidation

Significant effort by numerous groups has been devoted to the development of transition metal catalysts capable of selectively oxidizing C-H bonds without the use of a substrate-bound directing group. As a result, oxidation selectivity is determined by the steric and electronic properties of the substrate. Use of a non-directed catalyst system offers several advantages, notably, the minimization of concession steps required for the installation and removal of a directing functionality. However, the trade-off is reduced site- and chemoselectivity, especially as substrates become more functional group rich and complex. To overcome this hurdle, the development of novel ligand frameworks and optimized reaction conditions have been leveraged to provide predictable selectivity using these systems.

In most cases, non-directed C-H oxidation catalysts operate under a different mechanism from that of their directed analogs. Instead of metalation of a C-H bond to form a C-[M] complex as is common with many directed systems, non-directed catalysts are oxidized to form a high-valent metal-oxo or peroxo- species. The oxidized metal can then oxidize C-H bonds through a rapid, two-step hydrogen atom abstraction/hydroxyl rebound process, by a concerted, 3-centered oxygen insertion, or a [3+2] addition process. Alternatively, catalysts can oxidize alkanes through the generation of reactive oxygen free radicals. Irrespective of the mechanistic pathway, the process remains an outer-sphere transformation.[10] Numerous metal systems using Mn,[28] Ni,[29] Co,[30,31] Cr,[32] Fe,[33] Re,[34] Cu,[35] Pt,[36] Ir,[37] and Ru[38] catalysts have been developed for these oxidation processes. The recent development of two catalyst systems will be the focus of the remainder of this section.

The use of electrophilic, non-heme iron catalysts are one of the thoroughly investigated systems for aliphatic C-H bond oxidation. The use of a tetradentate N-donor ligand serves as a mimic for the porphyrin ring seen in heme containing enzymes and stabilizes the formation of an iron (V) oxo as the reactive oxidation intermediate.[39] The White group has developed a discreet iron catalyst capable of selective sp^3 C-H oxidation in good yields. Initial investigations into an iron (II) catalyst stabilized with the bulky (*S*,*S*-PDP) ligand resulted in selective oxidation of 3° carbons over 2° and 1° (Scheme1.8A).[40] Subsequent studies showed that the same catalyst was effective for the oxidation of unactivated methylenes to ketones when the appropriate substrate is chosen.[41] Predictable functionalization of electron rich carbons is observed as oxidation occurs at the most highly substituted carbon distal from electron withdrawing substituents.

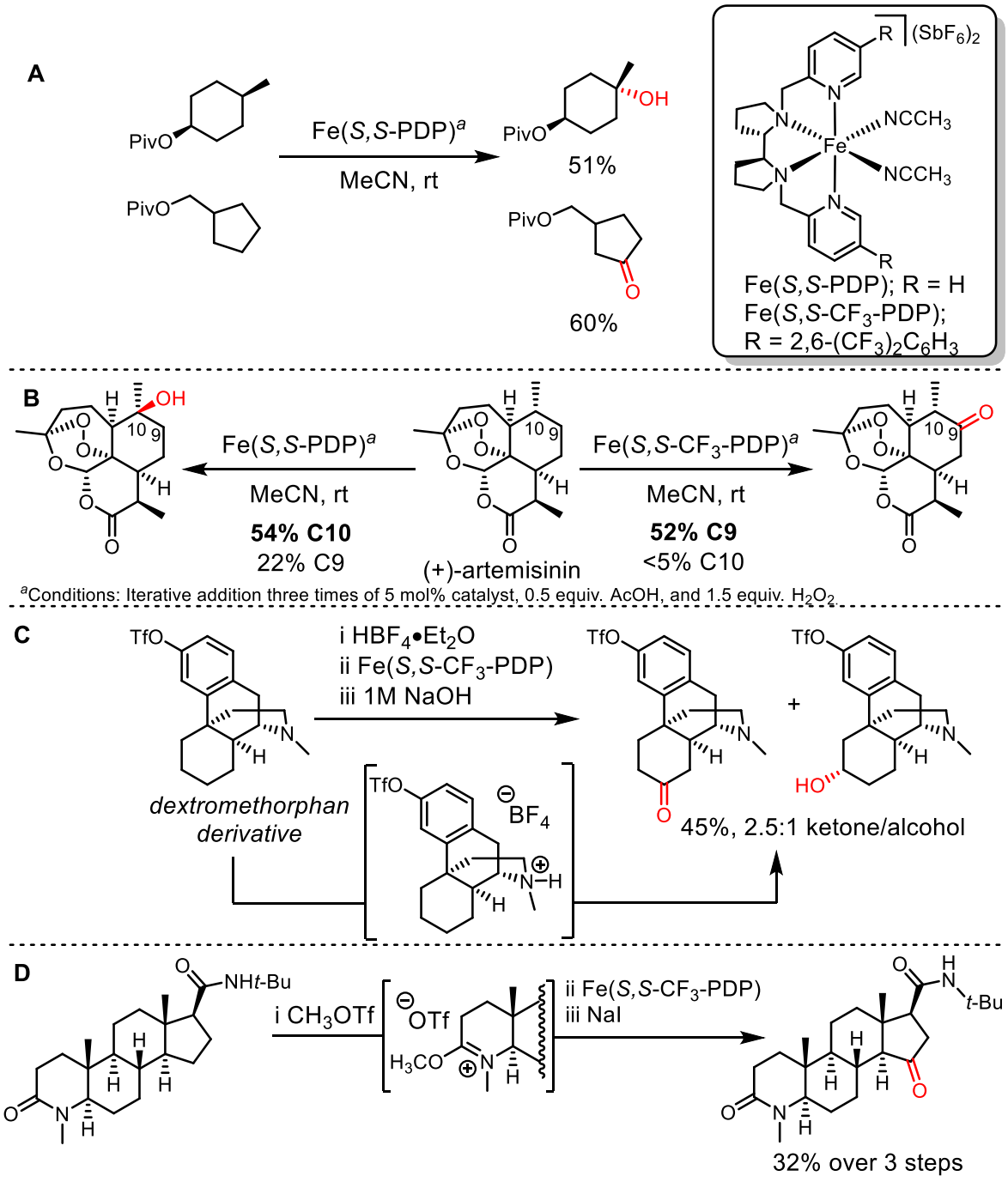

Scheme 1.8: Reactions using White's non-heme iron catalysts. **A**. 3° and 2° oxidation using Fe(*S*,*S*-PDP). **B**. Differential oxidation of artemisinin by employing catalyst control. **C**. Directing oxidation using Fe(PDP) catalysts by masking amines as the ammonium salt. **D**. Influencing the oxidation site by transiently masking amides as the electron deficient methyl ether.

White and coworkers also developed a sterically bulkier variant of the PDP catalyst containing two 2,6-trifluoromethylphenyl substituents that was selective for 2° oxidations in the presence of 3° carbons.[42] The enhanced selectivity is attributed to the electron withdrawing nature of the added substituents to the 5-positions of the pyridine ring attenuating catalyst reactivity towards more electron rich carbons. Additionally, added steric bulk restricts access to the transiently generated high-valent iron species. The authors demonstrated the effectiveness of this catalyst on the selective oxidation of artemisinin (Scheme 1.8B). Recent efforts have been focused on developing strategies to direct the site of functionalization using these iron catalysts by transiently masking specific functional groups. Amine-containing substrates can be oxidized at remote carbons by masking the nitrogen as the HBF_4 salt or BF_3 adduct (Scheme 1.8C).[43] Also, amide substrates could be oxidized at distal methylenes upon O-methylation with MeOTf (Scheme 1.8D).[44]

The Du Bois lab has made significant progress in the development of Ru-based reactions for non-directed C-H oxidation. Early work resulted in a 3-selective reaction using a $RuCl_3$ precatalyst and $KBrO_3$ oxidant.[45] Under these conditions, the transient formation of a RuO_4 species that was proposed to undergo C-H oxidation via [3+2] addition transition state (Scheme 1.9A) . Further investigations showed that the use of the Me_3tacn ligand increased conversions and selectivity when compared to the $RuCl_3$ system (Scheme 1.9B).[46] A recent disclosure from the Du Bois and Sigman groups involves the development of a non-directed reaction catalyzed by cis-[$Ru(dtbpy)_2Cl_2$] that does not oxidize nitrogen groups such as pyridines and amines (Scheme 1.9C).[47] Using an acid-stable Ru catalyst allows the reaction to be performed using acetic acid as a co-

solvent and stochiometric trifluoromethanesulfonic acid. With these conditions, basic nitrogen groups are protonated and thus protected from further chemical oxidation. C-H oxidations performed using this reaction are stereoretentive, a significant improvement over the previous stereoablative [Ru(Me3tacnCl3)] system.

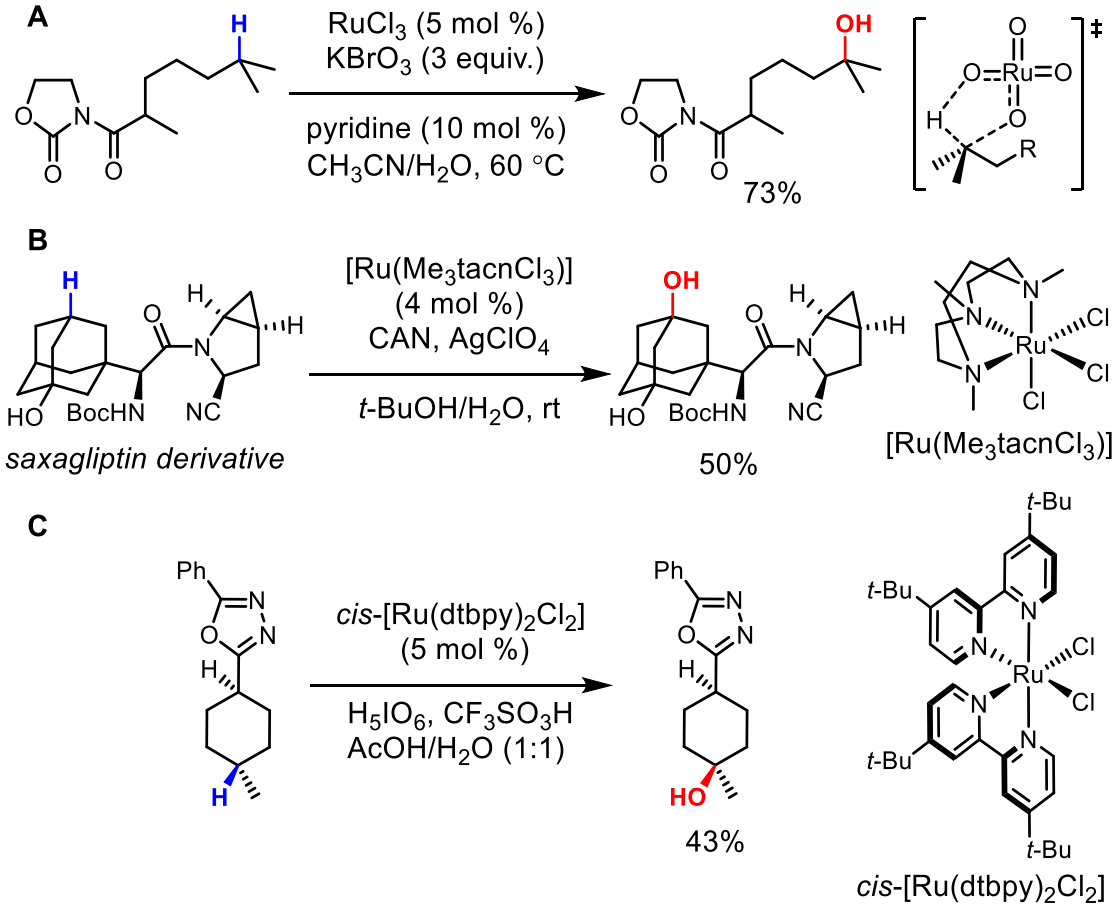

Scheme 1.9: Du Bois' development of electrophilic Ru catalysts for C-H oxidation. **A**. Employing simple ruthenium salts. **B**. Using the discreet tacn ligand framework. **C**. Oxidation of basic nitrogen-containing substrates in acidic aqueous solvent using a discreet ruthenium catalyst.

1.2.3 Biomimetic C-H Bond Oxidation

Nature employs enzymes as powerful catalysts for the selective oxidation of C-H bonds with selectivity determined by a myriad of weak non-covalent interactions within the enzyme active site. De novo design of an entirely new enzyme for selective oxidation

has not been achieved. Breslow,[48–53] Hennig,[54] and others[55,56] have attempted to replicate the selectivity observed through enzymatic catalysis with the development of biomimetic C-H oxidation catalysts. Based on the reactive co-factor of cytochrome P450 enzymes, these catalysts employ a metal-porphyrin decorated with a macrocyclic cyclophane or cyclodextrin groups. Over the past several decades, Breslow has developed a manganese catalyst with four appended B-cyclodextrin rings (Scheme 1.10A).[51] Substrates modified with tert-butylphenyl containing auxiliaries are positioned near the reactive metal center through hydrophobic interactions between the auxiliaries and cyclodextrin rings. This approached was applied to the benzylic hydroxylation of dihydrostilbene substrates with good conversion.[49] Further efforts afforded the highly selective oxidation of the alpha face of the B-ring of androstane-3,17-diol using 10 mol% of Mn catalyst **1** (Scheme 1.10B).[52] Improved Mn catalyst **2** containing perfluoroaryl groups which were predicted to prevent oxidative decomposition of the catalyst resulted in greater catalytic efficiency for the hydroxylation of the androstane diol substrate.[50,53]

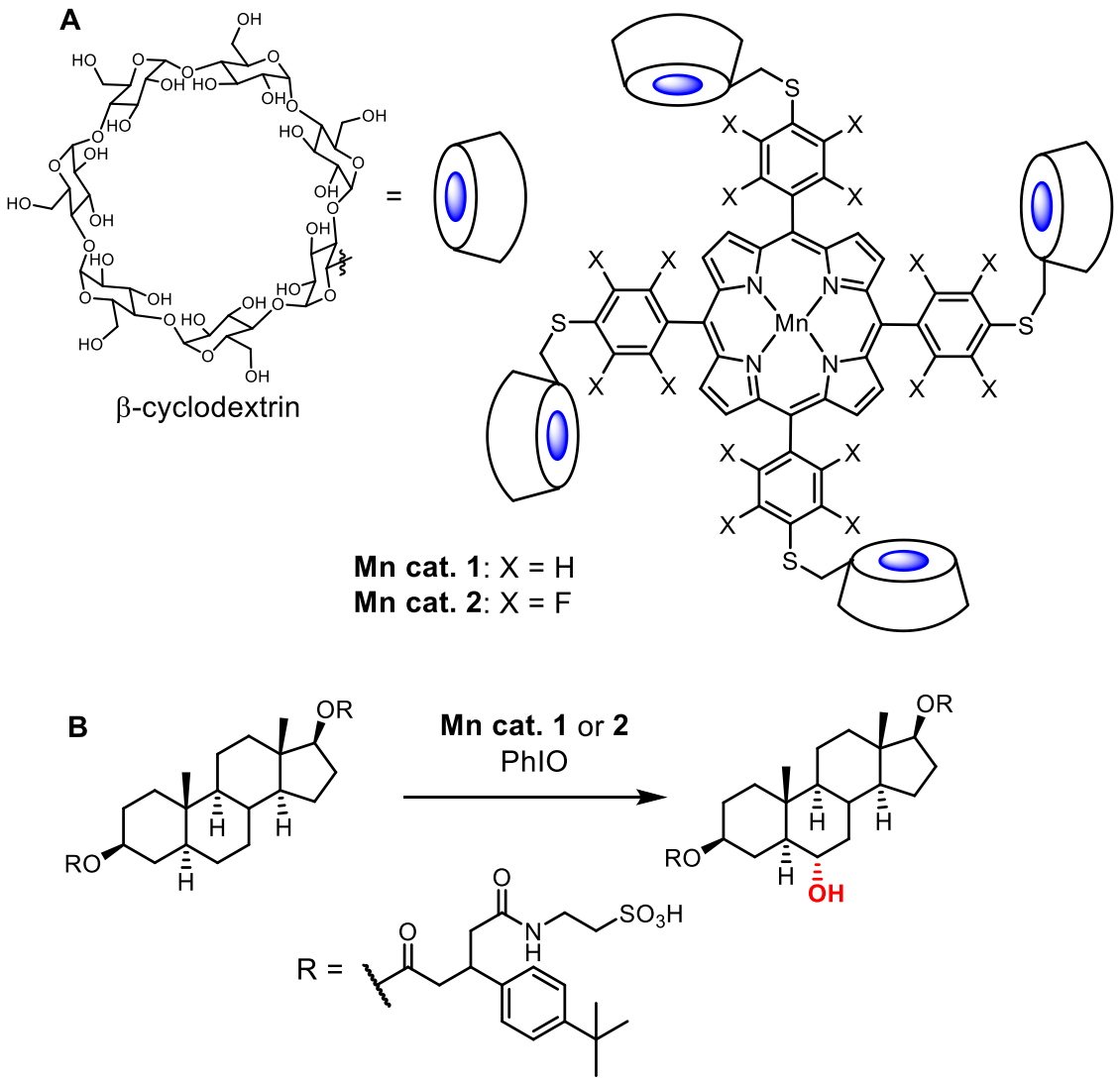

Scheme 1.10: Breslow's biomimetic manganese catalysts. **A**. The structure of the manganese porhyrin catalyst with four pendant β-cyclodextrin rings. **B**. Application of Mn catalysts for the selective oxidation of a steroid framework.

1.3 Organic C-H Bond Oxidation Methods

Electrophilic O-atom transfer reagents are a useful alternative to metal-based C-H oxidation methods. Dioxiranes are among the most commonly used class of organic reagents used for these types of transformations. Pioneered by Murray[57] and Curci,[58,59] dimethyldioxirane (DMDO) and trifluoromethyldioxirane (TFDO) can be prepared from the corresponding ketones and stored for long terms at low temperatures. These compounds

are proposed to insert directly into sp^3 C-H bonds through a concerted oxygen transfer to furnish the resulting hydroxylated product and an equivalent of ketone, but there is also evidence for a stepwise radical-based process (Scheme 1.11A).[58] Selectivity for C-H insertion favors more electron rich carbons. Despite the high reactivity and thermal instability of these compounds, they have been successfully employed for the late-stage hydroxylation of organic compounds. Baran utilized TFDO for the installation of a tertiary hydroxyl group en-route to the synthesis of the terpene natural product 4-epiajanol (Scheme 1.11B).[60] The highly-selective equatorial C-H oxidation in the presence of several other 3° carbons was attributed to substrate strain release in the transition state of the oxygen transfer.[61] Wender leveraged a DMDO oxidation for the selective hemiketalization of an electron rich pyran ring of a bryostatin analogue in high yield (Scheme 1.11C).[62] The latter example is a remarkable demonstration of the application of these reagents as both free hydroxyl groups, electron rich, and electron deficient olefins are tolerated.

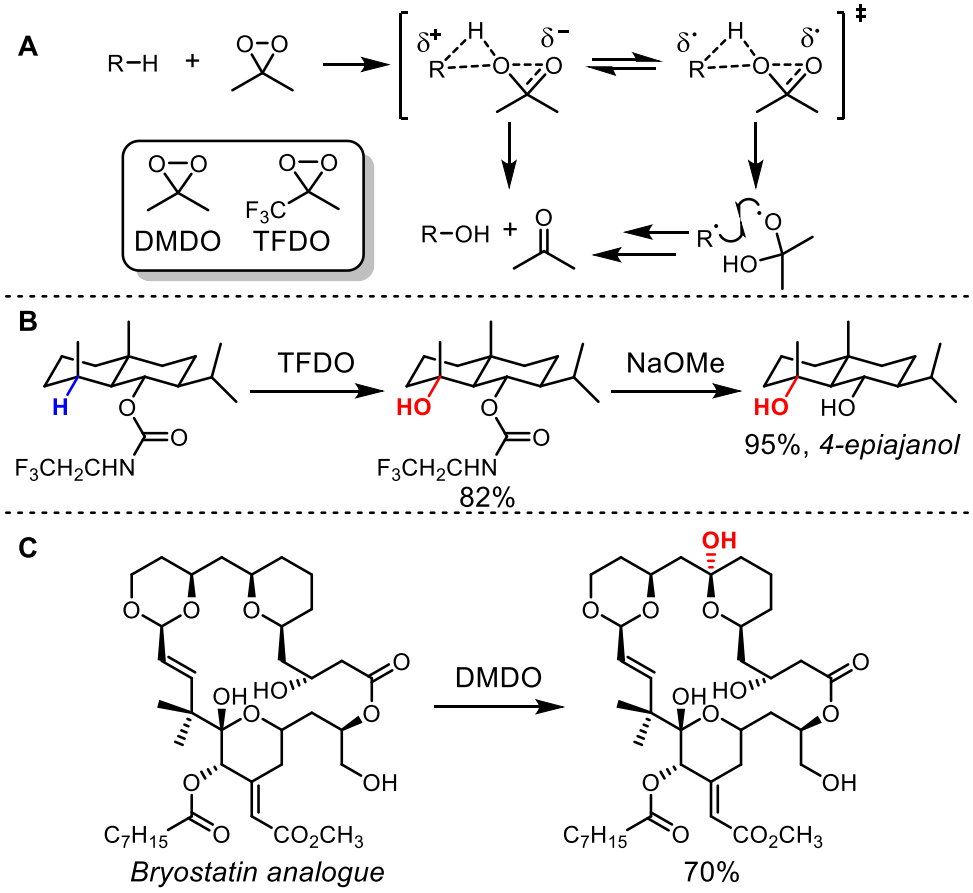

Scheme 1.11: C-H functionalization using dioxirane reagents. **A**. Proposed mechanism for dioxirane C-H oxidation. **B**. Baran's application of TFDO in the synthesis of 4-epiajanol. **C**. Wender's application of DMDO in the synthesis of hydroxylated bryostatin analogues.

A significant hurdle to the more mainstream application of these reagents is their instability, requiring storage at cryogenic temperatures for extended use.[57] Additionally, stoichiometric use of these oxidants is required. An attractive alternative to the use of TFDO and DMDO is the use of a suitably reactive ketone that can be oxidized into a dioxirane in situ from inexpensive oxidants, such as hydrogen peroxide or persulfates. Hilinski and Pierce developed a trifluoromethyl aryl ketone catalyst that could be used in 20 mol % for C-H oxidation with hydrogen peroxide as the oxidant (Scheme 1.12A).[63] Du Bois and coworkers engineered benzoxathiazine catalysts capable of in situ oxidation to

the corresponding oxaziridine as the active species (Scheme 1.12B).[64] In both examples, the oxidation selectivity is analogous to DMDO and TFDO oxidations. In lieu of a catalyst for intramolecular oxidation, Inoue created a removable trifluoromethyl ketone auxiliary for intramolecular hydroxylation (Scheme 1.12C).[65] This group could promote the 1,3-axial hydroxylation of cyclohexanols and steroids. It was observed that the oxidation selectivity was significantly eroded when an equatorial alcohol was used to tether the auxiliary to the substrate.

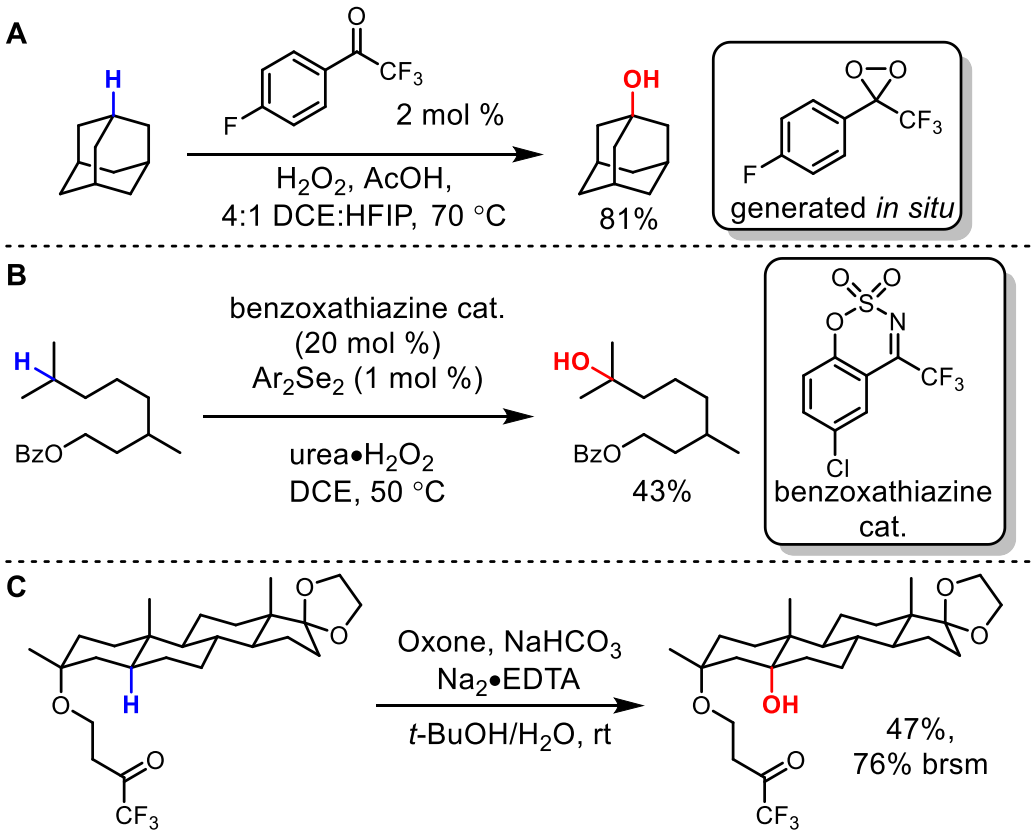

Scheme 1.12: *In situ* generated dioxiranes and oxaziridines for C-H oxidation. **A**. Wender's trifluoromethyl aryl ketone catalyst. **B**. DuBois' benzoxathiazine catalyst. **C**. A tethered auxiliary for in situ dioxirane generation.

1.4 Biocatalytic C-H Oxidation Methods

The greatest challenge in chemical oxidation methods is controlling the site- and stereoselectivity of functionalization. As mentioned earlier, nature has overcome these hurdles by implementing metalloenzymes for aliphatic C-H oxidation. One of the largest classes of enzymes leveraged for this transformation across species ranging from bacteria and fungi to humans is the cytochrome P450. As an alternative approach to small molecule methods, scientists have sought to harness the natural reactivity of these enzymes for the selective oxidation of non-native substrates.

1.4.1 Conserved Structural Features and the Cytochrome P450 Catalytic Cycle

Aside from the sequence homology among different cytochrome P450 enzymes, one of the main conserved structural features is the iron protoporphyrin IX cofactor (Scheme 1.13A) with an axial cysteine ligand. This metal center serves as the reactive site for oxygenation while the surrounding residues determine the orientation of the substrate within the active site through a myriad of non-covalent interactions.

The resting state of the enzyme is an Fe(III) species with an axial water ligand. Upon substrate binding to the enzyme, the water ligand is removed and the spin state of the iron changes to allow single electron reduction of the iron by a redox partner (Scheme 1.13A).[66–68] The redox partner can exist as a separate domain within the P450, or in an entirely different protein. The electrons provided to the redox partner typically come from the oxidation of NADH or NADPH. The reduction of the P450 Fe(III) to Fe(II) allows the incorporation of an axial oxygen. Another single electron transfer from the redox partner and double protonation allows for the reductive scission of the oxygen-oxygen bond and

results in the formation of an Fe(IV) oxo with a radical cation delocalized in the surrounding porphyrin cofactor. This intermediate, commonly known as compound I, is the reactive species that oxidizes proximal substrate C-H bonds. Once the substrate is oxidized, it is ejected from the enzyme and replaced by a water ligand to return the enzyme to its Fe(III) resting state.

Numerous deuterium labelling and radical clock experiments have determined that substrate oxidation by compound I proceeds through a radical rebound mechanism (Scheme 1.13B).[68] This occurs through a stepwise process where a hydrogen atom is abstracted from the substrate to generate a radical and an Fe(IV) hydroxyl species. The substrate radical can then recombine with the iron hydroxyl to install form the oxidized product and reduce the iron species to Fe(III). Independent syntheses of Fe(IV) hydroxyl compounds with modified porphyrin rings have been shown to undergo hydroxyl rebound when subjected to the trityl radical to give Fe(III) and the corresponding organic alcohol.[69] This radical rebound process is so rapid that the substrate radical cannot isomerize or reorient within the active site. Thus, reactions performed by P450s are stereoretentive despite proceeding through a short lived radical.

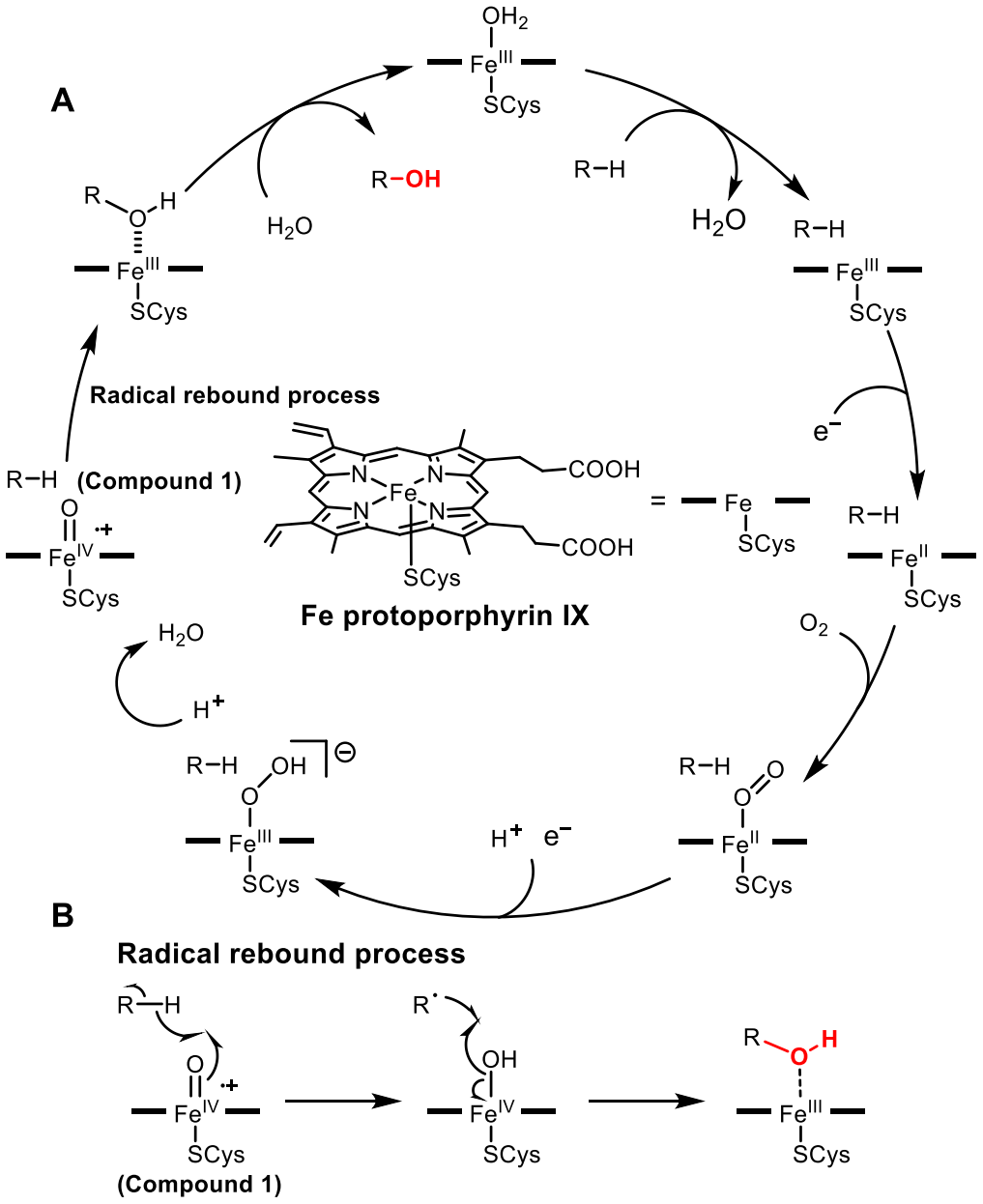

Scheme 1.13: The P450 catalytic cycle. **A**: General catalytic cycle for P450 mediated C-H hydroxylation. **B**. Radical rebound oxidation of substrates from compound 1.

1.4.2 Methods for Modifying Enzymatic Reactivity

Cytochrome P450 enzymes are highly efficient catalysts for their native substrate. However, it is typically observed that their effectiveness decreases as substrates deviate from the natural scaffold. Repurposing enzymes to accept substrates of varying size and

complexity remains a challenge in the implementation of biocatalysis. To overcome this problem, the sequence of the protein can be altered through amino acid mutation. Rational mutagenesis and directed evolution are the two strategies routinely used to alter enzyme activity.

Rational mutagenesis[70] requires knowledge of the enzyme structure either through crystal structure or modeling of the active site. Using this information, mutations can be made at specific sites to alter the reactivity of the enzyme. Directed evolution[67,70,71] relies on the random generation of numerous mutants, then assessing their reactivity using an assay for a specific trait (i.e. reactivity towards a new substrate). Mutants that displayed improved characteristics can then be subjected to additional rounds of mutation/assaying in an iterative process to further increase efficiency. Since this process occurs through random mutation, little to no structural knowledge of the enzyme is required. These methods are not restricted to the alteration of the enzyme substrate tolerance. Rational and directed mutagenesis can be used to increase site selectivity, stereoselectivity, thermal stability, coupling efficiency, and organic solvent tolerance to name a few traits.

A third approach that has recently been pioneered by Watanabe[72,73] and Reetz[74] is the use of non-oxidizable activators to trick the enzyme into accepting unusual substrates. These activators bind the P450 and induce the formation of compound I, but do not undergo oxidation. Instead, compounds that are unsuitable substrates can enter the active site and undergo oxidation by the activated P450.

1.4.3 Examples of Biocatalytic C-H Oxidation

The strategies previously described have been used with remarkable success for the implementation of P450s for the oxyfunctionalization of aliphatic C-H bonds. The Urlacher group employed a rational mutagenesis approach to develop mutants of the P450 BM3 from *Bacillus megaterium* for the regioselective allylic hydroxylation of β-cembrenediol (Scheme 1.14A).[75] The two mutants displayed exquisite regiocontrol for two adjacent allylic positions, however minimal diastereoselectivity was observed.

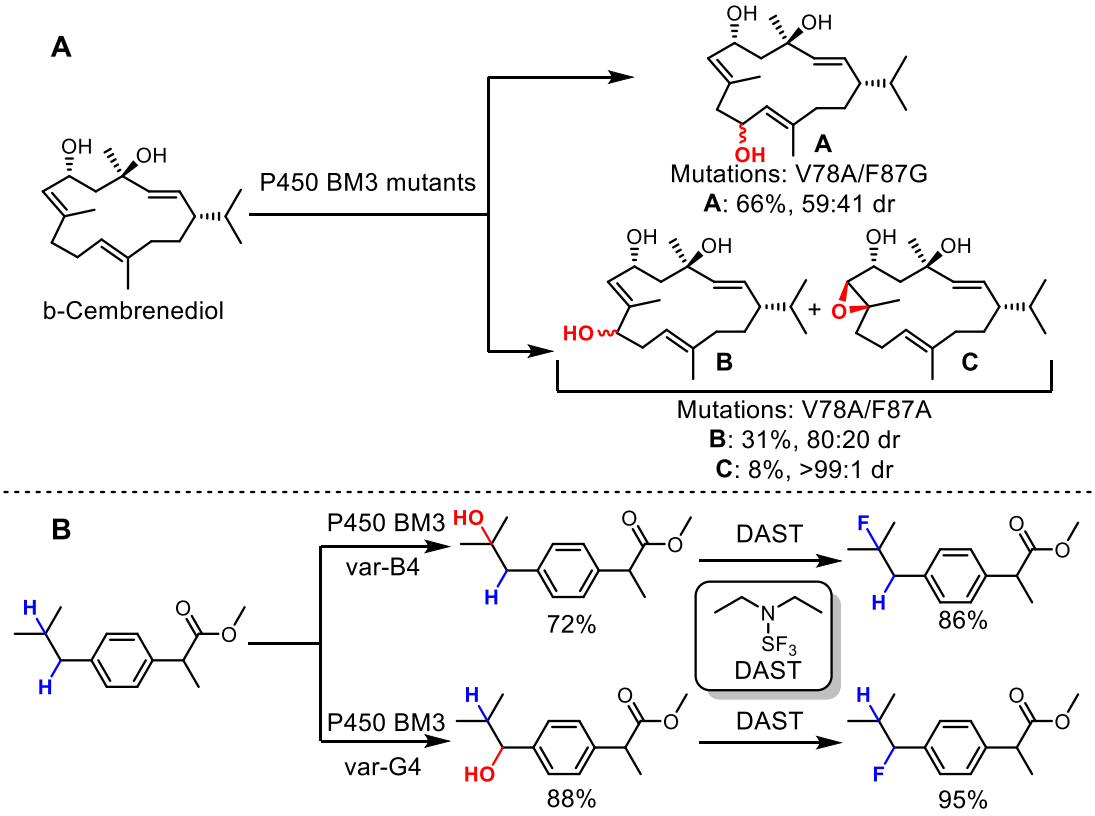

Scheme 1.14: Applications of P450 engineering for divergent selectivity. **A**. Rational mutagenesis applied to the generation of BM3 mutants for the oxidation of β-cembrenediol. **C**. Directed evolution of BM3 variants for a combined chemoenzymatic fluorination protocol.

Arnold leveraged a directed evolution approach to identify several BM3 mutants capable of selective hydroxylation of a series of small molecule scaffolds (Scheme 1.14B).[76] Using the BM3 mutant var-G4, oxidation of the benzylic methylene of ibuprofen was obtained, which offers analogous selectivity to Crabtree's manganese-terpyridine catalyst (vide supra). Switching to mutant var-B4 afforded methine oxidation. Enzymatically oxidized products were then subjected to deoxygenative fluorination using DAST to demonstrate a two-step protocol for late-stage chemoenzymatic fluorination. Finally, Watanabe exploited the use of perfluorinated carboxylic acid activators to promote the P450 BM3 catalyzed hydroxylation of small hydrocarbons.

While the highlighted examples showcase the utility of P450s as a robust method for oxygen incorporation, methods that display the orthogonality of biocatalysis compared to chemical methods are of interest. This is especially so in the context of late-stage oxygenation of complex, functional group rich molecules. Fasan and coworkers identified several P450 BM3 mutants using a directed evolution/fingerprinting approach that displayed remarkable site-and stereoselectivity functionalization of artemisinin (Scheme 1.15A).[77,78] Using different mutants, hydroxylation of the C14 methyl and C9 methylene as either the *R* or *S* stereoisomer are obtained. In contrast, White's iron-based PDP approach is selective for functionalization of the C10 methine of artemisinin and over-oxidation of C9 to the corresponding ketone.[42] Recently, Arnold and Stoltz disclosed a fantastic example of the unique selectivity of P450s compared to chemical methods for the completion of the total synthesis of nigelladine A (Scheme 1.15B).[79] Numerous chemical allylic oxidation methods based on Se, Cr, Pd, and Rh failed to oxidize the desired C7 position and resulted an undesired selectivity or a mixture of products. After

screening a library of engineered P450s, a single variant was identified that was selective for hydroxylation at C7. The synthesis was completed after DMP oxidation to the corresponding ketone in 21% yield over two steps.

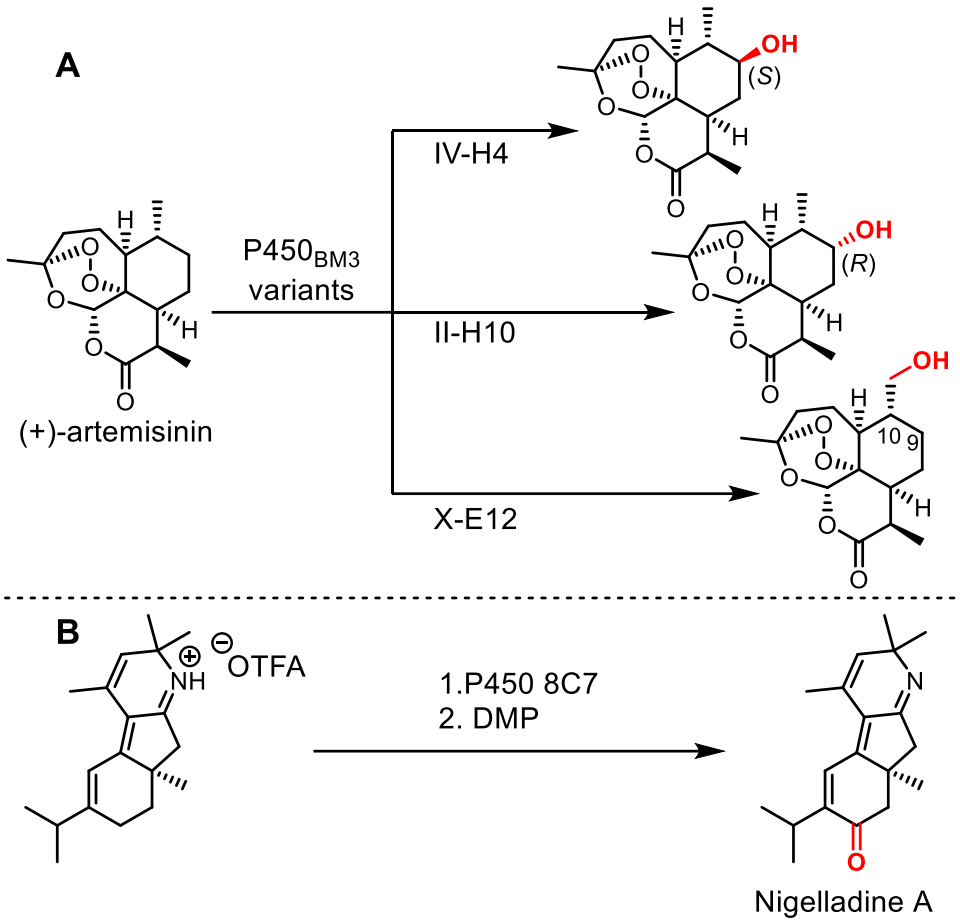

Scheme 1.15: Biocatalytic oxidation applied to late-stage synthesis. **A**. Biocatalytic oxidation to generate artemisinin derivatives. **B**. Selective installation of the final site of oxidation by biocatalysis to complete the total synthesis of nigelladine A.

1.5 Conclusions and Outlook

With the ubiquity of the C-H bond in organic molecules, it is abundantly clear that no single aliphatic C-H bond oxidation method can conduct every desired transformation. Instead, chemists must carefully select the appropriate method from the available toolbox of C-H oxidation technologies. New methods are constantly under development that

operate under unique principles for controlling selectivity, with the underlying goal of targeting a previously inaccessible class of C-H bonds for oxidation. As briefly outlined in this chapter, biocatalysis offers unique modes of determining selectivity as well as oxidation patterns that are analogous or orthogonal to chemical methods. Enzymes can be mutated to target unactivated bonds regardless of steric or electronic environments.

Chapter 2 focuses on a specific cytochrome P450, PikC, from its discovery in the genome *of Streptomyces venezualae* through its development into a robust biocatalyst. Within these studies, discovery of the unique mode of substrate binding allows for elements of directed oxidation as well as enzymatic methods to be incorporated in a single platform. Chapter 3 outlines the use of this biocatalyst to perform oxidation on unnatural scaffolds where regioselectivity is determined by the identity of the directing group.

Chapter 2: Development of the Cytochrome P450 PikC as a Biocatalyst for Late-Stage C-H Oxidation

2.1 Introduction

As delineated in the previous chapter, biocatalysis is a powerful complement to chemical aliphatic C-H oxidation methods. Unlike chemical systems that are created upon the fundamental understanding of chemical reactivity, suitable biocatalysts need to be discovered in nature. This is often achieved by probing biosynthetic pathways in bacteria, fungi, and plants. This chapter entails the discovery, characterization, and development of a unique cytochrome P450 as a potent biocatalyst for late-stage C-H hydroxylation.

2.2 The Biosynthesis of Natural Product Macrolide Antibiotics Encoded in the pik Gene Cluster in *Streptomyces venezualae*

Macrolides are an important class of bacterial antibiotics, with erythromycin (Figure 2.1A) being the first to see clinical use. Since then, several other potent macrolides have been adopted for human use. These antibiotics are capable of binding to the 23S bacterial ribosome subunit and preventing translation ultimately resulting in cell death.[80] Understanding the mechanism of their biological synthesis would allow the manipulation of the bacterial genome to create new antibiotic analogs.[81,82]

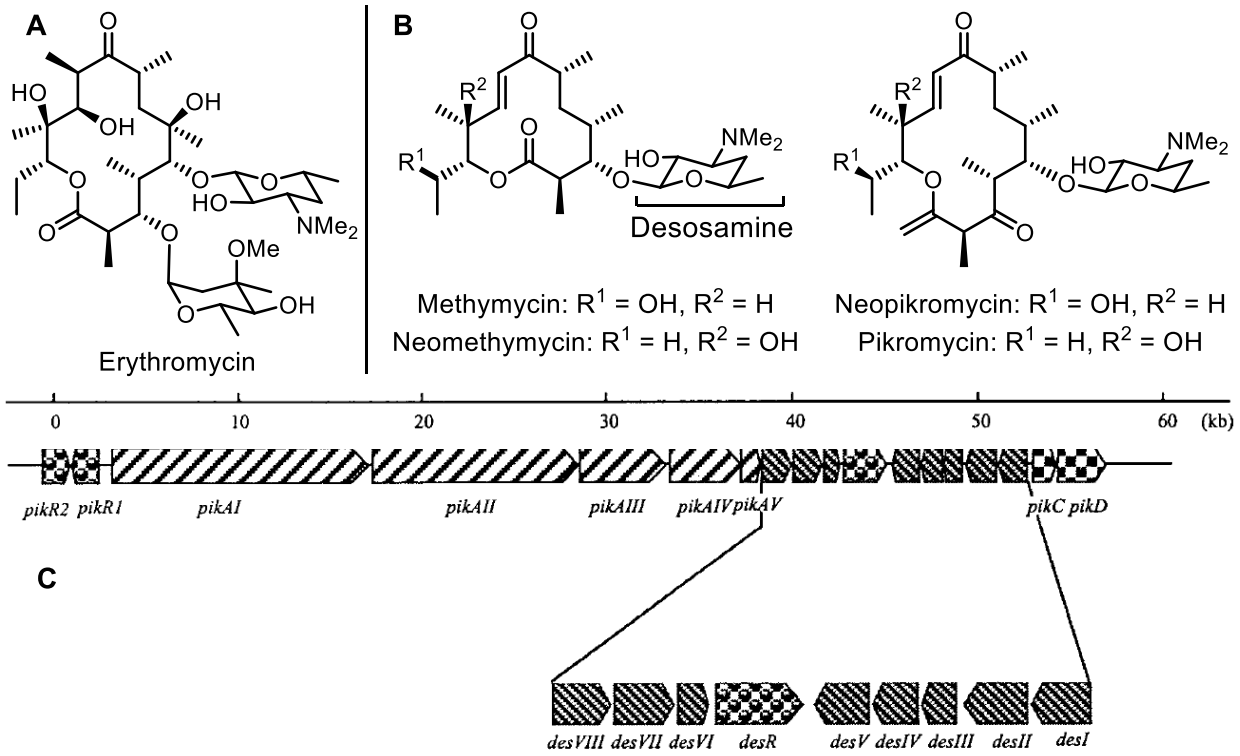

Figure 2.1: Macrolide antibiotics **A**. Clinically used macrolide antibiotic Erythromycin. **B**. Macrolide antibiotics produced by *Streptomyces venezuelae*. **C**. The gene cluster encoding the four macrolide antibiotics shown in panel **B**.

Methymycin, neomethymycin, pikromycin, and narbomycin are four macrolides produced by the bacteria *Streptomyces venezuelae* (Figure 2.1B). Investigations by Sherman and coworkers have shown that the ~60 kB pik gene cluster contains the biosynthetic machinery responsible for the synthesis of all four macrolide natural products (Figure 2.1C).[83] The pik cluster is comprised of 18 genes. Of note, pikAI, pikAII, pikAIII, and pikAIV encode a polyketide synthase (PKS), a multifunctional series of proteins responsible for the synthesis of the polyketide backbone. These PKS systems are observed across numerous macrolide and polyketide biosynthetic pathways.[84,85] The pik PKS is comprised of six modules, which are responsible for the synthesis of the linear backbone of the macrolide aglycone. Subsequent macrolactonization by a thioesterase (TE) encoded in pikAIV or pikAV affords 12-membered aglycone 10-deoxymethynolide

(10-dml) from PKS module 5 or 14-membered aglycone narbonolide from PKS module 6. Downstream of pikA are the seven genes comprising pikB. These are responsible for the synthesis of the deoxyaminosugar desosamine. A single flexible glycosyltransferase encoded in desVII appends desosamine to both 10-dml and narbonolide aglycones to make YC-17 and narbomycin (Figure 2.2).

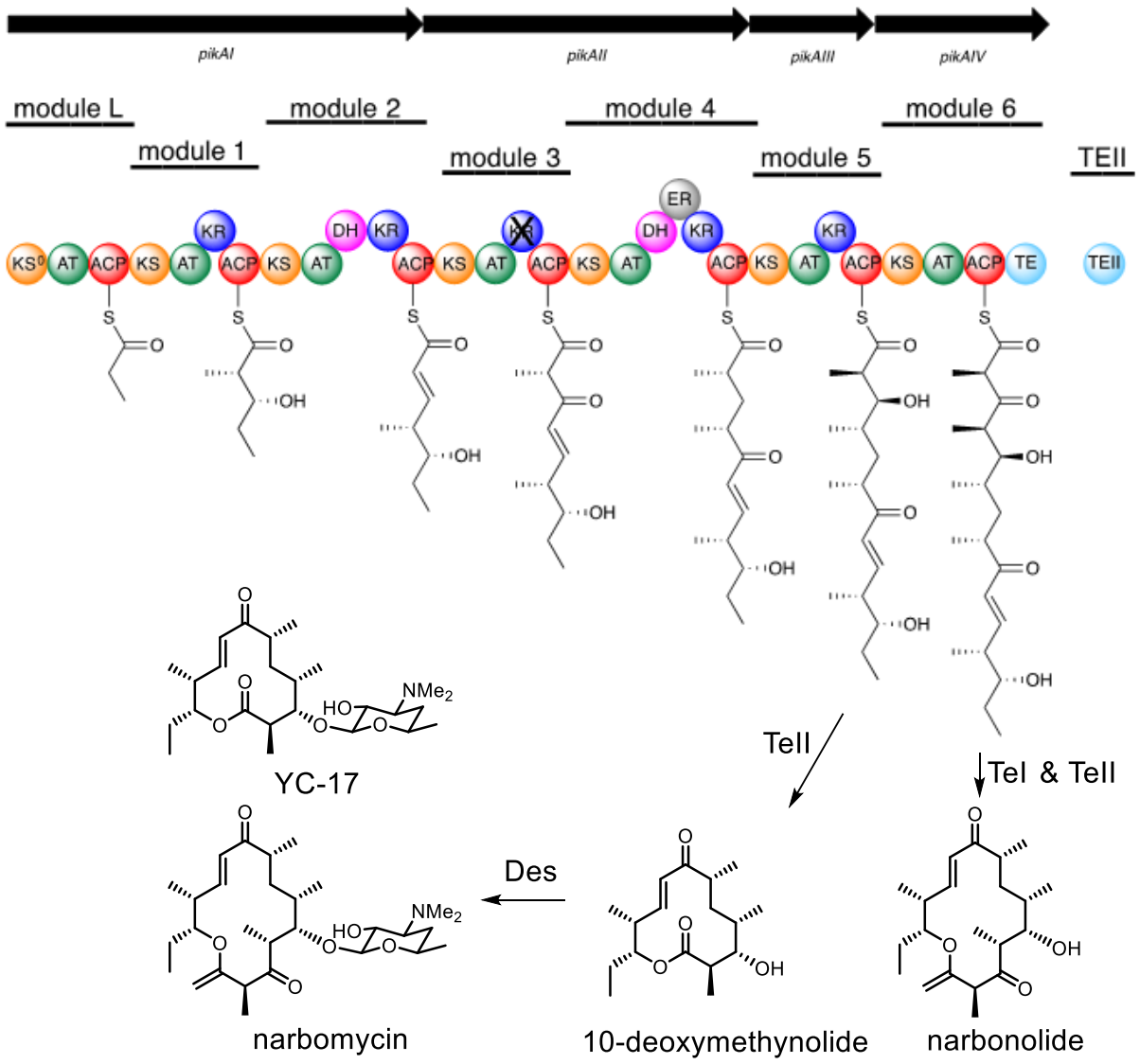

Figure 2.2: The structure and biosynthesis of 10-dml, narbonolide, YC-17, and narbomycin.

Further downstream, the gene pikC encodes a single cytochrome P450 monooxygenase. The PikC enzyme is responsible for the hydroxylation of both C10 and C12 of YC-17 to form methymycin and neomethymycin in a 1:1 ratio (Scheme 2.1). Additionally, PikC catalyzes the hydroxylation of 14-membered narbomycin to pikromycin and neopikromycin in a 38:1 ratio.[86] The final incorporation of a hydroxyl group enhances the effectiveness of these compounds as antibiotics compared to their unfunctionalized analogs. Post-synthetic modifications to increase activity, such as hydroxylation, are common in biosynthetic pathways.

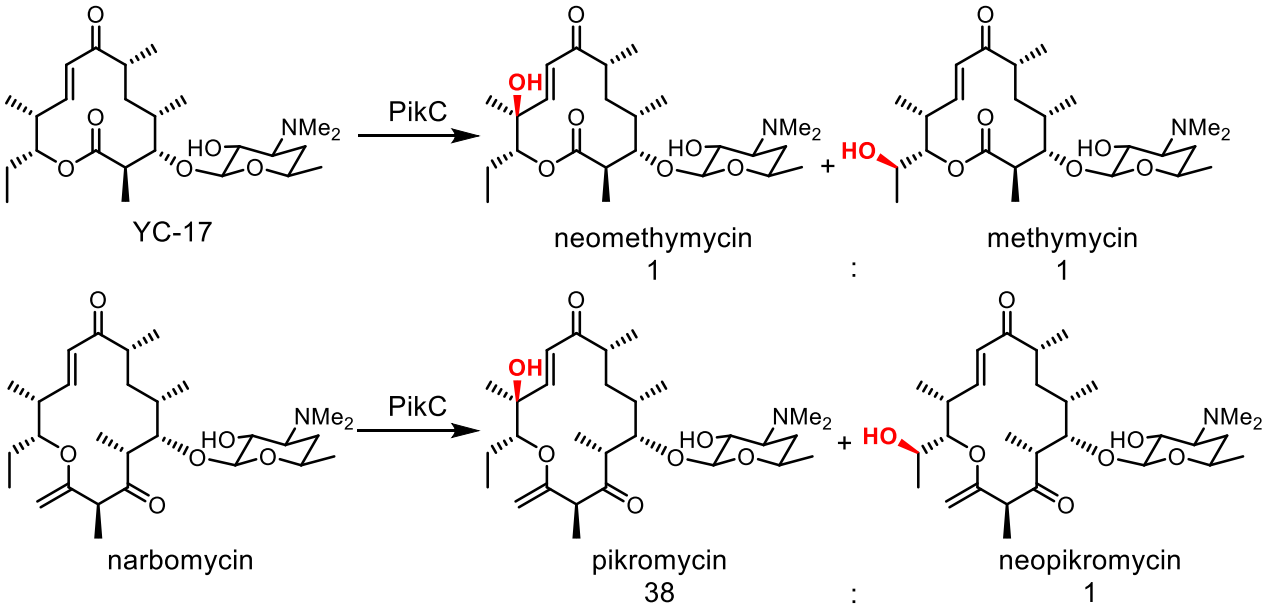

Scheme 2.1: Endogenous reactions of the cytochrome P450 PikC.

Analysis of the co-crystal structures of 10-dml and narbomycin bound to PikC reveals a unique mode of substrate binding.[87] PikC contains a buried pocket and a solvent-exposed pocket both adjacent to the heme-containing active site. Within these remote pockets are carboxylate containing residues that form salt bridge and electrostatic interactions with the protonated aminosugar desosamine present in both endogenous substrates. The dimethylamine moiety of desosamine was calculated to have a pK_a of

8.85, thus adopting a protonated state at biological pH further enhancing the stability of necessary electrostatic interactions. Subsequently, the distal hydrophobic macrolactone is positioned adjacent to the iron heme through hydrophobic interactions. The desosamine of YC-17 occupies the buried pocket of PikC, forming a salt bridge with E94 and an ionic pair with E85 (Figure 2.3A). Alternatively, the desosamine of narbomycin is anchored in the solvent exposed binding pocket through a salt bridge with E85 and an electrostatic interaction with D50 (Figure 2.3B).

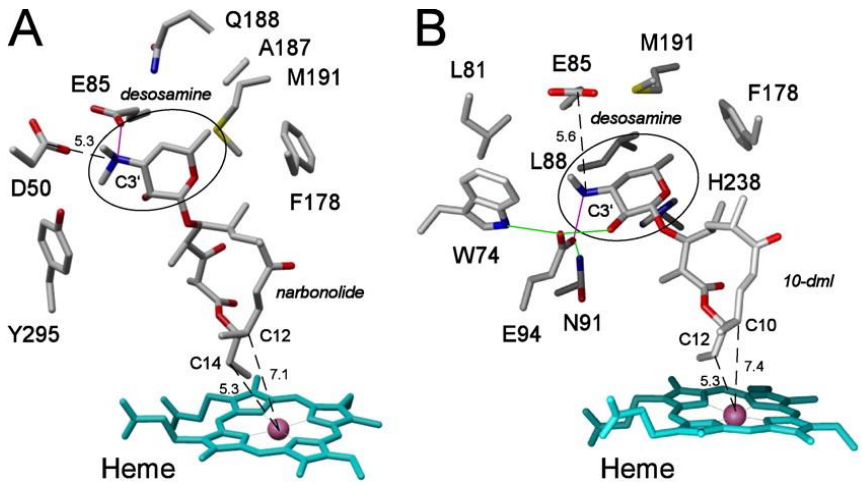

Figure 2.3: Co-crystal structures of native substrates with PikC. **A**. Co-crystal structure of narbonolide bound PikC. **B**. Co-crystal structure of YC-17 bound PikC.

2.3 Initial Developments of the Cytochrome P450 PikC

PikC is unique among cytochrome P450s due to its ability to accept large substrates of varying ring sizes. Such substrate flexibility is rare among enzymes and many engineering efforts are focused on increasing the size of the active site to accommodate larger substrates. Altering site-selectivity requires additional modifications as well. A biocatalyst that has the innate ability to oxidize large molecules with flexibility as seen in the oxidation of 10-dml to two distinct products in a 1:1 ratio would serve as a

robust platform for further enzyme engineering efforts. Additionally, the anchoring mode of substrate binding is seldom observed compared to the usual induced fit binding mechanism with only a few examples reported to date.[88,89] These atypical characteristics warrant further development of PikC into a biocatalytic platform.

2.3.1 Initial Enhancements to PikC Through Rational Mutagenesis

The discovery of the unique binding of endogenous substrates to PikC via co-crystal structures facilitates site-directed mutagenesis to probe the requirements of the electrostatic interaction between the protonated dimethylamine moiety and carboxylate residues Asp-50, Glu-85, and Glu-94. Mutating Glu-94 to non-polar alanine or polar glutamine eliminates PikC reactivity with YC-17 and produces minimal conversion of narbomycin. Analogous mutations to Glu-85 greatly reduce conversion of both endogenous substrates. These results align with the binding shown in the co-crystal structure as YC-17 associates with Glu-85 and Glu-94 in the buried pocket and narbomycin with Glu-85 and Asp-50 in the solvent exposed pocket. The respective ionic contacts formed with these residues 85 and 94 are essential for catalysis. Interestingly, mutation of Asp-50 to asparagine (D50N) results in enhanced catalytic activity towards both YC-17 and narbomycin.[87]

Analysis of the co-crystal structure of $PikC_{D50N}$ with narbomycin reveals a shift in binding from the surface exposed pocket (Figure 2.4A) to the buried pocket (Figure 2.4B) with ionic contacts between the protonated dimethylamine and Glu-85 and Glu-94. This structural insight coupled with the enhanced catalytic reactivity of $PikC_{D50N}$ with narbomycin indicates that binding to the surface exposed pocket is transient and serves to facilitate the transition of substrates to the buried, catalytically active pocket.[90] Kinetic

binding studies show that PikC$_{D50N}$ binds faster to narbomycin than wild type PikC (PikC$_{WT}$) (822.8 s^{-1} vs. 703.0 s^{-1}). Glu-85 likely aids substrate relocation from the transient to the catalytic pocket as it is essential for productive binding to both pockets. The mutation of this residue to glutamine drastically reduces the binding rate to 421.4 s^{-1}. From the PikC$_{D50N}$ co-crystal structures as well as kinetic data, it is evident that substrate binding to PikC occurs in two steps: substrate binding to the transient, solvent exposed pocket followed by a rate-limiting transition to the catalytically active buried pocket. The D50N mutation destabilizes the interaction between the substrate and the transient pocket, thus lowering the kinetic barrier for relocation to the catalytic buried pocket. A general reaction coordinate for substrate binding is shown in Figure 2.4D.

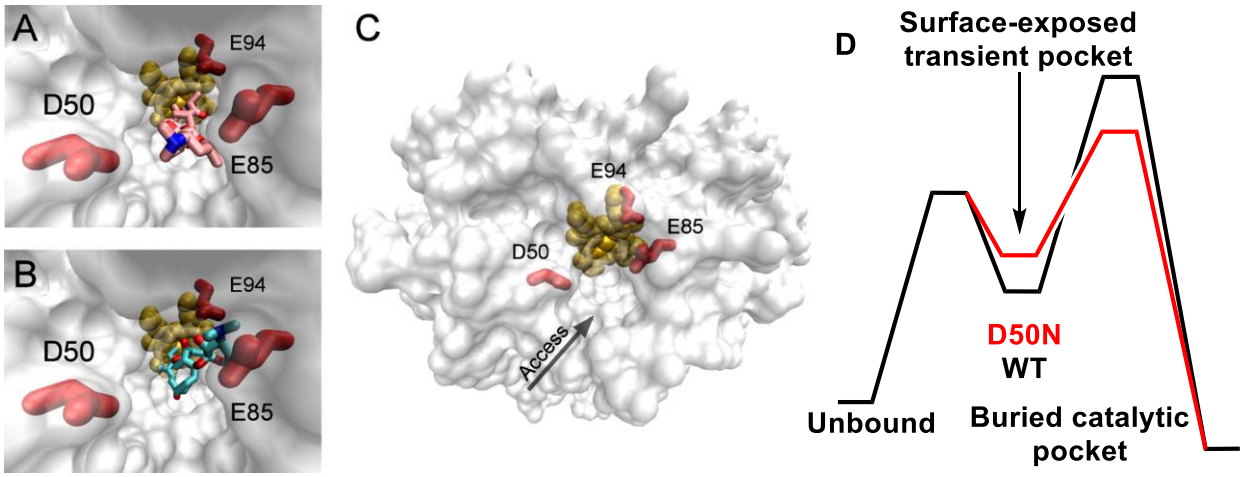

Figure 2.4: Narbomycin bound to PikC. **A**. Narbomycin bound in the transient pocket. **B**. Narbomycin bound in the catalytically active pocket. **C**. Dispersion of charged residues. **D**. General reaction coordinate for substrate binding to PikC$_{WT}$ (black) and PikC$_{D50N}$ (red).

2.3.2 Development of a Catalytically Self-Sufficient PikC Fusion Protein and Incorporation of a NADPH Recycling System

An integral component of P450 catalysis is the presence of a reductase, which shuttles electrons from NADPH to the heme iron allowing the reductive scission of

molecular oxygen and subsequent generation of reactive compound I. A desirable trait among P450s developed as biocatalysts, such as BM3, is the presence of an endogenous reductase domain that allows the enzyme to be catalytically self-sufficient.[91] Without this endogenous domain, expensive exogenous reductase partners are required to reconstitute P450 activity *in vitro*. This presents a significant barrier to the implementation of many enzymes as biocatalysts.

PikC does not contain an endogenous reductase domain and *in vitro* reconstitution requires the use of expensive spinach ferrodoxin reductase (Fdr) and ferrodoxin (Fdx), a system that is commonly employed (Figure 2.5A).[92,93] This necessitates the use of three independent components to achieve PikC reactivity and is highly cumbersome. To circumvent this drawback, PikC was covalently linked at the N-terminus to RhFRED, a reductase domain from the bacteria *Rhodococcus* sp. NCIMB 9784 (Figure 2.5B).[94] The resulting fusion protein can be expressed as a single catalytically active unit, thus eliminating the need for expensive exogenous partners. The PikC-RhFRED fusion protein displays enhanced catalytic activity towards the native substrates, YC-17 and narbomycin, when compared to the three component PikC/Fdr/Fdx system. This shows that the fused protein complex is more efficient at transferring electrons from NADPH.[95]

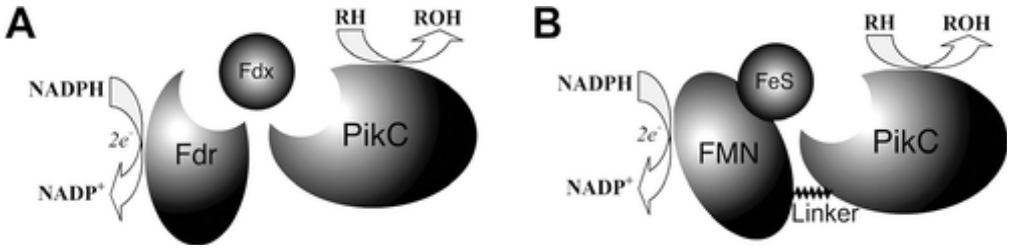

Figure 2.5 Two PikC redox partner systems. **A**. The three-component redox system. **B**. The one component RhFRED system.

Another improvement to the PikC reaction conditions is eliminating the use of stochiometric NADPH as a reducing agent as it is expensive and unstable. This can be achieved by coupling the reaction of PikC-RhFRED to glucose-6-phosphate dehydrogenase.[96] This added enzyme catalyzes the oxidation of inexpensive glucose-6-phosphate to 6-phosphoglucono-δ-lactone with concurrent reduction of the less expensive $NADP^+$ to NADPH (Figure 2.6). With this recycling system, glucose-6-phosphate serves as an alternative terminal reducing reagent for NADPH, which is generated catalytically *in situ* from $NADP^+$.

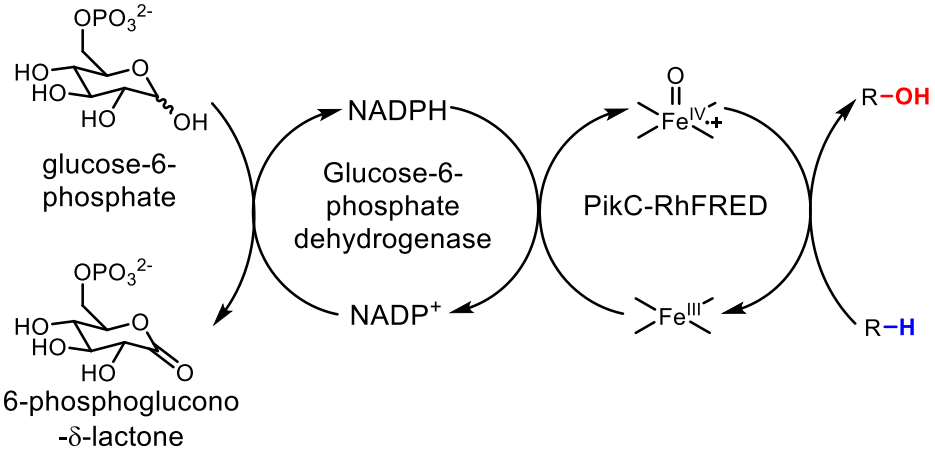

Figure 2.6: NADPH recycling system catalyzed by glucose 6-phosphate dehydrogenase (G6PDH).

2.4 The Substrate Engineering Approach to PikC Biocatalysis

The unique salt bridge anchoring of substrates to PikC allows a substrate engineering approach[97] to be employed for the use of PikC as a biocatalyst. This strategy entails functionalizing substrates with a PikC-compatible auxiliary (termed anchoring group) that contains a basic tertiary amine moiety capable of forming the necessary salt-bridge and electrostatic interactions (Figure 2.7A). This substrate can then be subjected to the PikC oxidation conditions to obtain hydroxylated product(s) (Figure 2.7B).

Subsequently, the anchoring group can be removed. The overall strategy is analogous to transition metal based directing group approaches outlined in chapter 1. However, with the PikC system functionalization occurs distal to the directing/anchoring functionality whereas most of contemporary approaches promote oxidation proximal to the directing group.

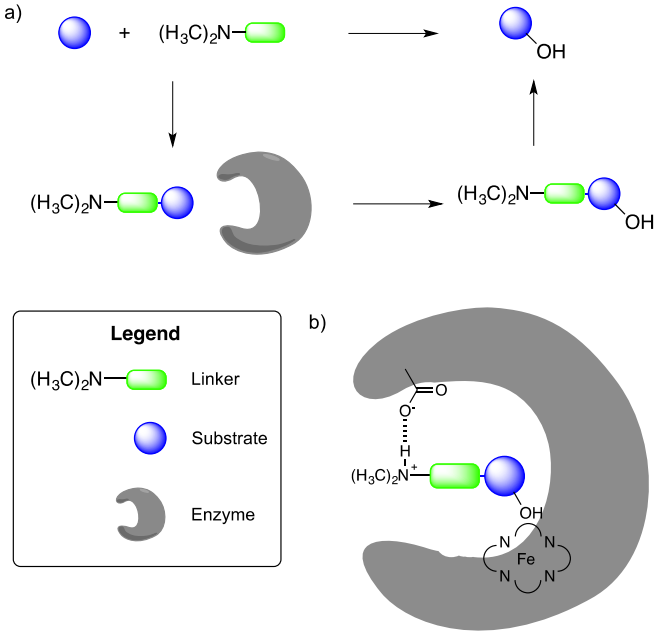

Figure 2.7: The substrate engineering approach to biocatalysis. **A**. The general method used to functionalize substrates for PikC oxidation. **B**. Representation of the enzyme/substrate interaction promoted by the removable anchoring group.

2.4.1 Desosamine as an Anchoring Group

Initial investigations into the substrate engineering approach with PikC focused on the use the endogenous aminosugar desosamine as a competent directing group for the oxidation of non-native aglycones. Instead of chemically synthesizing desosamine, the sugar was obtained via hydrolysis from erythromycin A (Scheme 2.2).[98] The harvested sugar was then protected and converted to the glycosyl fluoride.[99] The resulting desosamine fluoride (Des-F) was then used as a donor for facile desosaminylation of a

variety of aglycones. Glycosylations with Des-F were performed in good yield and were highly selective for the β-anomer. PikC compatible substrates were prepared from alcoholic aglycones ranging from 12- to 15-membered carbocycles, bicycles, steroids, and aromatics.[100]

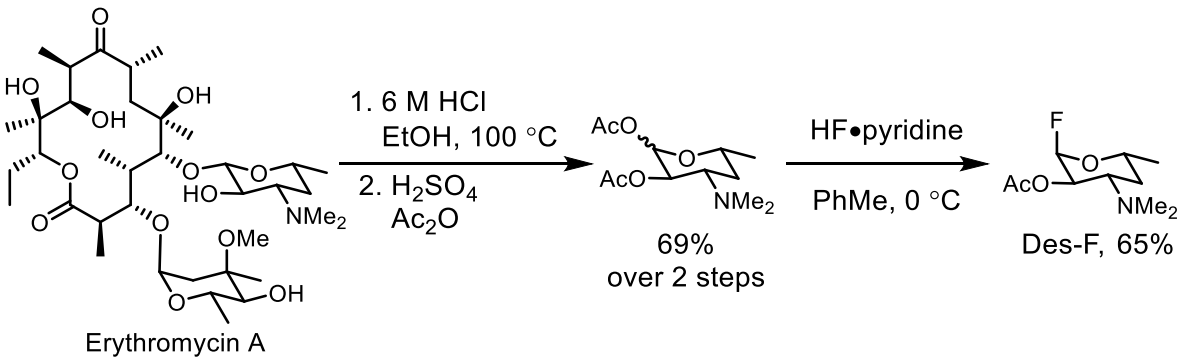

Scheme 2.2: Synthesis of desosamine fluoride (Des-F) from erythromycin A.

Glycosylated substrates were subjected to enzymatic oxidation using the single mutant PikC fusion protein $PikC_{D50N}$-RhFRED and the reactions analyzed by LCMS (Table 2.1). Larger carbocyclic substrates were shown to be effectively hydroxylated by PikC with the 13-membered substrate undergoing 65% conversion. Despite good reactivity, these substrates were converted to ≥6 oxidation products compared to only two products obtained using the endogenous substrate YC-17. The lack of selectivity was attributed to the flexibility of the 12- to 15-membered carbocycles within the active site indiscriminately positioning sp^3 C-H bonds adjacent to the heme iron. Comparison of the LCMS retention times of authentic standards of putative hydroxylated products of the 12-membered carbocyclic substrate and showed that PikC oxidation occurs at the methylenic carbons distal to the desosamine anchoring group. Co-crystal structures of the 12-membered carbocyclic substrate with PikC corroborated these results, indicating that the three distal methylenes (two of which are degenerate) are all within ~1 A of the heme iron.

These results demonstrate that PikC is an effective catalyst for remote-directed sp^3 C-H hydroxylation.

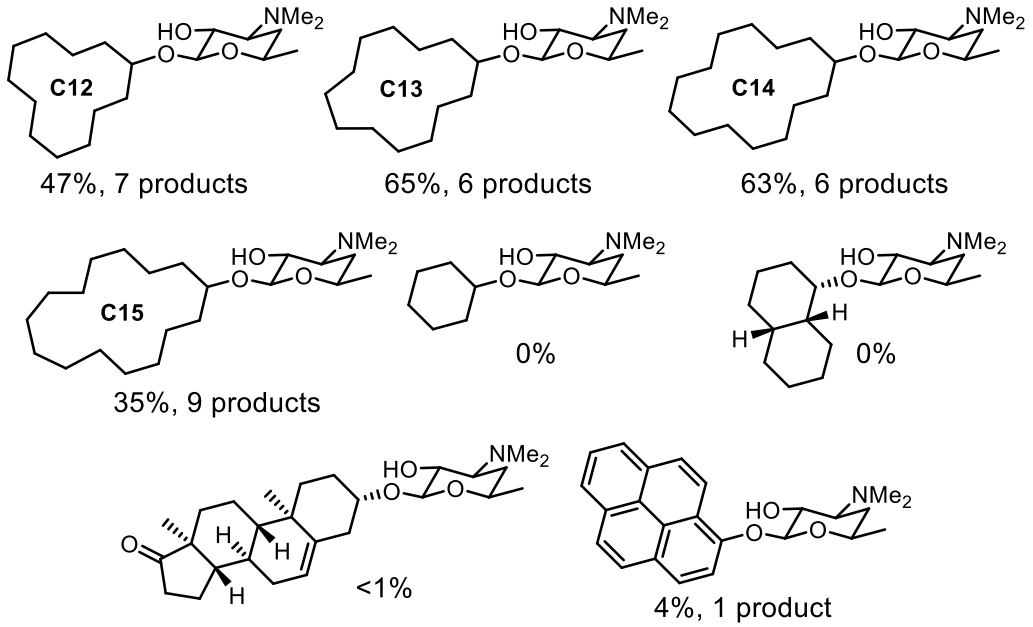

Table 2.1: Hydroxylation of desosamine anchored unnatural aglycones with $PikC_{D50N}$-RhFRED.

Smaller cyclohexanol and *trans*-decalin did not undergo PikC hydroxylation, which was attributed the inability of the substrate to reach the heme iron while bound to the catalytic buried pocket due to size limitations. Alternatively, a rigid steroid was not hydroxylated as it was presumed to be too large to fit into the active site. An aromatic substrate was oxidized in 4% to a single product. This is of interest as the reaction of PikC with sp^2 C-H bonds was previously unknown and the instability of an aryl radical generated through the radical rebound mechanism of P450 oxidation.

2.4.2 Synthetic PikC Anchors

With the demonstrated success of the substrate engineering approach using desosamine as an anchoring group, ensuing efforts focused on the development of more

synthetically useful PikC anchors. This stemmed from the non-trivial removal of desosamine following PikC oxidation. New synthetic PikC anchors were designed to be appended to substrates by an ester linkage rather than an anomeric bond. Such a connection facilitates rapid attachment to substrates from the corresponding carboxylic acid and easy removal under hydrolytic conditions. Additionally, a variety of spacing groups separating the ester linkage from the necessary tertiary amine could be sampled to identify optimal anchor structures to enhance PikC/substrate binding.[101]

Synthetic anchors were appended to the endogenous aglycone 10-dml and the resulting substrates subjected to oxidation using $PikC_{D50N}$-RhFRED accompanied by the NADPH regenerating system (Table 2.2). Linear aliphatic anchors ranging from 1 to 3 methylene spacers were effective at promoting monohydroxylation in greater than 80% conversion. Of note, marginal hydroxylation regiocontrol was observed using different synthetic anchors. Shorter aliphatic anchors with 1 or 2 methylene spacers resulted in a slight preference for oxidation at exocyclic methylene C12 while a longer 3 methylene spaced anchor favored oxidation at tertiary allylic C10.

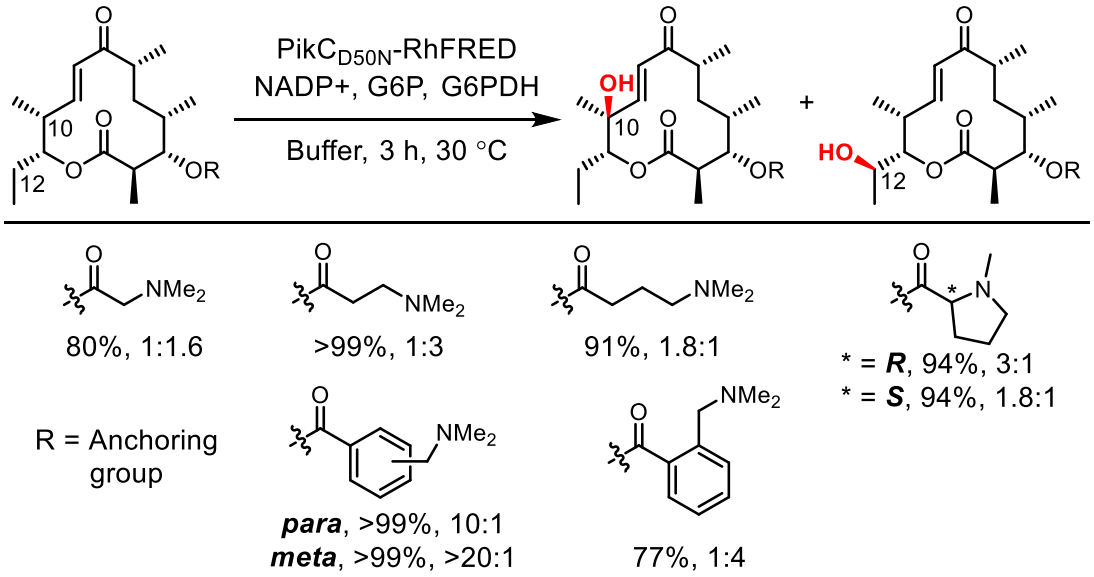

Percentages represent % conversion. Ratios refer to to C10:C12 hydroxylation sites.

Table 2.2: Hydroxylation of 10-dml using synthetic anchoring groups.

It was hypothesized that increasing the rigidity of the anchor would result in increased selectivity for a single hydroxylated product. Employing (*R*)- or (*S*)-N-methylproline resulted in >90% conversion with increased selectivity for C10 oxidation (3:1 and 1.8:1, respectively). The discrepancy in selectivity between the two proline enantiomers was attributed to a match/mismatch relationship between the chirality of the anchors and the inherently chiral environment of the enzyme active site. Use of *para*- and *meta*- benzyl amine based anchors resulted in the greatest C10:C12 selectivity with the former producing 10:1 selectivity and the latter >20:1. These results are in stark contrast to the endogenous directing group, desosamine, which only affords a 1:1 ratio of C10:C12 oxidation. Employing an *ortho*- benzyl amine anchor resulted in a reversal of hydroxylation selectivity, affording a 1:4 ratio of C10:C12. The unprecedented control of the C10:C12 oxidation site represents the first demonstration of regiocontrol determined

by the structure of the anchoring group. Leveraging this strategy on different substrates would allow regiochemical alterations without altering the P450 through mutation.

2.5 Computationally-Guided Mutagenesis and Small Molecule Oxidation with PikC

PikC has shown remarkable success for the oxidation of substrates similarly sized to that of the native aglycones 10-dml and narbonolide. However, deviation from these scaffolds results in a dramatic loss of enzymatic activity. Expansion of the accepted substrate classes is warranted to make PikC a broadly applicable biocatalyst. As previously shown, small ring systems such as cyclohexane and cis-decalin are unable to be oxidized by PikC using desosamine as an anchor. A combined synthetic, computational, and biochemical approach was used to develop a robust PikC mutant for the oxidation of small molecules using synthetic anchoring groups.

2.5.1 Development of a Highly Active PikC Triple Mutant

Menthol was selected as the initial substrate for enzymatic studies as it possesses several methyl, methylene, and methines in varying steric environments. Several groups have used the menthol core for C-H oxidation studies with transition metal-based catalysts,[40,102–104] which allows the comparison of PikC reactivity and selectivity to previously disclosed methods. A suite of (+)- or (-)-menthol substrates with appended PikC synthetic anchors were prepared (Table 2.3). Anchoring groups were selected to maximize varying length and rigidity. Aliphatic substrates **1**-**4** ranging from two to six carbons. Rigid *ortho*-, *meta*-, and *para*- benzyl amine compounds **5**-**7** were also prepared.[105]

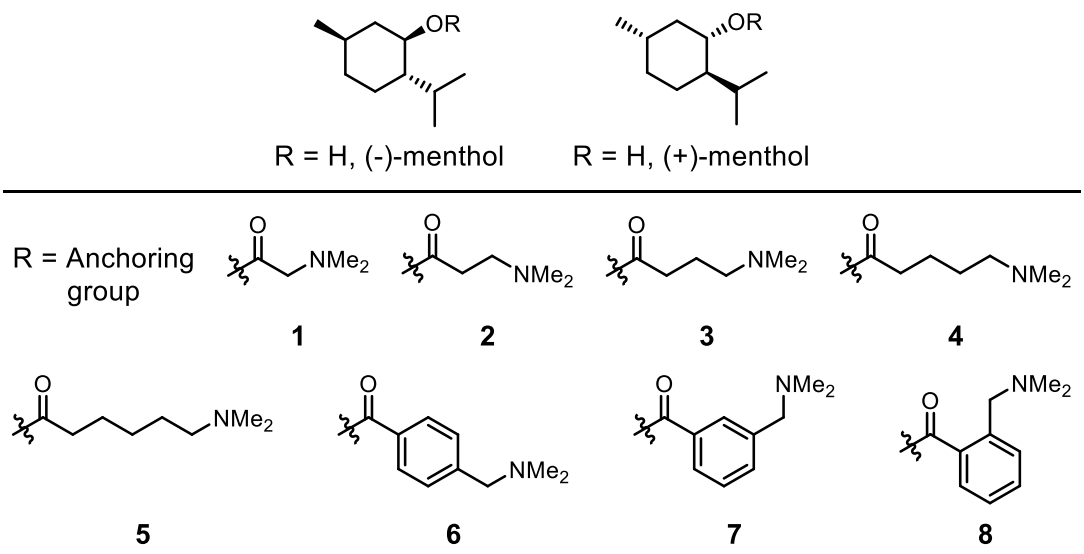

Table 2.3: Menthol derived substrates with synthetic anchors.

Molecular dynamics (MD) simulations using $PikC_{WT}$ and $PikC_{D50N}$ revealed that compound **1** possessing a short dimethyl glycine anchor is unable to form favorable electrostatic contacts with residues E85 and E94 in the catalytic buried pocket (Figure 2.8A). Instead, the substrate forms a catalytically unproductive hydrogen bond with nearby E246. Substrate interactions with this residue cause a shift in the tertiary structure of the protein to the *apo*, or "open," form. This has previously been shown to be a conformation of PikC unbound to substrate, and thus catalytically inactive (Figure 2.8B). Simulations of (-)-menthol substrates (-)-**5** and (-)-**6** possessing a longer anchor favors electrostatic interactions with E85 and E94 in the catalytically active buried pocket. A new interaction between the protonated amine and E48 located in the buried pocket is also observed and is not seen in previous crystallographic studies. Despite substrate binding in the desired buried pocket, noticeable fluctuations between the unfavorable 'open' and active 'closed' conformation are observed, which is attributed to dynamic binding between the E85/E94/E48 triad.

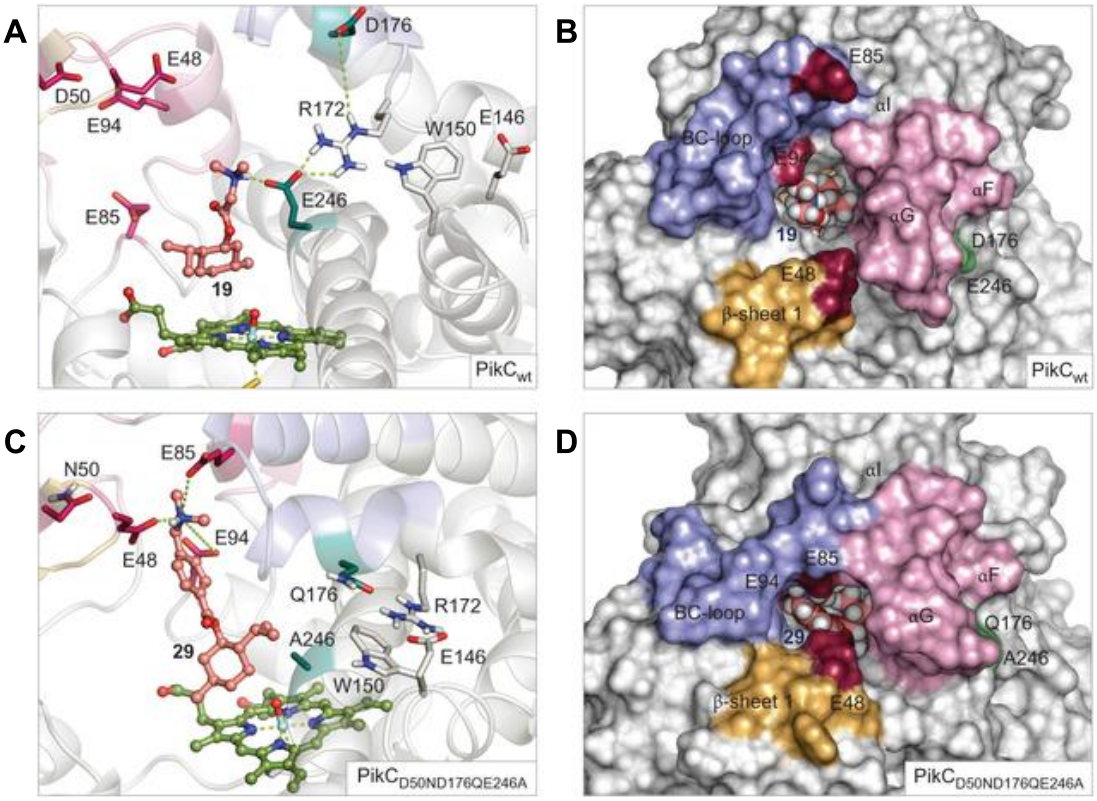

Figure 2.8: Substrate binding and tertiary structure of PikC variants observed in MD simulations. **A**. Detrimental binding of (-)-**1** to E246 in PikC$_{WT}$. **B**. Space-filling representation of (-)-**1** bound in PikC$_{WT}$ in the open conformation. **C**. Desired binding of (-)-**6** to PikC$_{D50ND176QE246A}$ showing electrostatic contacts to key residues E85/E94/E48. **D**. Space-filling representation of (-)-**6** bound PikC$_{D50ND176QE246A}$ in the desired closed conformation.

Based on these simulations, it was hypothesized that increasing the persistence of substrate binding to E85 would favor the desired 'closed' tertiary structure, thus enhancing catalytic activity. This could be accomplished by eliminating residues that lead to unproductive binding, namely E246 and D176, which were identified through MD simulations (Figure 2.8C and 2.8D). Incorporation of mutations at E246 and D176 to the already reactive D50N mutant lead to the creation of a PikC$_{D50ND176QE246A}$ that could be combined with the exogenous RhFRED domain to create catalytically a self-sufficient triple mutant fusion protein PikC$_{D50ND176QE246A}$-RhFRED. As predicted, additions of the E246A and D176Q mutations as well as use of longer anchors as in substrate (-)-**6** favor

binding to the buried pocket as well as a 'closed' catalytically active tertiary structure. Use of this computationally derived triple mutant resulted in dramatically increased total turnover numbers (TTN) for (-)-menthol substrates **1**-**8** when compared to reactions employing PikC$_{WT}$-RhFRED or PikC$_{D50N}$-RhFRED.

Computational studies using (+)-menthol derivatives **1**-**8** with PikC$_{WT}$ and PikC$_{D50N}$ resulted in unilaterally unfavorable binding due to unfavorable interactions between substrate and enzyme chirality. This is corroborated by experimental data showing low TTNs with this series of substrates. Changing biocatalysts to the triple mutant improves TTNs, however the change is not as significant as observed with the (-)-menthol series of substrates.

2.5.2 Site-Selectivity and Scope of Enzymatic Small Molecule Oxidations

Upon development of a more active PikC mutant, efforts were focused on determining the site- and stereoselectivity of enzymatic oxidation products. Density functional theory (DFT) and quantum mechanics (QM) calculations of the hydrogen atom abstraction transition states between a truncated (-)-menthol substrate and iron oxo compound I indicated favorable reactivity at the C4 position. MD simulations of (-)-**5** in the PikC active site revealed that the C4 equatorial hydrogen is located closer to the iron oxo and is bound closer to the calculated transition state geometry throughout the lifetime of the simulation when compared to its geminal axial counterpart. Scaled up reactions of both (-)-**5** and (-)-**6**, followed by product isolation and subsequent removal of the anchoring group by $LiAlH_4$ reduction matched the computationally predicted selectivity to afford diol **9** (Scheme 2.3). This outcome contrasts with other small molecule oxidation methods that preferentially oxidize the more electron-rich tertiary carbons of menthol.

The orthogonal selectivity obtained through PikC demonstrates the use of this system to achieve new reactivity rather than a complement to other small molecule approaches.

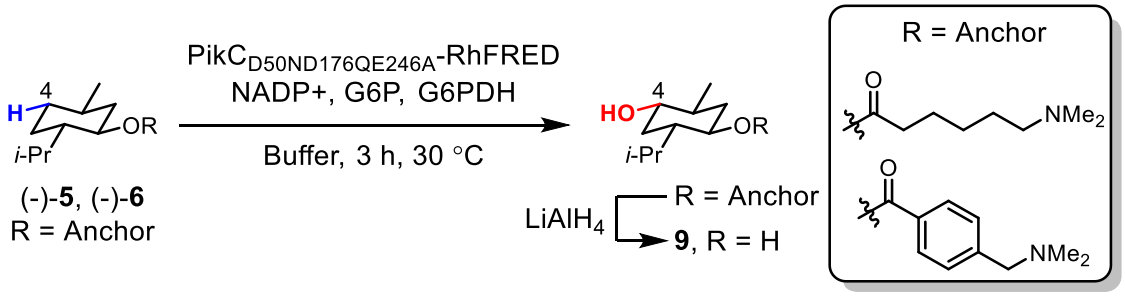

Scheme 2.3: PikC$_{D50ND176QE246A}$-RhFRED hydroxylation of (-)-**5** and (-)-**6**.

As a control, desosamine bound (-)-menthol **10** was subjected to oxidation by the PikC triple mutant. No conversion to hydroxylated product was observed indicating that desosamine is unsuitable for bridging the gap between the catalytically active buried pocket and the iron oxo (Table 2.4). This result further validates use of synthetic anchors over the endogenous directing group for unnatural substrate oxidation.

Experimental examination of (+)-menthol based substrates **1-8** align with computationally predicted reactivity in that reactions result in low conversion and at least five isomeric products. The broad utility of the PikC triple mutant was demonstrated across a series of stereodefined small molecules (Table 2.4). Terpene substrates derived from (+)-α-terpineol and (-)-isopulegol are hydroxylated at the allylic methyl and C4 methylene to give **11** and **12**. Enantioenriched tetrahydronaphthol and indanol based substrates are oxidized at the most electronically activated benzylic position to give **13** and **14**. Finally, bridged bicyclic (+)-fenchol based substrate is oxidized at a distal methylene to afford **15**. In each instance of methylene oxidation, the hydroxylation stereochemistry is *anti-* to that of the site of anchor attachment, resulting in predictable selectivity for this small molecule oxidation approach.

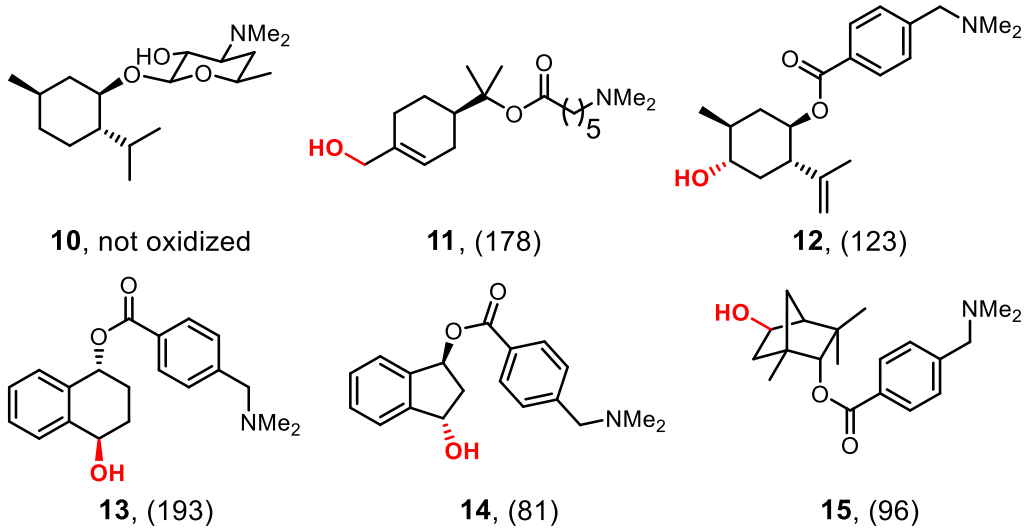

Table 2.4 Scope of site-selective oxidation with PikC$_{D50ND176QE246A}$-RhFRED. Sites of hydroxylation are indicated in red. Values in parentheses are total turnover numbers (TTN)

2.6 Conclusions and Outlook

From its discovery in the genome of *Streptomyces venezuelae* to the generation of a self-sufficient triple mutant fusion protein, significant strides have been made in the development of PikC as a general and robust biocatalyst for late-stage C-H oxidation. However, despite the numerous successes with large and small molecule oxidation, the ability to control hydroxylation regiochemistry based on the anchoring group has only been demonstrated on the native aglycone 10-dml with the less active PikC$_{D50N}$-RhFRED fusion protein.

Advances in anchoring group technology, while significantly improved over the use of desosamine, require further refinement before further exploration of regiochemical alterations can be made. The ensuing chapter will focus on the development of a new, modular class of PikC compatible anchors and their implementation to control oxidation regiochemistry using unnatural substrates and the triple mutant fusion protein described in this chapter.

2.7 Acknowledgements

For the work conducted in *chapter 2.5*,[105] Michael M. Gilbert, Alison R. H. Narayan, Solymar Negretti, and Wangxiang Zhao synthesized substrates and characterized products. Alison R. H. Narayan conducted the biochemical experiments. Gonzalo Jimenez-Oses, Peng Liu, Ragunath O. Ramabhadran, Yun-Fang Yang, and Lawrence R. Furan performed the computational experiments.

Chapter 3: Synthesis of Diverse 11- and 12-Membered Macrolactones From a Common Linear Substrate Using a Single Biocatalyst

3.1 Introduction

The late-stage functionalization of sp^3 C-H bonds is a powerful strategy for the incorporation of oxidative functionality to increase molecular diversity. Chemists have access to numerous methods based on transition metals, biocatalysts, and reactive organic reagents to target specific bonds for oxidation, as outlined in chapter 1. For a given method, selectivity for a specific hydrogen is governed by different factors and altering the site of oxidation often requires employing a different catalyst or reagent. The development of a method that allowed tunable site selectivity using a single catalyst would drastically reduce the need to screen different oxidation conditions.

While the late-stage functionalization approach allows for the rapid generation of oxidized analogs, a disadvantage is that preparation of a late-stage intermediate often requires a significant linear synthesis that ultimately leads to derivatives with a similar core structure. To change make significant structural changes to the scaffold, the synthesis of the common intermediate needs to be redesigned. This problem can be solved by the incorporation of a regiodivergent process that allows the cyclization of a single substrate to form two or more different scaffolds. Coupling a regiodivergent synthesis with late-

stage C-H oxidation would streamline the synthesis of a variety of compounds varying in core structure and oxidation patterns (Figure 3.1).

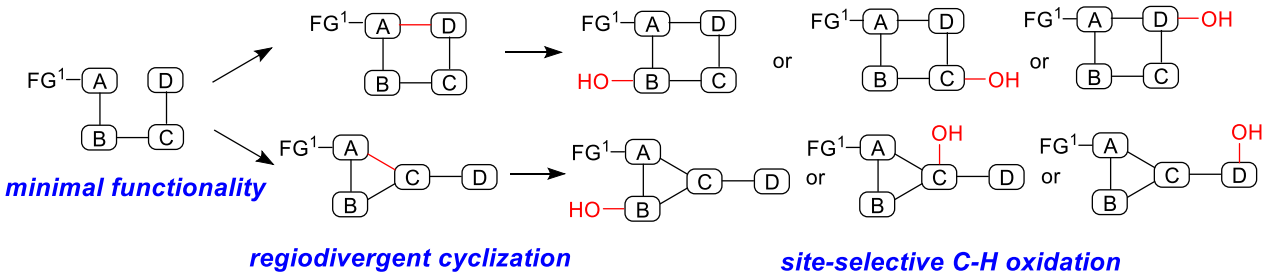

Figure 3.1: General approach for combining a regiodivergent cyclization followed by site-selective C-H oxidation into a diversity-oriented synthesis.

This chapter focuses on the regiodivergent synthesis of macrocyclic substrates from a common intermediate via nickel-catalyzed reductive coupling. Diverse scaffolds prepared by this method are then hydroxylated using PikC$_{D50ND176QE246A}$-RhFRED. The site of oxidation can be tuned to specific C-H bonds by employing a new class of triazole-based PikC anchors and does not require any modifications to the biocatalyst.

3.2 A Brief Overview of Regiocontrol in Inter- and Intramolecular Nickel-Catalyzed Reductive Couplings of Aldehydes and Alkynes

The nickel-catalyzed reductive coupling of aldehydes and alkynes is a powerful tool for the construction of C-C bonds. The allylic alcohol motif obtained from these reactions is commonly seen across many natural products and can be used for further synthetic manipulations.[106] The Montgomery[107] group and others[108,109] have longstanding interests in the discovery, development, understanding, and application of this technology for the synthesis of complex molecules. Recently, the discoveries of N-heterocyclic carbene (NHC) ligands as effective promotors and silanes as competent reducing agents have allowed remarkable advances in regiocontrol of the coupling of

aldehydes with unsymmetrical alkynes. The combination of a small NHC ligand, such as IMes or *i*-Pr-BAC with a small silane favors C-C bond formation with the less hindered alkyne terminus (Scheme 3.1A). Use of large ligands such as SIPr or **21** results in coupling of the more hindered alkyne terminus (scheme 3.1B).[110] Mechanistic studies[111] have shown that these reactions proceed through a rate-determining metallocyclization with the regiochemistry determined by the interaction between alkyne and ligand sterics.[112] A post rate-limiting sequential sigma bond metathesis with the silane and reductive elimination regenerates the Ni(0) catalyst.

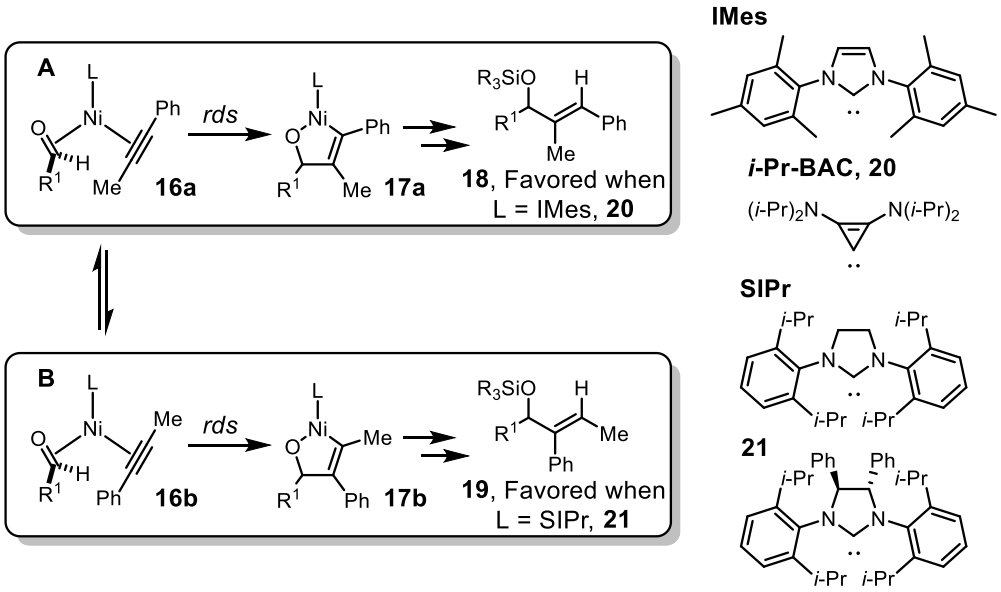

Scheme 3.1: Reductive coupling regiochemistry determined by ligand sterics. **A**. Small ligand protocol. **B**. Large ligand protocol.

Alternatively, coupling of the hindered alkyne terminus can be achieved employing *both* a large NHC ligand (SIPr) and large silane (i.e. (*t*-Bu)$_2$MeSiH).[113] Greater regioselectivities can be achieved using this protocol, which employs a commercially available ligand, thus conferring a significant preparative advantage (Scheme 3.2). Kinetic studies of the large ligand large silane protocol show that formation of major and

minor regioisomers **18** and **19** form under different mechanistic pathways. Unlike previously studied reactions, the cyclization of **16a** to **17a** is reversible and the rate-determining step is the sigma bond metathesis between **17a** and silane. Employing a bulky silane greatly increases the barrier for this step and favors the irreversible cyclization to form **17b**, which can undergo a post rate limiting sigma bond metathesis with the bulky silane due to greater steric accessibility of the nickel center.

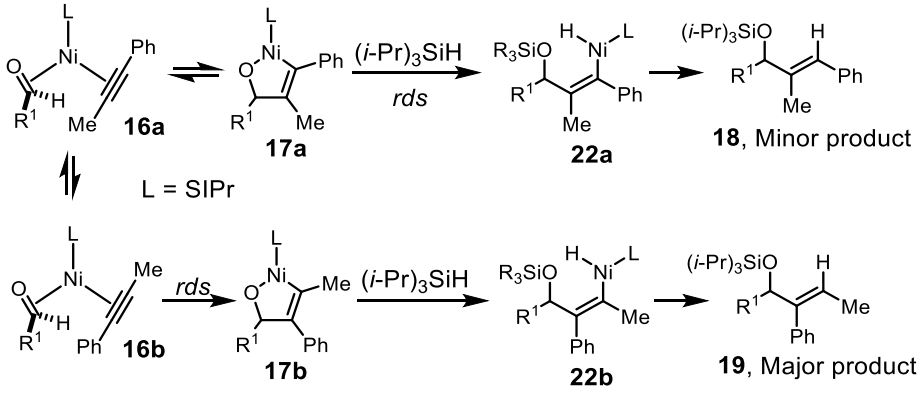

Scheme 3.2: Reductive coupling regiochemical control using the large ligand and large silane protocol.

Advances in the regiocontrol of intermolecular aldehyde/alkyne reductive couplings using different NHC/silane combinations were applied to intramolecular reactions to afford macrocyclic products. The ability to control ring size through the synthesis of exo- or endo-macrocycles using this approach was first demonstrated in the chemical synthesis of 10-dml.[114] A key disconnection in this approach is the use of a nickel catalyzed reductive coupling of **23** using the small NHC ligand IMes and small silane Et_3SiH to afford silyl-protected allylic alcohol **25** in 58% as an inconsequential 4:1 mixture of diastereomers as deprotection and oxidation afforded the desired natural product aglycone (Scheme 3.3). If the ligand used in the macrocyclization of **23** is changed to bulky DP-IPr, 11-membered exo-macrocycle **24** is obtained in 59% as a single

diastereomer. Subsequent investigations afforded a general and highly regioselective exo-macrocyclization protocol using the bulky, electron deficient NHC IPr^{Cl} and *i*-Pr_3SiH.[115] Exo-cyclizations using this approach are proposed to operate under a similar mechanistic pathway outlined in scheme 3.2, with cyclization to form the endo-metallacycle proceed through a reversible metallocyclization followed by an unfavorable rate-determining sigma bond metathesis with the bulky silane reducing agent leading to favorable formation of the exo-product.

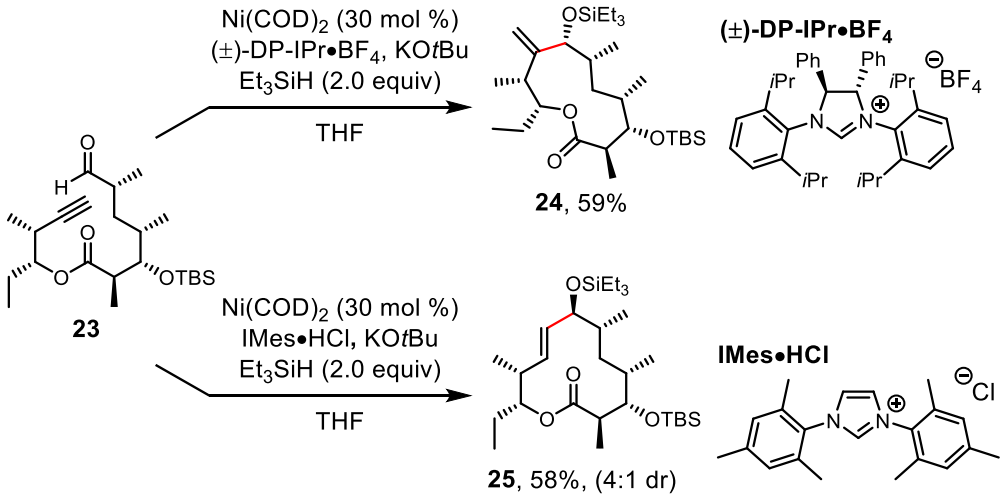

Scheme 3.3: Regiodivergent nickel-catalyzed macrocyclization applied in the synthesis of 10-dml and unnatural regioisomer **24**.

3.3 Substrate Design and the Regiodivergent Synthesis of 11- and 12-Membered Macrolactone Substrates

Several factors need to be considered in the design of macrocyclic substrates to accomplish a synthesis that incorporates a regiodivergent cyclization as well as controllable site-selective C-H oxidation. Arguably the most significant hurdle is the development of substrate scaffolds that are capable of undergoing differential oxidation by PikC based solely on synthetic anchoring group structure; a transformation that has

not been accomplished on an unnatural substrate. Surveying substrates subjected to PikC oxidation revealed that unfunctionalized carbocyclic substrates afforded numerous oxidation products indicating that multiple oxidation products could be achieved, but with little possibility of site control (Figure 3.2).[100] At the other end of the spectrum, the native aglycone 10-dml as a substrate results in exquisite regiocontrol for two sites of oxidation,[101] but structures derived from this scaffold would be too complex for a streamlined synthetic approach. It was hypothesized that substrates of intermediate complexity would be suitable for this study as incorporated functionality would mitigate indiscriminate PikC reactivity and substrates would be synthetically accessible.

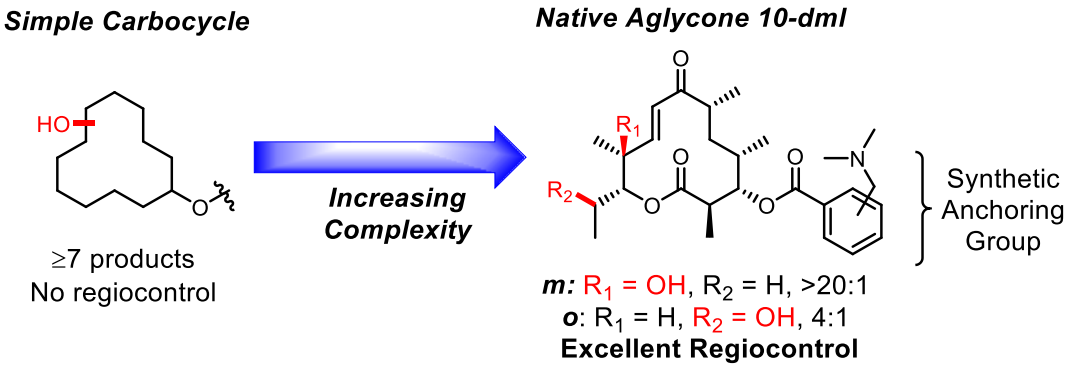

Figure 3.2: Spectrum of macrocyclic substrates subjected to PikC oxidation.

Another major consideration is the nature of the regiodivergent reaction to be employed. The nickel-catalyzed reductive coupling reaction of aldehydes and alkynes has been demonstrated to be suitably robust for the regiodivergent cyclization of late-stage intermediates in preparatively useful yields, which makes it an optimal choice for this application. Prepared substrates would also need to be enantioenriched to avoid complicated diastereo- and regioisomeric mixtures that would arise from the matched/mismatched reaction of chiral PikC with a racemic substrate. While significant strides have been made in the development of intermolecular enantioselective reductive

coupling reactions using enantioenriched NHC ligands,[116,117] an analogous asymmetric intramolecular variant for the synthesis of macrocycles has yet to be developed. Fortuitously, Ni(0) macrocyclizations have been demonstrated to be highly diastereoselective. Employing an enantioenriched ynal would therefore lead to a single enantiomer of an allylic alcohol.[115]

3.3.1 The Synthesis of Enantioenriched Ynal Starting Material

Ynal **33** was selected as a common linear intermediate for regiodivergent cyclization and site-selective oxidation studies. Previous studies had shown that the exo-macrocyclization proceeds with both high diastereo- and regioselectivity. Therefore, a synthesis was developed to produce **33** on multigram scales in high enantiomeric excess (Scheme 3.4). Enantioenriched alcohol serves as the starting material and is commercially available from the chiral pool. TBDPS protection of the alcohol and controlled DIBAL-H reduction of the resulting silyl ether affords aldehyde intermediate **27**. Horner-Wadsworth-Emmons olefination using *in-situ* deprotonated phosphonocrotonate ester affords **28** as an inconsequential mixture of E/Z diastereomers. The mixture of dienes is carried on to a Pd/C hydrogenation to give silyl ether **29** in 77% yield over four steps. Basic hydrolysis of **29** affords the corresponding carboxylic acid, which was carried on directly to the Steglich esterification with but-3-yn-1-ol to give alkyne **31** in 91% over two steps. Subsequent TBAF deprotection unmasks primary alcohol **32**, which can then be oxidized to desired aldehyde **33**. Owing to the instability of aliphatic aldehydes, alcohol oxidation was performed immediately prior to macrocyclization to avoid decomposition or epimerization of the chiral alpha-carbon. The Dess-Martin periodinane (DMP) oxidant

was selected for this reaction as it proceeds to full conversion in ~1 h and is sufficiently mild.

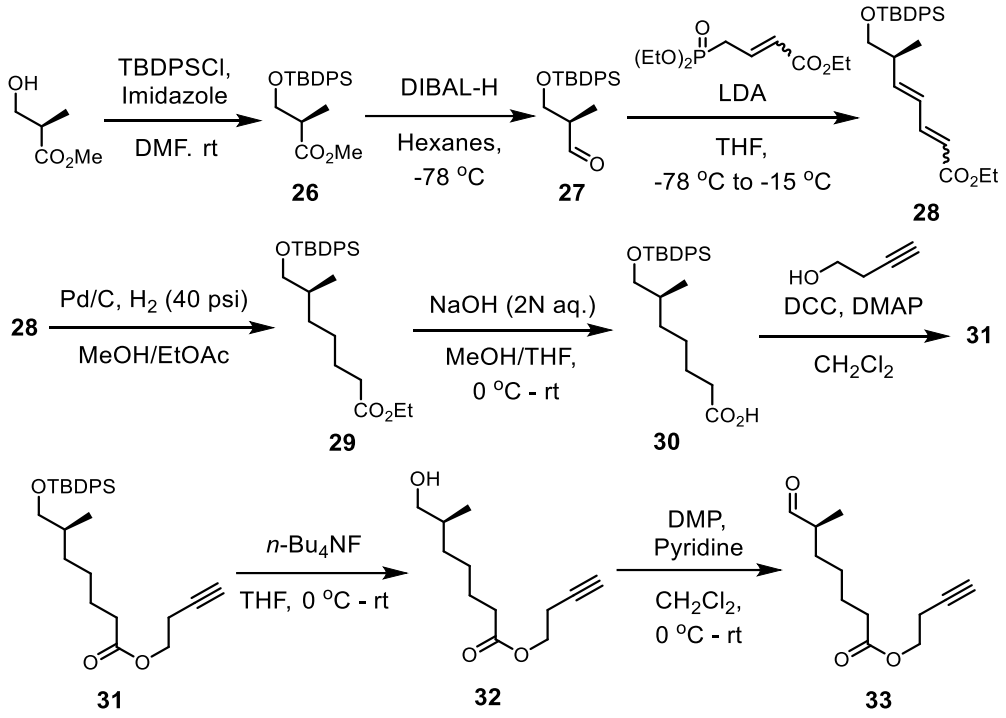

Scheme 3.4: Synthesis of enantioenriched ynal **33**.

3.3.2 Regiodivergent Macrocyclizations

With ynal **33** in hand, efforts were focused on implementation of Ni(0) cyclization. Subjection of **33** to published exo-cyclization conditions using IPr^{Cl}•HCl and KO*t*-Bu resulted in good yield of desired product **34** in >95:5 dr and rr. Upon TBAF deprotection and acylation to form the corresponding Mosher ester, it was apparent that the er of the product had eroded from >99% to 84:16 (Table 3.1, entry 1). It was reasoned that epimerization of the alpha methyl group during the reaction was responsible for the loss of enantiopurity. Using the free carbene of IPr^{Cl} instead of an *in-situ* deprotonation to eliminate the needed for the potentially culpable KO-*t*-Bu base resulted in nearly identical yield and er (Table 3.1, entry 2). Lowering the reaction temperature from 90 °C to 60 °C

resulted in an improvement in yield to 61% and an er of 95:5 (Table 3.1, entry 3). Further reduction of the temperature led to both diminished yields and er (Table 3.1, entries 4-6). Due to the ease of preparation and reaction assembly, the free carbene of IPr^{Cl} was continued to be used instead of the HCl salt even though KO-*t*-Bu was shown not to be detrimental to the reaction.

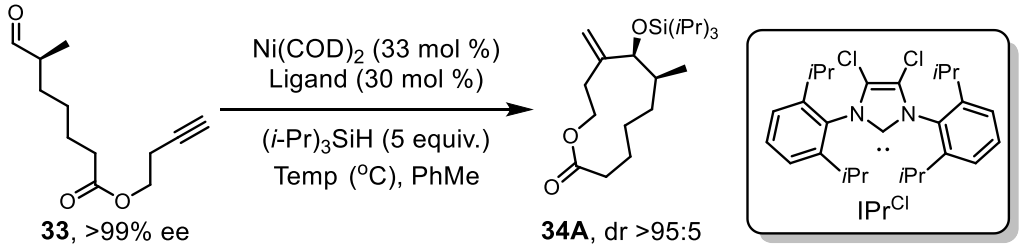

Entry	Ligand	Additive	Temp (°C)	Yield (%)	er[a]
1	IPr^{Cl}•HCl	KO-tBu	90	50	81:19
2	IPr^{Cl}	-	90	41	80:20
3	IPr^{Cl}	-	60	61	95:5
4	IPr^{Cl}	-	50	56	93:7
5	IPr^{Cl}	-	40	45	86:14
6	IPr^{Cl}	-	r.t.	23	74:26

[a]er determined by deprotection to give **34b** and conversion to the Mosher ester.

Table 3.1: Optimization of the nickel-catalyzed exo-macrocyclization of **33**.

Previously published reaction conditions for the endo-macrocyclization using IMes and Et_3SiH afforded the desired macrolactone in good yields, >95:5 rr, and 97:3 dr. Gratifyingly, no loss in enantiopurity was observed upon deprotection of the silyl ether and conversion to the corresponding Mosher ester. In both exo- and endo-cyclizations, the stereochemistry of the resulting allylic alcohol is *syn* to the vicinal methyl group as determined by both NOE. The *syn* stereochemical assignment is corroborated in both cases by the assignment of the absolute stereochemistry using Mosher ester analysis.

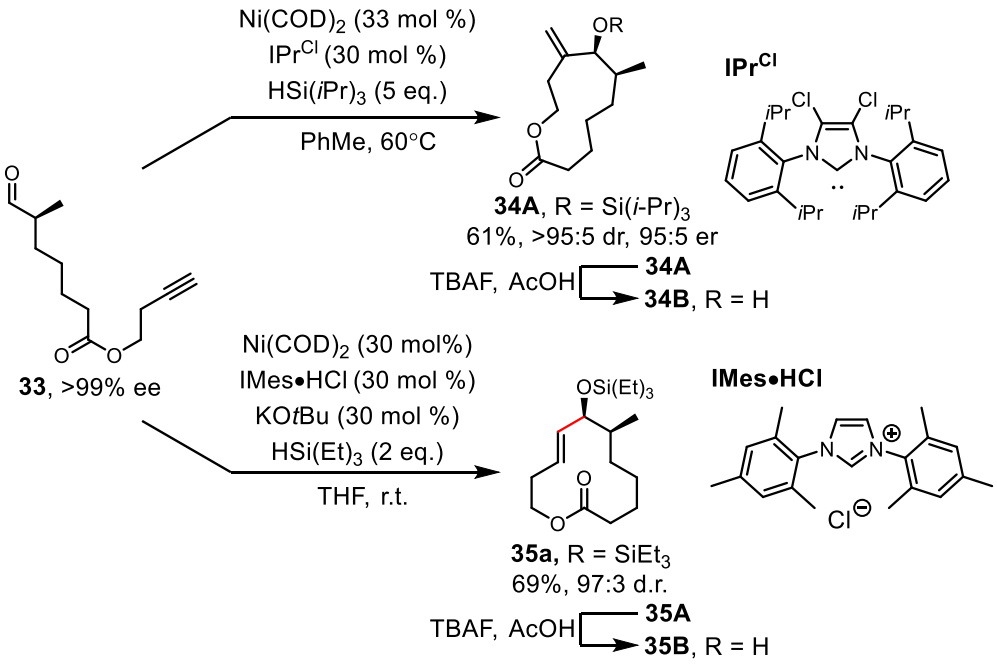

Scheme 3.5: Regiodivergent nickel-catalyzed macrocyclization of **33**.

The high diastereoselectivity of both cyclizations is rationalized by the ability of **33** to adopt a favorable conformation, where the aliphatic alkyne substituent is perpendicular to the aldehyde carbonyl (Scheme 3.6). In this conformation, the Ni(0) NHC catalyst can coordinate to the aldehyde and alkyne to give putative intermediates **36a** and **36b**. The orientation of the alkyne substituent in **36a**/**36b** is determined by the identity of the NHC ligand, with the large ligand large silane combination favoring the formation of **37a** and small ligand/ small silane favoring **37b**.[115] Post-oxidative cyclization steps afford **34A** and **35A** with the observed stereochemical outcome.

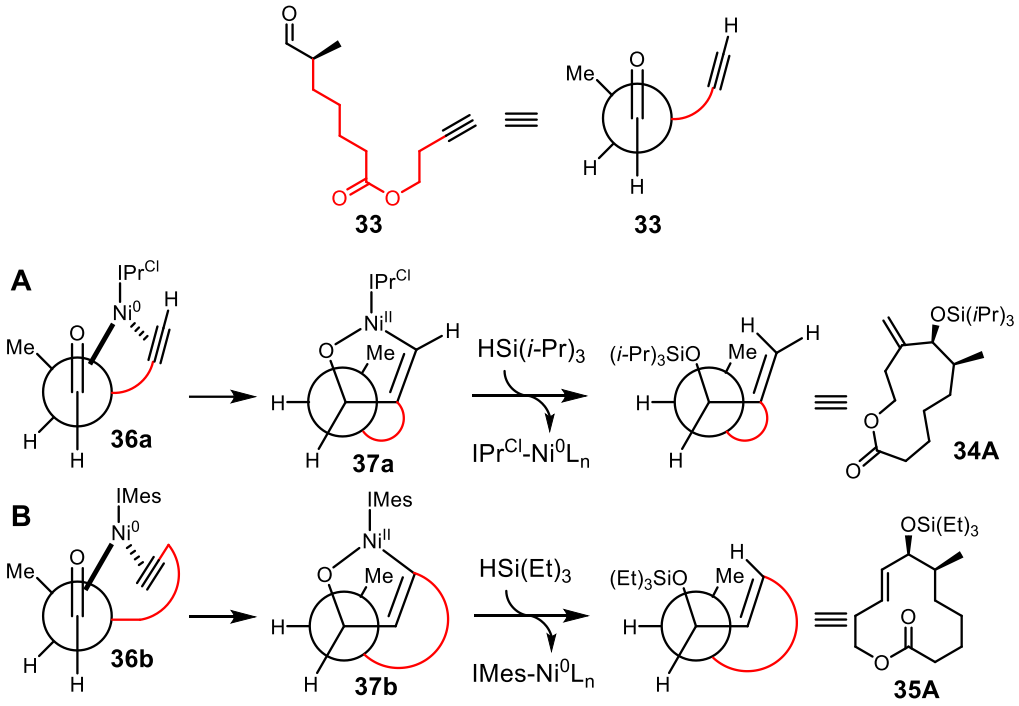

Scheme 3.6: Rationale behind the observed macrocyclization diastereoselectivities. **A**. Exo-cyclization to give **34A**. **B**. Endo-cyclization to give **35A**.

3.4 Triazole-Based Anchors

Previous studies have shown the utility of benzyl amine-based anchors as a synthetically useful alternative to the endogenous desosamine for PikC reactions. However, a new versatile anchoring strategy is needed discover the unknown structural requirements for PikC oxidation where the identity of the anchor determines the site of hydroxylation using a non-native substrate. The envisaged approach necessitates modular assembly to maximize structural diversity, the ability for high-throughput synthesis, and facile removal of the anchor following PikC oxidation. A strategy combining these factors was developed based on a 1,2,3-triazole assembled through a metal-catalyzed azide/alkyne cyclization (scheme 3.7). Anchors are appended to a substrate through a two-step sequence first undergoing an esterification with an azido-acid and then a metal catalyzed cyclization with an acetylenic amine (scheme 3.7A).

An important feature of this anchoring strategy is the access of a variety of modular components. Azido acid building blocks are easily accessed from amino acids through a stereoretentive diazo transfer reaction. As such, the wealth of natural and unnatural amino acids can serve as potential scaffolds for anchor assembly. Also, numerous acetylenic amines are commercially available. Changing the metal catalyst used in the azide/alkyne cyclization can also alter the regiochemistry of the anchor scaffold allowing another method to control anchor structure. Employing a copper catalyst gives the 1,4-triazole[118,119], while using a ruthenium catalyst affords the 1,5- regioisomer (Scheme 3.7B).[120] Sharpless and Fokin have shown that both metal reactions are highly regioselective for their respective isomer and can tolerate a myriad of functional groups, affording high yields under mild conditions. Using this modular approach, it was hypothesized that the identity of spacer elements S1 and S2 as well as the triazole regioisomer would dictate which substrate C-H bond is positioned proximal to the Fe heme upon binding to PikC (Scheme 3.7C). Since this anchoring strategy is broadly applicable, it was reasoned that regiodivergent oxidation could be rapidly optimized for different macrocycles **34A**, and **35A**.

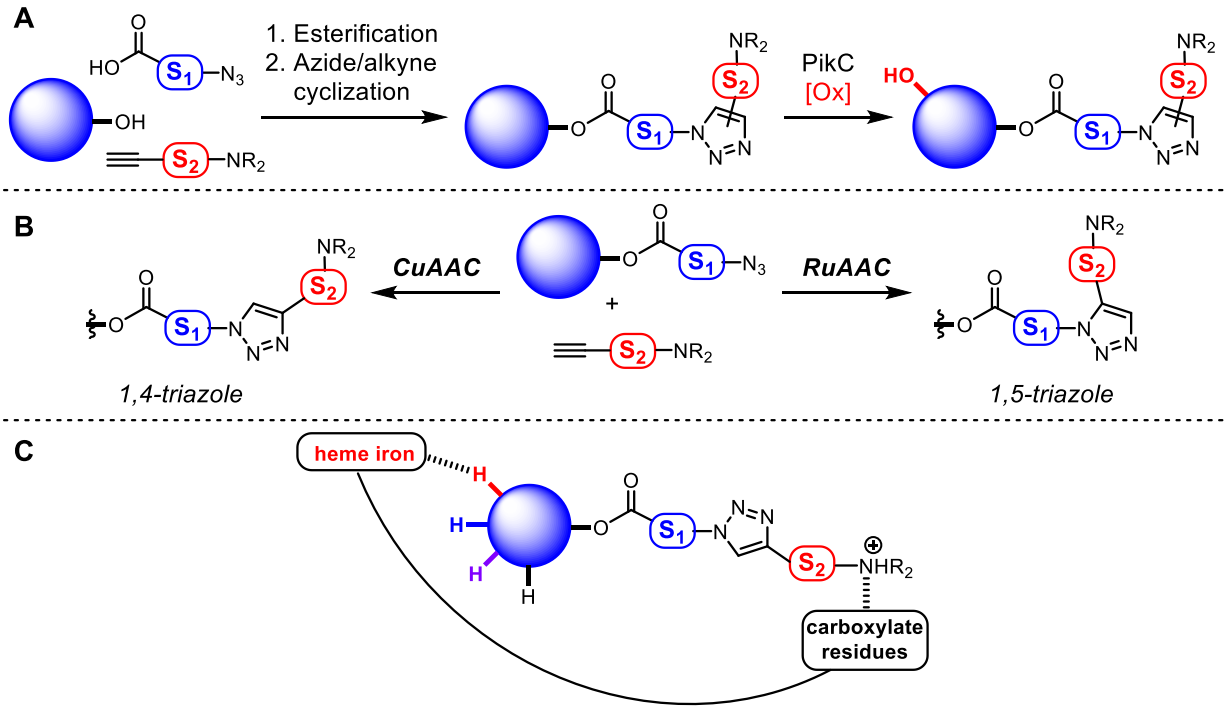

Scheme 3.7: General approach towards the synthesis of triazole-based anchors. **A.** Two-step assembly. **B.** Regiodivergent azide/alkyne cyclization. **C.** Representation of triazole substrates bound to PikC where S1 and S2 elements determine which hydrogen are proximal to the heme iron.

3.5 PikC Catalyzed Macrolactone Oxidation

3.5.1 Oxidation of an 11-Membered Macrolactone

The triazole based anchoring strategy outlined in section 3.4 was applied to the 11-membered exo-macrocycle **34A** synthesized using nickel catalysis as the key cyclization step. Macrocycle **34A** was deprotected using TBAF buffered with AcOH to remove the silyl protecting group and prevent transesterification with the resulting hydroxide. With the free alcohol in hand, a suite of triazole-based anchors were appended to give **38a-n**, which were then subjected to PikC oxidation using the self-sufficient triple mutant fusion protein $PikC_{D50ND176QE246A}$-RhFRED on an analytical scale.

Upon quenching, the crude reactions were analyzed by reverse phase LCMS to determine conversions and the number of hydroxylation isomers.

From the analytical reactions, it was observed that 1,5-triazole anchors based on glycine or alanine (**a**-**d**) resulted in low conversion to hydroxylated products with anchor **d** achieving the highest selectivity among this series in a 4:1 ratio in favor of a single oxidation product (Table 3.2 entries 1-4). The use of the analogous 1,4- regioisomers **e**-**h** conferred higher selectivity and better conversion (Table 3.2 entries 5-8). Anchor, **h** displayed the highest selectivity for a single product in a 96:4 ratio. Interestingly, the *S* enantiomer **g** resulted in a mixture of five oxidation products, indicating that the selective incorporation of chirality in the anchor can serve as a means of effectively controlling product distribution. Longer, more rigid biaryl triazole anchors **i**-**l** were also surveyed (Table 3.2 entries 9-12). Anchors **j**-**l** all resulted in >30% conversion with at least a ~3:1 selectivity for a major product. Switching from *para*- anchor **j** to *ortho*- anchor **l** resulted in a change in the order of elution of the major product from the LCMS, indicating a potential change in hydroxylation regiochemistry. Control substrate **38m** containing an isopropyl group instead of a dimethylamine was not oxidized by PikC, showing the necessity of the key electrostatic interaction between the protonated substrate and the enzyme (Table 3.2 entry 13). Switching the dimethylamine for a basic imidazole as in **38n** did not result in oxidation, indicating that a tertiary amine is the optimal basic functionality for this transformation (Table 3.2 entry 14).

To determine the site- and stereochemistry of hydroxylation, PikC reactions of interest were scaled, the products isolated by preparative HPLC and characterized by 2D NMR spectroscopy. Alternatively, the product identification was accomplished through

the chemical synthesis of authentic standards. These compounds were used to identify PikC reaction products by the comparison of their LCMS retention times in single injection and co-injection experiments as well as through ^{1}H NMR analysis. The synthesis and application of these authentic standards for product characterization will be discussed in the following section.

Rigid biaryl anchors **j** and **k** afforded allylic oxidation product **39j** and **39k**, respectively, as the major product. With both anchors, the allylic product is obtained as a single diastereomer *syn* to the adjacent ester and methyl functionalities (Table 3.3). Switching to a shorter alanine anchor **h** resulted in a shift of oxidation site to give alpha hydroxyl **40h**. A third site of oxidation is obtained using the *ortho*- biaryl anchor **l** giving **41l**, where oxidation occurs β- to the macrolactone. β-macrolactone oxidation selectivity is of interest as oxidation at this position does not benefit from stabilization of a radical intermediate from the presence of neighboring pi systems and oxidation at this position occurs in the presence of more reactive C-H bonds. Characterized minor oxidation products are shown to be regioisomeric mixtures of **39**, **40** or **41**, with other diastereomers not observed. Additionally, epoxidation of the exocyclic olefin or formation of the corresponding N-oxides was not observed displaying the high functional group tolerance of this enzymatic approach. These results represent the first example of anchor-controlled selective oxidation of an unnatural substrate using PikC. The ability of PikC to control the site of oxidation based on substrate/anchor conformation and geometry within the active site, thus overriding steric or electronic factors, shows the complementarity of this approach in relation to other C-H oxidation methods.

Entry	Anchor	Conversion[a]	Ratio[b,c]
1	a	12	23:77
2	b	27	18:82
3	c	18	31:69
4	d	25	15:80:2:3
5	e	19	21:76:3
6	f	29	14:76:10
7	g	32	16:72:2:4:6
8	h	39	6:94
9	i	28	8:42:46:4
10	j	62	3:14:82:1
11	k	55	1:22:73:4
12	l	31	71:24:4:1
13	m	0	-
14	n	0	-

[a]Values are percent conversion to (M+H+16) as determined by LCMS. [b]Ratios for (M+H+16) in order of elution from the LCMS.

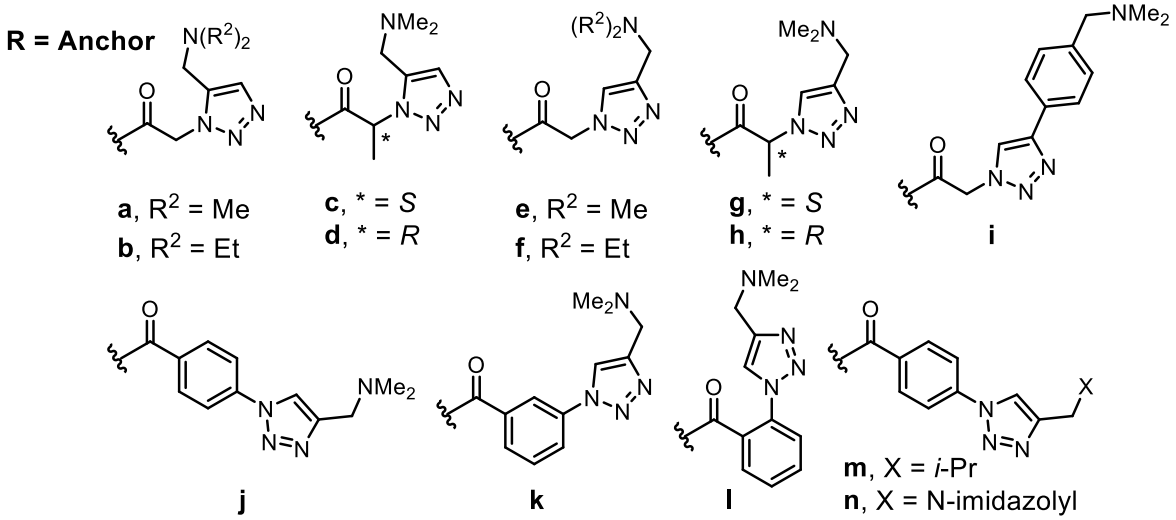

Table 3.2: PikC oxidation of exo-macrocycle substrates functionalized with triazole anchors.

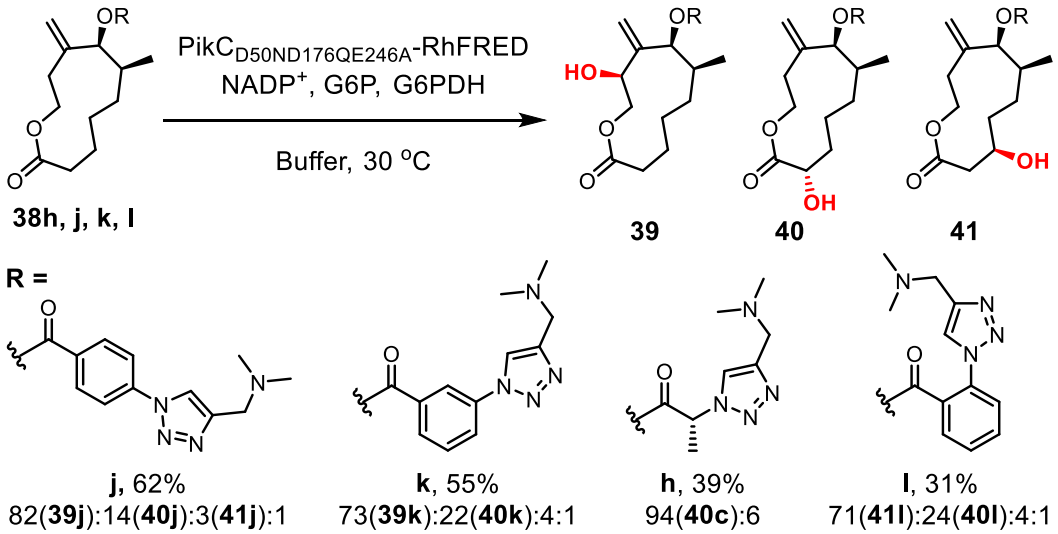

Table 3.3: Anchor-controlled site-selective hydroxylation of macrolactone **38**.

Subjecting acetylated macrolactone **34c** to contemporary aliphatic C-H oxidation approaches, such as White's non-heme Fe catalyst,[40,41] resulted in epoxidation as the sole product (Scheme 3.8). While unsuccessful at hydroxylation, the exploration of PikC oxidation of more highly oxidized substrates is of interest. Chemical oxidation of **34B** to spirocyclic epoxide **43** is achieved quantitatively and as a single diastereomer upon switching oxidants to mCPBA. Subsequent attachment of para-biaryl anchor **j** and subjection to PikC oxidation gives alpha hydroxyl **44** in 41% and a 95:5 ratio. The shift in the oxidation site of **44j** compared to **39j** is likely due to the loss of allylic stabilization of the radical intermediate upon conversion to the epoxide.

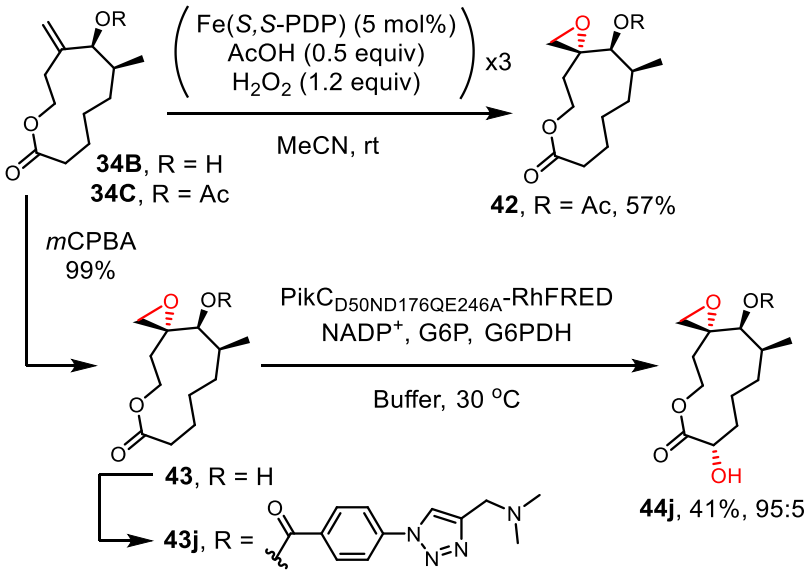

Scheme 3.8: Combined chemical and enzymatic oxidation.

3.5.2 Synthesis of 11-Membered Macrolactone Authentic Standards

Several PikC oxidation products were characterized by the comparison to putative authentic standards as mentioned earlier. Upon discovery of the three major sites of oxidation **39**-**41** though scaled reactions and product isolation, syntheses were devised to prepare authentic allylic and alpha- oxidation products for further compound elucidation (Scheme 3.9). The synthesis of alpha hydroxyl standards was first accomplished by deprotonation of macrocycle **34** using KHMDS, then treatment of the in situ formed enolate with Davis' oxaziridine to furnish **45** as a single diastereomer. Absolute stereochemical assignment of this product was determined using Mosher ester analysis. Deprotection of monoprotected diol **45** using TBAF afforded **46**, which was used for the assignment of **40h** by ^{1}H comparison. A two-step protecting group manipulation sequence afforded alpha- monoprotected THP diol **47** in 88% over two steps. Esterification of the free alcohol with *ortho*-, *meta*-, or *para*- azidobenzoic acid and subsequent removal of the THP group gave **48a-c** in good yields. Finally, copper-

catalyzed azide/alkyne cyclization gave chemically prepared standards **40j**, **40k**, and **40l**. Comparison of the LCMS retention times of these standards to PikC reactions conclusively showed that these three compounds are products of their respective enzymatic reactions.

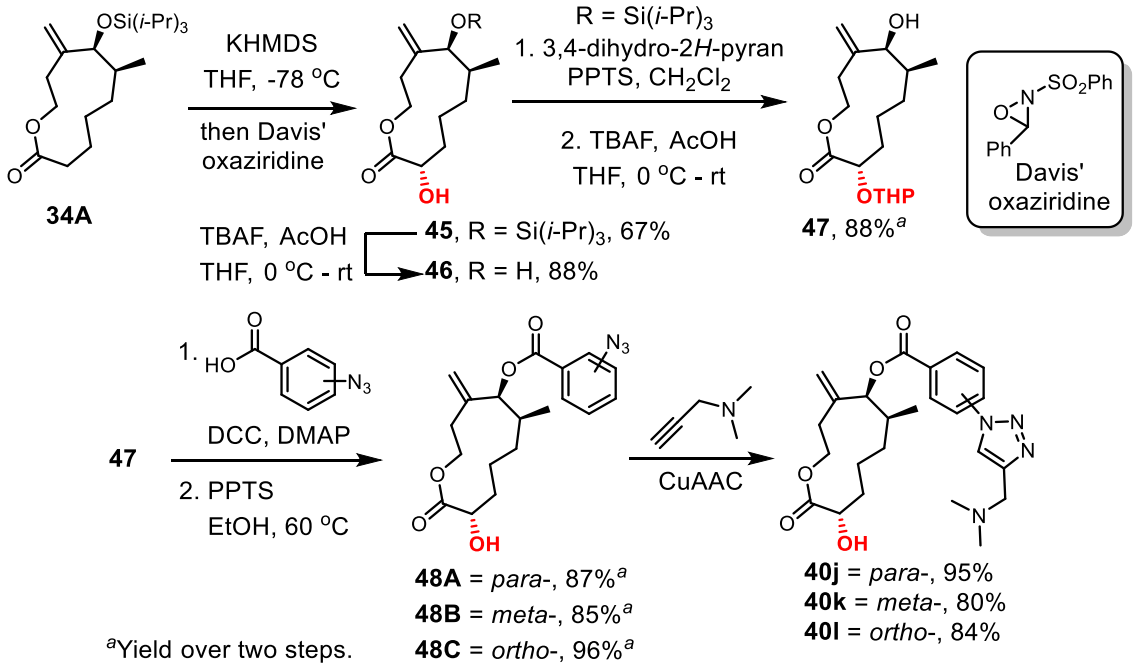

Scheme 3.9: Synthesis of α-hydroxylated authentic standards

Allylic oxidation standard **39k** was prepared using **49**, an intermediate prepared en route to **38k** (Scheme 3.10A). Subjection of this compound to oxidation conditions using SeO_2 and pyridine N-oxide resulted in the formation of **50** as a single diastereomer in 48% yield. The remaining mass balance was converted to the corresponding unsaturated ketone. The copper-catalyzed cyclization of **50** gave chemically prepared **39k**, the stereochemistry of which was determined by NOE and matched the LCMS retention time of its PikC counterpart. The site of oxidation of **44j** was determined by 2D NMR methods, but direct stereochemical assignment of this isolated product remained elusive. An authentic standard was prepared by first epoxidizing intermediate **48a** using mCPBA to

give **51** as a 94:6 mixture of diastereomers (Scheme 3.10B). The stereochemistry of the intermediate was not determined as copper azide/alkyne cyclization gave **44j**, the ^{1}H specrtrum of which matched its enzymatically prepared counterpart allowing both the assignment of the epoxide and the alpha hydroxyl.

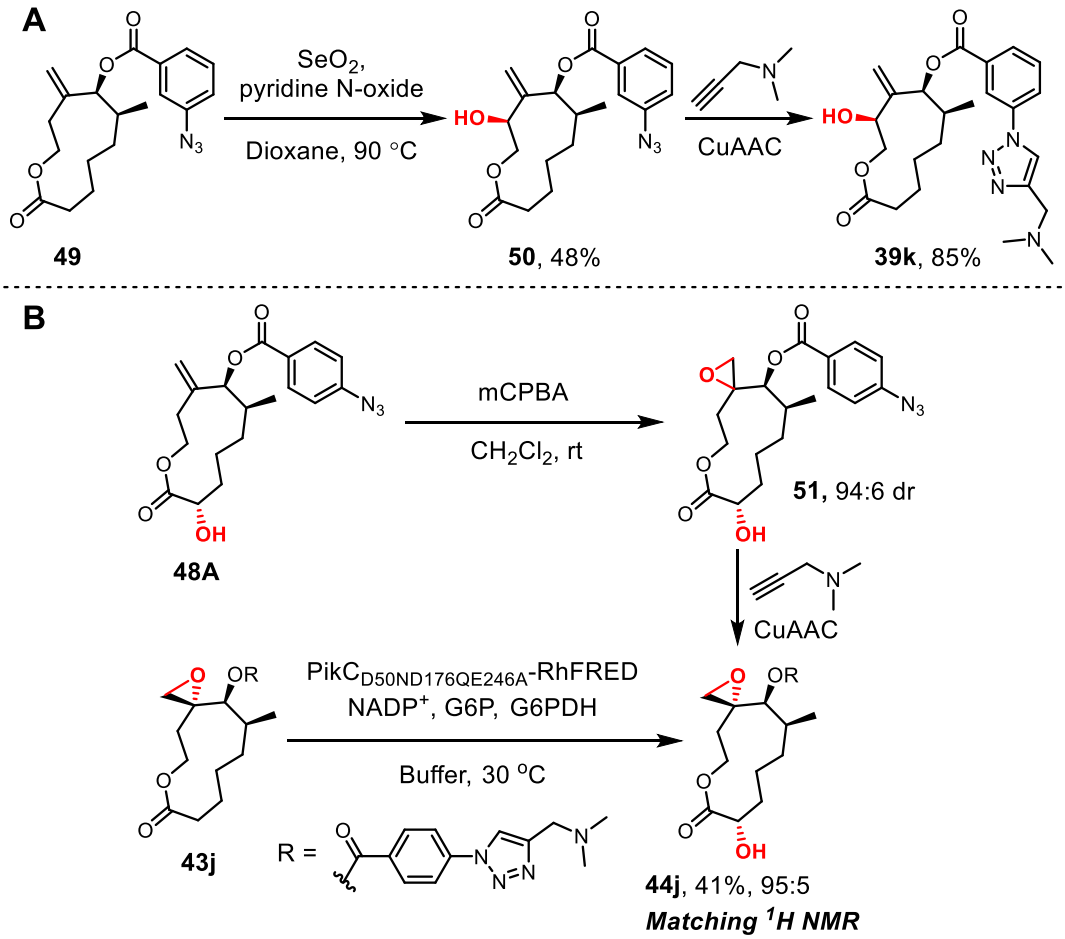

Scheme 3.10: Synthesis of additional oxidation standards. **A**. Synthesis of allylic standard **39k**. **B**. Synthesis of epoxide standard **44j**.

3.5.3 Enzymatic Oxidation of the Enantiomeric 11-Membered Macrocycle

Studies conducted with PikC and the menthol series of substrates showed that substrate chirality has a dramatic impact on conversion as well as product distribution. To probe whether chirality of **38** has an effect on enzymatic reactivity, the (*R*,*R*)

enantiomer of the 11-membered macrolactone, **52**, was prepared. This macrocycle was prepared following the same steps in the preparation of **33** to give (*R*)-**33**, upon which Ni(0) cyclization afforded the corresponding macrocycle with identical yield, dr, rr, and er. Subsequently, **52** was functionalized with anchors **j**, **k**, **h**, and **l** and subjected to PikC oxidation conditions. Products from the enzymatic reactions were characterized by comparison to authentic standards through LCMS retention times and ^{1}H NMRs. Unlike **38j** and **38k**, the major product of **52** with anchors **j** and **k** is α-hydroxylation rather than allylic oxidation (Table 3.4). Furthermore, anchor **h** is selective for β-oxidation product **54** rather than α-oxidation as seen with **38**. Despite the drastic differences in site-selectivity observed with the previous three anchors, **l** results in the same β-oxidation site and relative stereochemistry with both **38** and **52**. The discrepancies between oxidation profiles of the two macrocycle enantiomers indicate that anchor optimization is necessary between substrates, supporting the use of this modular, high-throughput approach.

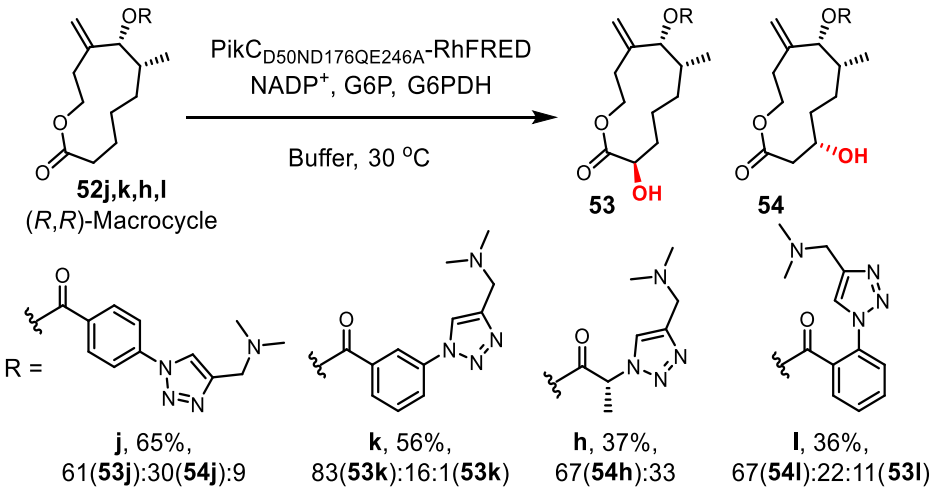

Table 3.4: PikC oxidation of (*R*,*R*) macrocycle **52**.

3.5.4 12-Membered Endo-Macrolactone PikC Oxidation

Upon Ni(0) cyclization using the small NHC ligand IMes and small silane Et_3SiH, the resulting 12-membered macrolactone **35** was deprotected and functionalized with several PikC triazole anchors to give **55j,l,o** (Table 3.5). Para-biaryl triazole anchor **j** afforded allylic oxidation product 56j in a ~2:1 ratio. The same site of oxidation was obtained using alanine anchor **o**, albeit with significantly greater selectivity. The use of a diethylamine in **o** instead of the dimethylamine used in **h** was found to decrease the amount of demethylation byproduct. As with the 11-membered macrolactone series, anchor **o** directed oxidation β- to the macrolactone ester with the minor oxidation product affording allylic oxidation. These results show that the ability to control hydroxylation regiochemistry is not limited to a single substrate and has the potential to be broadly applicable.

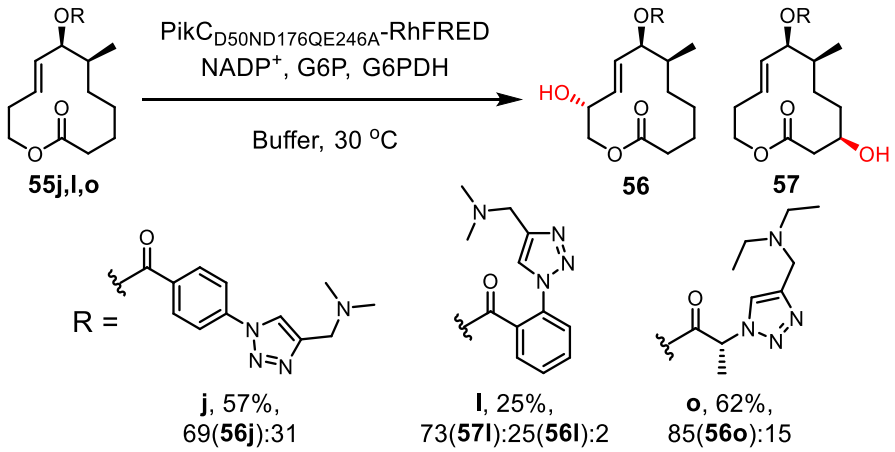

Table 3.5: PikC oxidation of the 12-membered endo-macrolactone **55**.

3.6 Anchoring Group Removal

A critical component of directing group design is facile removal following C-H functionalization. The choice of an ester linkage in previous and current anchoring groups was to allow removal under basic conditions. Employing macrolactone substrates presents the added complication of chemoselectivity. To probe if this can be accomplished, unoxidized **38h** was subjected to transesterification using K_2CO_3 in MeOH and macrolactone **34B** was cleanly recovered in 81%. However, subjecting PikC hydroxylated product **40h** to the same conditions resulted in macrolactone transesterification to give a linear triol product (Scheme 3.11). It was hypothesized that the addition of the α-hydroxyl group could increase the electrophilicity of the macrolactone carbonyl by engaging in intramolecular hydrogen bonding. Protection of **40h** as the TBS-ether followed by hydrolysis was able successfully remove the anchor to give monoprotected diol **58**.

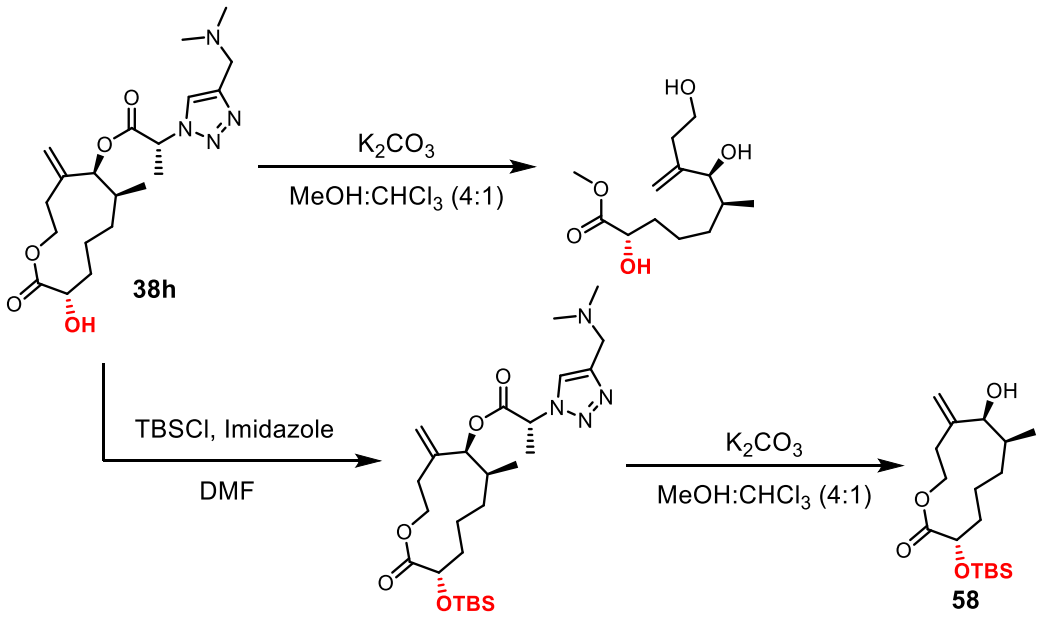

Scheme 3.11: Two-step removal of PikC anchors.

Removal of the biaryl triazole anchors from **38j**, **38k**, and **38l** proved to be significantly more challenging as the same conditions used on **38h** exclusively resulted in macrolactone scission. Screening commonly employed hydrolysis and transesterification conditions were unable to provide the desired reactivity (Table 3.6 entry 1). To overcome this pitfall, it was hypothesized that the incorporation of electron withdrawing groups *ortho*- to the triazole would increase the electrophilicity of the aryl ester allowing for selective removal. Fluorine was selected as the desired substituent as to maintain a similar steric profile to anchor **j** to give fluorinated anchor **p**. Subjection of **38p** to methanolysis resulted in a 68% yield of **34B** (Table 3.6 entry 2). Further optimization showed that anchor **p** can be removed in 90% using a mixture of THF/H_2O and LiOH (Table 3.6 entry 3). To prove that modified anchor **p** affords a similar reaction to profile to its non-fluorinated analog, the reaction of **38p** was scaled and the major product was confirmed as **39p**, the same oxidation selectivity afforded by **38j** (Table 3.7). Upon TBS- protection, anchor **p** was successfully cleaved from **39p** in 69% over two steps.

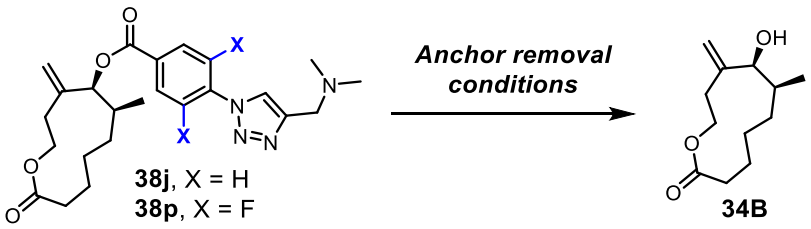

Entry	X	Conditions	Yield (%)[a]
1	H	K_2CO_3, MeOH	0
2	F	K_2CO_3, MeOH	68
3	F	LiOH, THF/H_2O	90

[a]Isolated yields.

Table 3.6: Removal of the fluorinated aryl anchor.

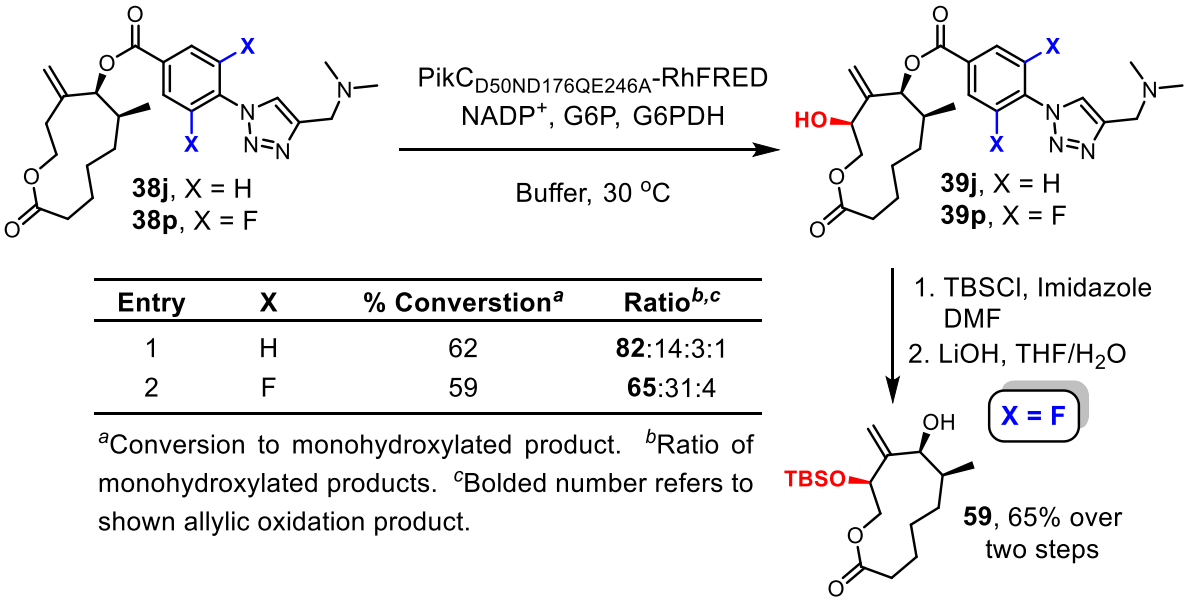

Entry	X	% Converstion[a]	Ratio[b,c]
1	H	62	**82**:14:3:1
2	F	59	**65**:31:4

[a]Conversion to monohydroxylated product. [b]Ratio of monohydroxylated products. [c]Bolded number refers to shown allylic oxidation product.

Table 3.7: PikC oxidation of fluorinated substrate **38p**.

3.7 Computationally Rationalized PikC Selectivity

PikC directed biocatalytic oxidations do not rely on C-H bond strength, acidity, steric accessibility, inductive influences, or proximity to the directing functionality. Instead selectivity is dictated by interactions between the active site residues matched with the structure, stereochemistry, and conformation of the substrate and triazole anchors. The compounded weak interactions that lead to differential selectivity make rationalization difficult. Therefore, a combined density functional theory (DFT) and molecular dynamics (MD) approach was used to simulate structural interactions within the PikC active site to elucidate the factors controlling hydroxylation regioselectivity. This combined approach was applied to rationalize the selective formation of **39j**, **40c**, and **41l** derived from **38j,c,l** (Table 3.3).

3.7.1 DFT Calculations of Low Energy Conformers and Transition States

DFT calculations were first used to determine the lowest energy conformers of a truncated methyl ester derivative of **38**. From these calculations, two low energy conformers were identified that differ by 0.9 kcal/mol (Figure 3.3A). The next highest energy conformer was >2 kcal/mol higher in energy than conformer 1, making it unlikely to be accessible. The spatial orientations of hydrogens within conformers 1 and 2 are largely identical, the only major difference between the two being the configuration of the macrolactone carbonyl relative to the exocyclic olefin (conformer 1: syn, conformer 2: anti). Following ground state optimization, the DFT barriers to hydrogen atom abstraction were computed for C3 and C10 for both conformers. The barriers for abstraction shown in purple and green were the lowest for each site and corresponded to the observed products **39** and **40** (Figure 3.3A).

Next, the optimal transition state geometries of the four possible monohydroxylation products at C3 and C10 in conformer 1 were computed using an isolated heme iron-oxo compound 1. Inspection of the transition state structures reveals that pseudo-equatorial hydrogen (purple) at C3 benefits from developing conjugation with the neighboring exocyclic olefin (Figure 3.3B). In contrast, the germinal C3 hydrogen is perpendicular to the olefin in the transition state and does not benefit from the resulting allylic radical stabilization (Figure 3.3C). A similar conjugation effect is seen for the oxidation at C10 with the green hydrogen benefitting from overlap with the adjacent carbonyl (Figure 3.3D). For the C10 blue hydrogen to overlap with the carbonyl, the macrolactone ring must distort, which results in a higher energy conformation, and is thus thermodynamically unfavorable (Figure 3.3E).

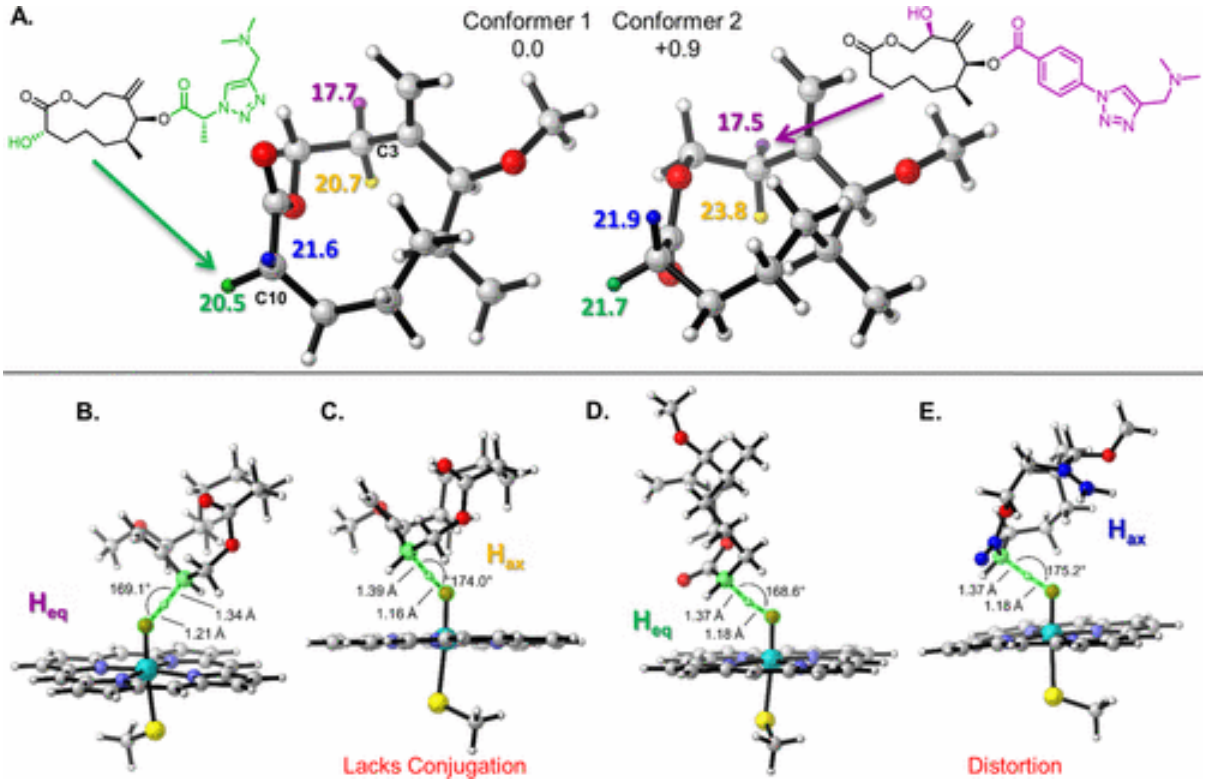

Figure 3.3: DFT computed low energy conformers and optimized transition states **A**. Lowest energy conformers of a model of structure **38**, with DFT barriers (kcal/mol) to C-H abstraction at C3 and C10. **B**. Transition structure of C3 (purple) hydrogen abstraction. **C**. Transition structure of C3 (yellow) hydrogen abstraction. **D**. Transition structure of C10 (green) hydrogen abstraction. **E**. Transition structure of C10 (blue) hydrogen abstraction.

3.7.2 Molecular Dynamics Simulations

Molecular dynamics (MD) simulations were performed using $PikC_{D50ND176QE246A}$ and conformer 1 with anchors **j** and **h** appended. The simulations were conducted for 500 ns, during which interconversion between conformer 1 and 2 was observed. The critical salt bridge interaction between residues E85 and E94 was also observed with both substrates **38j** and **38h**. Although the anchors result in similar binding, their length, flexibility, and stereochemistry results in different oxidation selectivity. Determining how these factors lead to different products is the goal of the MD simulations.

Figures 3.4A and 3.4B show that anchor **h** positions C3 closest to the iron oxo with an average distance of 3.3 A during the lifetime of the simulation. Conversely, **j** positions

C10 closest with an average distance of 4.1 A. During the lifetime of the simulation, the purple pseudo-equatorial hydrogen of **38j** is closer on average to the iron oxo than the germinal yellow hydrogen (Figure 3.4C). Analysis of the plot of the $H_{substrate}$-O_{iron} distances versus the C-H-O angles over the lifetime of the simulation using **38j** shows that the purple hydrogen is closest to the computed DFT transition state (shown in red) (Figure 3.4D). Collectively, the calculations show that the purple hydrogen is intrinsically more reactive as shown by the DFT barriers to abstraction as well as being positioned closest to the iron oxo using anchor **j**. Figures 3.3E and 3.3F show that the blue hydrogen of C10 is closest to the iron oxo as well as the optimized transition state geometry throughout the lifetime of the simulation. However, the barrier to abstraction of the blue hydrogen is 1.1 kcal/mol greater than that of the green hydrogen. Even though **h** can position C10 closest to the iron oxo, the intrinsic reactivity of the green hydrogen overrides the proximity of the blue hydrogen.

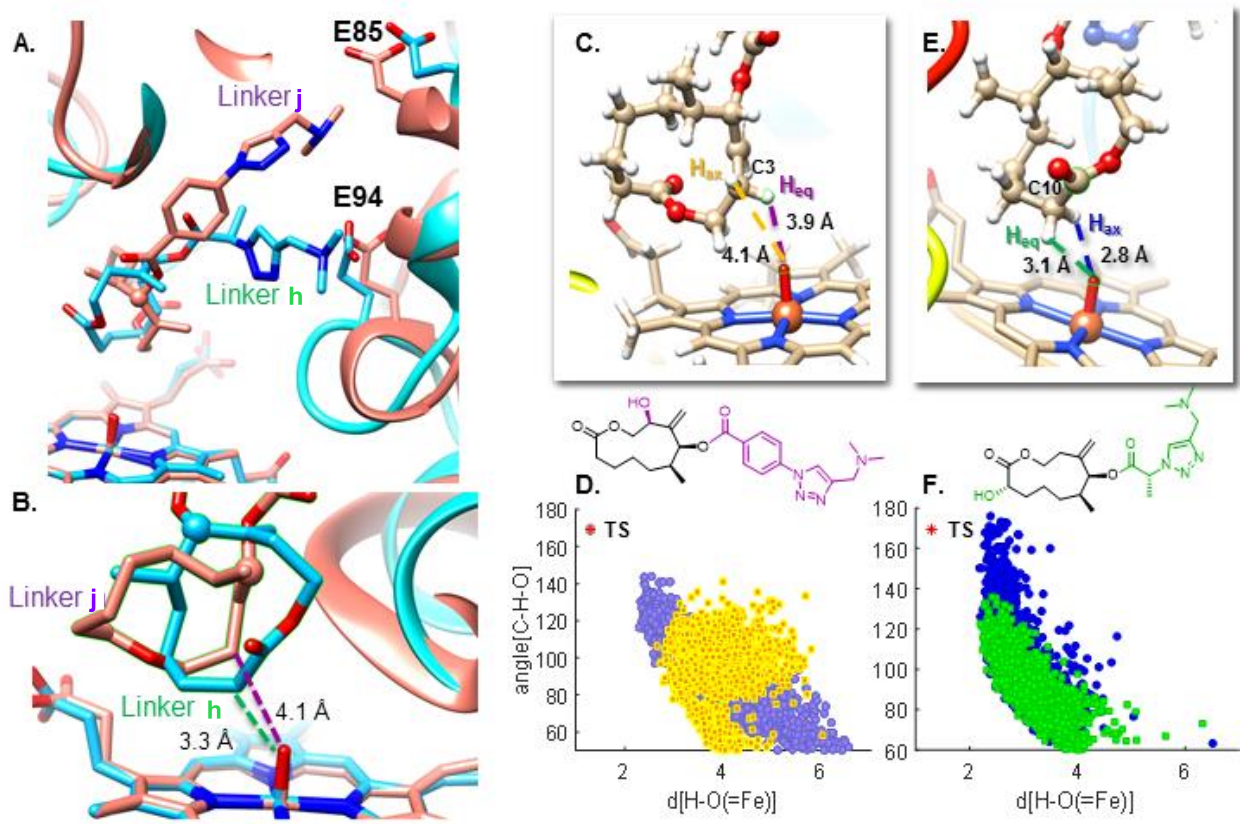

Figure 3.4: Molecular dynamics simulations. **A**. Snapshot of MD trajectory of **38h** overlaid with a snapshot of **38j**. **B**. Closeup of Figure 3.4A snapshot with average C-OFe distances shown. **C**. Snapshot of **38j** with average H-O bond distances shown. **D**. Plot of hydrogen abstraction (of substrate C3) to oxygen (of iron-oxo) distances vs C-H-O angles throughout the MD trajectory with transition state (TS) geometry shown in red. **E**. Snapshot of **38h** with average H-O distances shown. **F**. Plot of hydrogen (of substrate C10) to oxygen (of iron-oxo) distances and C-H-O angles throughout the MD trajectory, with TS geometry shown in red.

3.7.3 Rationalization of β-Oxidation Selectivity

Determining the factors contributing to the β-oxidation of **38l** is of a fundamental interest as the oxidized hydrogens do not benefit from conjugative overlap with neighboring π-systems. The stereochemistry of β-hydroxylated product **41l** was conclusively determined by 2D NOESY. Analysis of proton coupling constants and through-space interactions facilitated the development of a low energy conformer of **41l**, which agreed with computationally derived conformers of this product (Figure 3.5 A and

B). Upon inspection of the computed barriers to hydrogen atom abstraction of conformer 1, it was observed that oxidation of the β-up hydrogen of **38l** to give **41l** was disfavored by >4 kcal/mol (Figure 3.5C). A dramatic shift in abstraction barrier energy for both β hydrogens was observed upon rotation to conformer 2 favoring the oxidation of the β-up hydrogen by >6 kcal/mol (Figure 3.5D). The basis for this large change in abstraction energy is not fully understood, but a likely contributor is the change in dipole of the carbonyl inductively influencing abstraction barriers. MD simulations of **38l** show that the β-up hydrogen resulting in **41l** is closest to the iron oxo for the majority of the simulation, but is removed from the reactive center after ~300 ns (Figure 3.6 A and B). The β-down hydrogen remains ~4 Å from the iron center, which is seemingly too far removed to facilitate catalysis.

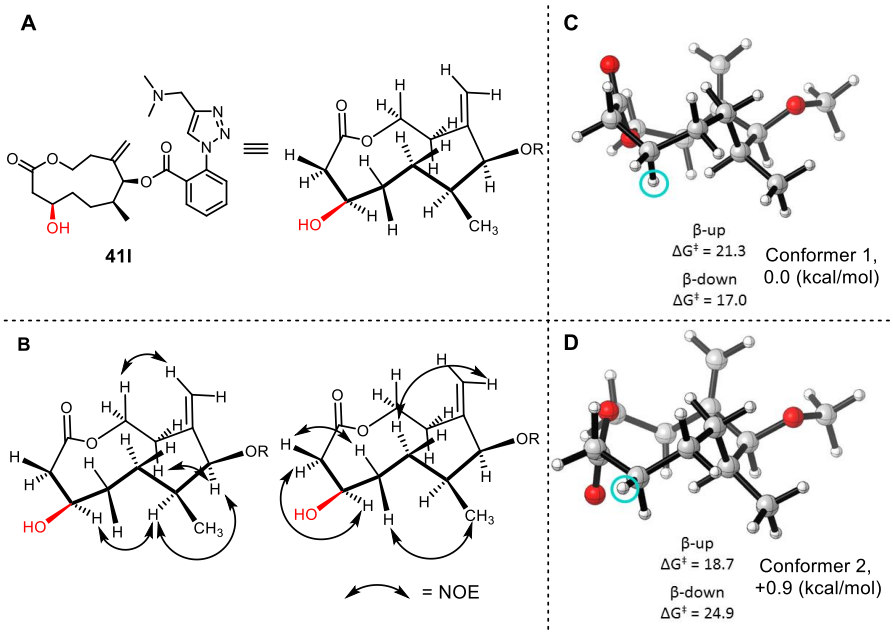

Figure 3.5: Stereochemical assignment and lowest energy conformers of **41l**. **A**. Truncated conformer of **41l** elucidated by 2D NOESY. **B**. Selected key NOE correlations. **C**. Low energy conformer of truncated **38** with unfavorable computed barriers to H abstraction (in kcal/mol) for observed stereochemistry. **D**. Higher energy conformer of truncated **38** with favorable computed barriers to H abstraction (in kcal/mol) for observed stereochemistry.

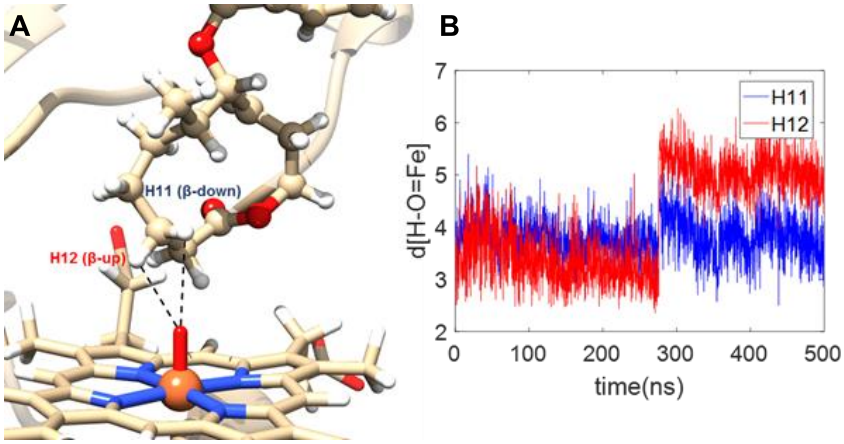

Figure 3.6: **A**. MD simulation of **41l**. **B**. Plot of simulation time (ns) vs hydrogen atom distance from the iron-oxo.

3.8 Computationally Guided Mutagenesis to Develop PikC Tetramutants

An interesting observation was made during the analysis of the MD simulations involving substrates **38h** and **38j**. During the lifetime of the simulation, anchor j is more proximal to E85 while anchor h favors interactions with E94 as seen in Figure 3.7. It was hypothesized that eliminating a favorable electrostatic contact by selective mutation of one of these residues to non-interacting alanine could promote a reorientation of the substrate within the active site resulting in a new oxidation profile. To this end, two novel PikC tetramutant fusion proteins, PikC$_{D50ND176QE246AE85A}$-RhFRED (Triple+E85A) and PikCD$_{50ND176QE246AE94A}$-RhFRED (Triple+E94A), were created.

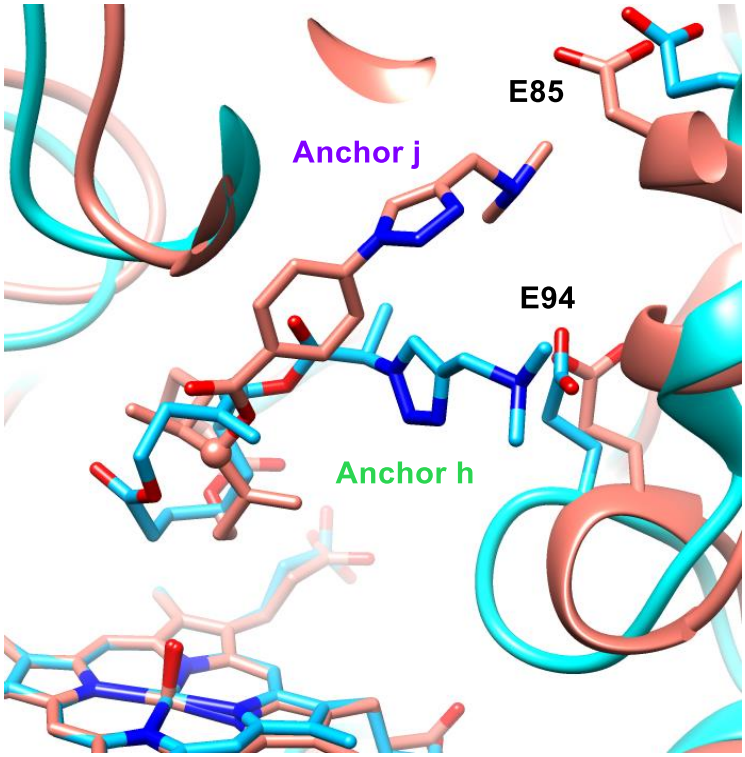

Figure 3.7: Overlaid MD snapshots of **38j** and **38h** showing the preferential electrostatic interaction of **j** with E85 and **h** with E94.

Compounds **38h,j,l** were subjected to oxidation employing both PikC tetramutants and the standard NADPH recycling system. Conversion to hydroxylation and product ratios were determined by LCMS. The major and minor products were identified whenever possible by comparison to the LCMS traces of the corresponding reactions performed with the PikC triple mutant. **38h** exhibited identical reactivity and selectivity with the PikC triple mutant and the Triple+E85A tetramutant to give **40h** (Table 3.8 entries 1-2). Use of the Triple+E94A tetramutant favored formation of **40h**, but with reduced conversion and selectivity (Table 3.8 entry 3). A loss of conversion and selectivity is expected as the E94 residue is favored by anchor **h**, however E85 alone can achieve a comparable level of reactivity. A similar trend is observed with **38j** and **38l** using the Triple+E85A tetramutant. The oxidation profiles are similar to the triple mutant, except

with reduced conversion and selectivity for the same major products **39h** and **41l** (Table 3.8 entries 5-6 and 9-10). Interestingly, using the Triple+E94A tetramutant with substrate **38j** results in **40j** formed as the major product (Table 3.8 entry 7). This change was unexpected as it was predicted that the mutation of E85 should result in a new mode of binding based on the MD simulations. The use of the Triple+E94A tetramutant with **38l** results in improved ~4:1 selectivity for **41l** compared to the ~3:1 selectivity obtained with the PikC triple mutant (Table 3.8 entry 11). Further investigation of the effects of these new PikC mutants is required for a better understanding of these key substrate/residue interactions.

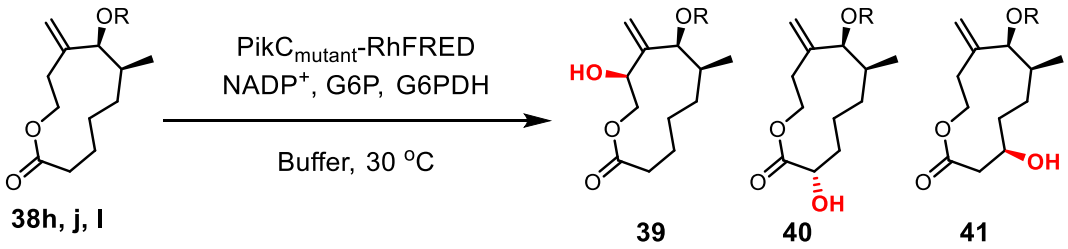

Entry	Anchor	Mutant	Conversion[a]	Ratio[b,c]
1	h	Triple	39	6:94(**40**)
2	h	Triple+E85A	39	6:94(**40**)
3	h	Triple+E94A	26	7:86(**40**):7
4	h	D50N	2	-
5	j	Triple	62	3(**41**):14(**40**):82(**39**):1
6	j	Triple+E85A	60	3(**41**):25(**40**):71(**39**):1
7	j	Triple+E94A	41	70(**40**):6(**39**):24
8	j	D50N	31	2(**41**):16(**40**):77(**39**):5
9	l	Triple	31	71(**41**):24(**40**):4:1
10	l	Triple+E85A	26	71(**41**):20(**40**):7:2
11	l	Triple+E94A	33	81(**41**):15(**40**):2:2

[a]Values are percent conversion to (M+H+16) as determined by LCMS. [b]Ratios for (M+H+16) in order of elution from the LCMS. [c]Known oxidation products shown in parentheses. Triple = D50ND176QE246A.

R = Anchor

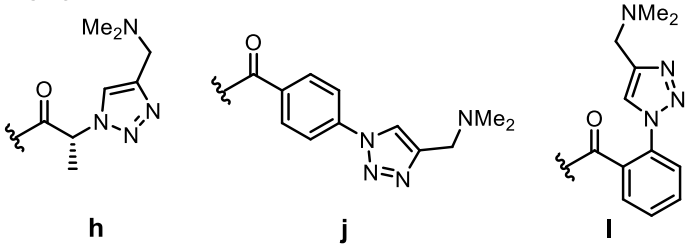

Table 3.8: Reactions of **38h**, **38j**, and **38l** with PikC triple mutant and PikC tetramutant fusion proteins.

3.9 Conclusion

This study[121] shows that a variety of macrocyclic compounds varying in ring size and oxidation patterns can be prepared from a single ynal substrate. Employing catalyst control, the ynal can be cyclized to give 11- or 12-membered macrolactones with high regio- and diastereoselectivity. Coupling this regiodivergent synthesis with late-stage C-H oxidation using a computationally engineered P450 PikC allows for the tunable site-

and stereoselective hydroxylation of obtained macrolactone cores using diverse, triazole-based PikC directing groups. This synthetic strategy has the potential to be applied to other scaffolds, increasing the molecular diversity obtained from a common intermediate.

3.10 Acknowledgements

For the work conducted in chapter 3.3 through chapter 3.8, synthetic chemistry was conducted by Michael M. Gilbert, Shoulei Wang, and Hengbin Wang. Biochemical oxidations and product analysis were conducted by Matthew D. DeMars, Michael M. Gilbert, and Alison R. H. Narayan. Computational studies were conducted by Song Yang and Jessica M. Grandner.

Chapter 4: Conclusions and Future Directions

4.1 Conclusions

In summary, the synthetic benefit for the application of a late-stage C-H oxyfunctionalization approach has been described. Due to the ubiquity of the C-H bond, several strategies for functionalization have been described. Special emphasis has been placed on biocatalysis as a method for the above transformation as the principles for selectivity are often drastically different compared to chemical transformations.

Studies from the Sherman, Houk, Podust, and Montgomery labs have engineered PikC from a wild type P450 to a potent catalyst for remote directed C-H bond hydroxylation. The development of a triple mutant fusion protein, $PikC_{D50ND176QE246A}$-RhFRED, combined with synthetic anchors has expanded the class of substrates to small molecules. Oxidations performed using this approach are predictably selective and can be rationalized through quantum mechanical and molecular dynamics simulations. Hydroxylations are performed with exquisite site- and regioselectivity.

Further investigations into anchoring group structures have yielded modular, triazole-based anchors. This high-throughput anchoring strategy has been applied to the late-stage, site-selective hydroxylation of 11- and 12-membered macrolactones, which were prepared via regiodivergent, nickel-catalyzed macrocyclization from a common linear intermediate. The result is an overall synthetic approach where multiple scaffolds can be accessed from a single substrate, then oxidized at specific C-H bonds using a

single PikC mutant (Scheme 4.1). The selectivity of these oxidations is dictated by the structure of the anchoring group as well as the stereochemical configuration of the substrate and its interactions with the PikC active site.

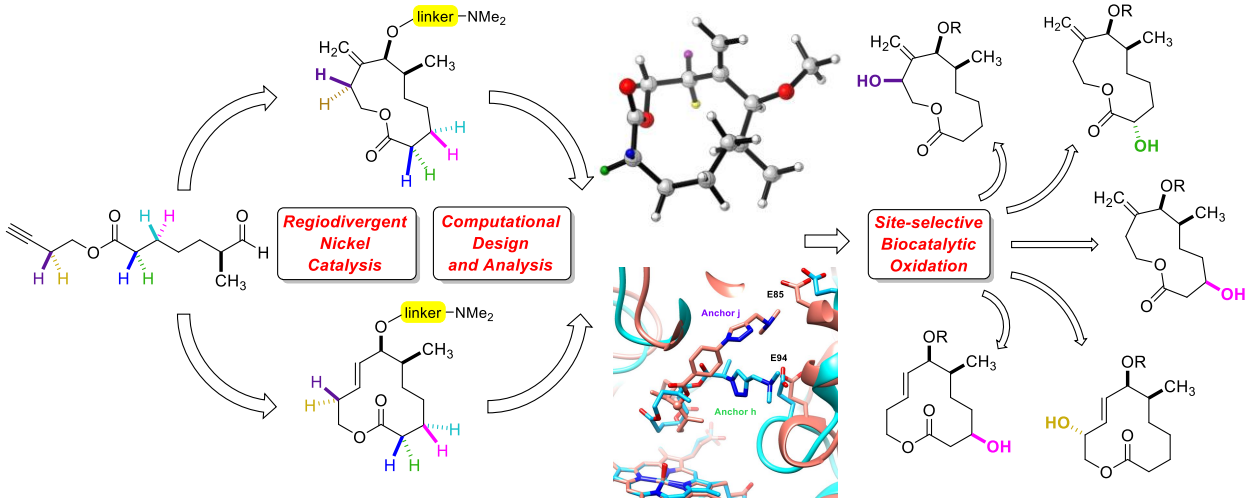

Scheme 4.1 Regiodivergent cyclization of a common intermediate followed by selective PikC hydroxylation.

4.1 Future Directions

Three sites of oxidation of macrocycle 38 have been obtained by only varying the identity of the PikC anchor. However, studies have shown that mutations to the PikC triple mutant are capable of drastically altering the oxidation profile of **38** in combination with various triazole anchors. Future studies will focus on the synergy between computationally guided mutagenesis of PikC and triazole anchors to target new sites C-H bonds of **38** for oxidation. This could be achieved by moving the key salt bridge forming residues to different positions in the active site, thus forcing derivatives of **38** to be repositioned in the active site.

Alternatively, the use of a P450 homologous to PikC that relies on critical salt bridge interactions for substrate binding could result in unique selectivity. Such enzymes, (i.e. JuvD) have been isolated by the Sherman group and been recently employed in chemoenzymatic syntheses.[122] The use of these unexplored enzymes with triazole anchored substrates has the potential to result in unique oxidation patterns not observed with PikC.

Chapter 5: Experimental Supporting Information

5.1 General Protocols

Unless otherwise noted, all reactions were conducted in flame-dried or oven-dried glassware with magnetic stirring under an atmosphere of dry nitrogen. Solvents were purified under nitrogen using a solvent purification system (Innovative Technology, inc., Model #SPS-400-3 and PS-400-3). Unless otherwise noted, all other chemical reagents were obtained from commercial sources and used as received. Silanes were purified by passing through alumina. $Ni(COD)_2$ (Strem Chemicals, Inc.), all N-heterocyclic carbene salts (Aldrich), potassium tert-butoxide (Strem Chemicals, Inc.) were stored and weighed in an inert atmosphere glovebox. Reaction temperatures were controlled by a JKEM Scientific (Model 210) temperature modulator. Analytical thin layer chromatography (TLC) was performed on SilicaPlate TLC 60Å F-254 (250 μm silica gel) and compounds were visualized with phosphomolybdic acid, ceric ammonium molybdate, or aqueous $KMnO_4$ stain. Flash column chromatography was performed using SiliaFlash® P60 (230-400 mesh) silica gel.

1 H-Nuclear Magnetic Resonance (1 H-NMR) and 13 C Nuclear Magnetic Resonance (13 C-NMR) spectra were recorded on Varian MR 400, Vnmrs 500, INOVA 500 and Vnmrs 700 MHz. NMR spectra were recorded in deuterated chloroform ($CDCl_3$) at rt unless otherwise stated. The NMR data were presented as follows: chemical shift in

ppm with the proton signal of the residual of chloroform (δ 7.26 for 1 H-NMR) and (δ = 77.0 ppm for 13 C-NMR) as internal standards, multiplicity (s = singlet; d = doublet; t = triplet; q = quartet; m = multiplet, dd = doublet of doublets; ddd = doublet of doublets of doublets; dddd = doublet of doublets of doublets of doublets; tt = triplet of triplets; dq = doublet of quartets), coupling constant (J/Hz), integration. In many instances, the quaternary triazole carbon could not be observed directly due to signal broadening. Whenever possible, this peak was assigned indirectly by HMBC and is noted as such in the compound characterization. High resolution mass spectra were recorded on a VG 70-250-s spectrometer manufactured by Micromass Corp. (Manchester UK) at the University of Michigan Mass Spectrometry Laboratory. IPr^{Cl} free carbene was prepared from commercially available IPr free carbene following a previously reported procedure.[123] Imidazole-1-sulfonyl azide was prepared according to established protocols and purified by chromatography (50% EtOAc/hex) prior to use.[124] Fe(*S,S*-PDP) was purchased from Aldrich and handled in a nitrogen-filled glovebox.

5.2 Chapter 2 Experimental

5.2.1 Starting Material Characterization

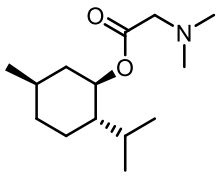

(1*R*,2*S*,5*R*)-2-isopropyl-5-methylcyclohexyl dimethylglycinate, ((–)-1):

A flame-dried round-bottom flask was charged with (0.42 g) N,N-dimethylamino glycine•HCl (1.5 equiv), 0.62 g DCC (1.5 equiv), and 0.37 g DMAP (1.5 equiv). The contents of the flask were suspended in 20 mL of CH_2Cl_2 and allowed to stir for ~5 min.

0.47 mL of distilled triethylamine (1.7 equiv) was added dropwise and the reaction was stirred for an additional 5 min before 0.31 g of (–)-menthol (1.0 equiv) was added. The reaction was stirred for 7 d and was then filtered through a cotton plug. The solvent was removed by under reduced pressure, and 1 M HCl was added to the resulting yellow residue until the pH was between 2 and 3. The aqueous solution was extracted 3x with 25 mL of 30% EtOAc/hexanes, and the remaining aqueous layer was adjusted to pH 8-9 with a saturated aqueous sodium bicarbonate solution. The solution was extracted 3x with 30 mL of CH_2Cl_2. The resulting organic layers were combined, dried over sodium sulfate, and filtered. The solvent was removed under reduced pressure to afford the crude material, which was purified by column chromatography (the column was packed with 5% EtOAc, 5% triethylamine, and 90% hexanes and run on a gradient of 30% EtOAc/hexanes to 7:2:1 EtOAc: MeCN: MeOH) to yield 0.28 g (57%) of the title compound as a clear oil.

^{1}H NMR (500 MHz, $CDCl_3$) δ 4.77 (td, J = 10.9, 4.4 Hz, 1H), 3.14 (s, 2H), 2.34 (s, 6H), 2.04 – 1.94 (m, 1H), 1.92 – 1.78 (m, 1H), 1.76 – 1.61 (m, 2H), 1.58 – 1.44 (m, 1H), 1.43 – 1.34 (m, 1H), 1.12 – 0.95 (m, 2H), 0.93 – 0.81 (m, 7H), 0.76 (d, J = 6.9 Hz, 3H)

^{13}C NMR (126 MHz, $CDCl_3$) δ 170.2, 74.4, 60.8, 46.9, 45.3, 40.9, 34.2, 31.4, 26.3, 23.3, 22.0, 20.7, 16.2

HRMS (ESI) m/z calculated for [M+H]+ 242.2115, found 242.2112.

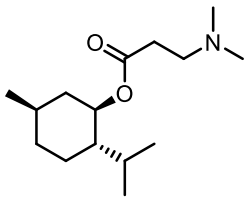

(1*R*,2*S*,5*R*)-2-isopropyl-5-methylcyclohexyl 3-(dimethylamino)propanoate ((–)-2):

Following the procedure used to synthesize (1R,2S,5R)-2-isopropyl-5-methylcyclohexyl dimethylglycinate, (–)-menthol (0.31 g), 3-(N,N-dimethylamino)propionic acid•HCl (0.46 g), DCC (0.62 g), DMAP (0.37 g), and triethylamine (0.47 mL) was employed to give 0.096 g (19%) of the title compound as a clear oil after purification by column chromatography (silica gel, packed with 5% EtOAc, 5% triethylamine, and 90% hexanes and run on a gradient of 30% EtOAc/hexanes to 7:2:1 EtOAc: MeCN: MeOH).

^{1}H NMR (401 MHz, $CDCl_3$) δ 4.69 (td, J = 10.9, 4.4 Hz, 1H), 2.83 – 2.70 (m, 2H), 2.67 – 2.51 (m, 2H), 2.36 (s, 6H), 2.03 – 1.92 (m, 1H), 1.92 – 1.78 (m, 1H), 1.75 – 1.61 (m, 2H), 1.56 – 1.42 (m, 1H), 1.42 – 1.30 (m, 1H), 1.13 – 0.93 (m, 2H), 0.93 – 0.79 (m, 8H), 0.75 (d, J = 7.0 Hz, 3H)

^{13}C NMR (126 MHz, $CDCl_3$) δ 172.1, 74.2, 54.8, 47.0, 45.2, 40.9, 34.3, 33.3, 31.4, 26.2, 23.4, 22.0, 20.8, 16.3

HRMS (ESI) m/z calculated for [M+H]+ 256.2271, found 256.2274.

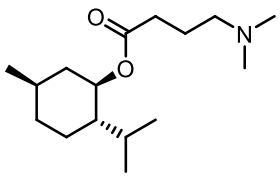

(1*R*,2*S*,5*R*)-2-isopropyl-5-methylcyclohexyl 4-(dimethylamino)butanoate ((–)-3):

(–)-(1*R*,2*S*,5*R*)-menthol (200 mg, 1.28 mmol), 3-N,N-dimethylaminobutyric acid hydrochloride (325 mg, 1.92 mmol), triethylamine (304 µL, 2.18 mmol), DCC (400 mg, 1.92 mmol) and DMAP (237 mg, 1.92 mmol) were dissolved in 12.5 mL of CH_2Cl_2 and stirred at rt for 4 d, then the reaction mixture was filtered through cotton and evaporated to dryness in vacuo. The crude residue was transferred to a separatory funnel by washing the flask with 0.1 M HCl and 30% EtOAc in hexanes. The acidified aqueous phase was

extracted three times with 30% EtOAc in hexanes. Then, the aqueous layer was basified with saturated aqueous $NaHCO_3$ solution until it reached a pH of approximately 8-9, measured by pH paper. The aqueous layer was extracted three times with EtOAc. The EtOAc layers were combined, dried over anhydrous sodium sulfate, filtered, and evaporated to dryness in vacuo. The crude residue was chromatographed over silica gel (gradient from 30% EtOAc in hexanes to 20% MeCN, 10% MeOH in EtOAc) to yield 168 mg (49% yield) of the desired ester derivative as a colorless oil.

^{1}H NMR (400 MHz, $CDCl_3$) δ 4.67 (ddd, J = 10.8, 10.8, 4.4 Hz, 2H), 2.35 – 2.24 (m, 4H), 2.22 (s, 6H), 2.06 – 1.93 (m, 1H), 1.91 – 1.74 (m, 3H), 1.72 – 1.62 (m, 2H), 1.54 – 1.42 (m, 1H), 1.41 – 1.31 (m, 1H), 1.11 – 0.80 (m, 9H), 0.75 (d, J = 6.8 Hz, 3H);

^{13}C NMR (175 MHz, $CDCl_3$) δ 173.1, 74.0, 58.9, 47.0, 45.4, 40.9, 34.2, 32.4, 31.3, 26.2, 23.4, 23.1, 22.0, 20.7, 16.3; IR (thin film, cm-1) 2925, 2865, 2812, 2764, 1728, 1456; **HRMS (ESI)** m/z calculated for [M+H]+ 270.2433, found 270.2431.

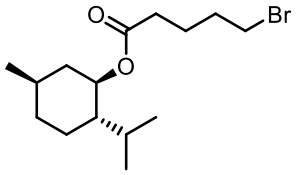

(1*R*,2*S*,5*R*)-2-isopropyl-5-methylcyclohexyl 5-bromopentanoate ((-)-S1)):

Following the procedure used to synthesize (1*R*,2*S*,5*R*)-2-isopropyl-5-methylcyclohexyl 6- bromohexanoate, (–)-menthol (0.23 g), DCC (0.46 g), DMAP (0.027 g), 5-bromovaleric acid (0.45 g), and CH_2Cl_2 (23 mL) were employed. 0.48 g of the title compound was obtained after purification by column chromatography (Silica gel, 5% EtOAc/hexanes to 10% EtOAc/hexanes).

^{1}H NMR (400 MHz, $CDCl_3$) δ 4.68 (td, J = 10.9, 4.4 Hz, 1H), 3.42 (t, J = 6.6 Hz, 2H), 2.32 (t, J = 7.2 Hz, 2H), 2.02 – 1.94 (m, 1H), 1.94 – 1.73 (m, 4H), 1.72 – 1.63 (m, 2H), 1.56 –

1.42 (m, 1H), 1.41 – 1.32 (m, 1H), 1.12 – 0.93 (m, 2H), 0.93 – 0.80 (m, 7H), 0.75 (d, J = 6.9 Hz, 3H);

^{13}C NMR (126 MHz, $CDCl_3$) δ 172.6, 74.2, 47.0, 40.9, 34.2, 33.7, 33.0, 32.0, 31.4, 26.3, 23.6, 23.5, 23.4, 22.0, 20.7, 16.3.

HRMS (ESI) m/z calculated for $[M+Na]^+$ 341.1087, found 341.1082.

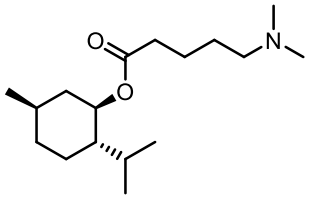

(1*R*,2*S*,5*R*)-2-isopropyl-5-methylcyclohexyl 5-(dimethylamino)pentanoate, ((–)-4):

Following the procedure to synthesize (1*R*,2*S*,5*R*)-2-isopropyl-5-methylcyclohexyl 6- (dimethylamino)hexanoate, (1*R*,2*S*,5*R*)-2-isopropyl-5-methylcyclohexyl 5-bromopentanoate (0.16 g), 40% w/w aqueous dimethylamine (0.32 mL) and DMF (2.2 mL) was employed to give 0.12 g (88%) of the desired product after purification by column chromatography (Silica gel, 30% EtOAc/hexanes to 98%CH_2Cl_2, 2%, Et_3N).

^{1}H NMR (400 MHz, $CDCl_3$) δ 4.68 (td, J = 10.9, 4.4 Hz, 1H), 2.36 – 2.16 (m, 10H), 2.03 – 1.93 (m, 1H), 1.93 – 1.78 (m, 1H), 1.75 – 1.57 (m, 4H), 1.56 – 1.41 (m, 3H), 1.41 – 1.30 (m, 1H), 1.13 – 0.92 (m, 2H), 0.92 – 0.78 (m, 7H), 0.75 (d, J = 7.0 Hz, 3H);

^{13}C NMR (126 MHz, $CDCl_3$) δ 173.1, 73.9, 59.4, 47.0, 45.5, 41.0, 34.6, 34.3, 31.4, 27.2, 26.3, 23.4, 23.0, 22.0, 20.8, 16.3.

HRMS (ESI) m/z calculated for $[M+H]^+$ 284.2584, found 284.2595.

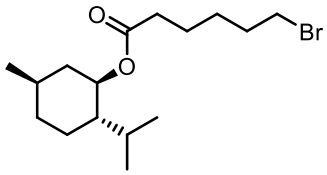

(1*R*,2*S*,5*R*)-2-isopropyl-5-methylcyclohexyl 6-bromohexanoate (-)-S2:

A flame-dried round-bottom flask was charged with 0.62 g of dicyclohexylcarbodiimide (DCC) (3.0 mmol), 0.037 g 4-dimethylaminopyridine (DMAP) (0.30 mmol), and 0.58 g of 6-bromohexanoic acid (3.0 equiv). The contents of the flask were suspended in 21 mL of CH_2Cl_2, and allowed to stir for 10 min. Then, 0.31 g of (–)-menthol (2.0 mmol) was added and the reaction was stirred until all the (–)-menthol was consumed as judged by TLC. The reaction mixture was filtered through a cotton plug and the solvent was removed under reduced pressure to afford a white residue. The crude material was purified by column chromatography (silica gel, gradient 5% EtOAc/hexanes to 10% EtOAc/hexanes) to yield 0.66 g (99%) of the title compound as a clear oil.

^{1}H NMR (401 MHz, $CDCl_3$) δ 4.68 (td, J = 10.9, 4.4 Hz, 1H), 3.40 (t, J = 6.8 Hz, 2H), 2.30 (t, J = 7.4 Hz, 2H), 2.02 – 1.93 (m, 1H), 1.93 – 1.78 (m, 3H), 1.75 – 1.59 (m, 4H), 1.55 – 1.42 (m, 3H), 1.41 – 1.31 (m, 1H), 1.12 – 0.93 (m, 2H), 0.93 – 0.79 (m, 6H), 0.75 (d, J = 6.9 Hz, 3H)

^{13}C NMR (126 MHz, $CDCl_3$) δ 173.0, 74.0, 47.0, 40.9, 34.4, 34.2, 33.5, 32.4, 31.4, 27.6, 26.3, 24.2, 23.4, 22.0, 20.8, 16.3

HRMS (ESI) m/z calculated for $[M+Na]^+$ 355.1243, found 355.1240.

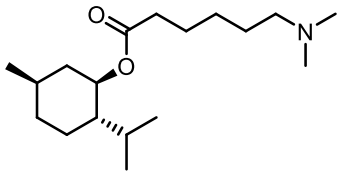

(1*R*,2*S*,5*R*)-2-isopropyl-5-methylcyclohexyl 6-(dimethylamino)hexanoate, ((–)-5):

A flame-dried round-bottom flask was charged with 0.16 g of (1*R*,2*S*,5*R*)-2-isopropyl-5- methylcyclohexyl 6-bromohexanoate (0.47 mmol). (1*R*,2*S*,5*R*)-2-isopropyl-5-methylcyclohexyl 6- bromohexanoate was suspended in 2.2 mL DMF and allowed to stir for ~5 min, followed by addition of 0.31 mL of 40% w/w aqueous dimethylamine (2.5 mmol). The mixture was stirred until all the starting material was consumed as monitored by TLC analysis. The reaction was quenched with 6 mL of saturated sodium bicarbonate solution and extracted with EtOAc (3 x 15 mL). The resulting organic layers were combined, dried with sodium sulfate, filtered and concentrated under reduced pressure. The resulting clear oil was chromatographed (Silica gel, 30% EtOAc/Hex to 99% CH_2Cl_2, 1% Et_3N) to yield 0.13 g (90%) of the title compound as a clear oil.

^{1}H NMR (401 MHz, $CDCl_3$) δ 4.67 (td, J = 10.9, 4.4 Hz, 1H), 2.34 – 2.15 (m, 10H), 2.02 – 1.93 (m, 1H), 1.93 – 1.77 (m, 1H), 1.75 – 1.58 (m, 4H), 1.48 (quint, J = 7.8 Hz, 3H), 1.41 – 1.26 (m, 3H), 1.15 – 0.93 (m, 2H), 0.93 – 0.79 (m, 7H), 0.75 (d, J = 6.9 Hz, 3H).

^{13}C NMR (126 MHz, $CDCl_3$) δ 173.3, 73.9, 59.6, 47.0, 45.5, 40.9, 34.7, 34.3, 31.4, 27.4, 27.0, 26.2, 23.4, 22.0, 20.8, 16.3.

HRMS (ESI) m/z calculated for $[M+H]^+$ 298.2741, found 298.2747.

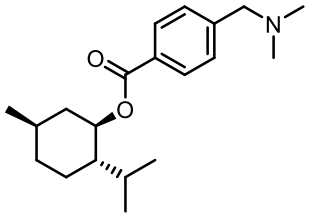

(1*R*,2*S*,5*R*)-2-isopropyl-5-methylcyclohexyl 4-((dimethylamino)methyl)benzoate, ((–)-6):

Following the procedure used to synthesize (1*R*,2*S*,5*R*)-2-isopropyl-5-methylcyclohexyl dimethylglycinate, (-)-(1*R*,2*S*,5*R*)-menthol (100 mg, 0.640 mmol), 172 mg of 4- ((dimethylamino)methyl)benzoic acid (0.960 mmol, 1.50 equiv), 200 mg of dicyclohexylcarbodiimide (0.960 mmol, 1.5 equiv) and 118 mg 4-dimethylaminopyridine (0.960 mmol, 1.5 equiv) were employed to yield 166 mg (82%) of the desired ester derivative as a colorless oil after chromatography over silica gel (gradient from 30% EtOAc in hexanes to 100% EtOAc).

^{1}H NMR (700 MHz, $CDCl_3$) δ 7.99 (d, J = 8.4 Hz, 2H), 7.38 (d, J = 8.4 Hz, 2H), 4.93 (ddd, J = 11.2, 11.2, 4.2 Hz, 1H), 3.47 (s, 2H), 2.25 (s, 6H), 2.12 (d, J = 11.9 Hz, 1H), 1.96 (sept-d, J = 7.0, 2.8 Hz, 1H), 1.75 – 1.70 (m, 2H), 1.61 – 1.53 (m, 2H), 1.14 (td, J = 13.7, 3.2 Hz, 1H), 1.09 (t, J = 12.0 Hz, 1H), 0.97 – 0.88 (m, 7H), 0.79 (d, J = 7.0 Hz, 3H)

^{13}C NMR (125 MHz, $CDCl_3$) δ 166.0, 144.1, 129.6, 129.5, 128.8, 74.7, 64.0, 47.2, 45.3, 41.0, 34.3, 31.4, 26.5, 23.6, 22.0, 20.8, 16.5.

IR (thin film, cm^{-1}) 2923, 2856, 2767, 1712, 1611, 1454.

HRMS (ESI) m/z calculated for [M+H]+ 318.2433, found 318.2420.

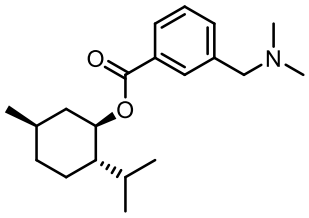

(1*R*,2*S*,5*R*)-2-isopropyl-5-methylcyclohexyl 3-((dimethylamino)methyl)benzoate, ((–)-7):

Following the procedure used to synthesize (1*R*,2*S*,5*R*)-2-isopropyl-5-methylcyclohexyl dimethylglycinate, (-)-(1*R*,2*S*,5*R*)-menthol (160 mg, 1.02 mmol), 154 mg of 3- ((dimethylamino)methyl)benzoic acid (1.54 mmol, 1.50 equiv), 320 mg of dicyclohexylcarbodiimide (1.54 mmol, 1.50 equiv) and 190 mg 4-dimethylaminopyridine (1.54 mmol, 1.50 equiv) to yield 105 mg (33%) of the desired ester derivative as a colorless oil after chromatography over silica gel (gradient from 30% EtOAc in hexanes to 100% EtOAc).

^{1}H NMR (400 MHz, $CDCl_3$) δ 7.97 – 7.92 (m, 2H), 7.52 (d, J = 7.5 Hz, 1H), 7.40 (d, J = 7.5 Hz, 2H), 4.94 (ddd, J = 11.0, 11.0, 4.5 Hz, 1H), 3.49 (d, J = 13.0 Hz, 1H), 3.45 (d, J = 13.0 Hz, 1H), 2.25 (s, 6H), 2.11 (dtd, J = 11.5, 3.5, 2.0 Hz, 1H), 1.96 (sept-d, J = 7.0, 2.5 Hz, 1H), 1.73 – 1.69 (m, 2H), 1.63 – 1.52 (m, 2H), 1.18 – 1.06 (m, 2H), 0.92 (t, J = 6.5 Hz, 6H), 0.79 (d, J = 7.5 Hz, 3H).

^{13}C NMR (175 MHz, $CDCl_3$) δ 166.0, 139.2, 133.3, 130.8, 130.0, 128.3, 128.2, 74.7, 63.9, 47.1, 45.2, 40.9, 34.2, 31.4, 26.4, 23.6, 22.0, 20.7, 16.4.

IR (thin film, cm^{-1}) 2949, 2864, 2815, 2767, 1711, 1455, 1360.

HRMS (ESI) m/z calculated for $[M+H]^+$ 318.2433, found 318.2440.

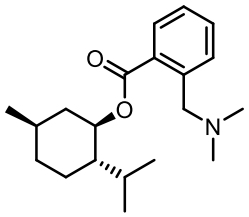

(1*R*,2*S*,5*R*)-2-isopropyl-5-methylcyclohexyl 2-((dimethylamino)methyl)benzoate, ((–)-8):

2-((dimethylamino)methyl)benzoic acid (57 mg, 0.32 mmol) was dissolved in 1 mL CH_2Cl_2. To this mixture was added one drop of N,N-dimethylformamide followed by oxalyl chloride (33 µL, 0.38 mmol). The reaction was stirred at rt for 1.5 h before the solvent was evaporated and the crude acid chloride was resuspended in 1 mL CH_2Cl_2. The acyl chloride suspension was added dropwise to an ice cooled solution of (–)-(1*R*,2*S*,5*R*)-menthol (100 mg, 0.64 mmol), DMAP (0.16 mmol, 20 mg) and triethylamine (180 µL, 1.3 mmol) in 3.4 mL CH_2Cl_2. The reaction mixture was stirred as it was warmed to rt. After 12 h, the reaction was quenched by the addition of saturated sodium bicarbonate solution. The aqueous phase was washed with EtOAc (3x), dried over sodium sulfate, filtered and concentrated. The crude residue was transferred to a separatory funnel by washing the flask with 0.1 M HCl and 30% EtOAc in hexanes. The acidified aqueous phase was extracted three times with 30% EtOAc in hexanes. Then, the aqueous layer was basified with saturated aqueous $NaHCO_3$ solution until it reached a pH of approximately 8-9, measured by pH paper. The basic aqueous layer was extracted three times with EtOAc. The EtOAc organic layers were combined, dried over anhydrous sodium sulfate, filtered, and evaporated to dryness in vacuo. The crude residue was chromatographed over silica gel (gradient from 5% EtOAc in hexanes to 100% EtOAc) to yield 44 mg (44%) of the desired ester as a colorless oil.

^{1}H NMR (500 MHz, $CDCl_3$) δ 7.70 (d, J = 8.0 Hz, 1H), 7.48 (d, J = 7.5 Hz, 1H), 7.42 (t, J = 7.5 Hz, 1 H), 7.29 (t, J = 7.5 Hz, 1H), 4.91 (ddd, J = 11.0, 11.0, 4.5 Hz, 1 H), 3.80 (d, J = 14.0 Hz, 1H), 3.65 (d, J = 13.5 Hz, 1H), 2.22 (s, 6H), 2.17 (d, J = 11.5 Hz, 1H), 2.02 (sept-d, J = 7.0, 2.5 Hz, 1H), 1.77 – 1.69 (m, 2H), 1.62 – 1.47 (m, 2H), 1.18 – 1.05 (m, 2H), 0.98 – 0.86 (m, 7H), 0.82 (d, 6.5 Hz, 3H).

^{13}C NMR (175 MHz, $CDCl_3$) δ 167.8, 139.9, 132.0, 130.8, 130.0, 129.3, 126.6, 76.8, 74.6, 61.2, 47.2, 45.2, 40.9, 34.2, 31.4, 26.2, 23.4, 22.1, 20.8, 16.3.

IR (thin film, cm^{-1}) 2951, 2868, 2815, 2765, 1715, 1454, 1366;

HRMS (ESI) m/z calculated for $[M+H]^+$ 318.2433, found 318.2436.

(3*R*,4*S*,6*R*)-4-(dimethylamino)-6-methyltetrahydro-2H-pyran-2,3-diyl diacetate, S3

Following the literature procedure,[100] 7.0 g (9.5 mmol) of erythromycin was added to a round bottom flask followed by 50 mL of EtOH. 125 mL of a 6 N HCl solution was added, and the mixture was heated at reflux at 100 °C for 4 h. The reaction mixture was transferred to a separatory funnel and extracted with $CHCl_3$ (3 x 50 mL). The organic layer was discarded, and the solvent was removed from the red/orange aqueous layer. After vacuum drying overnight, crude 4-(dimethylamino)-6- methyltetrahydro-2H-pyran-2,3-diol was obtained as a red/orange solid and was carried on to the next step without further purification. The crude compound was transferred to a round bottom flask and suspended in 50 mL Ac_2O. 2 mL of concentrated sulfuric acid was added at 0 °C. The resulting mixture was stirred overnight at rt. The reaction mixture was poured into ice water and neutralized with solid sodium bicarbonate and extracted with EtOAc. The combined organic layers were concentrated and purified by column chromatography (80% EtOAc

20% Hexanes to 2% MeOH in EtOAc) to afford 4- (dimethylamino)-6-methyltetrahydro-2H-pyran-2,3-diyl diacetate (1.5 g, 5.7 mmol, 60 % over 2 steps) as a yellow oil. Spectral data of the compound was identical with that previously reported.[100]

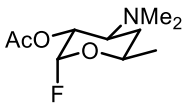

(2*R*,3*R*,4*S*,6*R*)-4-(dimethylamino)-2-fluoro-6-methyltetrahydro-2H-pyran-3-yl acetate, S4

To a stirring solution of HF pyridine (7.2 mL) in a dry polyethylene vial at 0 °C was added 1.2 g (4.4 mmol) of 4-(dimethylamino)-6-methyltetrahydro-2H-pyran-2,3-diyl diacetate as a solution in toluene (4.8 mL). The reaction was stirred at 0 °C for 2.5 h. The reaction mixture was diluted with 10 mL of a brine solution and quenched with a saturated sodium bicarbonate solution. The mixture was extracted with EtOAc and dried over Na_2SO_4, filtered, and concentrated. The crude material was chromatographed (100% EtOAc) to yield 0.48 g (2.2 mmol) of the α-anomer of 4-(dimethylamino)-2- fluoro-6-methyltetrahydro-2H-pyran-3-yl acetate as a clear oil. Spectral data of the compound was identical with that previously reported.[100]

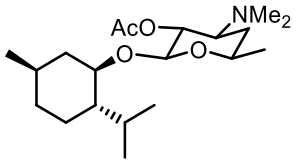

(2*S*,3*R*,4*S*,6*R*)-4-(dimethylamino)-2-(((1*R*,2*S*,5*R*)-2-isopropyl-5-methylcyclohexyl)oxy)-6- methyltetrahydro-2H-pyran-3-yl acetate, S5

A suspension of (–)-menthol (0.038 g, 0.24 mmol), 4-(dimethylamino)-2-fluoro-6-methyltetrahydro-2Hpyran-3-yl acetate (0.026 g, 0.12 mmol), and molecular sieves (4Å, 0.15 g) in 2 mL CH_2Cl_2 was stirred for 30 min at rt under an N_2 atmosphere. The

suspension was cooled to 0 °C and BF_3•OEt_2 0.060 mL (0.48 mmol, freshly distilled) was added. The reaction was stirred at 0 °C until the starting material was consumed as judged by TLC. The reaction was quenched with a solution of saturated sodium bicarbonate and extracted with EtOAc. The resulting organic layers were combined, dried over Na_2SO_4, filtered, concentrated, and purified by chromatography (5% MeOH in CH_2Cl_2) to yield 0.028 g (65%) of the title compound as a clear oil.

^{1}H NMR (401 MHz, $CDCl_3$) δ 4.77 (dd, J = 10.5, 7.6 Hz, 1H), 4.32 (d, J = 7.6 Hz, 1H), 3.63 – 3.42 (m, 1H), 3.32 (td, 1H), 2.77 (s, 1H), 2.41 – 2.18 (m, 7H), 2.06 (s, 3H), 2.01 – 1.91 (m, 1H), 1.80 – 1.69 (m, 1H), 1.69 – 1.55 (m, 2H), 1.45 – 1.13 (m, 8H), 1.03 – 0.77 (m, 9H), 0.74 (d, J = 6.9 Hz, 3H).

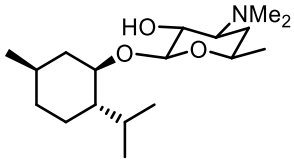

(2*S*,3*R*,4*S*,6*R*)-4-(dimethylamino)-2-(((1*R*,2*S*,5*R*)-2-isopropyl-5-methylcyclohexyl)oxy)-6- methyltetrahydro-2H-pyran-3-ol, (10):

To a solution of 2-((1*R*,2*S*,5*R*)-(-)-menthol)-4-(dimethylamino)-6-methyltetrahydro-2H-pyran-3-yl acetate 0.028 g (0.079 mmol) in 1.60 mL of MeOH was added 0.044 g of K_2CO_3 (0.32 mmol). The reaction was stirred at rt until all starting material was consumed as judged by TLC. The reaction was diluted with brine and extracted with EtOAc. The organic layers were combined, dried over Na_2SO_4, concentrated, and purified by chromatography (10% MeOH in CH2Cl2) to yield 0.023g (95%) of the title compound.

^{1}H NMR (401 MHz, $CDCl_3$) δ 4.29 (d, J = 7.3 Hz, 1H), 3.59 – 3.39 (m, 2H), 3.27 (dd, J = 10.2, 7.3 Hz, 1H), 2.63 (ddd, J = 12.3, 10.2, 4.1 Hz, 1H), 2.35 (s, 7H), 2.14 – 2.00 (m,

1H), 1.84 – 1.70 (m, 1H), 1.70 – 1.56 (m, 2H), 1.36 – 1.20 (m, 7H), 1.03 – 0.80 (m, 9H), 0.76 (d, J = 6.9 Hz, 3H).

^{13}C NMR (126 MHz, $CDCl_3$) δ 101.0, 76.6, 69.6, 69.1, 65.3, 47.6, 40.7, 40.3, 34.3, 31.5, 29.4, 24.9, 22.9, 22.1, 21.0, 20.9, 15.3.

HRMS (ESI) m/z calculated for $[M+H]^+$ 314.2690, found 314.2696.

Synthesis of (+)-menthol derivatives: The parallel set of (+)-menthol substrates were synthesized in an analogous manner to yield products matching the characterization data for the (–)-menthol enantiomer.

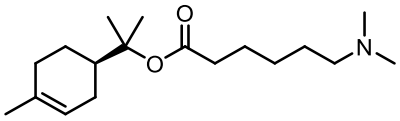

(*R*)-2-(4-methylcyclohex-3-en-1-yl)propan-2-yl 6-(dimethylamino)hexanoate, S6

A flame-dried round bottom flask was charged with 0.771 g (5.00 mmol) of (+)-α-terpineol, 1.545 g (7.50 mmol) of DCC, and 0.122 g (1.00 mmol) of DMAP. The contents of the flask were suspended in 25 mL of CH_2Cl_2 and allowed to stir for 5 minutes before 1.460 g (7.50 mmol) of 6-bromohexanoic acid. Upon completion, the reaction was filtered through a plug of cotton and the solvent removed. The crude material was purified by chromatography to yield the ester. A round bottom flask was charged with 0.404 g (1.22 mmol) of the ester. The contents of the flask were suspended in DMF and cooled to 0 °C. 0.289 g (6.42 mmol) of dimethylamine solution (40 wt. % in H_2O) was then added. Upon completion, the reaction was quenched with ethyl acetate and a solution of sat'd sodium bicarbonate. The organic layer was extracted twice with a solution of sat'd sodium

bicarbonate and once with a solution of brine. The solvent was removed from the organic layer and the resulting residue was suspended in 1 M HCl until pH ~2. The aqueous layer was extracted three times with diethyl ether and then basified to pH ~8 with a solution of sat'd sodium bicarbonate. The aqueous solution was extracted thrice with CH_2Cl_2, the organic layers combined, dried over sodium sulfate, and the solvent removed to yield 0.292 g (81%) of the desired product.

^{1}H NMR (400 MHz, $CDCl_3$): δ 5.38-5.32 (m, 1H), 2.29-2.16 (m, 11H), 2.07-1.92 (m, 4H), 1.85-1.73 (m, 2H), 1.63-1.54 (m, 4H), 1.52-1.45 (m, 2H), 1.42 (s, 3H), 1.40 (s, 3H), 1.35-1.25 (m, 3H).

^{13}C NMR (100 MHz, $CDCl_3$): δ 173.0, 133.9, 120.283, 84.6, 59.6, 45.4 (2C), 42.7, 35.6, 30.9, 27.3, 26.9, 26.3, 25.0, 23.8, 23.3, 23.3, 23.1.

HRMS (ESI) m/z calculated for $[M+H]^+$ 296.2584, found 296.2582.

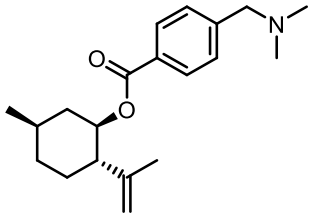

(1*R*,2*S*,5*R*)-5-methyl-2-(prop-1-en-2-yl)cyclohexyl-4-((dimethylamino)methyl)benzoate, S7

A flame-dried round bottom flask was charged with 0.462 g (3.00 mmol) of (-)-Isopulegol, 0.927 g (4.50 mmol) of DCC, and 0.073 g (0.60 mmol) of DMAP. The contents of the flask were suspended in 15 mL of CH_2Cl_2 and allowed to stir for 5 minutes before 0.675 g (4.50 mmol) of 4-formylbenzoic acid. Upon completion, the reaction was filtered through a plug of cotton and the solvent removed. The crude material was purified by chromatography to yield the ester. A flame-dried round bottom flask was charged with

0.772 g (2.70 mmol) of the ester and 0.284 g (3.51 mmol) of dimethylamine hydrochloride. The contents of the flask were suspended in CH_2Cl_2 and cooled to 0 °C. 0.859 g (4.05 mmol) of sodium triacetoxyborohydride was then added over half an hour. Upon completion, the reaction was quenched with ethyl acetate and a solution of sat'd sodium bicarbonate. The organic layer was extracted twice with a solution of sat'd sodium bicarbonate and once with a solution of brine. The solvent was removed from the organic layer and the resulting residue was suspended in 1 M HCl until pH ~2. The aqueous layer was extracted three times with diethyl ether and then basified to pH ~8 with a solution of sat'd sodium bicarbonate. The aqueous solution was extracted thrice with CH_2Cl_2, the organic layers combined, dried over sodium sulfate, and the solvent removed to yield 0.587 g (69%) of the desired product.

^{1}H NMR (400 MHz, $CDCl_3$): δ 7.94 (d, J = 8.0 Hz, 2H), 7.36 (d, J = 8.0 Hz, 2H), 5.01 (td, J = 10.9, 4.4 Hz, 1H), 4.78-4.75 (m, 1H), 4.71-4.67 (m, 1H), 3.47 (s, 2H), 2.33-2.20 (m, 7H), 2.19-2.11 (m, 1H), 1.90-1.55 (m, 6H), 1.53-1.40 (m, 1H), 1.13 (q, J = 11.8 Hz, 1H), 1.07-0.97 (m, 1H), 0.95 (d, J = 6.5 Hz, 3H).

^{13}C NMR (100 MHz, $CDCl_3$): δ 165.9, 146.1, 143.7, 129.7, 129.6, 128.8, 111.9, 74.2, 64.0, 50.9, 45.4 (2C), 40.5, 34.2, 31.4, 30.5, 22.0, 19.5.

HRMS (ESI) m/z calculated for $[M+H]^+$ 316.2271, found 316.2276.

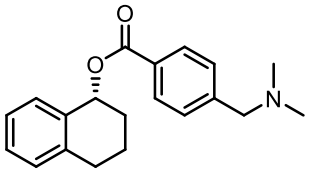

(*R*)-1,2,3,4-tetrahydronaphthalen-1-yl 4-((dimethylamino)methyl)benzoate, S8

A flame-dried round bottom flask was charged with 0.217 g (1.46 mmol) of (*R*)-1,2,3,4- tetrahydronaphthalen-1-ol, 0.453 g (2.20 mmol) of DCC, and 0.036 g (0.29 mmol)

of DMAP. The contents of the flask were suspended in 10 mL of CH_2Cl_2 and allowed to stir for 5 minutes before 0.330 g (2.20 mmol) of 4-formylbenzoic acid. Upon completion, the reaction was filtered through a plug of cotton and the solvent removed. The crude material was purified by chromatography to yield the ester. A flame-dried round bottom flask was charged with 0.381 g (1.40 mmol) of the ester and 0.143 g (1.78 mmol) of dimethylamine hydrochloride. The contents of the flask were suspended in CH_2Cl_2 and cooled to 0 °C. 0.445 g (2.10 mmol) of sodium triacetoxyborohydride was then added over half an hour. Upon completion, the reaction was quenched with ethyl acetate and a solution of sat'd sodium bicarbonate. The organic layer was extracted twice with a solution of sat'd sodium bicarbonate and once with a solution of brine. The solvent was removed from the organic layer and the resulting residue was suspended in 1 M HCl until pH ~2. The aqueous layer was extracted three times with diethyl ether and then basified to pH ~8 with a solution of sat'd sodium bicarbonate. The aqueous solution was extracted thrice with CH_2Cl_2, the organic layers combined, dried over sodium sulfate, and the solvent removed to yield 0.333 g (77%) of the desired product.

^{1}H NMR (400 MHz, $CDCl_3$) δ 7.99 (d, J = 8.2 Hz, 2H), 7.40 – 7.31 (m, 3H), 7.29 – 7.20 (m, 1H), 7.16 (m, 2H), 6.23 (t, J = 4.5 Hz, 1H), 3.45 (s, 2H), 2.96 – 2.86 (m, 1H), 2.85 – 2.74 (m, 1H), 2.22 (s, 6H), 2.15 – 1.98 (m, 3H), 1.87 (m, 1H);

^{13}C NMR (100 MHz, $CDCl_3$) δ 166.2, 144.1, 138.0, 134.7, 129.7, 129.5, 129.5, 129.0, 128.8, 128.0, 126.0, 70.5, 64.0, 45.4, 29.2, 29.0, 19.1.

HRMS (ESI) m/z calculated for [M+H]+ 310.1802, found 310.1808.

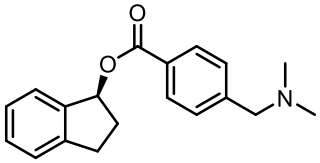

(*S*)-2,3-dihydro-1H-inden-1-yl 4-((dimethylamino)methyl)benzoate, S9

A flame-dried round bottom flask was charged with 0.200 g (1.50 mmol) of (*S*)-2,3-dihydro-1H-inden- 1-ol, 0.464 g (2.25 mmol) of DCC, and 0.027 g (0.225 mmol) of DMAP. The contents of the flask were suspended in 16 mL of CH_2Cl_2 and allowed to stir for 5 minutes before 0.338 g (2.25 mmol) of 4-formylbenzoic acid. Upon completion, the reaction was filtered through a plug of cotton and the solvent removed. The crude material was purified by chromatography (Hexanes to 20% ethyl acetate in hexanes) to yield 0.323 g (81%) of the desired product.

^{1}H NMR (700 MHz, $CDCl_3$) δ 10.09 (s, 1H), 8.19 (d, J = 8.4 Hz, 2H), 7.93 (d, J = 8.4 Hz, 2H), 7.50 (d, J = 7.5 Hz, 1H), 7.36 – 7.31 (m, 2H), 7.29 – 7.23 (m, 1H), 6.48 (dd, J = 7.1, 3.8 Hz, 1H), 3.21 (ddd, J = 15.3, 8.4, 6.2 Hz, 1H), 2.97 (ddd, J = 16.0, 8.6, 4.9 Hz, 1H), 2.69 – 2.61 (m, 1H), 2.31 – 2.23 (m, 1H).

^{13}C NMR (176 MHz, $CDCl_3$) δ 191.6, 165.5, 144.5, 140.7, 139.1, 135.5, 130.3, 129.4, 129.2, 126.8, 125.7, 124.9, 79.7, 32.4, 30.3;

IR (thin film, cm^{-1}) 2933, 2841, 1709, 1264.

A flame-dried round bottom flask was charged with 0.283 g (1.06 mmol) of (*S*)-2,3-dihydro-1H-inden- 1-yl 4-formylbenzoate and 0.112 g (1.38 mmol) of dimethylamine hydrochloride. The contents of the flask were suspended in DCM and cooled to 0 °C. 0.337 g (1.59 mmol) of sodium triacetoxyborohydride was then added over half an hour. Upon completion, the reaction was quenched with ethyl acetate and a solution of sat'd sodium bicarbonate. The organic layer was extracted twice with a solution of sat'd sodium

bicarbonate and once with a solution of brine. The solvent was removed from the organic layer and the resulting residue was suspended in 1 M HCl until pH ~2. The aqueous layer was extracted three times with diethyl ether and then basified to pH ~8 with a solution of sat'd sodium bicarbonate. The aqueous solution was extracted thrice with CH_2Cl_2, the organic layers combined, dried over sodium sulfate, and the solvent removed to yield 0.232 g (74%) of the desired product.

^{1}H NMR (500 MHz, $CDCl_3$) δ 8.03 – 7.96 (m, 2H), 7.49 (d, J = 7.5 Hz, 1H), 7.36 (d, J = 8.0 Hz, 2H), 7.33 – 7.30 (m, 2H), 7.28 – 7.21 (m, 1H), 6.45 (dd, J = 7.1, 4.1 Hz, 1H), 3.46 (s, 2H), 3.18 (ddd, J = 15.9, 8.5, 5.9 Hz, 1H), 2.95 (ddd, J = 16.0, 8.6, 5.2 Hz, 1H), 2.68 – 2.59 (m, 1H), 2.28 – 2.19 (m, 7H);

^{13}C NMR (176 MHz, $CDCl_3$) δ 166.5, 144.4, 144.3, 141.2, 129.7, 129.3, 128.9, 128.8, 126.7, 125.7, 124.8, 78.8, 64.0, 45.4, 32.5, 30.3.

IR (thin film, cm-^{1}) 2941, 2878, 2816, 2767, 1711, 1456, 1264.

HRMS (ESI) m/z calculated for $[M+H]^+$ 296.1645, found 296.1646.

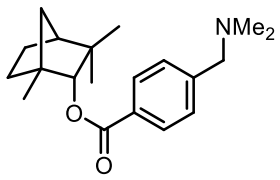

(1*R*,2*R*,4*S*)-1,3,3-trimethylbicyclo[2.2.1]heptan-2-yl-4-((dimethylamino)methyl)benzoate, S10

A flame-dried round bottom flask was charged with 1.000 g (6.50 mmol) of (+)-fenchol, 2.060 g (10.0 mmol) of DCC, and 0.159 g (1.30 mmol) of DMAP. The contents of the flask were suspended in 30 mL of CH_2Cl_2 and allowed to stir for 5 minutes before 1.500 g (10.00 mmol) of 4-formylbenzoic acid. Upon completion, the reaction was filtered through a plug of cotton and the solvent removed. The crude material was purified by

chromatography to yield the ester. A flame-dried round bottom flask was charged with 0.530 g (1.85 mmol) of the ester and 0.195 g (2.41 mmol) of dimethylamine hydrochloride. The contents of the flask were suspended in CH_2Cl_2 and cooled to 0 °C. 0.588 g (2.78 mmol) of sodium triacetoxyborohydride was then added over half an hour. Upon completion, the reaction was quenched with ethyl acetate and a solution of sat'd sodium bicarbonate. The organic layer was extracted twice with a solution of sat'd sodium bicarbonate and once with a solution of brine. The solvent was removed from the organic layer and the resulting residue was suspended in 1 M HCl until pH ~2. The aqueous layer was extracted three times with diethyl ether and then basified to pH ~8 with a solution of sat'd sodium bicarbonate. The aqueous solution was extracted thrice with CH_2Cl_2, the organic layers combined, dried over sodium sulfate, and the solvent removed to yield 0.414 g (71%) of the desired product.

^{1}H NMR (400 MHz, $CDCl_3$) δ 8.01 (d, J = 8.1 Hz, 2H), 7.40 (d, J = 8.1 Hz, 2H), 4.62 (s, 1H), 3.48 (s, 2H), 2.26 (s, 6H), 1.99 – 1.88 (m, 1H), 1.77 (d, J = 9.0 Hz, 2H), 1.67 (d, J = 11.7 Hz, 1H), 1.49 (s, 1H), 1.27 (s, 2H), 1.18 (s, 3H), 1.11 (s, 3H), 0.84 (s, 3H).

^{13}C NMR (126 MHz, $CDCl_3$) δ 166.8, 129.5, 128.9, 86.6, 64.0, 48.6, 48.4, 45.4, 41.5, 39.8, 29.8, 26.9, 25.9, 20.3, 19.5.

HRMS (ESI) m/z calculated for [M+H]+ 316.2271, found 316.2268.

5.2.2: Product Characterization

General protocol for anchoring group cleavage

A flame-dried round bottom flask was charged with lithium aluminium hydride (5.0 eq). Under N_2, the contents of the flask were suspended in 2 mL of THF and cooled to 0

°C. The solution of product from P450 oxidation in THF (1 mL) was then added dropwise via cannula. The reaction mixture was warmed to room temperature and stirred overnight, at which point H_2O (0.1 mL), 15% NaOH in H_2O (0.1 mL) and H_2O (0.2 mL) were added sequentially to quench the reaction. The mixture was diluted with EtOAc (10 mL), filtered to remove aluminum salts and the filtrate was concentrated. The residue obtained was purified by column chromatography to yield the product.

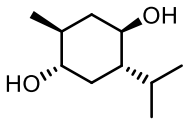

(1R,2S,4S,5S)-2-isopropyl-5-methylcyclohexane-1,4-diol (9)[125]**:**

^{1}H NMR (400 MHz, $CDCl_3$): δ 3.47 (td, J = 10.5, 4.4 Hz, 1H), 3.19 (ddd, J = 10.9, 9.7, 4.3 Hz, 1H), 2.19-2.10 (m, 1H), 1.96 (dt, J = 12.7, 4.1 Hz, 1H), 1.85 (ddd, J = 12.6, 4.3, 3.4 Hz, 1H), 1.47-1.23 (m, 4H), 1.17-1.04 (m, 2H), 1.03 (d, J = 6.5 Hz, 3H), 0.94 (d, J = 7.0 Hz, 3H), 0.83 (d, J = 6.9 Hz, 3H).

^{13}C NMR (176 MHz, $CDCl_3$): δ 76.0, 70.7, 48.5, 42.5, 38.3, 32.3, 25.8, 21.0, 18.2, 15.9;

IR (neat, cm^{-1}): 3230.0, 2926.2, 1456.0, 1095.8, 1026.9.

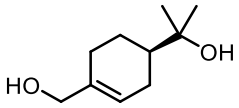

(R)-2-(4-(hydroxymethyl)cyclohex-3-en-1-yl)propan-2-ol, S11

^{1}H NMR (400 MHz, $CDCl_3$): δ 5.72-5.66 (m, 1H), 4.01 (t, J = 2.6 Hz, 2H), 2.22-2.01 (m, 3H), 2.00-1.93 (m, 1H), 1.92-1.80 (m, 1H), 1.60-1.50 (m, 1H), 1.35 – 1.25 (m, 3H), 1.20 (s, 3H), 1.19 (s, 3H).

^{13}C NMR (100 MHz, $CDCl_3$): δ 137.5, 122.4, 72.7, 67.1, 45.1, 27.4, 26.6, 26.5, 26.4, 23.6.

HRMS (ESI) m/z calculated for $[M+H]^+$ 171.1380, found 188.1645.

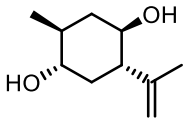

(1S,2S,4R,5S)-2-methyl-5-(prop-1-en-2-yl)cyclohexane-1,4-diol, S12

^{1}H NMR (400 MHz, $CDCl_3$): δ 4.94-4.90 (m, 1H), 4.87-4.84 (m, 1H), 3.52 (td, J = 10.5, 4.3 Hz, 1H), 3.31-3.21 (m, 1H), 2.13-2.00 (m, 2H), 1.92 (dt, J = 12.7, 3.9 Hz, 1H), 1.86-1.80 (m, 1H), 1.74-1.69 (m, 3H), 1.54-1.37 (m, 3H), 1.19-1.09 (m, 1H), 1.06 (d, J = 6.5 Hz, 3H).

^{13}C NMR (100 MHz, $CDCl_3$): δ 145.2, 113.6, 75.3, 69.6, 52.5, 40.3, 38.2, 38.0, 19.0, 18.2.

HRMS (ESI) m/z calculated for $[M+H]^+$ 171.1380, found 188.1654.

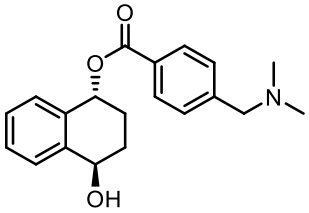

(1R,4R)-4-hydroxy-1,2,3,4-tetrahydronaphthalen-1-yl-4-((dimethylamino)methyl)benzoate, (13):

^{1}H NMR (400 MHz, $CDCl_3$) δ 7.98 (d, J = 8.2 Hz, 2H), 7.50 (d, J = 7.4 Hz, 1H), 7.41 – 7.33 (m, 4H), 7.30 (t, J = 7.4 Hz, 1H), 6.26 (t, J = 4.8 Hz, 1H), 4.92 (t, J = 4.7 Hz, 1H), 3.46 (s, 2H), 2.51 – 2.41 (m, 1H), 2.41 – 2.31 (m, 1H), 2.23 (s, 6H), 2.09 – 1.99 (m, 1H), 1.99 – 1.92 (m, 1H).

^{13}C NMR (100 MHz, $CDCl_3$) δ 166.1, 144.3, 139.4, 134.4, 129.7, 129.4, 129.2, 128.9, 128.8, 128.6, 128.3, 70.0, 67.5, 64.0, 45.4, 28.4, 25.0;

IR (thin film, cm^{-1}) 3398, 2940, 2776, 1708, 1453, 1263.

HRMS (ESI) m/z calculated for $[M+H]^+$ 326.1751, found 326.1753.

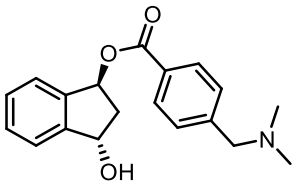

(1S,3S)-3-hydroxy-2,3-dihydro-1H-inden-1-yl 4-((dimethylamino)methyl)benzoate, (14):

^{1}H NMR (500 MHz, $CDCl_3$) δ 7.97 (d, J = 8.1 Hz, 2H), 7.53 (d, J = 7.5 Hz, 1H), 7.50 (d, J = 7.5 Hz, 1H), 7.43 (t, J = 7.4 Hz, 1H), 7.37 (m, 3H), 6.56 (dd, J = 6.7, 2.9 Hz, 1H), 5.56 (t, J = 5.7 Hz, 1H), 3.48 (s, 2H), 2.74 – 2.64 (m, 1H), 2.53 – 2.42 (m, 1H), 2.25 (s, 6H); **^{13}C NMR (126 MHz, $CDCl_3$)** δ 166.4, 145.9, 140.6, 129.8, 129.0, 128.9, 126.2, 124.4, 76.7, 74.4, 63.9, 45.3, 43.5.

IR (thin film, cm^{-1}) 3388, 2932, 1712, 1611, 1459, 1268, 1175.

HRMS (ESI) m/z calculated for $[M+H]^+$ 312.1594, found 312.1598.

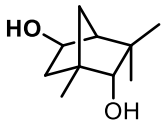

(1S,2R,4S,5R)-1,3,3-trimethylbicyclo[2.2.1]heptane-2,5-diol, S13

^{1}H NMR (500 MHz, $CDCl_3$) δ 4.17 – 4.13 (m, 1H), 3.23 (d, J = 1.6 Hz, 1H), 2.18 (ddd, J = 13.8, 6.7, 2.5 Hz, 1H), 1.70 (s, 1H), 1.56 (dd, J = 10.6, 1.6 Hz, 1H), 1.37 (d, J = 10.6 Hz, 1H), 1.20 (d, J = 6.2 Hz, 1H), 1.12 (s, 3H), 1.03 (s, 3H), 0.84 (s, 3H).

^{13}C NMR (126 MHz, $CDCl_3$) δ 83.5, 71.5, 55.6, 48.5, 38.8, 38.1, 36.5, 30.6, 19.5, 18.9;

IR (thin film, cm^{-1}) 3341, 2944, 1277, 1071.

LRMS (EI) m/z calculated for [M] 170.1, found 170.0.

5.3 Chapter 3 Experimental

5.3.1 Macrocycle Synthesis

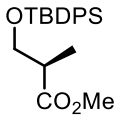

Methyl (*R*)-3-((tert-butyldiphenylsilyl)oxy)-2-methylpropanoate (26):

To an oven-dried flask equipped with stir bar was added 5.055 g (42.79 mmol) of methyl (*R*)-3-hydroxy-2-methylpropanoate, 120 mL of DMF, and 12.938 g (47.071 mmol) of TBDPSCl sequentially. The contents were stirred for ~5 min before the addition of 7.283 g (106.98 mmol) of imidazole. The reaction was stirred overnight. The following day, the reaction was quenched by transferring to a separatory funnel with H_2O and hexanes. The organic layer was washed four times with H_2O and once with brine. The organic layer was dried over $MgSO_4$, filtered, and concentrated. The spectra matched that of previous reports and the crude material was carried on without further purification.[126]

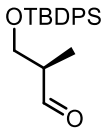

Methyl (*R*)-3-((tert-butyldiphenylsilyl)oxy)-2-methylpropanoate (27):

An oven-dried flask equipped with stir bar was charged with 12.0 g (33.66 mmol) of **26** and 166 mL of hexanes. The contents were cooled to -78 °C and 50.490 mL of a 1M solution of DIBAL-H in hexanes was added by syringe drive over 30 min. Upon complete addition the reaction was stirred for an additional 45 min. The reaction was quenched with the addition of 25 mL of MeOH at -78 °C and allowed to stir for 10 min. The reaction was transferred cold to a flask containing stirring sat'd aqueous Rochelle's salt and Et_2O. The solution was stirred vigorously until a biphasic mixture formed (~1 hour). Once

complete, the contents were transferred to a separatory funnel and the aqueous layer was extracted three times with Et_2O. The organic layers were combined, dried over $MgSO_4$, filtered, and concentrated to yield the title compound, which matched previously reported spectra and was carried on directly to the next reaction.[126]

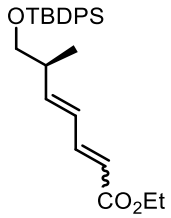

Ethyl (*S*,4*E*)-7-((tert-butyldiphenylsilyl)oxy)-6-methylhepta-2,4-dienoate (28):

To a solution of 13.50 mL (103 mmol) of diisopropylamine in THF (173 mL) cooled to -78 °C under a nitrogen atmosphere was added 27.46 mL (68.66 mmol) of *n*-BuLi dropwise. The solution was warmed to rt and stir for 20 min before being cooled to -78 °C. 20.15 mL (85.50 mmol) of ethyl 4-(diethoxyphosphoryl)but-2-enoate was then added dropwise and the solution allowed to warm to 0 °C and stir for 20 min before being cooled to -78 °C. 33.66 mmol of (*R*)-3-((tert-butyldiphenylsilyl)oxy)-2-methylpropanal (**27**) was then added dropwise as a solution in 30 mL of THF. The reaction was stirred at -78 °C for 15 min before warming to -15 °C and stirring for 2 hours. The reaction was quenched by the addition of sat'd aqueous NH_4Cl and transferred to a separatory funnel. The aqueous phase was extracted 3x with EtOAc/hexanes (1:1), and the organic layers were combined, dried over Na_2SO_4, filtered, and concentrated. The resulting residue was purified by column chromatography (6% EtOAc/hexanes) to yield the desired diene as a mixture of *E*/*Z* isomers, which was carried on directly to the hydrogenation.

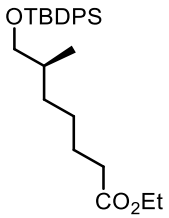

Ethyl (*S*)-7-((tert-butyldiphenylsilyl)oxy)-6-methylheptanoate (29):

28 was transferred with 4:1 MeOH/EtOAc to a flask containing a suspension of 1.682 mmol of 10% w/w Pd/C in 4:1 MeOH/EtOAc. The contents were shaken overnight in a Parr reactor at 40 psi. Upon completion, the reaction was quenched by removing the solvent until ~10 mL of solvent remained, and the resulting suspension was filtered through a plug of silica gel with ethyl acetate. The solvent was removed to yield 11.014 g (77% over four steps) of the title compound the spectra of which matched previous reports[13].

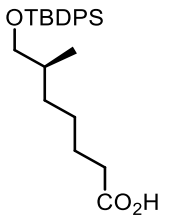

(*S*)-7-((tert-Butyldiphenylsilyl)oxy)-6-methylheptanoic acid (30):

A flask equipped with stir bar was charged with 11.014 g (25.813 mmol) of **29**, 153 mL of MeOH, and 100 mL of THF. The contents were cooled to 0 °C and 51.6 mL of 2M aqueous NaOH was added dropwise. Upon complete addition, the reaction stirred for 1h at 0 °C before warming to rt and stirring for an additional 1h. Additional aqueous 2M NaOH was added if starting material remained and stirring was continued. Upon complete consumption **29** as judged by TLC, the reaction was quenched with an aqueous potassium bisulfate solution until pH ~1-2. The aqueous layer was extracted three times with EtOAc, the organic layers combined, dried over $MgSO_4$, filtered, and concentrated

to yield the desired compound, which was carried on to the next step without further purification.[115]

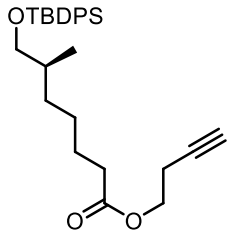

But-3-yn-1-yl (*S*)-7-((tert-butyldiphenylsilyl)oxy)-6-methylheptanoate (31):

An oven-dried flask equipped with stir bar was charged with 25.813 mmol of the crude **30**, 7.237 g (103.25 mmol) of but-3-yn-1-ol, and 210 mL of CH_2Cl_2. After stirring for 5min, 7.456 g (36.138 mmol) of DCC and 3.154 g (25.813 mmol) of DMAP were added sequentially. The reaction was stirred overnight before being quenched by dilution with hexanes, filtration, and removal of the solvent. The remaining residue was purified by chromatography (5% EtOAc/hexanes) to give 10.541 g (91% over two steps) of the title compound, whose spectra matched previous reports.[115]

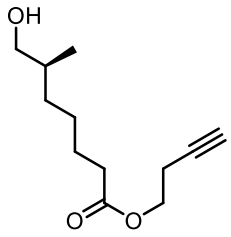

But-3-yn-1-yl (*S*)-7-hydroxy-6-methylheptanoate (32):

An oven-dried flask equipped with stir bar was charged with 10.541 g (23.389 mmol) of **31** and 54 mL of THF. The contents were cooled to 0 °C whereupon 52.86 mL of a 1M solution of *n*-Bu_4NF was added dropwise. The reaction was stirred for 1h at 0 °C before warming to rt. Upon consumption **31** as judged by TLC, the reaction was quenched with a sat'd solution of NH_4Cl and transferred to a separatory funnel. The aqueous layer was

extracted three times with Et_2O, the organic layers were combined, dried over $MgSO_4$, filtered, and concentrated. Purification of the crude material by chromatography (30% EtOAc/hexanes) afforded 4.419 g (89%) of the title compound as a clear oil whose spectra matched that of previous reports[13].[115]

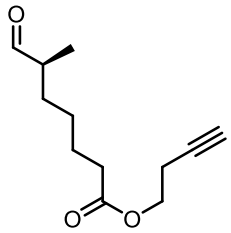

But-3-yn-1-yl (*S*)-6-methyl-7-oxoheptanoate (33):

To an oven dried vial equipped with stir bar was added 0.071g (0.333 mmol) of **S7**, 3.40 mL of CH_2Cl_2, and 0.145 mL (1.782 mmol) of pyridine. The contents were cooled to 0 °C and 0.378 g (0.891 mmol) of Dess-Martin periodinane was added in a single portion. After stirring at 0 °C for 10 min, the reaction was warmed to rt and stirred for 1 h. A 1:1 solution of sat'd aqueous sodium bicarbonate and sat'd aqueous sodium thiosulfate was added and the mixture stirred for 30 min. The aqueous layer was extracted three times with Et_2O, the organic layers were combined, dried over $MgSO_4$, filtered and concentrated. Purification by chromatography (15% EtOAc/hexanes) afforded 0.057 g (90%) of the title compound as a clear oil whose spectra matched previous reports.[115]

But-3-yn-1-yl (*R*)-6-methyl-7-oxoheptanoate (***R*-33)** was prepared in the same manner with matching ^1H spectra starting from methyl (*S*)-3-hydroxy-2-methylpropanoate.

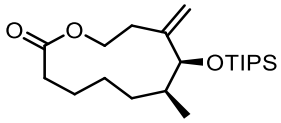

(7*S*,8*S*)-7-Methyl-9-methylene-8-((triisopropylsilyl)oxy)oxacycloundecan-2-one (34A):

In a glovebox, an oven-dried flask equipped with stir bar was charged with 0.019 g (0.069 mmol) of $Ni(COD)_2$ and 0.029 g (0.063 mmol) of IPr^{Cl}. The flask was capped with a septum, removed from the glovebox, and attached to a nitrogen line. The contents of the flask were suspended in toluene (6.3 mL) and allowed to stir for 20 min. The contents were diluted with an additional 31.4 mL of toluene and heated to 60 °C in an oil bath for 20 min. Triisopropylsilane (0.214 mL, 1.05 mmol) was then added in a single portion. Ynal **33** (0.044 g**,** 0.209 mmol) was then added by syringe drive over 1 hour as a 4.15 mL solution in toluene. The reaction was stirred overnight at 60 °C. The reaction was cooled to rt and the volatiles removed under vacuum. The crude residue was filtered through a plug of silica with EtOAc/Hexanes (1:1) and then purified by column chromatography (2% EtOAc/Hexanes) to yield 0.044 g (60%) of the title compound as a colorless oil.[115]

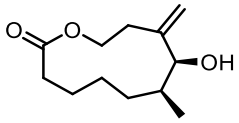

(7*S*,8*S*)-8-Hydroxy-7-methyl-9-methyleneoxacycloundecan-2-one (34B):

An oven-dried flask equipped with stir bar was charged with 0.047 g (0.127 mmol) of (7*S*,8*S*)-7-methyl-9-methylene-8-((triisopropylsilyl)oxy)oxacycloundecan-2-one and THF (5.11 mL). The contents of the flask were cooled to 0 °C and 0.015 mL (0.225 mmol) of acetic acid and 1.53 mL of a 1M solution of TBAF were added sequentially. The reaction was warmed to rt and stir until all the starting material was consumed as judged by TLC.

Upon completion, the reaction was quenched with sat'd aqueous NH_4Cl and transferred to a separatory funnel. The aqueous layer was extracted three times with Et_2O, and the organic layers were combined, dried over $MgSO_4$, filtered, and concentrated. The crude residue was purified by column chromatography (30% EtOAc/Hexanes) to yield the desired product as a white solid.

^{1}H NMR (700 MHz, $CDCl_3$) δ 5.29 – 5.26 (m, 1H), 5.20 (s, 1H), 4.91 (ddd, *J* = 13.3, 10.9, 2.5 Hz, 1H), 3.99 (s, 1H), 3.95 (ddd, *J* = 10.9, 4.1, 2.4 Hz, 1H), 2.49 (ddd, *J* = 16.0, 7.6, 1.8 Hz, 1H), 2.40 – 2.34 (m, 1H), 2.17 (dddd, *J* = 15.2, 13.0, 4.1, 2.0 Hz, 1H), 2.10 (ddd, *J* = 16.0, 11.9, 1.8 Hz, 1H), 2.07 – 2.00 (m, 1H), 1.91 – 1.83 (m, 1H), 1.67 – 1.59 (m, 1H), 1.59 – 1.53 (m, 1H), 1.48 (d, *J* = 4.6 Hz, 1H), 1.46 – 1.40 (m, 1H), 1.39 – 1.33 (m, 1H), 1.05 (d, *J* = 6.9 Hz, 3H), 1.03 – 0.98 (m, 1H).

^{13}C NMR (176 MHz, $CDCl_3$) δ 173.79, 148.01, 110.98, 79.70, 64.12, 35.24, 30.87, 29.18, 25.79, 23.41, 20.12, 16.92.

HRMS (ESI) *m/z* calculated for $[M+H]^+$ 213.1485, found 213.1475.

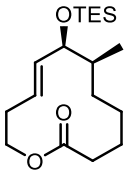

(7*S*,8*S*,*E*)-7-Methyl-8-((triethylsilyl)oxy)oxacyclododec-9-en-2-one (35A):

In a glovebox, an oven-dried flask equipped with stir bar was charged with 0.019 g (0.069 mmol) of $Ni(COD)_2$, 0.023 g (0.069 mmol) of IMes•HCl, and 0.008 g (0.069 mmol) of potassium *tert*-butoxide. The flask was sealed with a septum, removed from the glovebox, and attached to a nitrogen line. The contents of the flask were suspended in THF (16.60 mL) and stirred for 20 min at rt. Triethylsilane (0.073 mL, 0.456 mmol) was then added in a single portion. Ynal **33** (0.048 g, 0.228 mmol) was suspended in 16.6

mL of THF and added to the reaction by syringe drive over 3 h and was stirred overnight. The volatiles were removed under vacuum, the crude residue was filtered through a plug of silica with EtOAc/Hexanes (1:1), and the volatiles were removed under vacuum. The resulting residue was purified by column chromatography (4% EtOAc/Hexanes) to yield 0.051 g (69%) of the desired product as a clear oil.

^{1}H NMR (500 MHz, $CDCl_3$) δ 5.53 (dd, *J* = 20.0, 14.0 Hz, 1H), 5.39 (dt, *J* = 14.8, 7.1 Hz, 1H), 4.71 (dt, *J* = 11.0, 7.3 Hz, 1H), 4.13 (dd, *J* = 8.1, 4.7 Hz, 1H), 3.91 (dt, *J* = 11.0, 4.3 Hz, 1H), 2.42 – 2.36 (m, 2H), 2.33 – 2.28 (m, 2H), 1.92 – 1.83 (m, 1H), 1.75 – 1.66 (m, 1H), 1.49 – 1.38 (m, 1H), 1.35 – 1.27 (m, 3H), 0.97 – 0.88 (m, 13H), 0.60 – 0.52 (m, 6H).

^{13}C NMR (176 MHz, $CDCl_3$) δ 173.78, 133.70, 127.67, 74.99, 61.10, 37.57, 33.21, 32.41, 30.94, 24.25, 23.40, 16.08, 6.88, 4.98.

HRMS (ESI) *m/z* calculated for $[M+NH_4]^+$ 344.2615, found 344.2609.

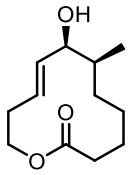

(7*S*,8S,*E*)-8-Hydroxy-7-methyloxacyclododec-9-en-2-one (35B):

To an oven-dried flask equipped with stir bar was added 0.051 g (0.156 mmol) of (7*S*,8*S*,*E*)-7-methyl-8-((triethylsilyl)oxy)oxacyclododec-9-en-2-one and THF (6.30 mL). The contents of the flask were cooled to 0 °C and 0.018 mL (0.312 mmol) of acetic acid and 1.87 mL of a 1M solution *of n*-Bu_4NF were added sequentially. The reaction was warmed to rt and stir until all the starting material was consumed as judged by TLC. The reaction was quenched by the addition of sat'd aqueous NH_4Cl. The contents of the flask were transferred to a separatory funnel, the aqueous phase was extracted three times with Et_2O, and the organic layers were combined, dried over $MgSO_4$, filtered, and

concentrated. The crude residue was purified by column chromatography (30% EtOAc/Hexanes) to yield 0.031 g (94%) of the desired product as a white solid.

^{1}H NMR (500 MHz, $CDCl_3$) δ 5.58 (dd, *J* = 15.3, 7.2 Hz, 1H), 5.55 – 5.47 (m, 1H), 4.63 (ddd, *J* = 11.0, 7.9, 5.5 Hz, 1H), 4.18 (dd, *J* = 7.2, 4.3 Hz, 1H), 3.98 (dt, *J* = 11.0, 4.7 Hz, 1H), 2.43 – 2.38 (m, 2H), 2.33 – 2.29 (m, 2H), 1.89 – 1.77 (m, 2H), 1.51 – 1.41 (m, 1H), 1.38 – 1.24 (m, 3H), 1.20 – 1.09 (m, 1H), 0.99 (d, *J* = 6.9 Hz, 3H).

^{13}C NMR (126 MHz, $CDCl_3$) δ 173.65, 133.51, 128.18, 74.70, 61.14, 36.33, 33.14, 32.60, 30.79, 24.19, 23.66, 16.08.

HRMS (ESI) *m/z* calculated for $[M+Na]^+$ 235.1305, found 235.1301.

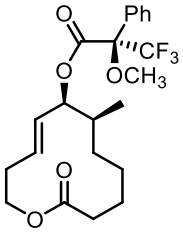

(6*S*,7*S*,*E*)-7-Methyl-12-oxooxacyclododec-4-en-6-yl (*R*)-3,3,3-trifluoro-2-methoxy-2-phenylpropanoate ((*R*)-MTPA-35B):

An oven-dried vial equipped with stir bar was charged with 0.005 g (0.024 mmol) of **35B**, 0.017 g (0.071 mmol) of (*R*)-3,3,3-trifluoro-2-methoxy-2-phenylpropanoic acid, 0.015 g (0.071 mmol) of DCC, 0.003 g (0.024 mmol) of DMAP and 0.50 mL of CH_2Cl_2 sequentially. Upon consumption of the starting material as judged by TLC, the reaction was filtered through a plug of cotton and the solvent removed. Purification by column chromatography (10% EtOAc/hex) of the resulting residue afforded 0.010 g (97%) of the desired product as a clear oil.

^{1}H NMR (500 MHz, $CDCl_3$) δ 7.54 – 7.46 (m, 2H), 7.44 – 7.35 (m, 3H), 5.61 (ddd, *J* = 14.6, 9.3, 5.1 Hz, 1H), 5.52 (dd, *J* = 8.5, 4.5 Hz, 1H), 5.46 (ddd, *J* = 15.1, 8.3, 1.3 Hz, 1H),

4.70 (td, *J* = 10.7, 4.0 Hz, 1H), 3.89 (dt, *J* = 11.0, 4.2 Hz, 1H), 3.52 (d, *J* = 1.3 Hz, 3H), 2.47 – 2.24 (m, 4H), 2.03 – 1.94 (m, 1H), 1.94 – 1.83 (m, 1H), 1.46 (dtt, *J* = 12.6, 8.0, 4.3 Hz, 1H), 1.42 – 1.28 (m, 3H), 1.24 – 1.12 (m, 1H), 0.96 (d, *J* = 6.9 Hz, 3H).

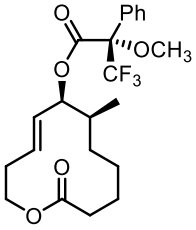

(6*S*,7*S*,*E*)-7-Methyl-12-oxooxacyclododec-4-en-6-yl (*S*)-3,3,3-trifluoro-2-methoxy-2-phenylpropanoate ((*S*)-MTPA-35B):

Following the same procedure used to synthesize **(**6*S*,7*S*,*E*)-7-methyl-12-oxooxacyclododec-4-en-6-yl (*R*)-3,3,3-trifluoro-2-methoxy-2-phenylpropanoate, 0.005 g (0.024 mmol) of **35B**, 0.017 g (0.071 mmol) of (*S*)-3,3,3-trifluoro-2-methoxy-2-phenylpropanoic acid, 0.015 g (0.071 mmol) of DCC, and 0.003 g (0.024 mmol) of DMAP were employed to give 0.010 g of the title compound.

^{1}H NMR (500 MHz, $CDCl_3$) δ 7.56 – 7.46 (m, 2H), 7.45 – 7.34 (m, 3H), 5.73 – 5.61 (m, 1H), 5.61 – 5.49 (m, 2H), 4.74 (ddd, *J* = 10.9, 9.0, 5.5 Hz, 1H), 3.89 (dt, *J* = 11.0, 4.1 Hz, 1H), 3.54 (s, 3H), 2.48 – 2.38 (m, 2H), 2.38 – 2.25 (m, 2H), 2.01 – 1.83 (m, 2H), 1.46 (ddq, *J* = 13.6, 8.8, 4.5 Hz, 1H), 1.35 (tq, *J* = 10.4, 4.9 Hz, 3H), 1.16 (td, *J* = 11.9, 11.4, 4.5 Hz, 1H), 0.85 (d, *J* = 6.9 Hz, 3H).

See Figure 5.1 for the stereochemical determination of the secondary allylic alcohol via ^{1}H NMR.

The products of the nickel-catalyzed macrocyclization of but-3-yn-1-yl (*R*)-6-methyl-7-oxoheptanoate (***R*-33**) and subsequent deprotection yielded **(*R,R*)-34A** and **(*R,R*)-34B** macrocycles whose spectra matched those of (**34A**) and (**34B**).

5.3.2: Triazole Anchor Assembly

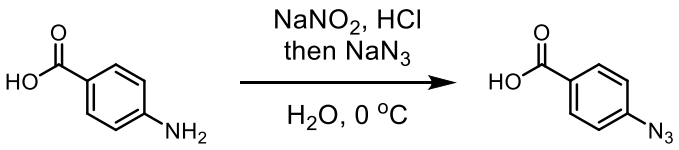

4-Azidobenzoic acid

A flask equipped with stir bar was charged with 5.0 g (36.46 mmol) of 4-aminobenzoic acid and suspended in 150 mL of 5% aqueous HCl. The flask was placed in the dark and cooled to 0 °C followed by the addition of 2.64 g (38.28 mmol) of $NaNO_2$ as a solution in 10 mL of H_2O over 10 min. The reaction was stirred for 20 min before the addition of 2.61 g (40.10 mmol) of NaN_3 as a solution in 10 mL of H_2O over 30 min. Stirring was continued for an additional 15 min before the reaction was quenched with the addition of 200 mL of Et_2O. The contents were transferred to a separatory funnel and the organic layer was extracted four times with H_2O and once with brine. The organic layer was dried over $MgSO_4$, filtered, and concentrated to yield 4.358 g (73%) of the title compound as a yellow powder that was used without further purification. ^1H spectra matched that of previously reported compound.[127]

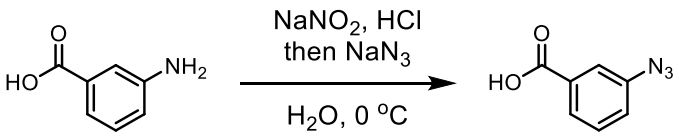

3-Azidobenzoic acid

The title compound was prepared in a method analogous to 4-azidobenzoic acid employing 5.0 g (36.46 mmol) of 3-aminobenzoic acid, 2.64 g (38.28 mmol) of $NaNO_2$, and 2.61 g (40.10 mmol) of NaN_3 to give 4.50 g (76%) of the desired compound as a yellow solid. ^1H spectra matched that of previously reported compounds.[128]

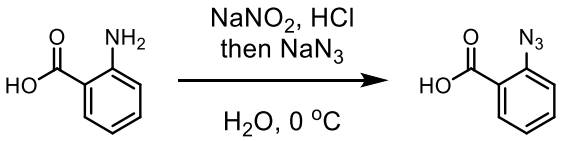

2-Azidobenzoic acid

The title compound was prepared in a method analogous to 4-azidobenzoic acid employing 5.0 g (36.46 mmol) of 2-aminobenzoic acid, 2.64 g (38.28 mmol) of $NaNO_2$, and 2.61 g (40.10 mmol) of NaN_3 to give 1.40 g (24%) of the desired compound as a yellow solid. ^1H spectra matched that of previously reported compounds.[128]

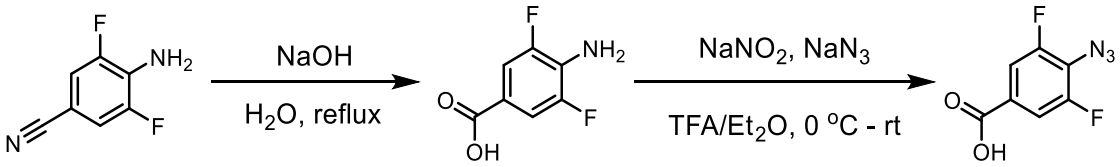

4-Azido-3,5-difluorobenzoic acid

The title compound was synthesized from commercially available 4-amino-3,5-difluorobenzonitrile according to previously reported procedures.[129,130]

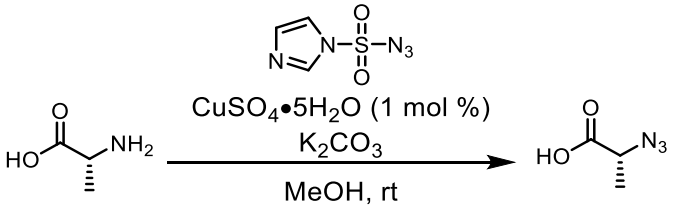

(*R*)-2-Azidopropanoic acid

The title compound was prepared according to literature precedent from D-Alanine. (*S*)-2-Azidopropanoic acid was prepared in an analogous method starting from L-Alanine.[131]

General Procedure for the attachment of PikC anchoring groups

Esterification: An oven-dried flask equipped with stir bar was charged with macrocycle, DCC, DMAP and CH_2Cl_2. The contents were stirred for 5 min before the addition of azido-

acid in a single portion. The contents were stirred until all starting material was consumed as judged by TLC. The reaction was filtered through a plug of cotton and the solvent removed under vacuum. The crude material was purified by column chromatography and carried on directly to either copper-catalyzed (CuAAC) or ruthenium-catalyzed (RuAAC) azide-alkyne cycloaddition reactions.

CuAAC: A flask equipped with stir bar was charged with azido-ester, H_2O/*t*-BuOH (1:1), and alkyne. The solution was stirred for 5 min before sequential addition of 10 mol % sodium ascorbate in 0.050 mL of H_2O and 1 mol% $CuSO_4 \cdot 5H_2O$ in 0.050 mL of H_2O. The reaction was stirred until the starting material was consumed as judged by TLC. Upon completion, the reaction was diluted with EtOAc and transferred to a separatory funnel containing sat'd aqueous sodium bicarbonate. The aqueous layer was extracted 3x with EtOAc, the organic layers combined, dried over $NaSO_4$, filtered, and concentrated. The crude residue was purified by column chromatography to yield the desired substrate.[119]

RuAAC: An oven-dried flask equipped with stir bar was charged with $Cp^*RuCl(PPh_3)_2$ in a glovebox. The flask was sealed with a septum, removed from the glovebox, and placed on a nitrogen line. Dioxane was then added and the solution stirred for 5 min. A solution of azido-ester and alkyne in dioxane was then added in a single portion. The reaction was then heated to 60 °C and allowed to stir until the starting material was consumed as judged by TLC. Upon completion, reaction was cooled to rt and the volatiles removed under vacuum. The crude residue was purified by column chromatography to yield the desired substrate.[120]

Several substrates could not be separated from trace triphenylphosphine oxide, in which case they were prepared using the following protocol:

An oven-dried flask equipped with stir bar was charged with Cp*RuCl(COD) in a glovebox. The flask was sealed with a septum, removed from the glovebox, and placed on a nitrogen line. Toluene was then added, and the solution was stirred for ~5 min. A solution of azido-ester and alkyne in toluene was then added in a single portion and reaction stirred until all the starting material was consumed as judged by TLC. Upon completion, the solvent was removed, and the crude residue was purified by column chromatography to yield the desired substrate.[120]

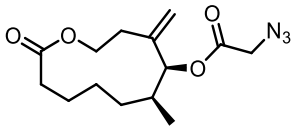

(5*S*,6*S*)-6-Methyl-4-methylene-11-oxooxacycloundecan-5-yl 2-azidoacetate (S14):

Following the general esterification procedure, the reaction of 0.035 g (0.165 mmol) of (7*S*,8*S*)-8-hydroxy-7-methyl-9-methyleneoxacycloundecan-2-one, 0.029 g (0.283 mmol) of 2-azidoacetic acid, 0.058 g (0.283 mmol) of DCC, 0.003 g (0.028 mmol) of DMAP, and 3.0 mL of CH_2Cl_2 afforded 0.045g (92%) of the desired ester after purification by column chromatography (15% EtOAc/Hexanes), which was carried on directly to the CuAAC reaction.

^{1}H NMR (500 MHz, $CDCl_3$) δ 5.24 (s, 1H), 5.18 (s, 1H), 5.03 (d, *J* = 2.0 Hz, 1H), 4.93 (ddd, *J* = 13.2, 10.9, 2.6 Hz, 1H), 3.99 – 3.86 (m, 3H), 2.58 – 2.42 (m, 2H), 2.30 – 2.08 (m, 3H), 1.94 – 1.79 (m, 1H), 1.70 – 1.39 (m, 4H), 1.08 (ddt, *J* = 14.4, 11.7, 3.8 Hz, 1H), 0.96 (d, *J* = 6.8 Hz, 3H).

^{13}C NMR (100 MHz, $CDCl_3$) δ 173.60, 167.70, 142.66, 112.22, 82.40, 63.88, 50.45, 35.21, 30.93, 28.70, 25.64, 24.64, 19.92, 16.46.

HRMS (ESI) *m/z* calculated for $[M+Na]^+$ 318.1424, found 318.1425.

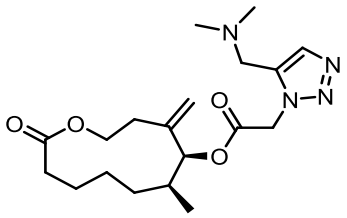

(5*S*,6*S*)-6-Methyl-4-methylene-11-oxooxacycloundecan-5-yl-2-(5-((dimethylamino)methyl)-1H-1,2,3-triazol-1-yl)acetate (38a):

Following one of the general RuAAC procedures, the reaction of 0.010 g (0.034 mmol) of (5*S*,6*S*)-6-methyl-4-methylene-11-oxooxacycloundecan-5-yl 2-azidoacetate, 0.005 mL (0.034 mmol) of N,N-dimethylprop-2-yn-1-amine, and $6.8x10^{-4}$ mmol of Cp*RuCl(COD) in 0.60 mL of toluene afforded 0.008 g (62%) of the title compound as a clear oil after purification by column chromatography (50% EtOAc/Hexanes to EtOAc).

^{1}H NMR (700 MHz, $CDCl_3$) δ 7.55 (s, 1H), 5.39 (s, 2H), 5.19 (s, 1H), 5.18 – 5.16 (m, 1H), 5.03 – 5.00 (m, 1H), 4.91 (ddd, *J* = 13.3, 10.9, 2.5 Hz, 1H), 3.92 (ddd, *J* = 10.9, 4.1, 2.3 Hz, 1H), 3.52 – 3.44 (m, 2H), 2.51 (ddd, *J* = 16.1, 7.5, 1.9 Hz, 1H), 2.46 – 2.40 (m, 1H), 2.26 – 2.06 (m, 9H), 1.91 – 1.80 (m, 1H), 1.67 – 1.52 (m, 3H), 1.51 – 1.36 (m, 2H), 0.99 – 0.79 (m, 4H).

^{13}C NMR (176 MHz, $CDCl_3$) δ 173.59, 166.12, 142.65, 134.68, 133.95, 112.12, 82.45, 63.85, 52.04, 49.43, 45.26, 35.21, 30.89, 28.68, 25.62, 24.52, 19.90, 16.44.

HRMS (ESI) *m/z* calculated for $[M+H]^+$ 379.234, found 379.2334.

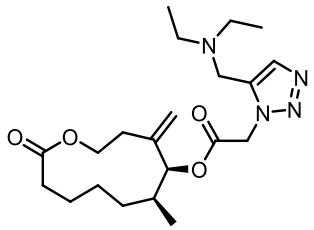

(5*S*,6*S*)-6-Methyl-4-methylene-11-oxooxacycloundecan-5-yl-2-(5-((diethylamino)methyl)-1H-1,2,3-triazol-1-yl)acetate (38b):

Following one of the general RuAAC procedures, the reaction of 0.010 g (0.034 mmol) of (5*S*,6*S*)-6-methyl-4-methylene-11-oxooxacycloundecan-5-yl 2-azidoacetate, 0.005 mL (0.034 mmol) of N,N-diethylprop-2-yn-1-amine, and 6.8×10^{-4} mmol of Cp*RuCl(COD) in 0.60 mL of toluene afforded 0.008 g (57%) of the title compound as a clear oil after purification by column chromatography (50% EtOAc/Hexanes to EtOAc).

^{1}H NMR (500 MHz, $CDCl_3$) δ 7.55 (s, 1H), 5.47 (s, 2H), 5.19 (s, 1H), 5.16 (s, 1H), 5.01 – 4.96 (m, 1H), 4.91 (ddd, *J* = 13.3, 10.9, 2.6 Hz, 1H), 3.92 (dt, *J* = 10.8, 3.2 Hz, 1H), 3.63 (s, 2H), 2.51 (dd, *J* = 16.0, 7.2 Hz, 1H), 2.44 (q, *J* = 7.2 Hz, 4H), 2.25 – 2.06 (m, 3H), 1.92 – 1.78 (m, 1H), 1.67 – 1.51 (m, 2H), 1.51 – 1.37 (m, 2H), 0.97 (t, *J* = 7.1 Hz, 6H), 0.94 – 0.86 (m, 4H).

^{13}C NMR (176 MHz, $CDCl_3$) δ 173.59, 166.26, 142.56, 135.18, 134.11, 112.25, 82.45, 63.83, 49.30, 46.61, 46.10, 35.20, 30.91, 28.70, 25.60, 24.51, 19.91, 16.48, 11.29.

HRMS (ESI) *m/z* calculated for $[M+H]^+$ 407.2653, found 407.2653.

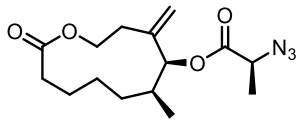

(5*S*,6*S*)-6-methyl-4-methylene-11-oxooxacycloundecan-5-yl (*S*)-2-azidopropanoate (S15):

An oven-dried vial equipped with stir bar was charged with 0.015 g (0.071 mmol) of (7*S*,8*S*)-8-Hydroxy-7-methyl-9-methyleneoxacycloundecan-2-one (**34B**), 0.024 g (0.212 mmol) of (S)-2-azidopropanoic acid, and 0.001 g (0.011 mmol) of DMAP. The contents were suspended in 1.5 mL of CH_2Cl_2 and allowed to stir before the addition of 0.041 g (0.212 mmol) of EDC. Upon completion as judged by TLC, the reaction was transferred to a separatory funnel with EtOAc. The organic layer was extracted twice with 1M aqueous HCl, once with a sat'd solution of sodium bicarbonate, and once with brine. The organic layer was dried over Na_2SO_4, filtered, and concentrated. Purification of the crude residue by column chromatography (gradient of hexanes to 40% EtOAc/hexanes) afforded 0.021 g (95%) of the title compound.

^{1}H NMR (500 MHz, $CDCl_3$) δ 5.20 (s, 1H), 5.18 (s, 1H), 5.05 (q, *J* = 1.9 Hz, 1H), 4.93 (ddd, *J* = 13.3, 10.9, 2.6 Hz, 1H), 4.01 – 3.91 (m, 2H), 2.52 (ddd, *J* = 16.1, 7.5, 1.9 Hz, 1H), 2.49 – 2.43 (m, 1H), 2.28 – 2.09 (m, 3H), 1.93 – 1.82 (m, 1H), 1.69 – 1.41 (m, 7H), 1.10 (ddt, *J* = 14.6, 11.7, 3.7 Hz, 1H), 0.96 (d, *J* = 6.8 Hz, 3H).

^{13}C NMR (126 MHz, $CDCl_3$) δ 173.62, 170.33, 142.72, 112.11, 82.19, 63.88, 57.61, 35.22, 30.95, 28.75, 25.66, 24.70, 19.93, 16.83, 16.42.

HRMS (ESI) *m/z* calculated for $[M+Na]^+$ 332.1581, found 332.1586.

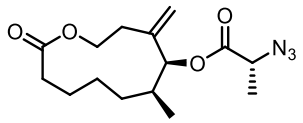

(5*S*,6*S*)-6-methyl-4-methylene-11-oxooxacycloundecan-5-yl (*R*)-2-azidopropanoate (S16):

An oven-dried vial equipped with stir bar was charged with 0.017 g (0.080 mmol) of (7*S*,8*S*)-8-Hydroxy-7-methyl-9-methyleneoxacycloundecan-2-one, 0.028 g (0.240 mmol) of (R)-2-azidopropanoic acid, and 0.001 g (0.011 mmol) of DMAP. The contents were suspended in 1.5 mL of CH_2Cl_2 and allowed to stir before the addition of 0.046 g (0.240 mmol) of EDC. Upon completion as judged by TLC, the reaction was transferred to a separatory funnel with EtOAc. The organic layer was extracted twice with 1M aqueous HCl, once with a sat'd solution of sodium bicarbonate, and once with brine. The organic layer was dried over Na_2SO_4, filtered, and concentrated. Purification of the crude residue by column chromatography (gradient of hexanes to 40% EtOAc/hexanes) afforded 0.023 g (92%) of the title compound.

^{1}H NMR (500 MHz, $CDCl_3$) δ 5.19 (s, 1H), 5.17 (s, 1H), 5.04 (s, 1H), 4.93 (ddd, J = 13.1, 11.1, 2.5 Hz, 1H), 4.01 – 3.89 (m, 2H), 2.56 – 2.41 (m, 2H), 2.28 – 2.07 (m, 3H), 1.87 (q, *J* = 12.8 Hz, 1H), 1.69 – 1.39 (m, 7H), 1.14 – 1.04 (m, 1H), 0.95 (t, *J* = 5.5 Hz, 3H).

^{13}C NMR (126 MHz, $CDCl_3$) δ 173.62, 170.35, 142.67, 112.15, 82.16, 63.90, 57.64, 35.22, 30.92, 28.70, 25.66, 24.70, 19.91, 16.92, 16.45.

HRMS (ESI) *m/z* calculated for $[M+Na]^+$ 332.1581, found 332.1584.

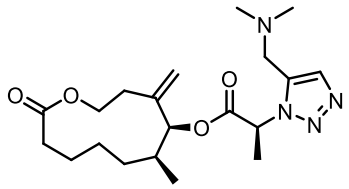

(5*S*,6*S*)-6-methyl-4-methylene-11-oxooxacycloundecan-5-yl-(*S*)-2-(5-((dimethylamino)methyl)-1H-1,2,3-triazol-1-yl)propanoate (38c):

Following the general RuAAC procedure, the reaction of 0.018 g (0.058 mmol) of (5*S*,6*S*)-6-methyl-4-methylene-11-oxooxacycloundecan-5-yl (*S*)-2-azidopropanoate, 0.012 mL (0.102 mmol) of N,N-dimethylprop-2-yn-1-amine, and 1.1 mg (3.0x10-3 mmol) of Cp*RuCl(COD) in 1.2 mL of toluene afforded 0.017 g (74%) of the title compound as a 4:1 inseparable mixture of diastereomers at the α-triazole stereocenter. The NMR data of the major diastereomer is reported.

^{1}H NMR (500 MHz, $CDCl_3$) δ 7.54 (s, 1H), 5.69 (q, *J* = 7.3 Hz, 1H), 5.16 – 5.10 (m, 2H), 4.96 – 4.85 (m, 2H), 3.89 (ddd, *J* = 11.0, 4.1, 2.3 Hz, 1H), 3.54 (d, *J* = 13.8 Hz, 1H), 3.42 (d, *J* = 14.0 Hz, 1H), 2.48 (ddd, *J* = 15.9, 7.6, 1.9 Hz, 1H), 2.42 (dq, *J* = 15.3, 2.0 Hz, 1H), 2.24 – 2.03 (m, 9H), 1.96 (d, *J* = 7.3 Hz, 3H), 1.89 – 1.76 (m, 1H), 1.60 – 1.29 (m, 4H), 0.81 (d, *J* = 6.8 Hz, 3H), 0.71 – 0.62 (m, 1H).

^{13}C NMR (126 MHz, $CDCl_3$) δ 173.60, 168.55, 142.82, 134.25, 133.68, 111.88, 82.22, 63.79, 56.06, 51.93, 45.26, 35.21, 30.92, 28.67, 25.59, 24.38, 19.85, 16.92, 16.21.

HRMS (ESI) *m/z* calculated for $[M+H]^+$ 393.2496, found 393.2502.

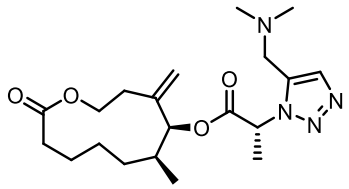

(5*S*,6*S*)-6-methyl-4-methylene-11-oxooxacycloundecan-5-yl-(*R*)-2-(5-((dimethylamino)methyl)-1H-1,2,3-triazol-1-yl)propanoate (38d):

Following the general RuAAC procedure, the reaction of 0.020 g (0.065 mmol) of (5*S*,6*S*)-6-methyl-4-methylene-11-oxooxacycloundecan-5-yl (*R*)-2-azidopropanoate, 0.013 mL (0.113 mmol) of N,N-dimethylprop-2-yn-1-amine, and 1.2 mg (3.25×10^{-3} mmol) of Cp*RuCl(COD) in 1.2 mL of toluene afforded 0.021 g (81%) of the title compound as an inseparable 9:1 mixture of diastereomers at the α-triazole stereocenter. The NMR data of the major diastereomer is reported.

^{1}H NMR (500 MHz, $CDCl_3$) δ 7.54 (s, 1H), 5.67 (q, *J* = 7.4 Hz, 1H), 5.14 (s, 1H), 5.12 (s, 1H), 4.93 – 4.84 (m, 2H), 3.91 (ddd, *J* = 10.9, 4.1, 2.3 Hz, 1H), 3.52 (d, *J* = 13.7 Hz, 1H), 3.40 (d, *J* = 13.9 Hz, 1H), 2.50 (dd, *J* = 16.0, 7.3 Hz, 1H), 2.41 (d, *J* = 15.4 Hz, 1H), 2.23 – 2.06 (m, 9H), 2.00 (d, *J* = 7.4 Hz, 3H), 1.89 – 1.78 (m, 1H), 1.66 – 1.50 (m, 2H), 1.49 – 1.35 (m, 2H), 0.93 – 0.80 (m, 4H).

^{13}C NMR (126 MHz, $CDCl_3$) δ 173.53, 168.70, 142.40, 134.29, 133.78, 112.20, 82.18, 63.86, 56.20, 51.91, 45.22, 35.16, 30.84, 28.67, 25.61, 24.62, 19.87, 16.91, 16.49.

HRMS (ESI) *m/z* calculated for $[M+H]^+$ 393.2496, found 393.2502.

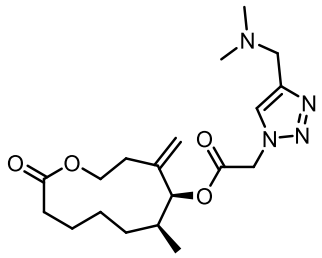

(5*S*,6*S*)-6-Methyl-4-methylene-11-oxooxacycloundecan-5-yl-2-(4-((dimethylamino)methyl)-1H-1,2,3-triazol-1-yl)acetate (38e):

Following the general CuAAC reaction procedure, the reaction of 0.010 g (0.034 mmol) of (5*S*,6*S*)-6-methyl-4-methylene-11-oxooxacycloundecan-5-yl 2-azidoacetate, 0.004 mL (0.034 mmol) N,N-dimethylprop-2-yn-1-amine, 3.40×10^{-4} mmol $CuSO_4 \bullet 5H_2O$, and 3.40×10^{-3} mmol of sodium ascorbate in 0.50 ml of H_2O/*t*-BuOH (1:1) afforded 0.013 g (99%) of the title compound as a clear oil after purification by column chromatography (gradient CH_2Cl_2 to 10% MeOH/CH_2Cl_2).

^{1}H NMR (700 MHz, $CDCl_3$) δ 7.66 (s, 1H), 5.25 – 5.17 (m, 3H), 5.16 – 5.13 (m, 1H), 3.91 (ddd, *J* = 10.9, 4.1, 2.4 Hz, 1H), 3.70 (s, 2H), 2.49 (ddd, *J* = 16.0, 7.6, 1.9 Hz, 1H), 2.45 – 2.39 (m, 1H), 2.31 (s, 6H), 2.23 – 2.05 (m, 3H), 1.88 – 1.78 (m, 1H), 1.63 – 1.51 (m, 2H), 1.46 – 1.34 (m, 2H), 0.96 – 0.80 (m, 4H).

^{13}C NMR (176 MHz, $CDCl_3$) δ 173.53, 165.49, 144.93, 142.34, 124.12, 112.28, 82.81, 63.79, 54.10, 50.86, 44.79, 35.15, 30.85, 28.70, 25.54, 24.44, 19.86, 16.45.

HRMS (ESI) *m/z* calculated for $[M+H]^+$ 379.2340, found 379.2332.

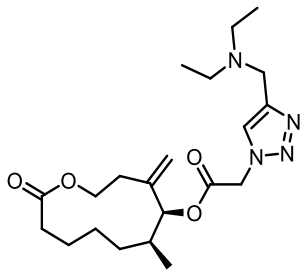

(5*S*,6*S*)-6-Methyl-4-methylene-11-oxooxacycloundecan-5-yl-2-(4-((diethylamino)methyl)-1H-1,2,3-triazol-1-yl)acetate (38f):

Following the general CuAAC reaction procedure, the reaction of 0.010 g (0.034 mmol) of (5*S*,6*S*)-6-methyl-4-methylene-11-oxooxacycloundecan-5-yl 2-azidoacetate, 0.005 mL (0.034 mmol) N,N-diethylprop-2-yn-1-amine, 3.40×10^{-4} mmol $CuSO_4 \cdot 5H_2O$, and 3.40×10^{-3} mmol of sodium ascorbate in 0.50 ml of H_2O/*t*-BuOH (1:1) afforded 0.013 g (93%) of the title compound as a clear oil after purification by column chromatography (gradient CH_2Cl_2 to 10% MeOH/CH_2Cl_2)

^{1}H NMR (700 MHz, $CDCl_3$) δ 7.88 (s, 1H), 5.26 – 5.17 (m, 3H), 5.14 (t, *J* = 1.7 Hz, 1H), 4.94 – 4.86 (m, 2H), 3.99 (s, 2H), 3.91 (ddd, *J* = 10.9, 4.2, 2.4 Hz, 1H), 2.72 (s, 4H), 2.49 (ddd, *J* = 16.1, 7.6, 1.9 Hz, 1H), 2.45 – 2.39 (m, 1H), 2.23 – 2.05 (m, 3H), 1.88 – 1.78 (m, 1H), 1.65 – 1.50 (m, 2H), 1.47 – 1.34 (m, 2H), 1.19 (t, *J* = 7.3 Hz, 6H), 0.94 – 0.82 (m, 4H).

^{13}C NMR (176 MHz, $CDCl_3$) δ 173.53, 165.43, 142.32, 125.33, 112.34, 82.85, 63.80, 50.89, 47.26, 46.44, 35.17, 30.87, 28.73, 25.57, 24.45, 19.86, 16.48, 10.78.

HRMS (ESI) *m/z* calculated for $[M+H]^+$ 407.2653, found 407.2665.

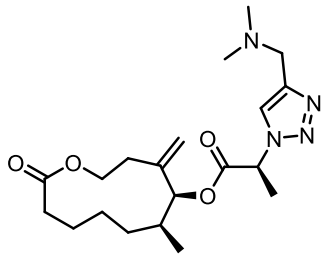

(5*S*,6*S*)-6-Methyl-4-methylene-11-oxooxacycloundecan-5-yl-(*S*)-2-(4-((dimethylamino)methyl)-1H-1,2,3-triazol-1-yl)propanoate (38g):

Following the general CuAAC reaction procedure, the reaction of 0.051 g (0.164 mmol) of (5*S*,6*S*)-6-methyl-4-methylene-11-oxooxacycloundecan-5-yl (*S*)-2-azidopropanoate, 0.014 g (0.164 mmol) of N,N-dimethylprop-2-yn-1-amine, 1.64×10^{-3} mmol of $CuSO_4 \cdot 5H_2O$, and 1.64×10^{-2} mmol of sodium ascorbate in 2.0 ml of H_2O/*t*-BuOH (1:1) afforded 0.061 g (95%) of the title compound as a clear oil after purification by column chromatography (gradient CH_2Cl_2 to 10% MeOH/CH_2Cl_2)

^{1}H NMR (500 MHz, $CDCl_3$) δ 7.70 (s, 1H), 5.51 (q, *J* = 7.5 Hz, 1H), 5.18 – 5.08 (m, 2H), 4.96 – 4.82 (m, 2H), 3.91 (ddd, *J* = 10.9, 4.2, 2.3 Hz, 1H), 3.67 (dd, *J* = 19.5, 14 Hz, 2H), 2.50 (dd, *J* = 16, 7 Hz, 1H), 2.46 – 2.38 (m, 1H), 2.31 (s, 6H), 2.25 – 1.97 (m, 3H), 1.94 – 1.69 (m, 4H), 1.69 – 1.49 (m, 2H), 1.48 – 1.27 (m, 2H), 0.96 – 0.76 (m, 4H).

^{13}C NMR (176 MHz, $CDCl_3$) δ 173.55, 168.49, 145.45, 142.41, 121.46, 112.10, 82.50, 63.78, 58.21, 54.43, 45.11, 35.15, 30.84, 28.67, 25.53, 24.40, 19.82, 18.00, 16.36.

HRMS (ESI) *m/z* calculated for $[M+H]^+$ 393.2496, found 393.2498.

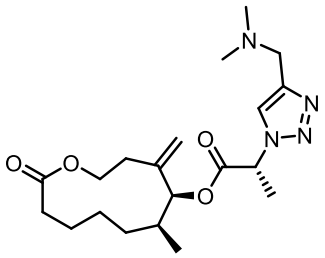

(5*S*,6*S*)-6-Methyl-4-methylene-11-oxooxacycloundecan-5-yl-(*R*)-2-(4-((dimethylamino)methyl)-1H-1,2,3-triazol-1-yl)propanoate (38h):

Following the general esterification procedure, the reaction of 0.022 g (0.104 mmol) of (7*S*,8*S*)-8-hydroxy-7-methyl-9-methyleneoxacycloundecan-2-one, 0.018 g (0.155 mmol) of (R)-2-azidopropanoic acid, 0.032 g (0.283 mmol) of DCC, 0.002 g (0.016 mmol) of DMAP, and 1.75 mL of CH_2Cl_2 afforded the desired ester after purification by column chromatography (15% EtOAc/Hexanes), which was carried on directly to the CuAAC reaction. Following the general CuAAC reaction procedure, the reaction of 0.104 mmol of (5S,6S)-6-methyl-4-methylene-11-oxooxacycloundecan-5-yl (R)-2-azidopropanoate, 0.0012 mL (0.104 mmol) N,N-dimethylprop-2-yn-1-amine, 1.04×10^{-3} mmol $CuSO_4 \bullet 5H_2O$, and 1.04×10^{-2} mmol of sodium ascorbate in 0.50 ml of H_2O/*t*-BuOH (1:1) afforded 0.030 g (75% over two steps) of the title compound after purification by column chromatography (gradient CH_2Cl_2 to 10% MeOH/CH_2Cl_2).

^{1}H NMR (500 MHz, $CDCl_3$) δ 7.72 (s, 1H), 5.50 (q, *J* = 7 Hz, 1H), 5.18 – 5.08 (m, 2H), 4.94 – 4.81 (m, 2H), 3.91 (ddd, *J* = 11.0, 4.2, 2.4 Hz, 1H), 3.78 – 3.66 (m, 2H), 2.50 (m, 1H), 2.45 – 2.37 (m, 1H), 2.33 (s, 6H), 2.25 – 1.98 (m, 4H), 1.95 – 1.72 (m, 4H), 1.67 – 1.49 (m, 2H), 1.48 – 1.34 (m, 2H), 0.96 – 0.79 (m, 3H).

^{13}C NMR (126 MHz, $CDCl_3$) δ 173.53, 168.51, 145.02, 142.25, 121.66, 112.19, 82.50, 63.81, 58.27, 54.30, 44.96, 35.13, 30.81, 28.69, 25.54, 24.44, 19.83, 17.98, 16.40.

HRMS (ESI) *m/z* calculated for $[M+H]^+$ 393.2496, found 393.2506.

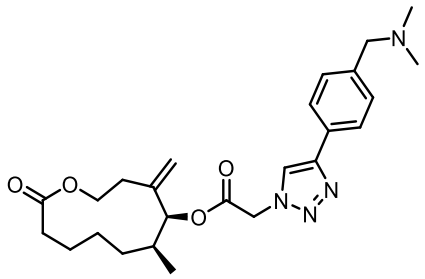

(5*S*,6*S*)-6-Methyl-4-methylene-11-oxooxacycloundecan-5-yl-2-(4-(4-((dimethylamino)methyl)phenyl)-1H-1,2,3-triazol-1-yl)acetate (38i):

Following the general CuAAC reaction procedure, the reaction of 0.014 g (0.047 mmol) of (5*S*,6*S*)-6-methyl-4-methylene-11-oxooxacycloundecan-5-yl 2-azidoacetate, 0.007 g (0.047 mmol) of 1-(4-ethynylphenyl)-N,N-dimethylmethanamine, 4.70×10^{-4} mmol of $CuSO_4 \bullet 5H_2O$, and 4.70×10^{-3} mmol of sodium ascorbate in 0.50 ml of H_2O/*t*-BuOH (1:1) afforded 0.007 g (33%) of the title compound as a clear oil after purification by column chromatography (gradient CH_2Cl_2 to 10% MeOH/CH_2Cl_2)

^{1}H NMR (401 MHz, $CDCl_3$) δ 7.90 (s, 1H), 7.81 (d, *J* = 7.9 Hz, 2H), 7.43 (d, *J* = 7.9 Hz, 2H), 5.31 – 5.21 (m, 3H), 5.17 (s, 1H), 4.97 (s, 1H), 4.90 (t, *J* = 2.3 Hz, 1H), 3.93 (dt, *J* = 10.8, 2.9 Hz, 1H), 3.60 (s, 2H), 2.56 – 2.29 (m, 8H), 2.28 – 2.04 (m, 3H), 1.92 – 1.75 (m, 1H), 1.66 – 1.51 (m, 2H), 1.51 – 1.32 (m, 2H), 0.93 (d, *J* = 6.9 Hz, 4H).

^{13}C NMR (176 MHz, $CDCl_3$) δ 173.58, 165.52, 147.96, 142.40, 133.89, 130.09, 125.99, 120.94, 112.33, 82.95, 63.81, 63.30, 50.95, 44.56, 35.16, 30.90, 28.76, 25.55, 24.48, 19.89, 16.52.

HRMS (ESI) *m/z* calculated for $[M+H]^+$ 455.2653, found 455.2637.

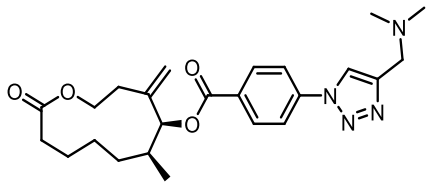

(5*S*,6*S*)-6-methyl-4-methylene-11-oxooxacycloundecan-5-yl-4-(4-((dimethylamino)methyl)-1H-1,2,3-triazol-1-yl)benzoate (38j):

Following the general esterification procedure, the reaction of 0.060 g (0.283 mmol) of (7*S*,8*S*)-8-hydroxy-7-methyl-9-methyleneoxacycloundecan-2-one, 0.231 g (1.413 mmol) of 4-azidobenzoic acid, 0.292 g (1.413 mmol) of DCC, 0.035 g (0.283 mmol) of DMAP, and 4.50 mL of CH_2Cl_2 afforded the desired azido ester, which was purified by column chromatography (15% EtOAc/hexanes) and carried on directly to the CuAAC reaction.

Following the general CuAAC reaction procedure, the reaction of 0.092 g (0.257 mmol) of (5*S*,6*S*)-6-methyl-4-methylene-11-oxooxacycloundecan-5-yl 4-azidobenzoate, 0.028 mL (0.257 mmol) N,N-dimethylprop-2-yn-1-amine, $2.57x10^{-3}$ mmol $CuSO_4•5H_2O$, and $2.57x10^{-2}$ mmol of sodium ascorbate in 1 ml of H_2O/*t*-BuOH (1:1) afforded 0.110 g (88% over two steps) of the title compound after purification by column chromatography (gradient CH_2Cl_2 to 10% MeOH/CH_2Cl_2)

^{1}H NMR (500 MHz, $CDCl_3$) δ 8.23 (d, *J* = 8.5 Hz, 2H), 8.12 (s, 1H), 7.87 (d, *J* = 8.4 Hz, 2H), 5.40 (s, 1H), 5.22 – 5.17 (m, 1H), 5.13 – 5.08 (m, 1H), 4.98 (ddd, *J* = 13.3, 10.9, 2.5 Hz, 1H), 3.98 (ddd, *J* = 10.9, 4.1, 2.3 Hz, 1H), 3.81 (s, 2H), 2.60 – 2.48 (m, 2H), 2.48 – 2.24 (m, 8H), 2.23 – 2.11 (m, 1H), 1.93 (q, *J* = 12.8 Hz, 1H), 1.77 – 1.45 (m, 4H), 1.36 – 1.17 (m, 1H), 1.03 (d, *J* = 6.8 Hz, 3H).

^{13}C NMR (126 MHz, $CDCl_3$) δ 173.67, 164.58, 146.49, 143.07, 140.27, 131.31, 130.22, 120.40, 119.87, 112.13, 81.73, 64.01, 54.37, 45.26, 35.30, 30.95, 29.01, 25.78, 24.99, 19.99, 16.67.

HRMS (ESI) *m/z* calculated for $[M+H]^+$ 441.2496, found 441.2500.

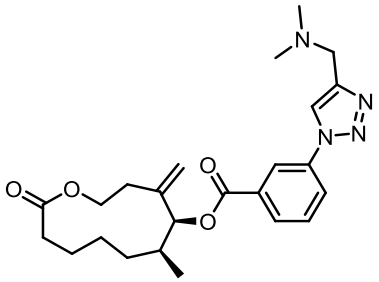

(5*S*,6*S*)-6-Methyl-4-methylene-11-oxooxacycloundecan-5-yl-3-(4-((dimethylamino)methyl)-1H-1,2,3-triazol-1-yl)benzoate (38k):

Following the general esterification procedure, the reaction of 0.007 g (0.033 mmol) of (7*S*,8*S*)-8-hydroxy-7-methyl-9-methyleneoxacycloundecan-2-one, 0.016 g (0.100 mmol) of 3-azidobenzoic acid, 0.021 g (0.100 mmol) of DCC, 0.001 g (0.008 mmol) of DMAP, and 0.50 mL of CH_2Cl_2 afforded 0.010 g (85%) the desired azido ester, after purification by column chromatography (15% EtOAc/Hexanes) and was carried on directly to the CuAAC reaction.

^{1}H NMR (700 MHz, $CDCl_3$) δ 7.84 (d, *J* = 7.8 Hz, 1H), 7.71 (s, 1H), 7.45 (t, *J* = 7.9 Hz, 1H), 7.23 (ddd, *J* = 8.0, 2.2, 1.1 Hz, 1H), 5.37 (s, 1H), 5.17 (s, 1H), 5.09 (d, *J* = 2.0 Hz, 1H), 4.96 (ddd, *J* = 13.3, 10.9, 2.5 Hz, 1H), 3.97 (ddd, *J* = 11.0, 4.2, 2.4 Hz, 1H), 2.55 (dd, *J* = 15.8, 6.9 Hz, 1H), 2.50 (d, *J* = 15.3 Hz, 1H), 2.34 – 2.24 (m, 2H), 2.16 (ddd, *J* = 16.1, 11.9, 1.9 Hz, 1H), 1.96 – 1.88 (m, 1H), 1.73 – 1.57 (m, 3H), 1.54 – 1.48 (m, 1H), 1.27 – 1.20 (m, 1H), 1.00 (d, *J* = 6.8 Hz, 3H).

^{13}C NMR (176 MHz, $CDCl_3$) δ 173.64, 164.80, 143.01, 140.64, 132.03, 129.89, 125.86, 123.38, 119.95, 112.07, 81.60, 63.98, 35.25, 30.91, 28.94, 25.74, 24.91, 19.96, 16.60.

HRMS (ESI) *m/z* calculated for $[M+Na]^+$ 380.1581, found 380.1582.

Following the general CuAAC reaction procedure, the reaction of 0.010 g (0.028 mmol) of (5*S*,6*S*)-6-methyl-4-methylene-11-oxooxacycloundecan-5-yl 3-azidobenzoate, 0.003 mL (0.028 mmol) N,N-dimethylprop-2-yn-1-amine, $2.80x10^{-4}$ mmol $CuSO_4•5H_2O$, and $2.8x10^{-3}$ mmol of sodium ascorbate in 0.50 ml of H_2O/*t*-BuOH (1:1) afforded 0.011 g (89%) of the title compound after purification by column chromatography (gradient CH_2Cl_2 to 10% MeOH/CH_2Cl_2)

^{1}H NMR (700 MHz, $CDCl_3$) δ 8.36 (s, 1H), 8.13 (d, *J* = 7.8 Hz, 1H), 8.07 (s, 1H), 8.05 – 8.01 (m, 1H), 7.63 (t, *J* = 7.9 Hz, 1H), 5.41 (s, 1H), 5.18 (s, 1H), 5.13 – 5.09 (m, 1H), 4.96 (ddd, *J* = 13.2, 11.0, 2.6 Hz, 1H), 3.98 (ddd, *J* = 11.0, 4.2, 2.3 Hz, 1H), 3.77 (s, 2H), 2.60 – 2.47 (m, 2H), 2.39 (s, 6H), 2.36 – 2.25 (m, 2H), 2.17 (ddd, *J* = 16.2, 11.9, 1.9 Hz, 1H), 1.97 – 1.87 (m, 1H), 1.74 – 1.65 (m, 2H), 1.61 (ddq, *J* = 13.2, 8.3, 3.6, 2.8 Hz, 1H), 1.52 (tq, *J* = 13.3, 3.1 Hz, 1H), 1.26 (ddd, *J* = 13.5, 9.0, 3.0 Hz, 1H), 1.02 (d, *J* = 6.8 Hz, 3H).

^{13}C NMR (176 MHz, $CDCl_3$) δ 173.7, 164.5, 145.7, 143.0, 137.4, 132.1, 130.1, 129.5, 124.9, 121.1, 120.9, 112.2, 82.0, 64.0, 54.2, 45.0, 35.3, 31.0, 29.0, 25.8, 25.0, 20.0, 16.6.

HRMS (ESI) *m/z* calculated for $[M+H]^+$ 441.2496, found 441.2485.

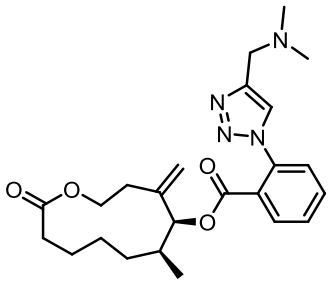

(5*S*,6*S*)-6-Methyl-4-methylene-11-oxooxacycloundecan-5-yl-2-(4-((dimethylamino)methyl)-1H-1,2,3-triazol-1-yl)benzoate (38l):

Following the general esterification procedure, the reaction of 0.040 g (0.188 mmol) of (7*S*,8*S*)-8-hydroxy-7-methyl-9-methyleneoxacycloundecan-2-one, 0.154 g (0.942 mmol) of 2-azidobenzoic acid, 0.194 g (0.942 mmol) of DCC, 0.023 g (0.188 mmol) of DMAP, and 4.0 mL of CH_2Cl_2 afforded the desired ester after purification by column chromatography (15% EtOAc/Hexanes), which was carried on directly to the CuAAC reaction.

Following the general CuAAC reaction procedure, the reaction of 0.065 g (0.183 mmol) of (5*S*,6*S*)-6-methyl-4-methylene-11-oxooxacycloundecan-5-yl 2-azidobenzoate, 0.021 mL (0.183 mmol) N,N-dimethylprop-2-yn-1-amine, 1.83×10^{-3} mmol $CuSO_4 \cdot 5H_2O$, and 1.83×10^{-2} mmol of sodium ascorbate in 3.0 ml of H_2O/*t*-BuOH (1:1) afforded 0.065 g (78% over two steps) of the title compound after purification by column chromatography (gradient CH_2Cl_2 to 10% MeOH/CH_2Cl_2)

^{1}H NMR (400 MHz, $CDCl_3$) δ 8.03 (dd, *J* = 7.8, 1.6 Hz, 1H), 7.79 (s, 1H), 7.68 (td, *J* = 7.7, 1.6 Hz, 1H), 7.60 (td, *J* = 7.6, 1.4 Hz, 1H), 7.49 (dd, *J* = 7.8, 1.3 Hz, 1H), 5.24 (s, 1H), 5.15 (s, 1H), 5.09 – 5.04 (m, 1H), 4.92 (ddd, *J* = 13.2, 10.9, 2.6 Hz, 1H), 3.93 (ddd, *J* = 11.0, 4.1, 2.5 Hz, 1H), 3.72 (s, 2H), 2.51 (dd, *J* = 15.1, 5.2 1H), 2.43 (d, *J* = 15.4 Hz, 1H),

2.35 (s, 6H), 2.28 – 2.07 (m, 3H), 1.87 (q, *J* = 12.8 Hz, 1H), 1.70 – 1.52 (m, 3H), 1.52 – 1.39 (m, 1H), 1.10 – 0.99 (m, 1H), 0.94 (d, *J* = 6.8 Hz, 3H).

^{13}C NMR (176 MHz, $CDCl_3$) δ 173.63, 163.76, 143.22, 142.72, 136.49, 132.73, 130.76, 129.94, 127.50, 127.40, 125.36, 112.24, 82.09, 63.96, 53.87, 44.61, 35.25, 30.95, 28.91, 25.71, 24.76, 19.95, 16.50.

The fully substituted triazole carbon was detected at 143.22 ppm by HMBC.

HRMS (ESI) *m/z* calculated for $[M+H]^+$ 441.2496, found 441.2513.

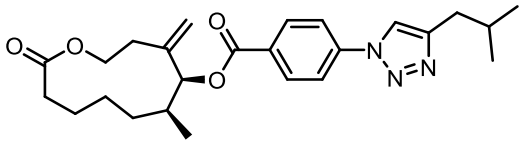

(5*S*,6*S*)-6-methyl-4-methylene-11-oxooxacycloundecan-5-yl-4-(4-isobutyl-1H-1,2,3-triazol-1-yl)benzoate (38m):

Following the general CuAAC reaction procedure, the reaction of 8.5 mg g (0.024 mmol) of (5*S*,6*S*)-6-methyl-4methylene-11-oxooxacycloundecan-5-yl 4-azidobenzoate, 10.0 mg (0.120 mmol) 4-methylpent-1-yne, $1.19x10^{-3}$ mmol $CuSO_4•5H_2O$, and $1.19x10^{-2}$ mmol of sodium ascorbate in 1 ml of H_2O/t-BuOH (1:1) afforded 9.0 mg (86%) of the title compound after purification by column chromatography (30% EtOAc/hex).

^{1}H NMR (700 MHz, $CDCl_3$) δ 8.21 (d, *J* = 8.6 Hz, 2H), 7.85 (d, *J* = 8.6 Hz, 2H), 7.78 (s, 1H), 5.39 (s, 1H), 5.20 – 5.17 (m, 1H), 5.11 (d, *J* = 2.0 Hz, 1H), 4.98 (ddd, *J* = 13.3, 10.9, 2.5 Hz, 1H), 3.97 (ddd, *J* = 11.0, 4.1, 2.3 Hz, 1H), 2.69 (d, *J* = 7.0 Hz, 2H), 2.55 (ddd, *J* = 16.2, 8.0, 1.8 Hz, 1H), 2.52 (d, *J* = 15.3 Hz, 1H), 2.36 – 2.26 (m, 2H), 2.17 (ddd, *J* = 16.2, 11.9, 1.9 Hz, 1H), 2.10 – 2.01 (m, 1H), 1.93 (q, *J* = 13.2 Hz, 1H), 1.74 – 1.59 (m, 4H), 1.55 – 1.49 (m, 1H), 1.32 – 1.26 (m, 1H), 1.02 (d, *J* = 6.8 Hz, 3H), 0.99 (d, *J* = 6.6 Hz, 5H).

^{13}C NMR (176 MHz, $CDCl_3$) δ 173.70, 164.65, 148.38, 143.07, 140.38, 131.25, 129.93, 119.76, 119.04, 112.12, 81.68, 64.01, 35.30, 34.67, 30.94, 28.97, 28.64, 25.77, 24.96, 22.31, 19.96, 16.67.

HRMS (ESI) m/z calculated for $[M+H]^+$ 440.2544, found 440.2544.

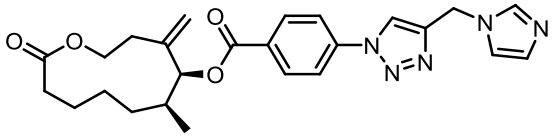

(5*S*,6*S*)-6-methyl-4-methylene-11-oxooxacycloundecan-5-yl 4-(4-((1H-imidazol-1-yl)methyl)-1H-1,2,3-triazol-1-yl)benzoate (38n):

Following the general CuAAC reaction procedure, the reaction of 8.5 mg g (0.024 mmol) of (5S,6S)-6-methyl-4methylene-11-oxooxacycloundecan-5-yl 4-azidobenzoate, 5.0 mg (0.048 mmol) 1-(prop-2-yn-1-yl)-1H-imidazole, $1.19x10^{-3}$ mmol $CuSO_4•5H_2O$, and $1.19x10^{-2}$ mmol of sodium ascorbate in 1 ml of H_2O/t-BuOH (1:1) afforded 6.0 mg (55%) of the title compound after purification by column chromatography (4% MeOH/CH_2Cl_2).

^{1}H NMR (700 MHz, $CDCl_3$) δ 8.22 (d, *J* = 8.6 Hz, 2H), 7.86 (s, 1H), 7.81 (d, *J* = 8.6 Hz, 2H), 7.65 (s, 1H), 7.12 (s, 1H), 7.07 (s, 1H), 5.39 (s, 1H), 5.37 (s, 2H), 5.18 (s, 1H), 5.09 (d, *J* = 2.0 Hz, 1H), 4.98 (ddd, *J* = 13.2, 11.0, 2.5 Hz, 1H), 3.97 (ddd, *J* = 10.9, 4.2, 2.4 Hz, 1H), 2.55 (ddd, *J* = 16.2, 7.6, 1.8 Hz, 1H), 2.51 (d, *J* = 15.8 Hz, 1H), 2.35 – 2.26 (m, 2H), 2.16 (ddd, *J* = 16.2, 12.0, 1.9 Hz, 1H), 1.97 – 1.89 (m, 1H), 1.74 – 1.58 (m, 3H), 1.55 – 1.48 (m, 1H), 1.30 – 1.22 (m, 1H), 1.02 (d, *J* = 6.8 Hz, 3H).

^{13}C NMR (176 MHz, $CDCl_3$) δ 173.68, 164.41, 144.85, 143.01, 139.77, 137.13, 131.37, 130.73, 130.21, 120.08, 119.98, 119.04, 112.12, 81.84, 63.98, 42.32, 35.29, 30.93, 28.96, 25.75, 24.95, 19.95, 16.67.

HRMS (ESI) m/z calculated for [M+H]+ 464.2292, found 464.2294.

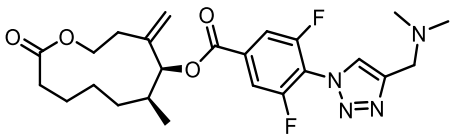

(5*S*,6*S*)-6-Methyl-4-methylene-11-oxooxacycloundecan-5-yl-4-(4-((dimethylamino)methyl)-1H-1,2,3-triazol-1-yl)-3,5-difluorobenzoate (38p):

Following the general esterification procedure, the reaction of 0.010 g (0.047 mmol) of (7*S*,8*S*)-8-hydroxy-7-methyl-9-methyleneoxacycloundecan-2-one, 0.047 g (0.236 mmol) of 4-azido-3,5-difluorobenzoic acid, 0.049 g (0.236 mmol) of DCC, 0.006 g (0.047 mmol) of DMAP, and 3.00 mL of CH_2Cl_2 afforded the desired azido ester, which was purified by column chromatography (15% EtOAc/Hexanes) and carried on directly to the CuAAC reaction.

Following the general CuAAC reaction procedure, the reaction of (0.047 mmol) of (5*S*,6*S*)-6-methyl-4-methylene-11-oxooxacycloundecan-5-yl 4-azido-3,5-difluorobenzoate, 0.005 mL (0.047 mmol) N,N-dimethylprop-2-yn-1-amine, 4.70×10^{-4} mmol $CuSO_4 \cdot 5H_2O$, and 4.7×10^{-3} mmol of sodium ascorbate in 1 ml of H_2O/*t*-BuOH (1:1) afforded 0.022 g (99% over two steps) of the title compound after purification by column chromatography (gradient CH_2Cl_2 to 10% MeOH/CH_2Cl_2)

^{1}H NMR (401 MHz, $CDCl_3$) δ 7.87 – 7.77 (m, 3H), 5.39 (s, 1H), 5.20 (s, 1H), 5.06 (d, *J* = 2.0 Hz, 1H), 4.97 (ddd, *J* = 13.3, 10.9, 2.7 Hz, 1H), 3.98 (ddd, *J* = 10.9, 4.1, 2.3 Hz, 1H), 3.77 (s, 2H), 2.62 – 2.45 (m, 2H), 2.41 – 2.24 (m, 7H), 2.17 (ddd, *J* = 16.0, 11.8, 1.7 Hz,

1H), 2.00 – 1.85 (m, 1H), 1.77 – 1.46 (m, 4H), 1.34 – 1.16 (m, 2H), 1.02 (d, *J* = 6.8 Hz, 3H).

^{13}C NMR (176 MHz, $CDCl_3$) δ 173.60, 162.54, 156.31 (dd, *J* = 257.9, 2.4 Hz) 145.11, 142.65, 133.14 (t, *J* = 8.5 Hz) 124.98, 118.97 (t, *J* = 15.8 Hz) 113.70 (dd, *J* = 21.8, 3.8 Hz) 112.24, 82.82, 63.90, 54.06, 45.08, 35.23, 30.93, 29.00, 25.71, 24.93, 19.95, 16.66.

HRMS (ESI) *m/z* calculated for $[M+H]^+$ 477.2308, found 477.2319.

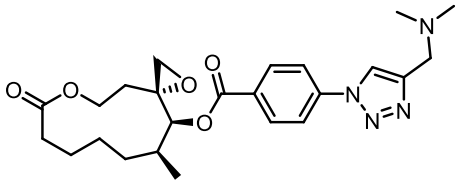

(3*R*,12*S*,13*S*)-12-Methyl-7-oxo-1,6-dioxaspiro[2.10]tridecan-13-yl-4-(4-((dimethylamino)methyl)-1H-1,2,3-triazol-1-yl)benzoate (43j):

To an oven-dried flask equipped with stir bar was added 0.014 g (0.061 mmol) of (3*R*,12*S*,13*S*)-13-hydroxy-12-methyl-1,6-dioxaspiro[2.10]tridecan-7-one, 0.007 g (0.061 mmol) of DMAP and 1 mL of CH_2Cl_2/Pyridine (1:1). The contents were cooled to 0 °C and 0.033 g (0.183 mmol) of 4-azidobenzoyl chloride was added dropwise as a solution in 1 mL of CH_2Cl_2. The reaction was warmed to rt and stir for 24 hours. The reaction was quenched with the addition of sat'd aqueous sodium bicarbonate and EtOAc. The aqueous layer was extracted 3x with EtOAc, the organic layers combined, dried over Na_2SO_4, filtered, and concentrated. The crude residue was purified by column chromatography (30% EtOAc/Hexanes) to yield 0.010 g (43%) of the desired product that was directly carried on to the CuAAC reaction

Following the general CuAAC reaction procedure, the reaction of 0.010 g (0.027 mmol) of (5*S*,6*S*)-6-methyl-4-methylene-11-oxooxacycloundecan-5-yl 4-azidobenzoate, 0.003 mL (0.027 mmol) N,N-dimethylprop-2-yn-1-amine, $2.73x10^{-4}$ mmol $CuSO_4•5H_2O$, and $2.57x10^{-3}$ mmol of sodium ascorbate in 1 ml of H_2O/*t*-BuOH (1:1) afforded 0.011 g (88%) of the title compound after purification by column chromatography (gradient CH_2Cl_2 to 10% MeOH/CH_2Cl_2).

^{1}H NMR (500 MHz, $CDCl_3$) δ 8.18 – 8.07 (m, 3H), 7.84 (d, *J* = 8.7 Hz, 2H), 5.41 (s, 1H), 4.74 (td, *J* = 12.1, 2.4 Hz, 1H), 3.95 (dt, *J* = 11.8, 3.6 Hz, 1H), 3.81 (s, 2H), 2.97 (d, *J* = 4.5 Hz, 1H), 2.91 (d, *J* = 4.5 Hz, 1H), 2.64 – 2.54 (m, 1H), 2.42 (s, 8H), 2.23 (ddd, *J* = 15.6, 11.6, 2.0 Hz, 1H), 2.07 – 1.92 (m, 2H), 1.80 – 1.63 (m, 3H), 1.62 – 1.52 (m, 1H), 1.42 – 1.31 (m, 1H), 1.01 (d, *J* = 6.8 Hz, 3H).

^{13}C NMR (176 MHz, $CDCl_3$) δ 173.84, 164.59, 145.24, 140.09, 131.29, 130.15, 121.08, 119.85, 76.74, 60.72, 57.25, 54.00, 48.23, 44.80, 35.29, 31.99, 29.75, 26.19, 25.63, 20.25, 16.81.

HRMS (ESI) *m/z* calculated for $[M+H]^+$ 457.2445, found 457.2447.

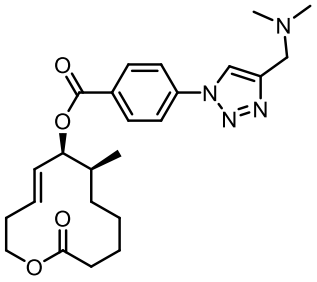

(6*S*,7*S*,*E*)-7-Methyl-12-oxooxacyclododec-4-en-6-yl-4-(4-((dimethylamino)methyl)-1H-1,2,3-triazol-1-yl)benzoate (55j):

Following the general esterification procedure, the reaction of 0.030 g (0.141 mmol) of (7*S*,8*S*,*E*)-8-hydroxy-7-methyloxacyclododec-9-en-2-one, 0.115 g (0.707 mmol) of 4-

azidobenzoic acid, 0.146 g (0.707 mmol) of DCC, 0.034 g (0.282 mmol) of DMAP, and 4.0 mL of CH_2Cl_2 afforded the desired ester after purification by column chromatography (15% EtOAc/Hexanes), which was carried on directly to the CuAAC reaction.

Following the general CuAAC reaction procedure, the reaction of (0.141 mmol) of (6*S*,7*S*,*E*)-7-methyl-12-oxooxacyclododec-4-en-6-yl 4-azidobenzoate, 0.016 mL (0.141 mmol) N,N-dimethylprop-2-yn-1-amine, $1.41x10^{-3}$ mmol $CuSO_4•5H_2O$, and $1.41x10^{-2}$ mmol of sodium ascorbate in 2.0 ml of H_2O/*t*-BuOH (1:1) afforded 0.055 g (89% over two steps) of the title compound after purification by column chromatography (gradient CH_2Cl_2 to 10% MeOH/CH_2Cl_2).

^{1}H NMR (700 MHz, $CDCl_3$) δ 8.19 (d, *J* = 7 Hz, 2H), 8.11 (s, 1H), 7.85 (d, *J* = 7 Hz, 2H), 5.69 – 5.60 (m, 2H), 5.57 (dd, *J* = 6.9, 4.5 Hz, 1H), 4.64 (ddd, *J* = 11.0, 9.4, 4.2 Hz, 1H), 4.01 (dt, *J* = 11.0, 4.5 Hz, 1H), 3.80 (s, 2H), 2.52 – 2.28 (m, 11H), 2.12 – 2.03 (m, 1H), 1.94 – 1.85 (m, 1H), 1.59 – 1.38 (m, 5H), 1.35 – 1.26 (m, 2H), 1.07 (d, *J* = 6.9 Hz, 3H).

^{13}C NMR (176 MHz, $CDCl_3$) δ 173.51, 164.56, 145.40, 140.00, 131.28, 131.26, 130.70, 128.51, 120.95, 119.81, 77.66, 60.93, 54.08, 44.91, 34.92, 33.30, 32.39, 30.90, 24.15, 23.25, 16.35.

HRMS (ESI) *m/z* calculated for $[M+H]^+$ 441.2496, found 441.2498.

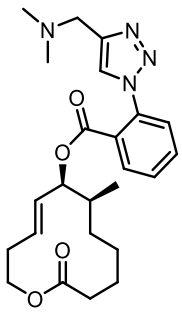

(6*S*,7*S*,*E*)-7-Methyl-12-oxooxacyclododec-4-en-6-yl-2-(4-((dimethylamino)methyl)-1H-1,2,3-triazol-1-yl)benzoate (55l):

Following the general esterification procedure, the reaction of 0.030 g (0.141 mmol) of (7*S*,8*S*,*E*)-8-hydroxy-7-methyloxacyclododec-9-en-2-one, 0.115 g (0.707 mmol) of 2-azidobenzoic acid, 0.146 g (0.707 mmol) of DCC, 0.034 g (0.282 mmol) of DMAP, and 4.0 mL of CH_2Cl_2 afforded the desired ester after purification by column chromatography (15% EtOAc/Hexanes), which was carried on directly to the CuAAC reaction.

Following the general CuAAC reaction procedure, the reaction of (0.141 mmol) of (6*S*,7*S*,*E*)-7-methyl-12-oxooxacyclododec-4-en-6-yl 2-azidobenzoate, 0.016 mL (0.141 mmol) N,N-dimethylprop-2-yn-1-amine, 1.41×10^{-3} mmol $CuSO_4 \cdot 5H_2O$, and 1.41×10^{-2} mmol of sodium ascorbate in 2.0 ml of H_2O/*t*-BuOH (1:1) afforded 0.050 g (80% over two steps) of the title compound after purification by column chromatography (gradient CH_2Cl_2 to 10% MeOH/CH_2Cl_2).

^{1}H NMR (500 MHz, $CDCl_3$) δ 7.96 (dd, *J* = 7.8, 1.6 Hz, 1H), 7.74 (s, 1H), 7.64 (td, *J* = 7.7, 1.6 Hz, 1H), 7.58 (td, *J* = 7.7, 1.3 Hz, 1H), 7.48 (dd, *J* = 7.8, 1.3 Hz, 1H), 5.62 (ddd, *J* = 14.5, 8.5, 5.9 Hz, 1H), 5.47 – 5.34 (m, 2H), 4.70 (ddd, *J* = 10.9, 9.1, 5.2 Hz, 1H), 3.91 (dt, *J* = 11.0, 4.2 Hz, 1H), 3.70 (s, 2H), 2.45 – 2.25 (m, 10H), 1.95 – 1.81 (m, 2H), 1.52 – 1.41 (m, 1H), 1.40 – 1.24 (m, 3H), 1.18 – 1.08 (m, 1H), 0.84 (d, *J* = 6.8 Hz, 3H).

^{13}C NMR (176 MHz, $CDCl_3$) δ 173.41, 164.33, 144.97, 136.17, 132.37, 132.33, 130.97, 129.63, 128.03, 127.56, 126.77, 124.37, 78.18, 60.86, 54.38, 45.24, 34.54, 33.27, 32.17, 30.96, 24.09, 23.01, 15.91.

HRMS (ESI) *m/z* calculated for $[M+H]^+$ 441.2496, found 441.2503.

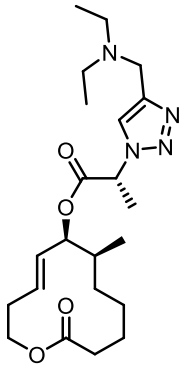

(6*S*,7*S*,*E*)-7-Methyl-12-oxooxacyclododec-4-en-6-yl-(R)-2-(4-((diethylamino)methyl)-1H-1,2,3-triazol-1-yl)propanoate (55o):

Following the general esterification procedure, the reaction of 0.056 g (0.264 mmol) of (7*S*,8*S*,*E*)-8-hydroxy-7-methyloxacyclododec-9-en-2-one, 0.065 g (0.565 mmol) of (R)-2-azidopropanoic acid, 0.117 g (0.565 mmol) of DCC, 0.017 g (0.142 mmol) of DMAP, and 4.50 mL of CH_2Cl_2 afforded 0.077 g (94%) the desired ester after purification by column chromatography (15% EtOAc/Hexanes), which was carried on directly to the CuAAC reaction.

Following the general CuAAC reaction procedure, the reaction of 0.077 g (0.249 mmol) of (6*S*,7*S*,*E*)-7-methyl-12-oxooxacyclododec-4-en-6-yl (*R*)-2-azidopropanoate, 0.035 mL (0.249 mmol) N,N-diethylprop-2-yn-1-amine, $2.49x10^{-3}$ mmol $CuSO_4•5H_2O$, and $2.49x10^{-2}$ mmol of sodium ascorbate in 2.0 ml of H_2O/*t*-BuOH (1:1) afforded 0.104 g (99%) of the title compound after purification by column chromatography (gradient CH_2Cl_2 to 10% MeOH/CH_2Cl_2).

^{1}H NMR (500 MHz, $CDCl_3$) δ 7.71 (s, 1H), 5.53 (ddd, *J* = 14.5, 8.2, 5.9 Hz, 1H), 5.48 – 5.38 (m, 2H), 5.32 (dd, *J* = 8.1, 4.5 Hz, 1H), 4.64 (ddd, *J* = 10.8, 8.9, 5.1 Hz, 1H), 3.98 – 3.81 (m, 3H), 2.71 – 2.52 (m, 4H), 2.45 – 2.21 (m, 4H), 1.96 – 1.76 (m, 5H), 1.52 – 1.40 (m, 1H), 1.37 – 1.21 (m, 3H), 1.20 – 1.06 (m, 7H), 0.87 (d, *J* = 6.9 Hz, 3H).

^{13}C NMR (126 MHz, $CDCl_3$) δ 173.34, 168.44, 144.25, 132.17, 127.39, 122.18, 78.74, 60.79, 58.34, 47.49, 46.65, 34.60, 33.21, 32.15, 30.67, 23.97, 22.96, 18.07, 15.85, 11.46. **HRMS (ESI)** *m/z* calculated for $[M+H]^+$ 421.2809, found 421.2806.

Substrates **55j, 55k, 55h, 55l,** and **(*R*,*R*)-34a** were synthesized following the same procedures used to make their corresponding enantiomers. The ^{1}H and ^{13}C spectra of these compounds matched those of the enantiomeric series.

5.3.3 PikC Oxidations

Preparation of PikC-RhFRED mutants

Using previously prepared pET28b_PikC$_{D50N/D176Q/E246A}$-RhFRED as template, site-directed mutagenesis was performed with the following primers: (E85A) 5'-CTGACCGAGGCCGCGGCCGCGCTCAAC-3' and (E94A) 5'-CCACAACATGCTGGCATCCGACCCGCCGC-3'.

Expression and purification of PikC-RhFRED

The plasmid encoding PikC$_{D50N/D176Q/E246A}$-RhFRED was transformed into *E. coli* BL21(DE3) cells, and an individual colony was selected for overnight growth (37 °C) in 250 mL of LB containing kanamycin (50 μg/mL).[105] 12 x 1.5 L of LB (2.8 L baffled Fernbach flasks) supplemented with kanamycin (50 μg/mL), thiamine (1 mM), and $FeCl_3$

(100 μM) were each inoculated with 15 mL of overnight seed culture and incubated at 37 °C (160 rpm). When the OD_{600} reached 0.6-1.0, the cultures were cooled in an ice-water bath (15-20 min) before addition of IPTG (0.1 mM) and δ-aminolevulinic acid (1 mM). The cultures were grown at 18 °C for 18-20 h before the cells were harvested and stored at -80 °C until used for protein purification. All subsequent steps were performed at 4 °C. The cells were thawed and resuspended in 180 mL of lysis buffer (50 mM NaH_2PO_4, 300 mM NaCl, 10 mM imidazole, 10% glycerol, 1 mM PMSF, pH 8) prior to lysis via sonication. The crude lysate was centrifuged at 50,000 x g for 30 min to remove cellular debris, and the clarified lysate was incubated with 20 mL of pre-equilibrated Ni-NTA resin on a nutating shaker for 1-2 h. The slurry was loaded onto an empty column, and the lysate was pushed through with gentle syringe pressure. The resin was washed with wash buffer (50 mM NaH_2PO_4, 300 mM NaCl, 20 mM imidazole, 10% glycerol, pH 8) to remove bulk protein contaminants prior to elution of PikC-RhFRED with elution buffer (50 mM NaH_2PO_4, 300 mM NaCl, 300 mM imidazole, 10% glycerol, pH 8). The protein was subsequently concentrated using 30-50 kD MWCO centrifugal filters and desalted by loading onto PD-10 columns and eluting with storage buffer (50 mM NaH_2PO_4, 1 mM EDTA, 0.2 mM DTT, 10% glycerol, pH 7.3). The purified enzyme was typically used right away for large-scale reactions; any unused enzyme was aliquoted, flash frozen in liquid N_2, and stored at -80 °C for subsequent use in analytical- and/or additional large-scale reactions. The yield of functional P450 (as assessed by obtaining CO difference spectra according to the established protocol was ~4-9 mg per 1 L of overexpression culture.[132]

Analytical-scale enzymatic reactions

Analytical-scale enzymatic reactions were carried out under the following conditions: 5 μM PikC-RhFRED, 1 mM substrate (5% DMSO, final concentration), 1 mM $NADP^+$, 5 mM glucose-6-phosphate, and 1 U/mL glucose-6-phosphate dehydrogenase in storage buffer (50 mM NaH_2PO_4 (pH = 7.3), 1 mM EDTA, 0.2 mM DTT, 10% (v/v) glycerol). The total volume of each reaction was 100 μL (carried out in a 1.7 mL Eppendorf tube), and reactions were incubated at 30 °C (200 rpm) for 14-18 h prior to quenching via extraction with chloroform (2 x 100 μL). The combined organic layers were dried under a gentle stream of N_2 and resuspended in methanol prior to LC-MS analysis. The subsequent liquid chromatography mass spectrometry (LC-MS) analysis was performed on an Agilent Q-TOF HPLC-MS (Department of Chemistry, University of Michigan) equipped with an high resolution electrospray mass spectrometry (ESI-MS) source and a Beckmann Coulter reverse-phase HPLC system using an Waters XBridge C18 3.5 μm, 2.1x150 mm under the following conditions: mobile phase (A = deionized water + 0.1% formic acid, B = acetonitrile + 0.1% formic acid), 10% to 100% B over 15 min, 100% B for 4 min; flow rate, 0.2 mL/min. Reactions were scanned for [M+H] (starting material), [M+H+16] (monohydoxylation), [M+H+32] (dihydroxylation), [M+H-14] (demethylated starting material), and [M+H+2] (demethylated monohydroxylated product). In instances where a diethylamine was used instead of a dimethylamine, the scanned mass values were adjusted to observe deethylation. The percent conversion was determined as outlined in Li et al.[100] Briefly, the percent conversion was calculated with (AUCtotal products/(AUCtotal products + AUCunreacted substrate) by assuming ionization

efficiency of substrate and hydroxylated products are the same, because the ionization site of this series of compounds should be the dimethylamino group.[100]

Preparative-scale enzymatic reactions

To an Erlenmeyer flask containing reaction buffer (50 mM NaH_2PO_4, 1 mM EDTA, 0.2 mM DTT, 10% (v/v) glycerol, pH 7.3) were added the following components sequentially: substrate (20 mM stock in DMSO, 1 mM final concentration), glucose-6-phosphate (100 mM stock in reaction buffer, 5 mM final concentration), glucose-6-phosphate dehydrogenase (100 U/mL stock in water, 1 U/mL final concentration), PikC-RhFRED (varied stock concentrations, 5 µM final concentration), and $NADP^+$ (20 mM stock in reaction buffer, 1 mM final concentration). The reaction mixture was capped with a milk filter and incubated at 30 °C overnight (14-16 h) with gentle shaking (100 rpm). Reactions were typically conducted on ~40-60 mg of each substrate (~90-130 mL total reaction volume) and performed in 500 mL Erlenmeyer flasks. After overnight incubation, the reaction was quenched by addition of acetone (2 x total reaction volume) and incubated at 4 °C for 2 h. The mixture was then filtered through celite, and the acetone was removed under reduced pressure. The remaining aqueous solution was saturated with NaCl, adjusted to pH 11, and extracted with ethyl acetate (3 x total reaction volume). The combined organic layers were dried over anhydrous Na_2SO_4 and evaporated under reduced pressure to afford a crude mixture of products and remaining starting material, which were purified by flash column chromatography. Mixtures that were recalcitrant to separation using standard column chromatographic techniques were further purified via semi-preparative HPLC using a Beckman Coulter System Gold HPLC equipped with a

Waters XBridge BEH C18 column (dimensions, 250 x 10 mm; particle size, 5 μm; pore size, 130 Å). The flow rate was maintained at 3 mL/min, and the mobile phase consisted of an acetonitrile/water mixture with formic acid (0.1%) included as a modifier. All crude material was dissolved in methanol and filtered through 0.20 μm PTFE filters (EMD Millipore) prior to manual HPLC injection. UV absorption was monitored at 240 nm and 260 nm.

Representative PikC preparative scale reaction

Following the preparative-scale PikC reaction protocol, the oxidation of **38j** was performed on 60 mg (1.36 mmol) of substrate. Upon completion of the reaction and workup, an aliquot of the reaction was analyzed by LCMS to assess conversion and product ratios. One quarter of the crude material (~45 mg) was purified by silica gel chromatography (CH_2Cl_2 to 10% MeOH/CH_2Cl_2) to give 3.1 mg (20% yield) of the oxidized product **39j**.

Explanation of Content for Tables S1, S2, and S3.

In tables S1, S2, and S3 the product ratios from crude LCMS analysis are provided for all triazole linkers tested. Entries that are reflected in manuscript Table 1 are depicted in bold in Tables S1, S2, and S3. Cases where product structures were determined by authentic standard comparisons are described in detail below the supplementary tables. All compounds identified in manuscript Table 1 were fully characterized by NMR methods as described starting on page S41.

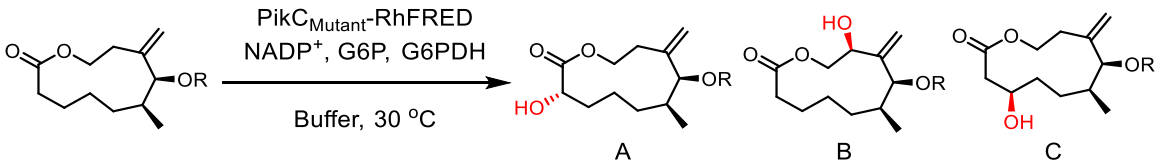

Entry	Substrate	Mutant	Conversion[a]	Ratio[b,c]	Major product
1	**38j**	**Triple**	**62**	**3(C):14(A):82(B):1**	**39j**
2	38j	Triple+E85A	60	3(C):25(A):71(B):1	-
3	38j	Triple+E94A	41	70(A):6(B):24	-
4	38j	D50N	31	2(C):16(A):77(B):5	-
5	**38k**	**Triple**	**55**	**1:22(A):73(B):4**	**39k**
6	**38h**	**Triple**	**39**	**6:94(A)**	**40c**
7	38h	Triple+E85A	39	6:94(A):0	-
8	38h	Triple+E94A	26	7:86(A):7	-
9	38h	D50N	2	-	-
10	**38l**	**Triple**	**31**	**71(C):24(A):4:1**	**41l**
11	38l	Triple+E85A	26	71(C):20(A):7:2	-
12	38l	Triple+E94A	33	81(C):15(A):2:2	-
13	38e	Triple	19	21:76:3	-
14	38f	Triple	29	14:76:10	-
15	38a	Triple	12	23:77	-
16	38b	Triple	27	18:82	-
17	38g	Triple	32	16:72:2:4:6	-
18	38d	Triple	25	15:80:2:3	-
19	38c	Triple	18	31:69	-
20	38i	Triple	28	8:42:46:4	-
21	38p	Triple	59	4:31:65(B)	-
22	38m	Triple	0	-	-
23	38n	Triple	0	-	-

[a]Values are percent conversion to M+H+16.

[b]Ratios for M+H+16 in order of elution from the LCMS.

[c]Known oxidation products shown in parentheses.

Table 5.1: PikC analytical reactions with the 11-membered macrocycle **38**.

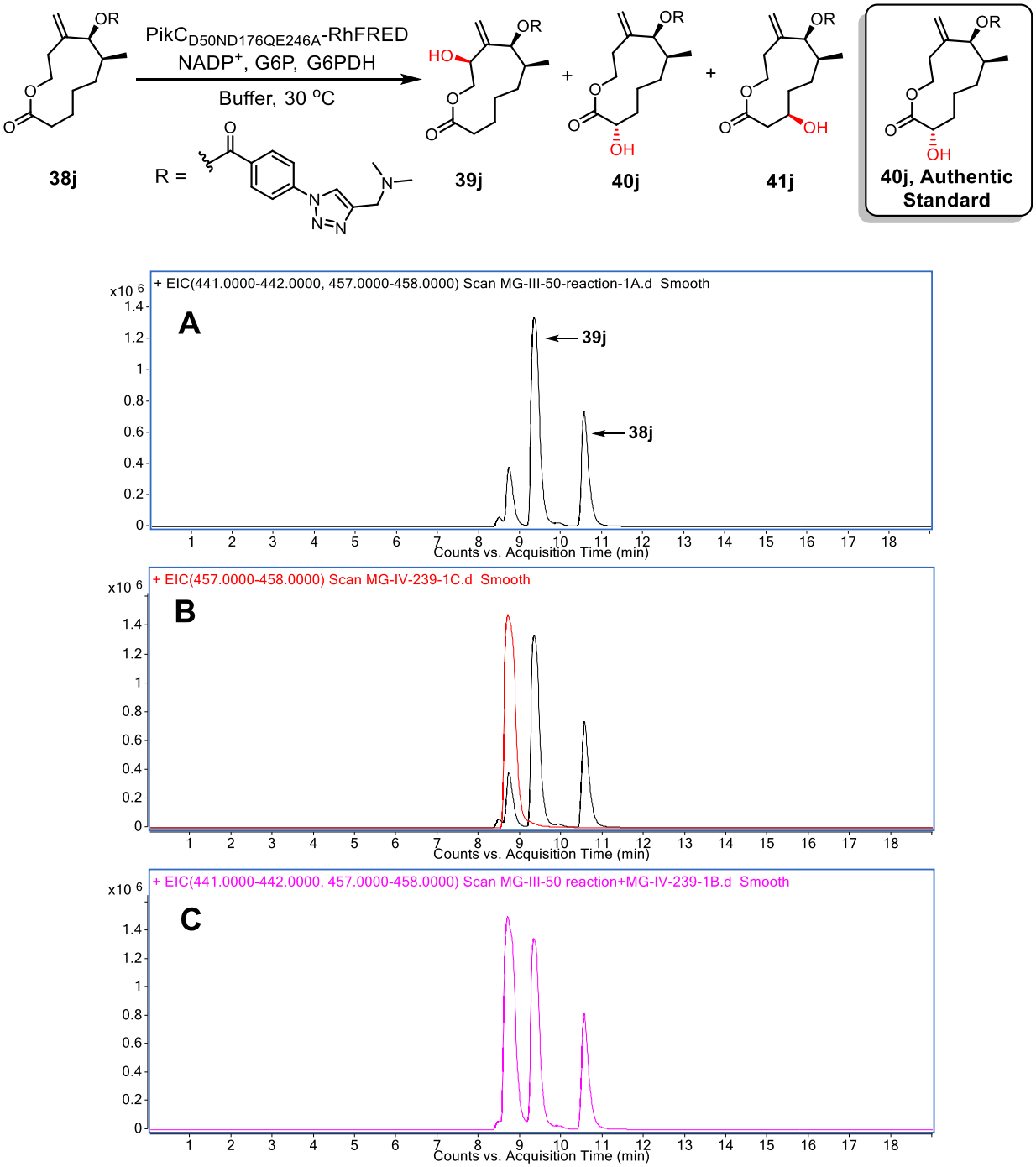

Figure 5.1: Identification of PikC product **40j** (Table 5.1, entry 1) with an authentic standard. **A**. The LCMS reaction profile of **38j** with PikC. **B**. The LCMS trace overlay of the PikC oxidation of **38j** (shown in black) and authentic standard (shown in red). **C**. The co-injection of the PikC oxidation of **38j** and authentic standard.

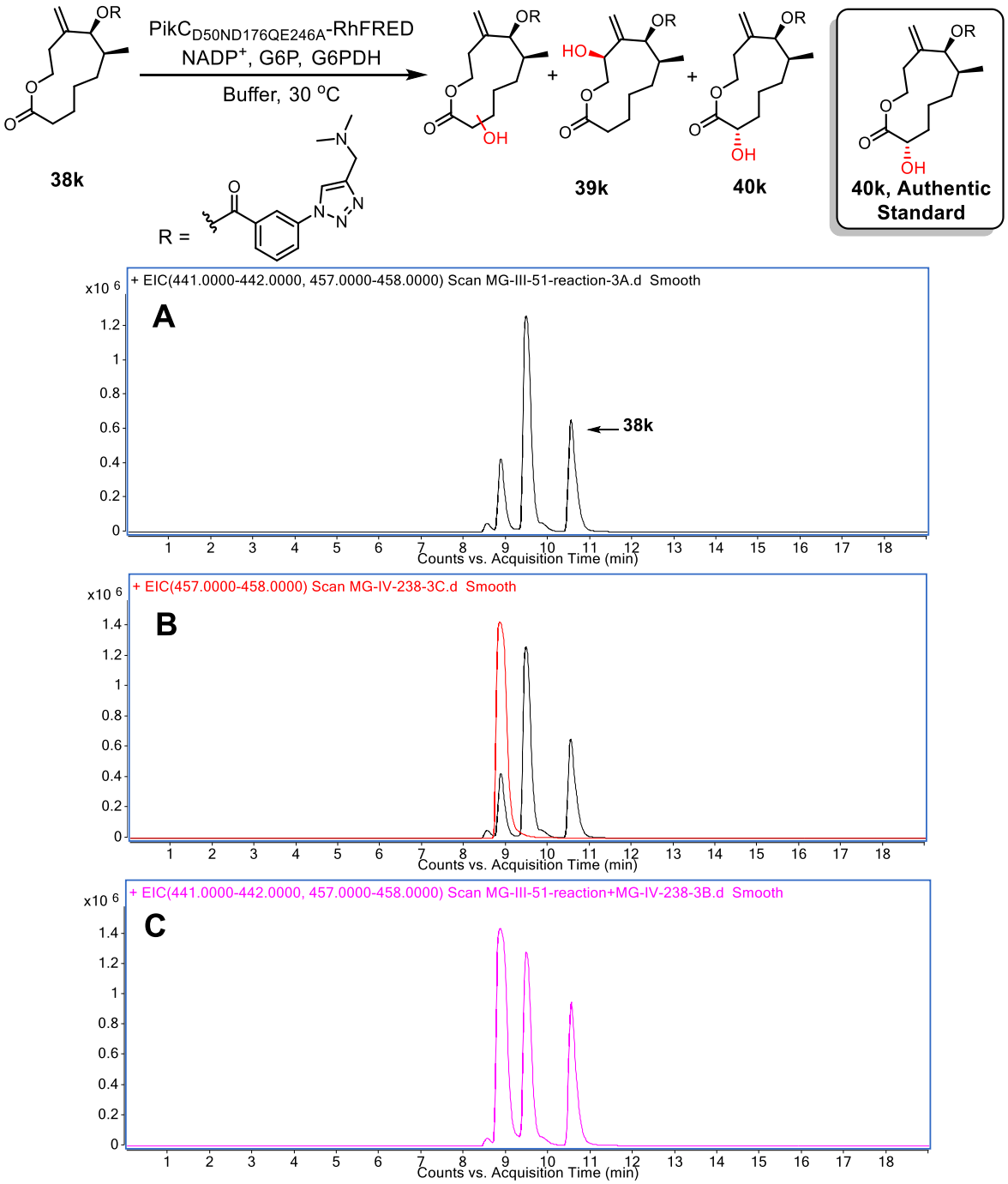

Figure 5.2: Identification of PikC product **40k** (Table 5.1, entry 5) with an authentic standard. **A**. The LCMS reaction profile of **38k** with PikC. **B**. The LCMS trace overlay of the PikC oxidation of **38k** (shown in black) and authentic standard (shown in red). **C**. The co-injection of the PikC oxidation of **38k** and authentic standard.

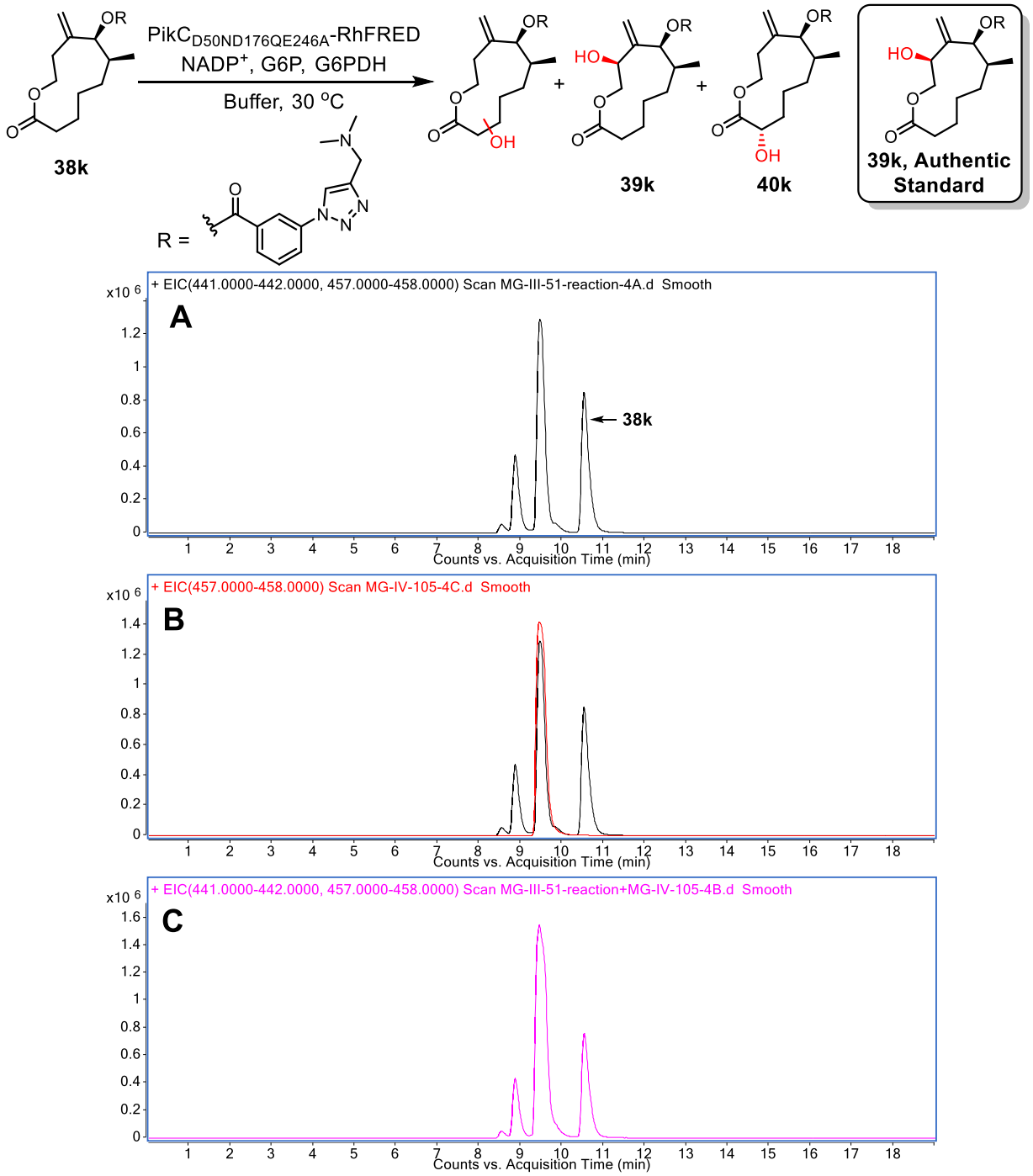

Figure 5.3: Identification of PikC product **39k** (Table 5.1, entry 5) with an authentic standard. **A.** The LCMS reaction profile of **38k** with PikC. **B**. The LCMS trace overlay of the PikC oxidation of **38k** (shown in black) and authentic standard (shown in red). **C**. The co-injection of the PikC oxidation of **38k** and authentic standard.

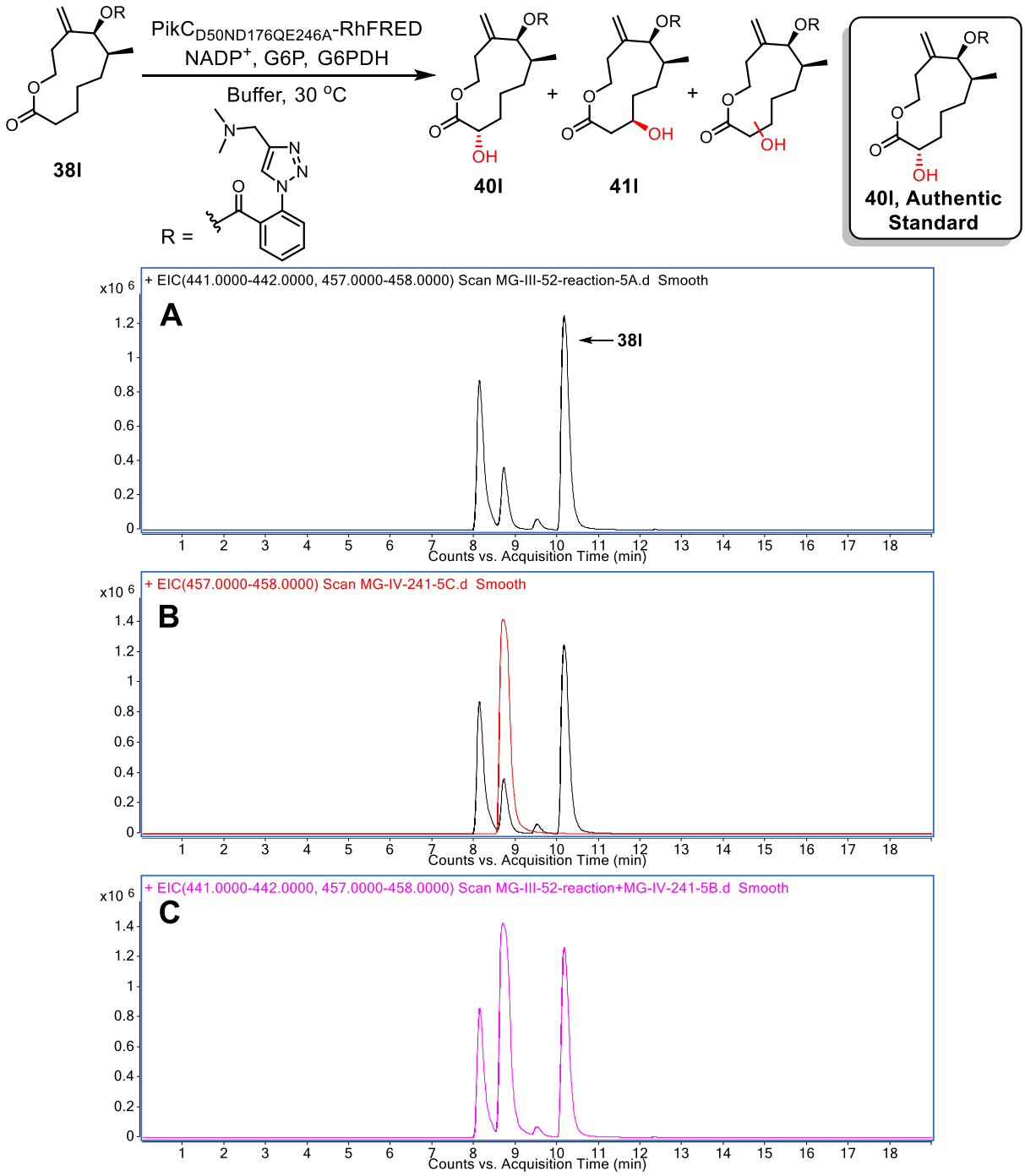

Figure 5.4: Identification of PikC product **40l** (Table 5.1, entry 10) with an authentic standard. **A**. The LCMS reaction profile of **38l** with PikC. **B**. The LCMS trace overlay of the PikC oxidation of **38l** (shown in black) and authentic standard (shown in red). **C**. The co-injection of the PikC oxidation of **4d** and authentic standard.

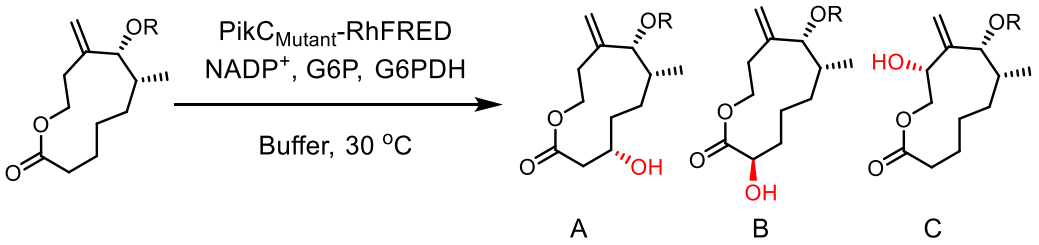

Entry	Substrate	Mutant	Conversion[a]	Ratio[b,c]	Major product
1	**52j**	**Triple**	**65**	**30(A):61(B):9(C)**	**53j**
2	52j	Triple+E94A	46	3(A):92(B):3(C):2	-
3	**52k**	**Triple**	**56**	**16:83(B):1(C)**	**53k**
4	52k	Triple+E94A	49	32:61(B):4(C):3	-
5	**52h**	**Triple**	**37**	**59:41[e]**	**54h**
6	**52l**	**Triple**	**36**	**67(A):22:11(B)**	**54l**
7	52l	Triple+E94A	45	86[d](A):12(B):2	-
8	52p	Triple	57	38:53:8:1	-
9	52p	Triple+E94A	32	3:93:4:0	

[a]Values are percent conversion to M+H+16.

[b]Ratios for M+H+16 in order of elution from the LCMS.

[c]Known oxidation products shown in parentheses.

[d]Multiple peaks overlap

[e]Prepartive ratio differs from the analytical scale ratio

Table 5.2: Analytical PikC reactions with the (*R*,*R*) 11-membered substrate **52**.

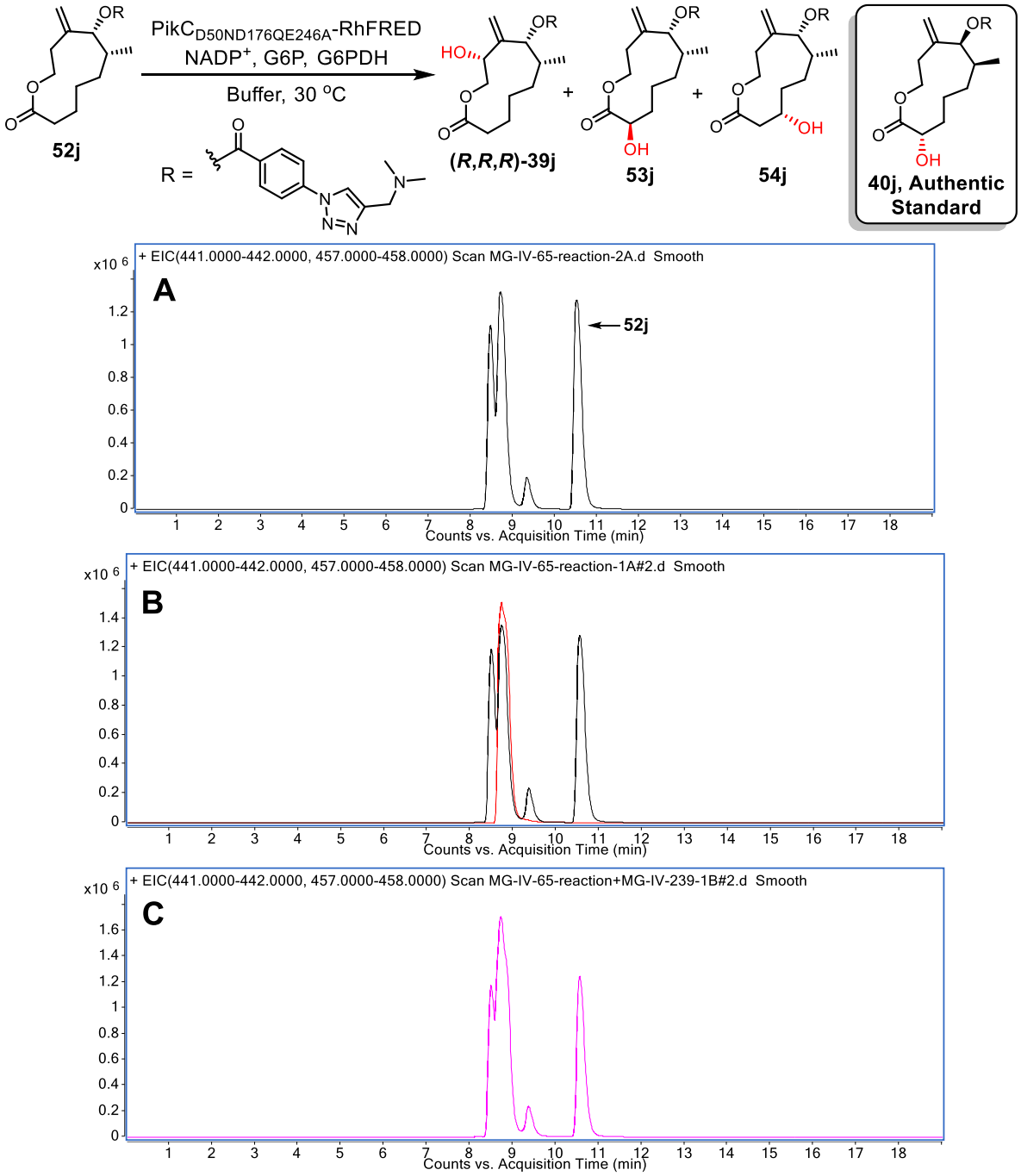

Figure 5.5: Identification of PikC product **53j** (Table 5.2, entry 1) with authentic standard **40j**. **A**. The LCMS reaction profile of **52j** with PikC. **B**. The LCMS trace overlay of the PikC oxidation of **52j** (shown in black) and authentic standard **40j** (shown in red). **C**. The co-injection of the PikC oxidation of **52j** and **40j**. Experiments are run under the assumption that enantiomeric compounds have identical LCMS retention times.

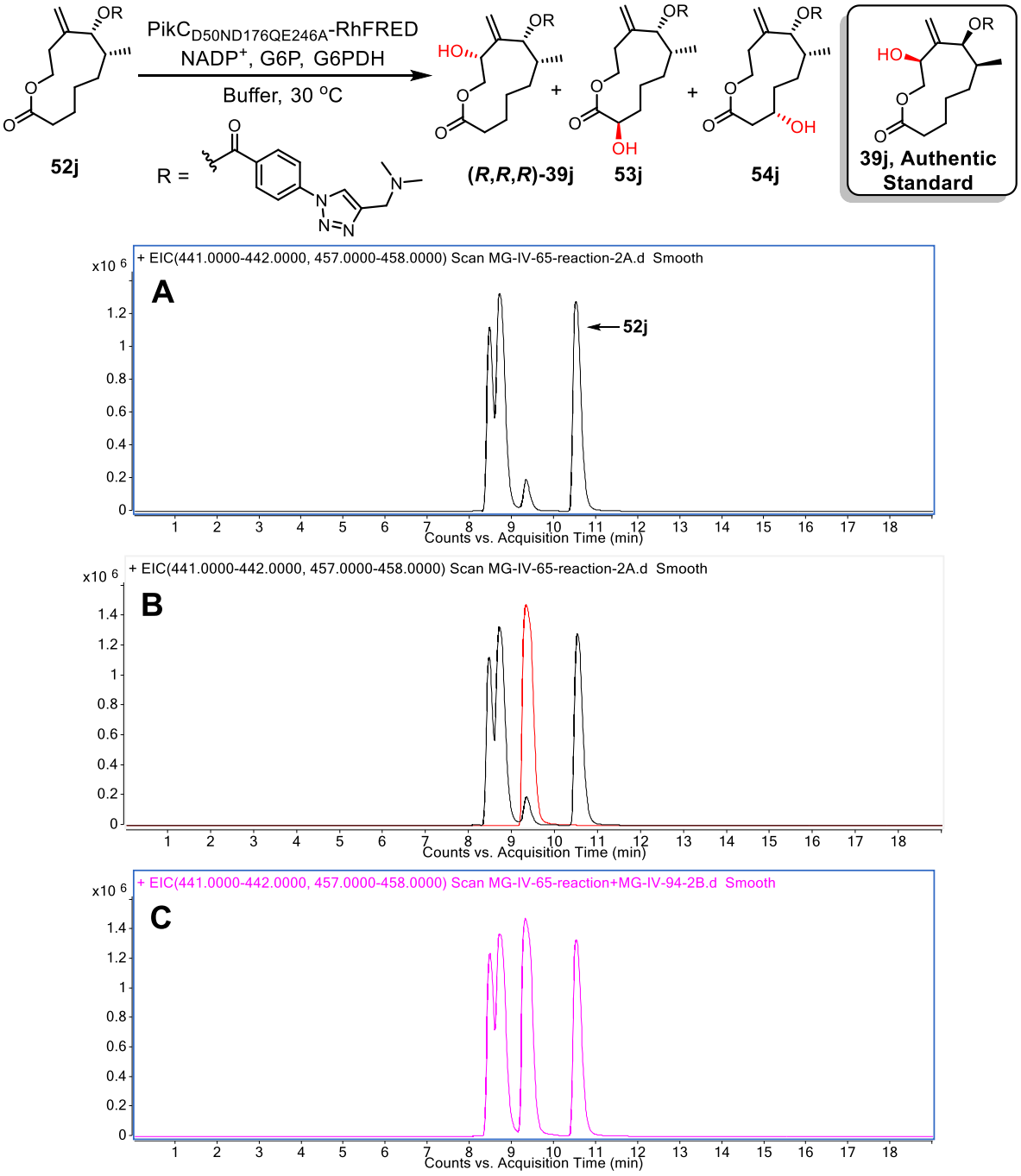

Figure 5.6: Identification of PikC product **(*R*,*R*,*R*)-39j** (Table 5.2, entry 1) with authentic standard **39j**. **A**. The LCMS reaction profile of **52j** with PikC. **B**. The LCMS trace overlay of the PikC oxidation of **52j** (shown in black) and authentic standard **39j** (shown in red). **C**. The co-injection of the PikC oxidation of **52j** and **39j**. Experiments are run under the assumption that enantiomeric compounds have identical LCMS retention times.

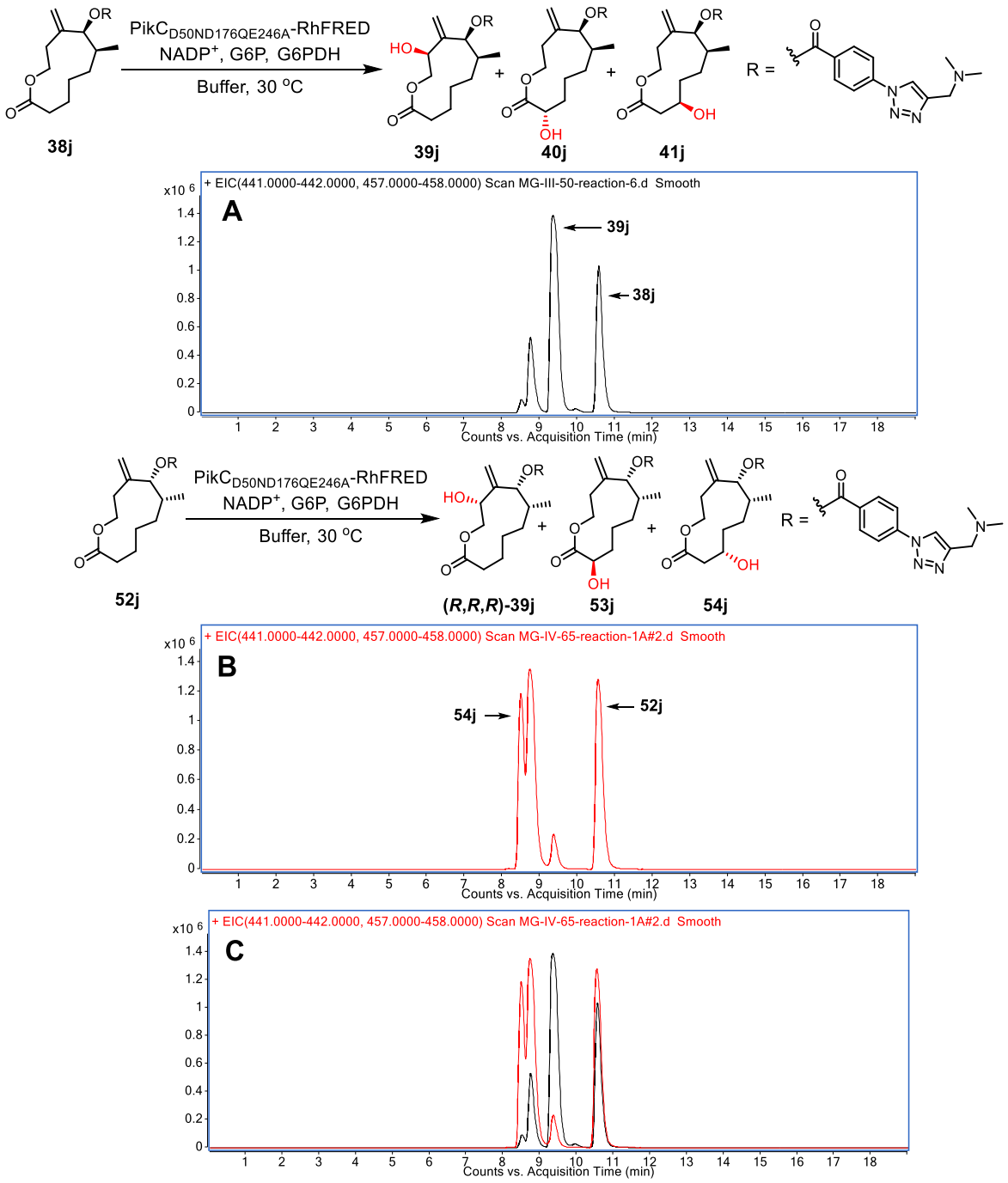

Figure 5.7: Identification of **41j** and **(*R*,*R*,*R*)-39j** (Table 5.2, entry 1) by the comparison of the LCMS retention times of the PikC reactions of **38j** and **52j**. Assignments are made under the assumption that enantiomeric compounds have identical retention times. **A**. The LCMS profile of the PikC oxidation of **38j** (repeated from table 5.1, entry 1). **B**. The LCMS profile of the PikC oxidation of **52j**. **C**. The overlay of LCMS profiles **A** and **B**.

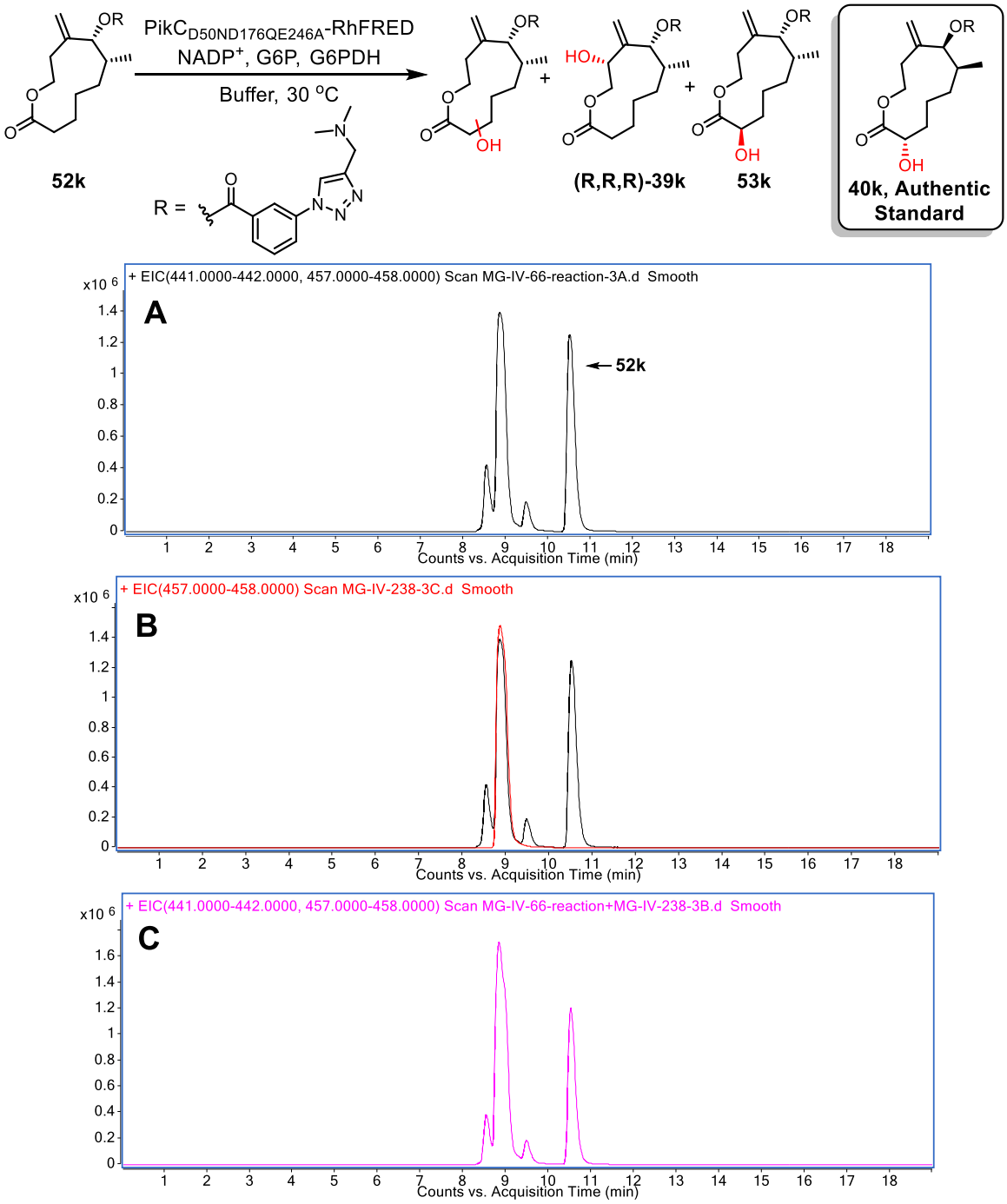

Figure 5.8: Identification of PikC product **53k** (Table 5.2, entry 3) with authentic standard **40k**. **A**. The LCMS reaction profile of **52k** with PikC. **B**. The LCMS trace overlay of the PikC oxidation of **52k** (shown in black) and authentic standard **40k** (shown in red). **C**. The co-injection of the PikC oxidation of **52k** and **40k**. Experiments are run under the assumption that enantiomeric compounds have identical LCMS retention times.

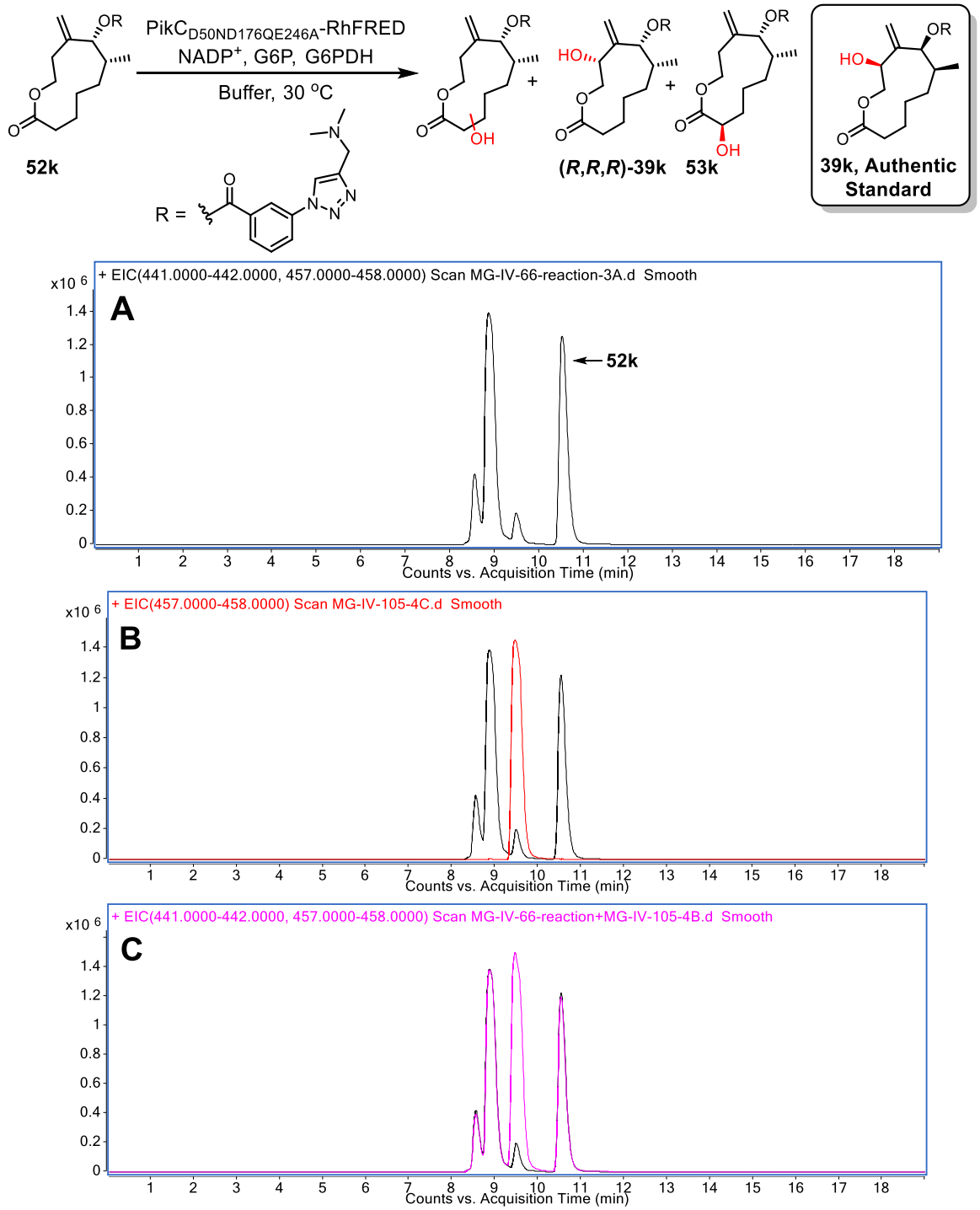

Figure 5.9: Identification of PikC product **(R,R,R)-39k** (Table 5.2, entry 3) with authentic standard **39k**. **A**. The LCMS reaction profile of **52k** with PikC. **B**. The LCMS trace overlay of the PikC oxidation of **52k** (shown in black) and authentic standard **39k** (shown in red). **C**. The co-injection of the PikC oxidation of **52k** and **39k**. Experiments are run under the assumption that enantiomeric compounds have identical LCMS retention times.

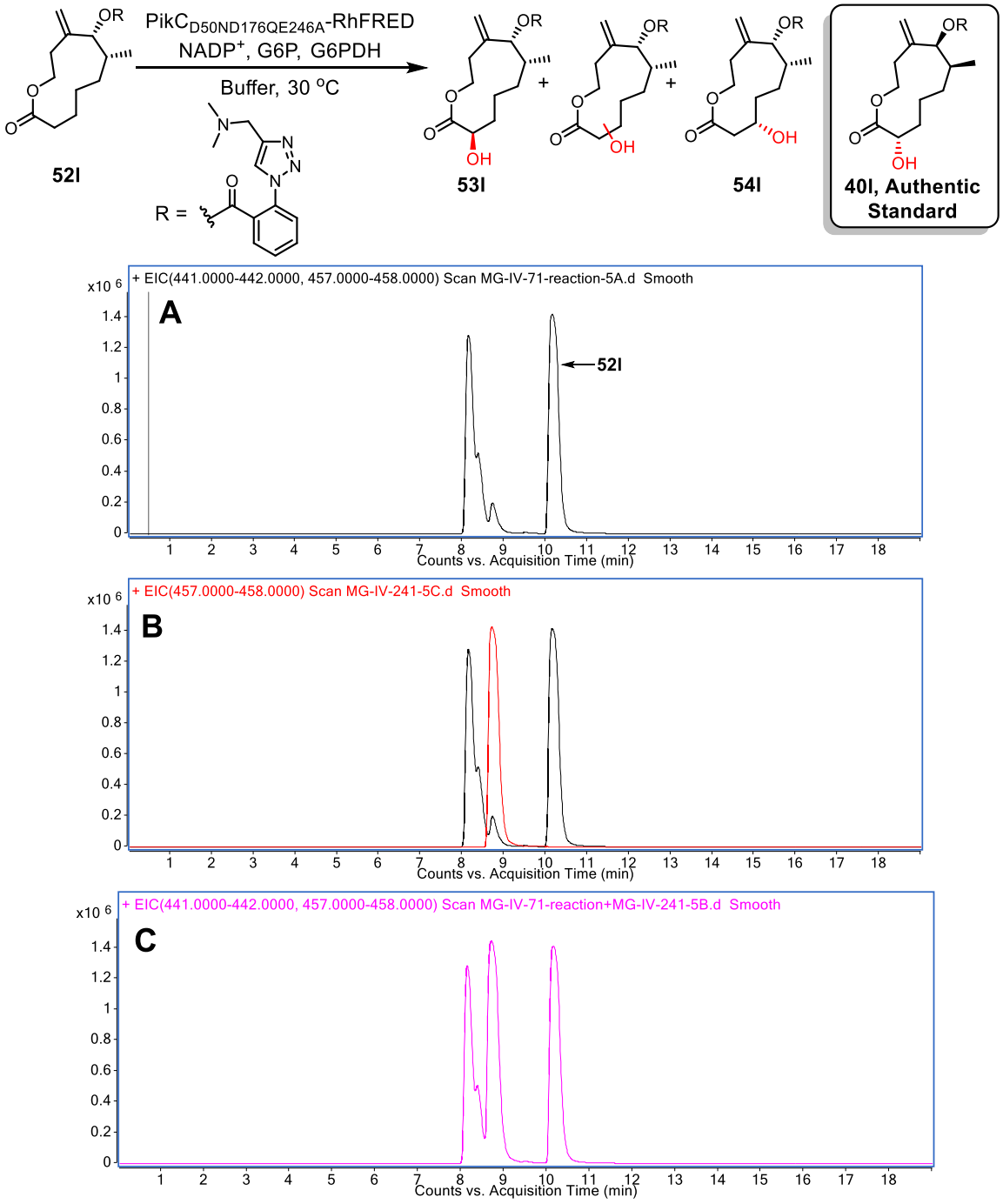

Figure 5.10: Identification of PikC product **53l** (Table 5.2, entry 6) with authentic standard **40l**. **A**. The LCMS reaction profile of **52l** with PikC. **B**. The LCMS trace overlay of the PikC oxidation of **52l** (shown in black) and authentic standard **40l** (shown in red). **C**. The co-injection of the PikC oxidation of **52l** and **40l**. Experiments are run under the assumption that enantiomeric compounds have identical LCMS retention times.

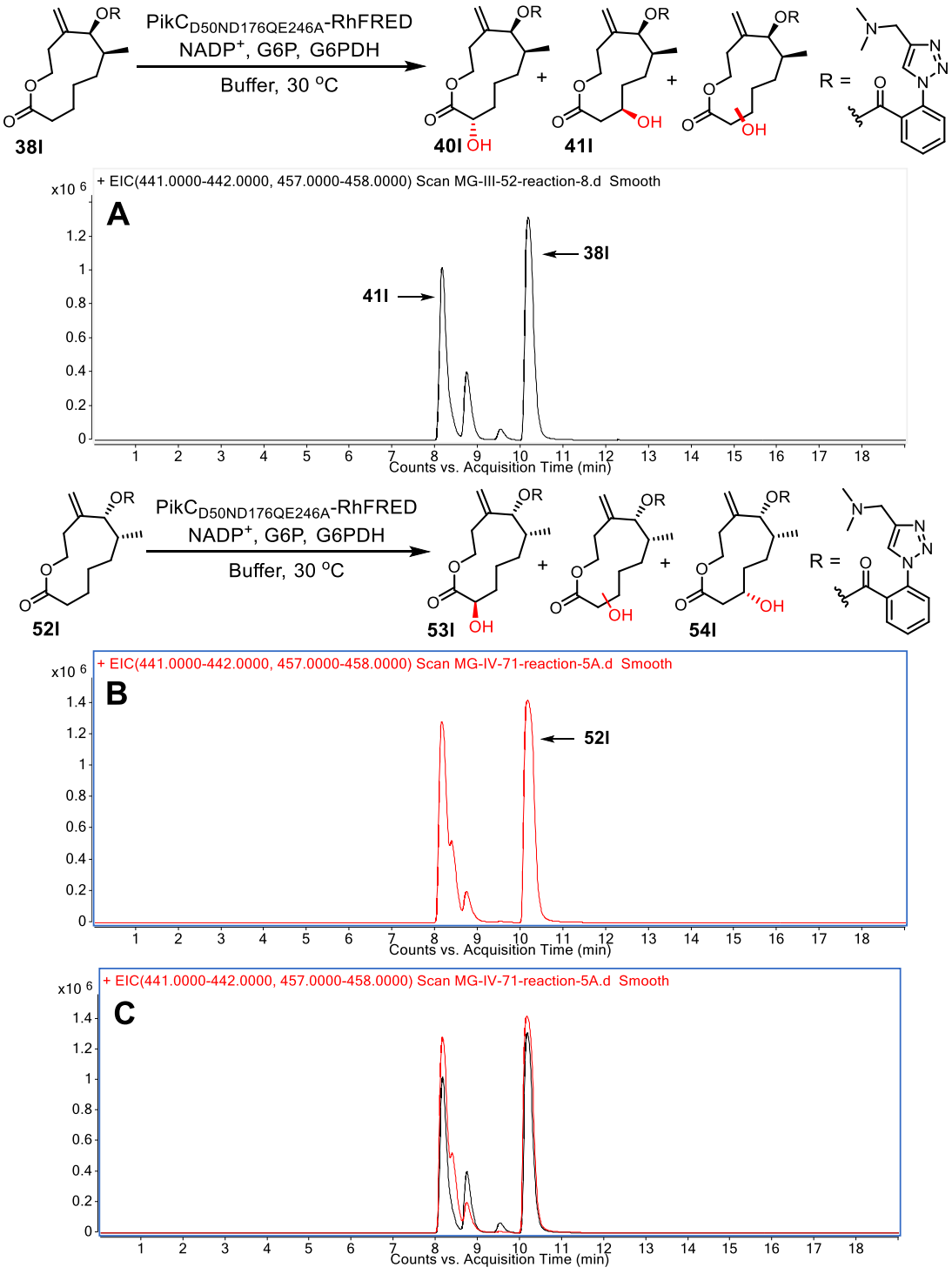

Figure 5.11: Identification of **54I** (Table 5.2, entry 6) by comparison of LCMS retention times of the PikC oxidation of **38I** and **52I**. Assignments are made under the assumption that enantiomeric compounds have identical retention times. **A**. The LCMS profile of the PikC oxidation of **38I** (Table 5.1, entry 10 repeated for comparison). **B**. The LCMS profile of the PikC oxidation of **52I**. **C**. The overlay of LCMS profiles **A** and **B**.

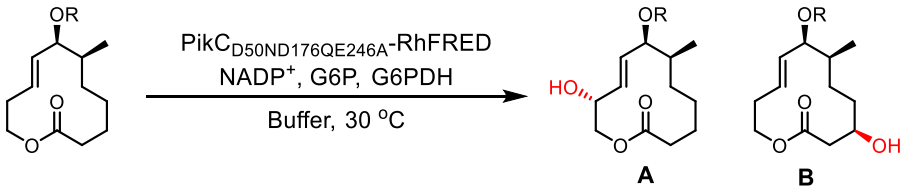

Entry	Substrate	Mutant	Conversion[a]	Ratio[b,c]	Major product
1	**55l**	**Triple**	**25**	**73(B):25(A):2**	**57j**
2	**55o**	**Triple**	**62**	**15:85(A)**	**56o**
3	55o	Triple+E85A	66	14:86(A)	56o
4	55o	Triple+E94A	42	29:71(A)	56o
5	55j	Triple	57	31:69(A)	56j

[a]Values are percent conversion to M+H+16.

[b]Ratios for M+H+16 in order of elution from the LCMS.

[c]Known oxidation products shown in parentheses.

Table 5.3: Analytical scale PikC reactions performed with the 12-membered macrolactone **55.**

5.3.4 Compounds Isolated from PikC Scale up Reactions

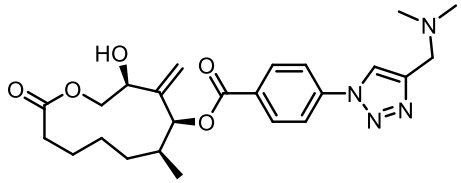

(3*S*,5*S*,6*S*)-3-Hydroxy-6-methyl-4-methylene-11-oxooxacycloundecan-5-yl-4-(4-((dimethylamino)methyl)-1H-1,2,3-triazol-1-yl)benzoate (39j):

The title compound was prepared following the preparative-scale enzymatic reaction protocol and isolated via benchtop chromatography (CH_2Cl_2 to 10% MeOH/CH_2Cl_2).

^{1}H NMR (700 MHz, $CDCl_3$) δ: 8.20 (d, *J* = 8.7 Hz, 2H), 8.14 (s, 1H), 7.87 (d, *J* = 8.6 Hz, 2H), 5.60 (d, *J* = 1.4 Hz, 1H), 5.54 (s, 1H), 5.25 (s, 1H), 4.85 (t, *J* = 10.6 Hz, 1H), 4.34 (dd, *J* = 10.6, 4.7, 1H), 4.01 (dd, *J* = 10.3, 4.7 Hz, 1H), 3.82 (s, 2H), 2.56 (ddd, *J* = 16.0, 7.5, 1.9 Hz, 1H), 2.43 (s, 7H), 2.17 (ddd, *J* = 16.2, 12.2, 1.9 Hz, 1H), 2.11 – 2.04 (m, 1H), 1.94 – 1.85 (m, 1H), 1.72 – 1.66 (m, 1H), 1.65 – 1.58 (m, 2H), 1.51 (td, *J* = 13.8, 13.2, 3.7 Hz, 1H), 1.30 – 1.23 (m, 1H), 1.05 (d, *J* = 6.8 Hz, 3H)

^{13}C NMR (176 MHz, $CDCl_3$) δ 172.70, 164.54, 149.02, 145.4, 140.24, 131.32, 130.07, 121.38, 120.01, 113.82, 80.63, 66.99, 65.69, 53.93, 44.70, 34.94, 30.14, 25.65, 24.51, 19.99, 16.61.

The fully substituted triazole carbon was detected at 145.4 ppm by HMBC.

HRMS (ESI) *m/z* calculated for $[M+H]^+$ 457.2445, found 457.2443.

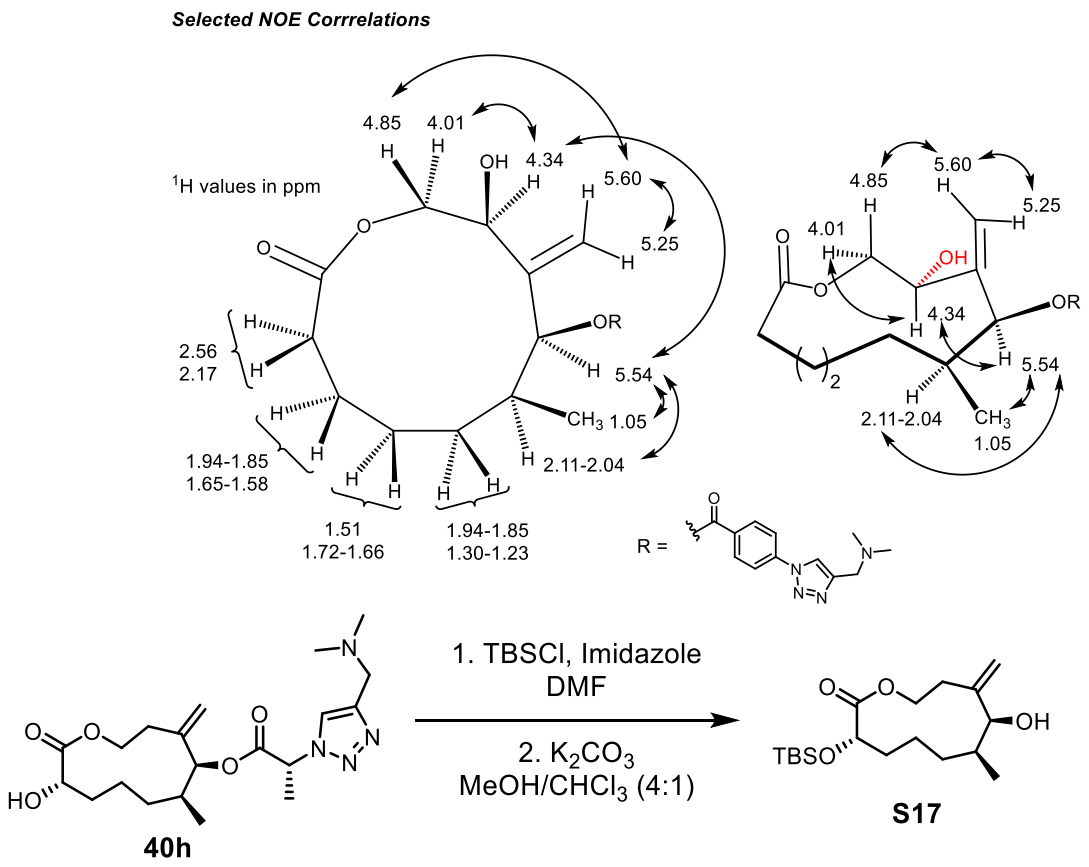

(3*S*,7*S*,8*S*)-3-((tert-Butyldimethylsilyl)oxy)-8-hydroxy-7-methyl-9-methyleneoxacycloundecan-2-one (S17):

Compound **40h** was prepared following the preparative-scale enzymatic reaction protocol using substrate **38h**. Prior to TBS protection and anchor methanolysis, most of the impurities from the crude PikC reaction were removed via column chromatography (CH_2Cl_2 to 10% MeOH/CH_2Cl_2).

An oven-dried vial equipped with stir bar was charged with the residue from the PikC oxidation reaction and 1.5 mL of DMF. TBSCl (40 eq.) and imidazole (60 eq.) were added sequentially and the contents stirred until the starting material was consumed as judged by TLC. Upon completion, the reaction was quenched by diluting with H_2O and EtOAc. The organic layer was extracted four times with H_2O and once with brine. Then, the organic layer was dried over Na_2SO_4, filtered, and concentrated. The resulting

residue with loaded onto a pad of silica gel and washed with CH_2Cl_2, then eluted with 10% MeOH/CH_2Cl_2. Removal of the solvent furnished the TBS protected compound, which was carried on directly to the methanolysis.

A vial containing the crude TBS protected product and a stir bar was suspended in 1.5 mL of MeOH/$CHCl_3$ (4:1) and allowed to stir for 5 min before the addition of K_2CO_3 (5.0 eq.). The contents were stirred until all of the starting material was consumed as judged by TLC. Upon completion, the reaction was quenched with pH 7 buffer and the aqueous layer extracted three times with EtOAc. The organic layers were combined, dried over Na_2SO_4, filtered, and concentrated. Purification of the crude residue by column chromatography (30% EtOAc/hexanes) afforded the title compound.

^{1}H NMR (500 MHz, $CDCl_3$) δ 5.28 (s, 1H), 5.21 (d, *J* = 1.9 Hz, 1H), 4.81 (ddd, *J* = 12.9, 10.7, 2.5 Hz, 1H), 4.15 (dt, *J* = 10.8, 3.4 Hz, 1H), 4.04 (dd, *J* = 9.9, 2.4 Hz, 1H), 3.99 (s, 1H), 2.39 (dd, *J* = 15.5, 3.3 Hz, 1H), 2.26 – 2.16 (m, 1H), 2.09 – 1.92 (m, 1H), 1.70 – 1.57 (m, 2H), 1.41 (s, 1H), 1.36 – 1.27 (m, 2H), 1.09 – 0.94 (m, 4H), 0.88 (s, 10H), 0.07 (s, 3H), 0.06 (s, 3H).

^{13}C NMR (176 MHz, $CDCl_3$) δ 173.19, 148.18, 111.14, 79.33, 73.89, 64.73, 31.96, 30.95, 30.06, 25.70, 24.25, 21.05, 18.24, 17.00, -5.02, -5.17.

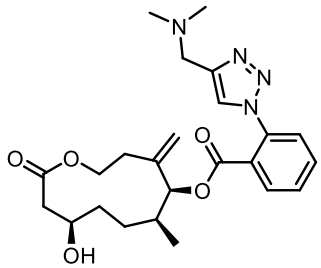

(5*S*,6*S*,9*R*)-9-Hydroxy-6-methyl-4-methylene-11-oxooxacycloundecan-5-yl 2-(4-((dimethylamino)methyl)-1H-1,2,3-triazol-1-yl)benzoate (41l):

The title compound was prepared following the preparative-scale enzymatic reaction protocol using substrate **38l** and isolated via preparative HPLC.

^{1}H NMR (700 MHz, $CDCl_3$) δ: 8.09 (s, 1H), 8.06 (d, *J* = 7.8 Hz, 1H), 7.71 (t, *J* = 7.7 Hz, 1H), 7.64 (t, *J* = 7.7 Hz, 1H), 7.51 (d, *J* = 7.9 Hz, 1H), 5.20 (s, 1H), 5.17 (s, 1H), 5.07 (s, 1H), 4.97 (ddd, *J* = 13.3, 11.2, 2.1 Hz, 1H), 4.28 – 4.21 (m, 1H), 4.05 (s, 2H), 3.95 (d, *J* = 11.2, 4.2, 2.1 Hz, 1H), 2.76 (d, *J* = 15.2 Hz, 1H), 2.58 (s, 6H), 2.46 – 2.37 (m, 2H), 2.23 – 2.14 (m, 1H), 2.13 – 2.06 (m, 1H), 1.92 – 1.84 (m, 1H), 1.66 – 1.59 (m, 1H), 1.57 – 1.51 (m, 1H), 1.20 – 1.12 (m, 1H), 1.02 (d, *J* = 6.8 Hz, 3H)

^{13}C NMR (176 MHz, $CDCl_3$) δ 170.29, 163.54, 142.25, 136.36, 132.96, 130.85, 130.22, 127.56, 127.33, 126.61, 112.57, 81.60, 66.03, 64.07, 53.81, 44.14, 43.57, 35.37, 30.73, 30.00, 23.90, 16.73

HRMS (ESI) *m/z* calculated for $[M+H]^+$ 457.2445, found 457.2442.

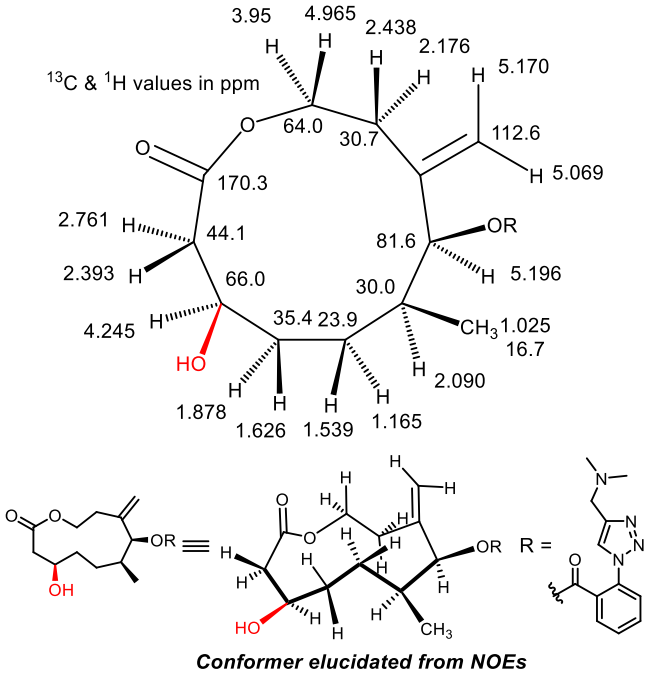

Conformer elucidated from NOEs

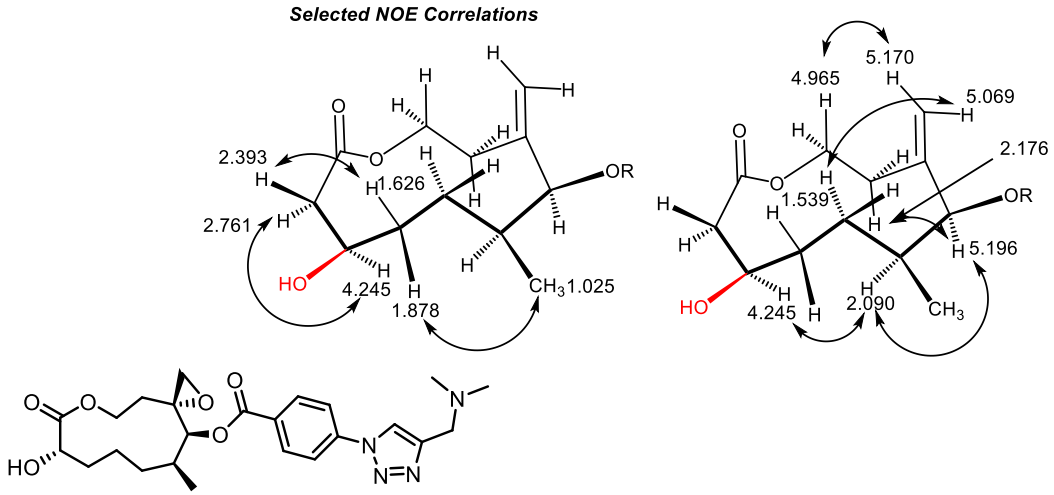

(3*R*,8*S*,12*S*,13*S*)-8-Hydroxy-12-methyl-7-oxo-1,6-dioxaspiro[2.10]tridecan-13-yl-4-(4-((dimethylamino)methyl)-1H-1,2,3-triazol-1-yl)benzoate (44j):

The title compound was prepared following the preparative-scale enzymatic reaction protocol using substrate **43j** and isolated via preparative HPLC.

^{1}H NMR (700 MHz, $CDCl_3$) δ 8.13 (d, *J* = 8.7 Hz, 2H), 8.01 (s, 1H), 7.85 (d, *J* = 8.7 Hz, 2H), 5.42 (s, 1H), 4.58 (dt, *J* = 11.6, 3.9 Hz, 1H), 4.24 – 4.18 (m, 1H), 4.15 (dd, *J* = 8.9, 2.1 Hz, 1H), 3.71 (s, 2H), 2.98 (d, *J* = 4.5 Hz, 1H), 2.92 (d, *J* = 4.6 Hz, 1H), 2.40 – 2.32 (m, 7H), 2.16 – 2.10 (m, 1H), 2.09 – 1.99 (m, 2H), 1.90 – 1.81 (m, 2H), 1.79 – 1.72 (m, 2H), 1.40 (ddt, *J* = 14.9, 10.3, 5.1 Hz, 1H), 1.01 (d, *J* = 6.8 Hz, 3H).

^{13}C NMR (176 MHz, $CDCl_3$) δ 174.91, 164.54, 146.60, 140.25, 131.31, 129.90, 120.35, 119.79, 75.96, 71.72, 62.30, 57.05, 54.37, 48.55, 45.29, 31.89, 31.20, 31.00, 27.41, 21.68, 17.06.

HRMS (ESI) *m/z* calculated for $[M+H]^+$ 473.2395, found 473.2396.

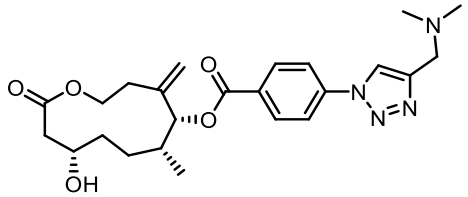

(5*R*,6*R*,9*S*)-9-Hydroxy-6-methyl-4-methylene-11-oxooxacycloundecan-5-yl 4-(4-((dimethylamino)methyl)-1H-1,2,3-triazol-1-yl)benzoate (54j):

Compound **54j** was prepared following the preparative-scale enzymatic reaction protocol using substrate **52j** and was purified by preparative HPLC.

^{1}H NMR (700 MHz, $CDCl_3$) δ: 8.22 (d, *J* = 8.7 Hz, 2H), 8.18 (s, 1H), 7.88 (d, *J* = 8.7 Hz, 2H), 5.37 (s, 1H), 5.20 (s, 1H), 5.12 (d, *J* = 2.0 Hz, 1H), 5.02 (ddd, *J* = 13.4, 11.0, 2.6 Hz, 1H), 4.30 (tt, *J* = 10.5, 2.9 Hz, 1H), 4.00 (ddd, *J* = 11.0, 4.2, 2.3 Hz, 1H), 3.88 (s, 2H), 2.81 (d, *J* = 15.4 Hz, 1H), 2.58 – 2.40 (m, 8H), 2.28 (dddd, *J* = 15.1, 13.0, 4.3, 1.9 Hz, 1H), 2.23 – 2.15 (m, 1H), 1.99 – 1.92 (m, 1H), 1.72 – 1.64 (m, 2H), 1.41 – 1.33 (m, 1H), 1.10 (d, *J* = 6.8 Hz, 3H)

^{13}C NMR (176 MHz, $CDCl_3$) δ 170.27, 164.46, 142.89, 142.57, 140.19, 131.33, 130.21, 121.45, 120.00, 112.42, 81.24, 66.05, 64.11, 53.48, 44.33, 44.25, 35.45, 30.72, 29.87, 24.13, 16.83.

The fully substituted triazole carbon was detected at 142.89 ppm by HMBC.

HRMS (ESI) *m/z* calculated for $[M+H]^+$ 457.2445, found 457.2448.

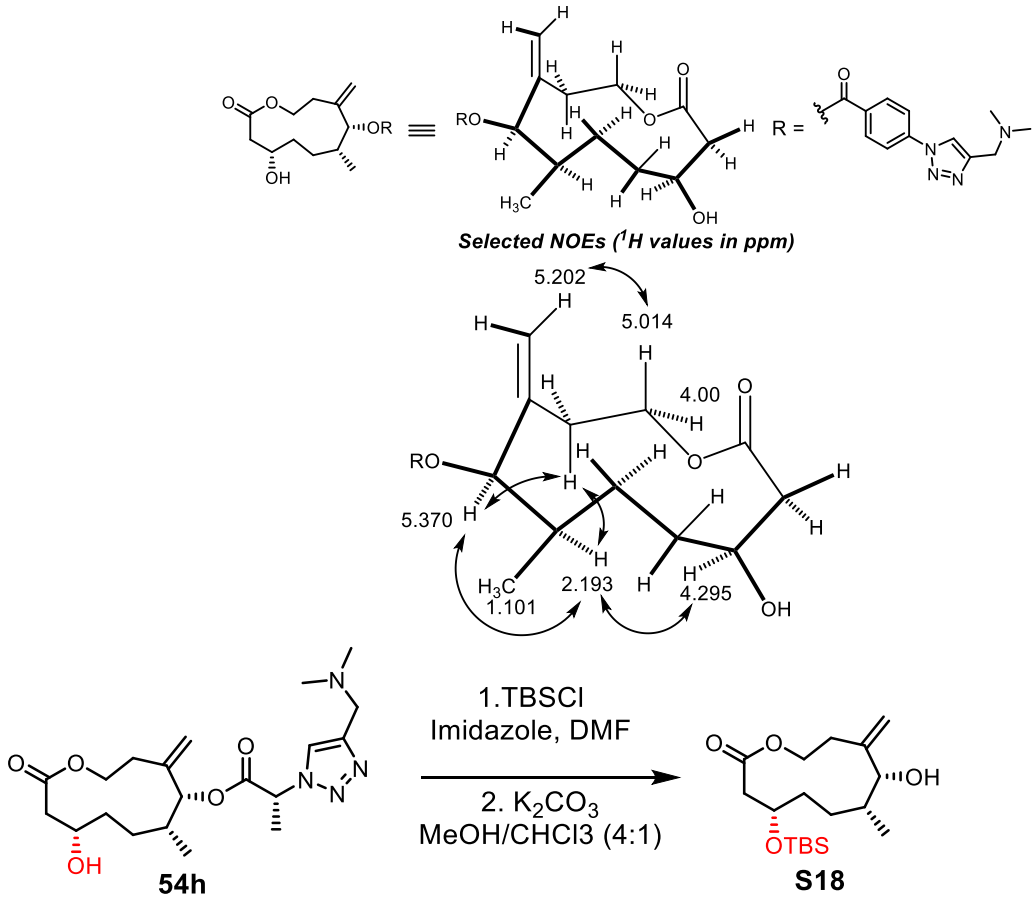

(4*S*,7*R*,8*R*)-4-((tert-butyldimethylsilyl)oxy)-8-hydroxy-7-methyl-9-methyleneoxacycloundecan-2-one (S18):

Compound **54h** was prepared following the preparative-scale enzymatic reaction protocol using substrate **52h**. Prior to TBS protection and anchor methanolysis, **13c** was purified by preparative HPLC.

An oven-dried vial equipped with stir bar was charged with the residue from the PikC oxidation reaction and 1.5 mL of DMF. TBSCl (40 eq.) and imidazole (60 eq.) were added sequentially and the contents stirred until the starting material was consumed as judged by TLC. Upon completion, the reaction was quenched by diluting with H_2O and EtOAc. The organic layer was extracted four times with H_2O and once with brine. Then, the organic layer was dried over Na_2SO_4, filtered, and concentrated. The resulting

residue with loaded onto a pad of silica gel and washed with CH_2Cl_2, then eluted with 10% MeOH/CH_2Cl_2. Removal of the solvent furnished the TBS protected compound, which was carried on directly to the methanolysis.

A vial containing the crude TBS protected product and a stir bar was suspended in 1.5 mL of MeOH/$CHCl_3$ (4:1) and allowed to stir for 5 min before the addition of K_2CO_3 (5.0 eq.). The contents were stirred until all the starting material was consumed as judged by TLC. Upon completion, the reaction was quenched with pH 7 buffer and the aqueous layer extracted three times with EtOAc. The organic layers were combined, dried over Na_2SO_4, filtered, and concentrated. Purification of the crude residue by column chromatography (30% EtOAc/hexanes) afforded the title compound.

^{1}H NMR (700 MHz, $CDCl_3$) δ 5.28 (d, *J* = 2.1 Hz, 1H), 5.21 (s, 1H), 4.93 (ddd, *J* = 13.4, 10.9, 2.7 Hz, 1H), 4.19 (tt, *J* = 10.6, 2.9 Hz, 1H), 3.99 (ddd, *J* = 10.9, 4.3, 2.2 Hz, 1H), 3.96 (s, 1H), 2.62 (d, *J* = 15.5 Hz, 1H), 2.40 (dd, *J* = 15.5, 10.3 Hz, 1H), 2.36 (d, *J* = 15.6 Hz, 1H), 2.16 (dddd, *J* = 15.2, 13.2, 4.3, 2.0 Hz, 1H), 1.95 – 1.88 (m, 1H), 1.82 – 1.76 (m, 1H), 1.56 (ddt, *J* = 14.2, 10.9, 4.2 Hz, 1H), 1.40 (s, 1H), 1.35 – 1.29 (m, 1H), 0.89 (s, 9H), 0.09 (s, 6H).

^{13}C NMR (176 MHz, $CDCl_3$) δ 170.71, 147.53, 111.12, 79.42, 66.77, 64.02, 45.00, 35.85, 30.60, 29.89, 25.80, 22.61, 18.06, 17.14, -4.69, -4.88.

HRMS (ESI) *m/z* calculated for $[M+Na]^+$ 365.2119, found 365.2121.

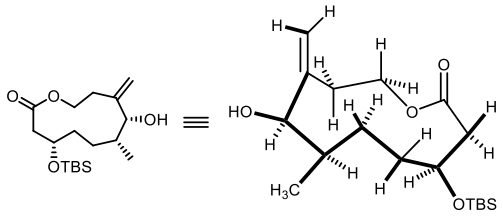

Selected NOEs (^{1}H values in ppm)

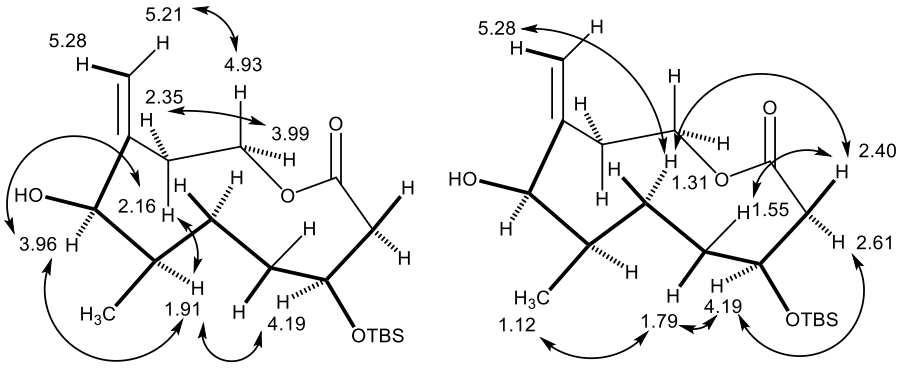

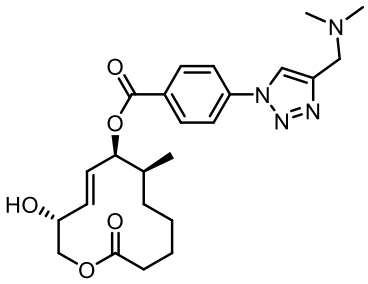

(3*R*,6*S*,7*S*,*E*)-3-Hydroxy-7-methyl-12-oxooxacyclododec-4-en-6-yl-4-(4-((dimethylamino)methyl)-1H-1,2,3-triazol-1-yl)benzoate (56j):

Compound **56j** was prepared following the preparative-scale enzymatic reaction protocol using substrate **55j** and was purified by preparative HPLC.

^{1}H NMR (700 MHz, $CDCl_3$) δ 8.20 (d, *J* = 8.7 Hz, 2H), 8.02 (s, 1H), 7.87 (d, *J* = 8.6 Hz, 2H), 5.90 (ddd, *J* = 15.5, 5.7, 1.3 Hz, 1H), 5.66 (td, *J* = 3.9, 1.8 Hz, 1H), 5.63 (ddd, *J* = 15.5, 5.6, 1.4 Hz, 1H), 4.45 – 4.42 (m, 1H), 4.36 (dd, *J* = 11.4, 3.9 Hz, 1H), 4.33 (dd, *J* = 11.4, 5.5 Hz, 1H), 3.71 (s, 2H), 2.43 (ddd, *J* = 14.6, 7.6, 4.1 Hz, 1H), 2.38 – 2.32 (m, 7H), 2.08 – 2.01 (m, 1H), 1.85 – 1.78 (m, 1H), 1.70 – 1.63 (m, 1H), 1.55 – 1.42 (m, 3H), 1.41 – 1.35 (m, 1H), 1.07 (d, *J* = 7.0 Hz, 3H).

^{13}C NMR (176 MHz, $CDCl_3$) δ 173.78, 164.60, 146.58, 140.23, 131.33, 130.75, 130.17, 129.11, 120.35, 119.85, 77.26, 70.92, 65.37, 54.36, 45.29, 35.22, 32.59, 29.89, 24.03, 23.75, 17.07.

HRMS (ESI) *m/z* calculated for $[M+H]^+$ 457.2445, found 457.2444.

The stereochemistry of **56j** was determined by Mosher ester derivatization (see the stereochemical determination and chemical correlation section for the comparison of the two ester ^{1}H NMRs and subsequent assignment).

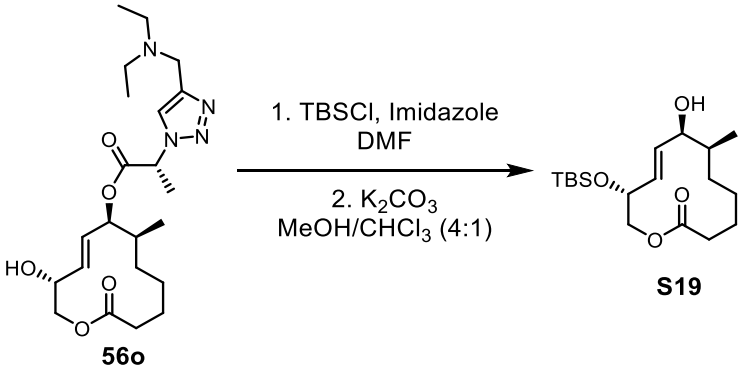

56o **S19**

(7*S*,8*S*,11*R*,*E*)-11-((tert-Butyldimethylsilyl)oxy)-8-hydroxy-7-methyloxacyclododec-9-en-2-one (S19):

Compound **56o** was prepared following the preparative-scale enzymatic reaction protocol using substrate **55o**. Prior to TBS protection and anchor methanolysis, **56o** was purified by column chromatography (CH_2Cl_2 to 10% MeOH/CH_2Cl_2).

An oven-dried vial equipped with stir bar was charged with the residue from the PikC oxidation reaction and 1.5 mL of DMF. TBSCl (40 eq.) and imidazole (60 eq.) were added sequentially and the contents stirred until the starting material was consumed as judged by TLC. Upon completion, the reaction was quenched by diluting with H_2O and EtOAc. The organic layer was extracted four times with H_2O and once with brine. Then, the organic layer was dried over Na_2SO_4, filtered, and concentrated. The resulting

residue with loaded onto a pad of silica gel and washed with CH_2Cl_2, then eluted with 10% MeOH/CH_2Cl_2. Removal of the solvent furnished the TBS protected compound, which was carried on directly to the hydrolysis.

A vial containing the crude TBS protected product and a stir bar was suspended in 1.5 mL of MeOH/$CHCl_3$ (4:1) and allowed to stir for 5 min before the addition of K_2CO_3 (5.0 eq.). The contents were stirred until all the starting material was consumed as judged by TLC. Upon completion, the reaction was quenched with pH 7 buffer and the aqueous layer extracted three times with EtOAc. The organic layers were combined, dried over Na_2SO_4, filtered, and concentrated. Purification of the crude residue by column chromatography (30% EtOAc/hexanes) afforded the title compound.

^{1}H NMR (700 MHz, $CDCl_3$) δ: 5.72 (dd, *J* = 15.4, 8.1 Hz, 1H), 5.50 (dd, *J* = 15.4, 8.0 Hz, 1H), 4.41 (dd, *J* = 10.6, 8.7 Hz, 1H), 4.33 (td, *J* = 8.3, 4.8 Hz, 1H), 4.22 (s, 1H), 3.89 (dd, *J* = 10.6, 4.8 Hz, 1H), 2.33 (dt, *J* = 14.4, 4.8 Hz, 1H), 2.27 (ddd, *J* = 14.7, 11.8, 3.8 Hz, 1H), 1.91 – 1.82 (m, 2H), 1.51 – 1.44 (m, 1H), 1.41 (s, 1H), 1.36 – 1.26 (m, 3H), 1.19 – 1.11 (m, 1H), 0.99 (d, *J* = 6.9 Hz, 3H), 0.89 (s, 9H), 0.08 (s, 3H), 0.06 (s, 3H)

^{13}C NMR (176 MHz, $CDCl_3$) δ 173.24, 133.05, 132.48, 75.21, 74.53, 71.87, 64.74, 36.34, 32.23, 30.50, 25.76, 24.12, 23.37, 18.14, 15.68, -4.28, -4.81.

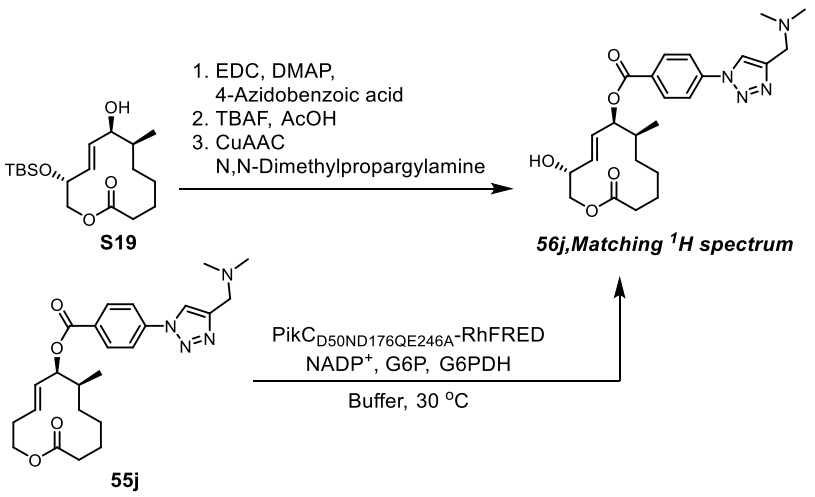

Scheme 5.1: Stereochemical assignment of **S19** by conversion to **56j**.

Stereochemical determination of S19 by chemical synthesis.

An oven-dried vial equipped with stir bar was charged with 3 mg (0.009 mmol) of **S19** and suspended in 1 mL of CH_2Cl_2. Then, 7 mg (0.045 mmol) of 4-azidobenzoic acid, 2 mg (0.018 mmol) of DMAP, and 7 mg (0.045 mmol) of EDC were added sequentially. The contents were stirred until all the starting material was consumed as judged by TLC. Upon completion, the reaction was quenched with a 1 M aqueous HCl solution and EtOAc. The organic layer was extracted twice with a 1 M aqueous HCl solution, once with sat'd aqueous sodium bicarbonate, and once with brine. The organic layer was dried over Na_2SO_4, filtered, concentrated, and carried on to the next step without further purification.

To an oven-dried vial equipped with stir bar was added the crude material from the EDC esterification and 0.50 mL of THF. The contents were cooled to 0 °C, whereupon 1 µL of AcOH and 0.108 µL of a 1 M solution of TBAF in THF where added sequentially. The reaction was warmed to rt and stir until all of the starting material was consumed as judged by TLC. Upon completion, the reaction was quenched with sat'd NH_4Cl and Et_2O.

The aqueous layer was extracted thrice with Et_2O, the organic layers combined, filtered, and concentrated to give the free alcohol. The crude material was carried on to the CuAAC cyclization without further purification.

Following the general CuAAC reaction procedure, the reaction of the crude material obtained from the deprotection, 0.005 mL (0.045 mmol) N,N-dimethylprop-2-yn-1-amine, $4.5x10^{-4}$ mmol $CuSO_4•5H_2O$, and $4.5x10^{-3}$ mmol of sodium ascorbate in 1.0 ml of H_2O/*t*-BuOH (1:1) afforded the desired adduct. After following the standard workup, the crude material was washed through a plug of silica with CH_2Cl_2 and then eluted with 10% MeOH/CH_2Cl_2 to afford the triazole, the ^1H NMR spectrum of which matched that of **S25** obtained through PikC oxidation (see the stereochemical determination and chemical correlation section for stacked ^1H NMRs).

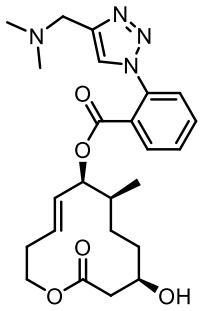

(6*S*,7*S*,10*R*,*E*)-10-hydroxy-7-methyl-12-oxooxacyclododec-4-en-6-yl-2-(4-((dimethylamino)methyl)-1H-1,2,3-triazol-1-yl)benzoate (57l):

Compound **57l** was prepared following the preparative-scale enzymatic reaction protocol using substrate **55l** and was purified by preparative HPLC.

^1H NMR (700 MHz, $CDCl_3$) δ 8.10 (s, 1H), 8.04 (d, *J* = 7.8 Hz, 1H), 7.70 (t, *J* = 7.7 Hz, 1H), 7.64 (t, *J* = 7.7 Hz, 1H), 7.50 (d, *J* = 7.8 Hz, 1H), 5.53 – 5.44 (m, 2H), 5.38 (t, *J* = 5.1 Hz, 1H), 4.43 – 4.36 (m, 1H), 4.27 – 4.19 (m, 3H), 4.14 – 4.07 (m, 1H), 2.68 (s, 6H), 2.62 (dd, *J* = 14.1, 4.3 Hz, 1H), 2.52 (dd, *J* = 14.2, 8.8 Hz, 1H), 2.45 – 2.39 (m, 2H),

1.99 – 1.93 (m, 1H), 1.65 – 1.56 (m, 2H), 1.53 – 1.47 (m, 1H), 1.33 – 1.27 (m, 1H), 0.94 (d, *J* = 7.0 Hz, 3H).

^{13}C NMR (176 MHz, $CDCl_3$) δ 171.28, 164.28, 144.88, 136.31, 132.53, 130.93, 130.15, 129.80, 128.75, 127.86, 126.88, 124.45, 77.80, 68.37, 61.08, 54.37, 45.22, 40.24, 34.36, 33.31, 30.74, 26.09, 15.74.

HRMS (ESI) *m/z* calculated for $[M+H]^+$ 457.2445, found 457.2445.

The stereochemistry of **57l** was determined by Mosher ester derivatization (see the stereochemical determination and chemical correlation section for the comparison of the two ester ^{1}H NMR and subsequent assignment).

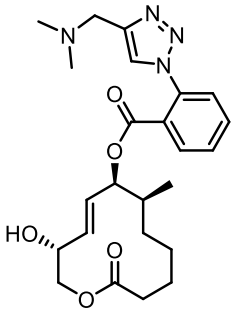

(6S,7S,E)-3-hydroxy-7-methyl-12-oxooxacyclododec-4-en-6-yl-2-(4-((dimethylamino)methyl)-1H-1,2,3-triazol-1-yl)benzoate (56l):

The title compound was isolated by preparative HPLC from the same product mixture as **57l** as the minor product.

^{1}H NMR (700 MHz, $CDCl_3$) δ 7.83 (dd, *J* = 7.7, 1.5 Hz, 1H), 7.73 (s, 1H), 7.64 (td, *J* = 7.7, 1.5 Hz, 1H), 7.57 (td, *J* = 7.6, 1.2 Hz, 1H), 7.48 (dd, *J* = 7.9, 1.2 Hz, 1H), 5.67 (dd, *J* = 14.1, 8.9 Hz, 1H), 5.51 – 5.44 (m, 2H), 4.63 (t, *J* = 10.1 Hz, 1H), 4.26 (td, *J* = 9.3, 5.1 Hz, 1H), 3.93 (dd, *J* = 10.5, 5.1 Hz, 1H), 3.68 (q, *J* = 13.5 Hz, 2H), 2.34 (s, 6H), 2.33 – 2.30 (m, 2H), 2.09 – 2.03 (m, 1H), 1.97 – 1.89 (m, 1H), 1.45 – 1.39 (m, 1H), 1.37 – 1.30 (m, 2H), 1.29 – 1.22 (m, 2H), 1.21 – 1.16 (m, 1H), 0.93 (d, *J* = 6.9 Hz, 3H).

^{13}C NMR (126 MHz, $CDCl_3$) δ 172.98, 165.09, 144.47, 137.77, 135.50, 131.97, 129.94, 129.61, 128.93, 126.51, 125.49, 124.11, 77.53, 71.20, 64.27, 54.21, 45.18, 33.72, 31.58, 31.17, 24.09, 22.46, 15.48.

HRMS (ESI) *m/z* calculated for $[M+H]^+$ 457.2445, found 457.2447.

The stereochemistry of **56l** was determined by Mosher ester derivatization (see the stereochemical determination and chemical correlation section for the comparison of the two ester ^{1}H NMR and subsequent assignment).

5.3.5: Authentic Standard Synthesis

Synthesis of Diol Standard 45

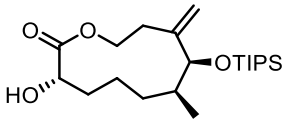

(3*S*,7*S*,8*S*)-3-Hydroxy-7-methyl-9-methylene-8-((triisopropylsilyl)oxy)oxacycloundecan-2-one (45):

To an oven-dried flask equipped with stir bar was added 0.171 g (0.464 mmol) of (7*S*,8*S*)-7-methyl-9-methylene-8-((triisopropylsilyl)oxy)oxacycloundecan-2-one and 9 mL of THF. The contents were cooled to -78 °C whereupon 0.696 mL of a 1M solution of KHMDS in THF was added dropwise. The reaction was stirred for 20 min before the addition of 0.182 g (0.696 mmol) of 3-phenyl-2-(phenylsulfonyl)-1,2-oxaziridine dropwise as a solution in 6 mL of THF. The reaction was stirred for an additional 20 mins at -78 °C before being quenched with sat'd aqueous NH_4Cl and transferred to a separatory funnel. The aqueous layer was extracted 3x with Et_2O, the organic layers combined, dried over $MgSO_4$, filtered, and concentrated under vacuum. The crude residue was purified by

column chromatography (CH_2Cl_2 to 1% MeOH/CH_2Cl_2) to give 0.120 g (67%) of the title compound as a clear oil.

^{1}H NMR (700 MHz, $CDCl_3$) δ 5.36 (s, 1H), 5.17 – 5.13 (m, 1H), 4.55 (ddd, *J* = 10.8, 4.4, 2.9 Hz, 1H), 4.40 (ddd, *J* = 12.3, 10.7, 3.1 Hz, 1H), 4.16 (t, *J* = 1.5 Hz, 1H), 4.05 – 3.99 (m, 1H), 2.59 (d, *J* = 5.7 Hz, 1H), 2.43 – 2.34 (m, 1H), 2.22 – 2.13 (m, 1H), 1.97 – 1.89 (m, 1H), 1.79 – 1.72 (m, 1H), 1.70 – 1.48 (m, 4H), 1.10 – 1.03 (m, 22H), 0.99 (d, *J* = 6.8 Hz, 3H).

^{13}C NMR (176 MHz, $CDCl_3$) δ 175.25, 147.25, 111.73, 80.58, 71.93, 65.49, 32.14, 32.05, 30.24, 25.18, 21.71, 18.31, 18.22, 17.65, 13.20.

HRMS (ESI) *m/z* calculated for $[M+Na]^+$ 407.2588, found 407.2585.

The stereochemistry of **45** was determined by Mosher ester analysis (see the stereochemical determination and chemical correlation section for the comparison of the two ester ^{1}H NMR and subsequent assignment).

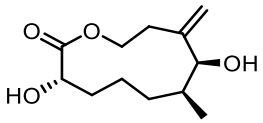

(3*S*,7*S*,8*S*)-3,8-Dihydroxy-7-methyl-9-methyleneoxacycloundecan-2-one (46):

To an oven-dried flask equipped with stir bar was added 0.023 g (0.060 mmol) of (3*S*,7*S*,8*S*)-3-hydroxy-7-methyl-9-methylene-8-((triisopropylsilyl)oxy)oxacycloundecan-2-one and 2.40 mL of THF. The contents were cooled to 0 °C and 0.007 mL (0.120 mmol) of acetic acid and 0.718 mL of a 1 M solution of TBAF in THF were added sequentially. The reaction was warmed to rt until all the starting material was consumed as judged by TLC. Upon completion, the reaction was quenched with sat'd aqueous NH_4Cl and transferred to a separatory funnel. The aqueous layer was extracted three times with Et_2O, the organic layers combined, dried over $MgSO_4$, filtered and the solvent removed.

The crude residue was purified by column chromatography (50% EtOAc/Hexanes) to yield 0.012 g (88%) of the title compound as a white solid.

^{1}H NMR (500 MHz, $CDCl_3$) δ 5.33 (d, *J* = 1.8 Hz, 1H), 5.18 (s, 1H), 4.62 (ddd, *J* = 10.7, 4.4, 2.4 Hz, 1H), 4.31 (ddd, *J* = 12.8, 10.7, 3.1 Hz, 1H), 4.05 – 3.95 (m, 2H), 2.68 (s, 1H), 2.47 – 2.34 (m, 1H), 2.22 (dddd, *J* = 15.1, 12.8, 4.5, 1.8 Hz, 1H), 2.01 – 1.90 (m, 1H), 1.77 (dqd, *J* = 13.9, 4.9, 4.4, 2.5 Hz, 2H), 1.73 – 1.56 (m, 2H), 1.52 (dddd, *J* = 13.8, 11.3, 4.5, 2.5 Hz, 2H), 1.12 – 1.00 (m, 4H).

^{13}C NMR (126 MHz, $CDCl_3$) δ 175.39, 147.78, 110.58, 79.19, 71.83, 65.89, 31.90, 30.45, 30.06, 24.55, 21.96, 17.12.

HRMS (ESI) *m/z* calculated for $[M+H]^+$ 251.1254, found 251.1250.

Synthesis of THP Monoprotected Diol Intermediate 47

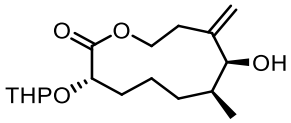

(3*S*,7*S*,8*S*)-8-Hydroxy-7-methyl-9-methylene-3-((tetrahydro-2H-pyran-2-yl)oxy)oxacycloundecan-2-one (47):

To an oven-dried vial equipped with stir bar was added 0.038 g (0.099 mmol) of (3*S*,7*S*,8*S*)-3-hydroxy-7-methyl-9-methylene-8-((triisopropylsilyl)oxy)oxacycloundecan-2-one and 2.0 mL of CH_2Cl_2. The contents were stirred for ~5 min before the sequential addition of 0.014 mL (0.148 mmol) of 3,4-dihydro-2*H*-pyran and 0.002 g (0.010 mmol) of PPTS. The reaction was stirred until all the starting material was consumed as judged by TLC. Upon completion, the reaction was quenched by diluting with a solution of sat'd aqueous sodium bicarbonate. The aqueous layer was extracted three times with EtOAc,

the organic layers combined, dried over Na_2SO_4, filtered and concentrated. The crude residue was carried on to the TIPS deprotection without further purification.

To a vial containing the THP protected diol was added 1.70 mL of THF. The contents were cooled to 0 °C and 0.010 mL (0.179 mmol) of acetic acid and 1.075 mL of a 1M solution of TBAF in THF were added sequentially. The reaction was warmed to rt and stir until all the starting material was consumed as judged by TLC. Upon completion, the reaction was quenched by diluting with a solution of sat'd aqueous NH_4Cl. The aqueous layer was extracted thrice with Et_2O, the organic layers combined, dried over $MgSO_4$, filtered and concentrated. The resulting residue was purified by column chromatography (30% EtOAc/Hexanes) to give 0.027 g (88% over two steps) of 1:1 mixtures of diastereomers at the THP chiral center.

^{1}H NMR (500 MHz, $CDCl_3$) δ 5.28 (s, 1H), 5.20 (s, 0.5H), 5.18 (s, 1H), 4.73 (ddd, *J* = 13.1, 10.8, 2.7 Hz, 0.5H), 4.67 (t, *J* = 3.7 Hz, 0.5H), 4.65 – 4.58 (m, 1H), 4.32 (dt, *J* = 10.8, 3.4 Hz, 1H), 4.25 (dt, *J* = 10.9, 3.4 Hz, 1H), 4.11 (dd, *J* = 10.1, 2.5 Hz, 0.5H), 3.98 (s, 1H), 3.89 (dd, *J* = 10.5, 2.7 Hz, 1H), 3.86 – 3.77 (m, 1H), 3.50 (dt, *J* = 10.7, 4.9 Hz, 1H), 3.43 (dt, *J* = 10.8, 4.7 Hz, 1H), 2.42 – 2.30 (m, 1H), 2.29 – 2.15 (m, 1H), 2.08 – 1.87 (m, 2H), 1.86 – 1.66 (m, 3H), 1.66 – 1.46 (m, 6H), 1.46 – 1.35 (m, 1H), 1.07 – 0.94 (m, 4H)

^{13}C NMR (126 MHz, $CDCl_3$) δ 172.67, 172.57, 147.99, 147.92, 110.97, 110.85, 98.64, 97.17, 79.25, 79.21, 78.41, 75.51, 64.77, 64.64, 62.55, 62.33, 30.58, 30.51, 30.48, 30.37, 29.67, 29.46, 29.26, 28.39, 25.27, 25.16, 24.03, 23.83, 21.90, 21.63, 19.23, 19.14, 16.92, 16.80.

HRMS (ESI) *m/z* calculated for $[M+H]^+$ 313.2010, found 313.2007.

Synthesis of Authentic Standard 40j

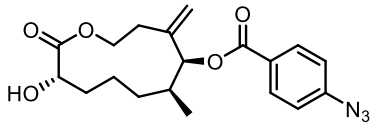

(5*S*,6*S*,10*S*)-10-Hydroxy-6-methyl-4-methylene-11-oxooxacycloundecan-5-yl 4-azidobenzoate (48A):

An oven-dried vial equipped with stir bar was charged with 0.008 g (0.026 mmol) of (3*S*,7*S*,8*S*)-8-hydroxy-7-methyl-9-methylene-3-((tetrahydro-2H-pyran-2-yl)oxy)oxacycloundecan-2-one, 0.021 g (0.128 mmol) of 4-azidobenzoic acid, 0.025 g (0.128 mmol) of EDC, and 0.008 g (0.0.064 mmol) of DMAP. The contents were suspended in 2.0 mL of CH_2Cl_2 and allowed to stir until all the starting material was consumed as judged by TLC. Upon completion, the reaction was filtered through a plug of silica gel and the solvent removed. The crude material was carried on to the THP deprotection without further purification.

An oven-dried vial equipped with stir bar was charged with the crude material from the above reaction and suspended in 3.0 mL of EtOH. 0.013 g (0.052 mmol) of PPTS was then added, the reaction heated to 60 °C and allowed to stir until all the starting material was consumed as judged by TLC. The reaction was quenched by diluting with a solution of sat'd aqueous sodium bicarbonate and EtOAc. The aqueous layer was extracted three times with EtOAc, the organic layers combined, dried over Na_2SO_4, filtered, and concentrated. The crude residue was purified by chromatography (10% EtOAc/Hexanes to 30% EtOAc/Hexanes) to yield 8.4 mg (87% over two steps) of the title compound as a clear oil.

^{1}H NMR (500 MHz, $CDCl_3$) δ 8.07 (d, *J* = 8.6 Hz, 2H), 7.09 (d, *J* = 8.7 Hz, 2H), 5.35 (s, 1H), 5.16 – 5.09 (m, 2H), 4.63 (ddd, *J* = 10.8, 4.5, 2.5 Hz, 1H), 4.35 (ddd, *J* = 12.6, 10.8,

3.1 Hz, 1H), 4.10 – 4.03 (m, 1H), 2.67 (s, 1H), 2.51 (d, *J* = 15.5 Hz, 1H), 2.40 – 2.30 (m, 1H), 2.08 – 1.92 (m, 2H), 1.89 – 1.60 (m, 3H), 1.32 – 1.27 (m, 1H), 0.99 (d, *J* = 6.7 Hz, 3H).

^{13}C NMR (126 MHz, $CDCl_3$) δ 175.21, 164.88, 144.95, 143.04, 131.40, 126.67, 118.95, 111.65, 80.71, 71.83, 65.79, 31.72, 30.26, 30.24, 26.11, 21.97, 16.84.

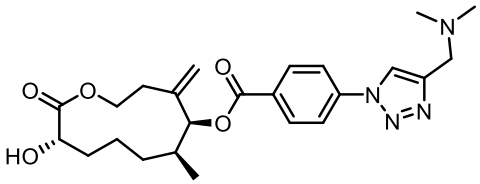

(5*S*,6*S*,10*S*)-10-Hydroxy-6-methyl-4-methylene-11-oxooxacycloundecan-5-yl4-(4-((dimethylamino)methyl)-1H-1,2,3-triazol-1-yl)benzoate (40j):

Following the general CuAAC reaction procedure, the reaction of 0.006 g (0.016 mmol) of (5*S*,6*S*,10*S*)-10-hydroxy-6-methyl-4-methylene-11-oxooxacycloundecan-5-yl 4-azidobenzoate, 0.006 mL (0.048 mmol) N,N-dimethylprop-2-yn-1-amine, $1.60x10^{-4}$ mmol $CuSO_4•5H_2O$, and $1.60x10^{-3}$ mmol of sodium ascorbate in 1.0 ml of H_2O/*t*-BuOH (1:1) afforded 0.007 g (95%) of the title compound after purification by column chromatography (gradient CH_2Cl_2 to 10% MeOH/CH_2Cl_2).

^{1}H NMR (500 MHz, $CDCl_3$) δ 8.23 (d, *J* = 8.6 Hz, 2H), 8.17 (s, 1H), 7.88 (d, *J* = 8.6 Hz, 2H), 5.40 (s, 1H), 5.19 – 5.10 (m, 2H), 4.63 (ddd, *J* = 10.8, 4.5, 2.5 Hz, 1H), 4.37 (ddd, *J* = 13.4, 11.0, 3.1 Hz, 1H), 4.08 (dd, *J* = 9.0, 2.0 Hz, 1H), 3.85 (s, 2H), 2.59 – 2.50 (m, 1H), 2.45 (s, 6H), 2.41 – 2.32 (m, 1H), 2.09 – 1.94 (m, 2H), 1.90 – 1.59 (m, 4H), 1.37 – 1.22 (m, 2H), 1.01 (d, *J* = 6.8 Hz, 3H)

^{13}C NMR (176 MHz, $CDCl_3$) δ 175.19, 164.50, 145.1, 142.89, 140.19, 131.34, 130.23, 121.21, 119.98, 111.75, 81.16, 71.83, 65.74, 54.00, 44.80, 31.71, 30.28, 30.27, 26.12, 21.95, 16.86.

The fully substituted triazole carbon was detected at 145.1 ppm by HMBC.

HRMS (ESI) *m/z* calculated for $[M+H]^+$ 457.2445, found 457.2449.

Synthesis of Authentic Standard 40l

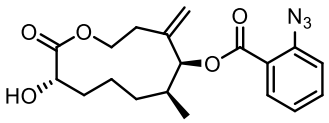

(5*S*,6*S*,10*S*)-10-Hydroxy-6-methyl-4-methylene-11-oxooxacycloundecan-5-yl 2-azidobenzoate (48C):

An oven-dried vial equipped with stir bar was charged with 0.008 g (0.026 mmol) of (3*S*,7*S*,8*S*)-8-hydroxy-7-methyl-9-methylene-3-((tetrahydro-2H-pyran-2-yl)oxy)oxacycloundecan-2-one, 0.042 g (0.260 mmol) of 2-azidobenzoic acid, 0.054 g (0.260 mmol) of DCC, and 0.016 g (0.130 mmol) of DMAP. The contents were suspended in 2.0 mL of CH_2Cl_2 and allowed to stir until all the starting material was consumed as judged by TLC. Upon completion, the reaction was filtered through a plug of silica gel and the solvent removed. The crude material was carried on to the THP deprotection without further purification.

An oven-dried vial equipped with stir bar was charged with the crude material from the above reaction and suspended in 3.0 mL of EtOH. 0.013 g (0.052 mmol) of PPTS was then added, the reaction heated to 60 °C and allowed to stir until all the starting material was consumed as judged by TLC. The reaction was quenched by diluting with a solution of sat'd aqueous sodium bicarbonate and EtOAc. The aqueous layer was extracted three times with EtOAc, the organic layers combined, dried over Na_2SO_4, filtered, and concentrated. The crude residue was purified by chromatography (10%

EtOAc/Hexanes to 30% EtOAc/Hexanes) to yield 9.3 mg (96% over two steps) of the title compound as a clear oil.

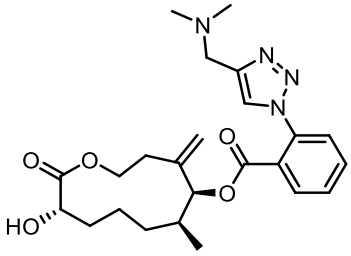

(5*S*,6*S*,10*S*)-10-Hydroxy-6-methyl-4-methylene-11-oxooxacycloundecan-5-yl-2-(4-((dimethylamino)methyl)-1H-1,2,3-triazol-1-yl)benzoate (40l):

Following the general CuAAC reaction procedure, the reaction of 0.004 g (0.011 mmol) of (5*S*,6*S*,10*S*)-10-hydroxy-6-methyl-4-methylene-11-oxooxacycloundecan-5-yl 2-azidobenzoate, 0.006 mL (0.048 mmol) N,N-dimethylprop-2-yn-1-amine, $1.11x10^{-4}$ mmol $CuSO_4•5H_2O$, and $1.11x10^{-3}$ mmol of sodium ascorbate in 1.0 ml of H_2O/*t*-BuOH (1:1) afforded 4.1 mg (84%) of the title compound after purification by column chromatography (gradient CH_2Cl_2 to 10% MeOH/CH_2Cl_2).

^{1}H NMR (500 MHz, $CDCl_3$) δ 8.13 – 8.03 (m, 2H), 7.70 (t, *J* = 7.7 Hz, 1H), 7.64 (t, *J* = 7.7 Hz, 1H), 7.52 (d, *J* = 7.8 Hz, 1H), 5.22 (s, 1H), 5.17 – 5.09 (m, 2H), 4.57 (ddd, *J* = 10.8, 4.4, 2.8 Hz, 1H), 4.33 (ddd, *J* = 13.8, 11.0, 3.1 Hz, 1H), 4.11 – 4.02 (m, 3H), 2.62 (s, 6H), 2.51 – 2.42 (m, 1H), 2.33 – 2.20 (m, 1H), 2.00 – 1.88 (m, 2H), 1.85 – 1.75 (m, 1H), 1.73 – 1.56 (m, 3H), 1.18 – 1.08 (m, 1H), 0.95 (d, *J* = 6.8 Hz, 3H)

^{13}C NMR (176 MHz, $CDCl_3$) δ 175.11, 163.45, 142.45, 136.36, 132.99, 130.84, 130.26, 127.56, 127.28, 126.77, 112.06, 81.38, 71.74, 65.67, 53.21, 43.75, 31.74, 30.45, 30.40, 26.19, 21.83, 16.77.

HRMS (ESI) *m/z* calculated for $[M+H]^+$ 457.2445, found 457.2447.

Synthesis of Authentic Standard 40k

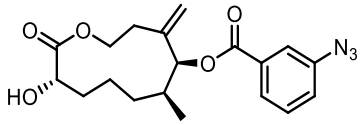

(5*S*,6*S*,10*S*)-10-Hydroxy-6-methyl-4-methylene-11-oxooxacycloundecan-5-yl 3-azidobenzoate (48B):

An oven-dried vial equipped with stir bar was charged with 0.008 g (0.026 mmol) of (3*S*,7*S*,8*S*)-8-hydroxy-7-methyl-9-methylene-3-((tetrahydro-2H-pyran-2-yl)oxy)oxacycloundecan-2-one, 0.042 g (0.260 mmol) of 3-azidobenzoic acid, 0.054 g (0.260 mmol) of DCC, and 0.016 g (0.130 mmol) of DMAP. The contents were suspended in 2.0 mL of CH_2Cl_2 and allowed to stir until all the starting material was consumed as judged by TLC. Upon completion, the reaction was filtered through a plug of silica gel and the solvent removed. The crude material was carried on to the THP deprotection without further purification.

An oven-dried vial equipped with stir bar was charged with the crude material from the above reaction and suspended in 3.0 mL of EtOH. 0.013 g (0.052 mmol) of PPTS was then added, the reaction heated to 60 C and allowed to stir until all of the starting material was consumed as judged by TLC. The reaction was quenched by diluting with a solution of sat'd aqueous sodium bicarbonate and EtOAc. The aqueous layer was extracted thrice with EtOAc, the organic layers combined, dried over Na_2SO_4, filtered, and concentrated. The crude residue was purified by chromatography (10% EtOAc/Hexanes to 30% EtOAc/Hexanes) to yield 8.2 mg (85% over two steps) of the title compound as a clear oil.

^{1}H NMR (500 MHz, $CDCl_3$) δ 7.85 (d, *J* = 7.8 Hz, 1H), 7.72 (t, *J* = 1.9 Hz, 1H), 7.46 (t, *J* = 7.9 Hz, 1H), 7.26 – 7.23 (m, 1H), 5.37 (s, 1H), 5.15 (s, 1H), 5.13 (d, *J* = 1.7 Hz, 1H),

4.63 (ddd, *J* = 10.8, 4.5, 2.5 Hz, 1H), 4.35 (ddd, *J* = 12.5, 10.8, 3.1 Hz, 1H), 4.08 (d, *J* = 8.9 Hz, 1H), 2.64 (d, *J* = 4.7 Hz, 1H), 2.53 (d, *J* = 15.6 Hz, 1H), 2.35 (dddd, *J* = 14.9, 12.7, 4.5, 1.7 Hz, 1H), 2.06 – 1.94 (m, 2H), 1.87 – 1.62 (m, 4H), 1.34 – 1.23 (m, 1H), 0.99 (d, *J* = 6.8 Hz, 3H).

^{13}C NMR (126 MHz, $CDCl_3$) δ 175.22, 164.80, 142.89, 140.71, 131.95, 129.95, 125.91, 123.47, 120.00, 111.75, 81.05, 71.82, 65.78, 31.73, 30.29, 30.25, 26.11, 21.95, 16.84.

HRMS (ESI) *m/z* calculated for $[M+Na]^+$ 396.1530, found 396.1525.

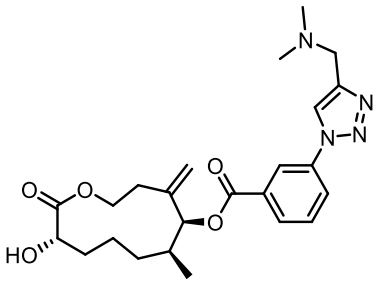

(5*S*,6*S*,10*S*)-10-Hydroxy-6-methyl-4-methylene-11-oxooxacycloundecan-5-yl-3-(4-((dimethylamino)methyl)-1H-1,2,3-triazol-1-yl)benzoate (40k):

Following the general CuAAC reaction procedure, the reaction of (0.141 mmol) of (6*S*,7*S*,*E*)-7-methyl-12-oxooxacyclododec-4-en-6-yl 2-azidobenzoate, 0.016 mL (0.141 mmol) N,N-dimethylprop-2-yn-1-amine, $1.41x10^{-3}$ mmol $CuSO_4•5H_2O$, and $1.41x10^{-2}$ mmol of sodium ascorbate in 2.0 ml of H_2O/*t*-BuOH (1:1) afforded 0.050 g (80% over two steps) of the title compound after purification by column chromatography (gradient CH_2Cl_2 to 10% MeOH/CH_2Cl_2).

^{1}H NMR (500 MHz, $CDCl_3$) δ: 8.39 (s, 1H), 8.20 – 8.09 (m, 2H) 8.03 (d, *J* = 8.1 Hz, 1H), 7.65 (t, *J* = 7.9 Hz, 1H), 5.42 (s, 1H), 5.21 – 5.09 (m, 2H), 4.63 (ddd, *J* = 10.9, 4.5, 2.6 Hz, 1H), 4.36 (ddd, *J* = 13.4, 10.9, 3.1 Hz, 1H), 4.08 (dd, *J* = 9.0, 2.1 Hz, 1H), 3.83 (s, 2H), 2.61 – 2.32 (m, 8H), 2.10 – 1.94 (m, 2H), 1.89 – 1.61 (m, 4H), 1.38 – 1.19 (m, 2H), 1.01 (d, *J* = 6.8 Hz, 3H)

^{13}C NMR (176 MHz, $CDCl_3$) δ 175.21, 164.41, 145.8, 142.83, 137.33, 132.00, 130.15, 129.60, 124.90, 121.31, 121.18, 111.85, 81.36, 71.81, 65.76, 54.03, 44.83, 31.73, 30.36, 30.29, 26.15, 21.96, 16.87.

The fully substituted triazole carbon was detected at 145.8 ppm by HMBC.

HRMS (ESI) *m/z* calculated for $[M+H]^+$ 457.2445, found 457.2448.

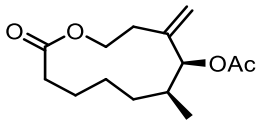

(5*S*,6*S*)-6-Methyl-4-methylene-11-oxooxacycloundecan-5-yl acetate (34C):

An oven dried flask equipped with stir bar was charged with 0.050 g (0.236) of (7*S*,8*S*)-8-hydroxy-7-methyl-9-methyleneoxacycloundecan-2-one, 0.003 g (0.024 mmol) of DMAP, and 1.67 mL of acetonitrile. The contents were stirred for ~5 min before the sequential addition of 0.029 mL (0.353 mmol) of pyridine and 0.033 mL (0.353 mmol) of acetic anhydride. The reaction was stirred until all of the starting material was consumed as judged by TLC. Upon completion, the reaction was quenched by diluting with Et_2O and transferred to a separatory funnel. The organic layer was extracted once with sat'd aqueous sodium bicarbonate, once with H_2O, and once with brine. The organic layer was dried over $MgSO_4$, filtered and the solvent removed. The crude residue was purified by column chromatography (20% EtOAc/Hexanes) to yield 0.056 g (93%) of the title compound as a clear oil.

^{1}H NMR (700 MHz, $CDCl_3$) δ 5.13 (s, 1H), 5.11 (s, 1H), 5.03 (s, 1H), 4.91 (ddd, *J* = 13.2, 10.9, 2.6 Hz, 1H), 3.93 (ddd, *J* = 10.9, 4.1, 2.5 Hz, 1H), 2.50 (dd, *J* = 16.0, 6.5 Hz, 1H), 2.46 – 2.40 (m, 1H), 2.22 (dddd, *J* = 15.2, 13.0, 4.1, 2.0 Hz, 1H), 2.16 – 2.08 (m, 5H), 1.92 – 1.83 (m, 1H), 1.67 – 1.59 (m, 1H), 1.59 – 1.53 (m, 1H), 1.52 – 1.46 (m, 1H), 1.46 – 1.39 (m, 1H), 1.06 (ddt, *J* = 15.0, 11.7, 3.9 Hz, 1H), 0.93 (d, *J* = 6.8 Hz, 3H).

^{13}C NMR (176 MHz, $CDCl_3$) δ 173.67, 170.38, 143.36, 111.74, 80.62, 64.03, 35.26, 30.92, 28.55, 25.70, 24.61, 20.86, 19.96, 16.42.

HRMS (ESI) *m/z* calculated for $[M+Na]^+$ 277.1410, found 277.1407.

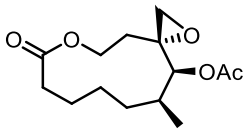

(3*R*,12*S*,13*S*)-12-Methyl-7-oxo-1,6-dioxaspiro[2.10]tridecan-13-yl acetate (42):

To a vial equipped with stir bar was added 0.014 g (0.055 mmol) of (5S,6S)-6-methyl-4-methylene-11-oxooxacycloundecan-5-yl acetate. 0.0026 g ($2.75x10^{-3}$ mmol) of Fe(*S,S*-PDP) and 0.0016 mL (0.0275 mmol) of acetic acid in 0.10 mL of acetonitrile was added . The solution was stirred vigorously and 0.004 mL of a 50% w/w solution of hydrogen peroxide diluted to 0.50 mL in acetonitrile was added dropwise over ~2 min. The reaction was stirred for 10 min. A second addition of 0.0026 g ($2.75x10^{-3}$ mmol) of Fe(*S,S*-PDP) and 0.0016 mL of acetic acid in 0.10 mL of acetonitrile was added followed by a solution of 0.004 mL of a 50% w/w solution of hydrogen peroxide diluted to 0.50 mL in acetonitrile over ~2 min. After stirring for 10 min, this process was repeated for a third time for a total of 15 mol% Fe(*S,S*-PDP), 1.5 equivalents of acetic acid, and 3.6 equivalents of hydrogen peroxide and a total reaction time of 30 min. The reaction was immediately quenched by diluting with sat'd aqueous sodium bicarbonate and the aqueous layer extracted three times with Et_2O. The combined organic layers were dried over $MgSO_4$, filtered and concentrated. The crude residue was purified by column chromatography (10% EtOAc/Hexanes to 20% EtOAc/Hexanes) to 8.5 mg (57%) of the title compound as a clear oil.

^{1}H NMR (700 MHz, C_6D_6) δ: 5.25 (s, 1H), 4.40 (td, *J* = 12.0, 2.4 Hz, 1H), 3.32 (dt, *J* = 11.6, 3.7 Hz, 1H), 2.65 (d, *J* = 4.9 Hz, 1H), 2.63 (d, *J* = 4.9 Hz, 1H), 2.11 (ddd, *J* = 15.3,

7.5, 2.1 Hz, 1H), 2.01 – 1.94 (m, 1H), 1.89 (ddd, *J* = 15.4, 11.7, 2.2 Hz, 1H), 1.76 (ddd, *J* = 16.2, 12.4, 3.9 Hz, 1H), 1.66 (s, 3H), 1.65 – 1.56 (m, 1H), 1.50 – 1.40 (m, 2H), 1.40 – 1.32 (m, 1H), 1.18 – 1.10 (m, 2H), 1.00 (ddt, *J* = 13.6, 11.2, 4.1 Hz, 1H), 0.78 (d, *J* = 6.8 Hz, 3H)

^{13}C NMR (126 MHz, C_6D_6) δ 172.83, 169.44, 75.43, 60.41, 56.79, 47.64, 35.27, 32.08, 29.70, 26.24, 25.79, 20.44, 20.21, 16.70.

HRMS (ESI) *m/z* calculated for $[M+H]^+$ 271.1540, found 271.1540.

Selected NOE Correlations (^{1}H values in ppm)

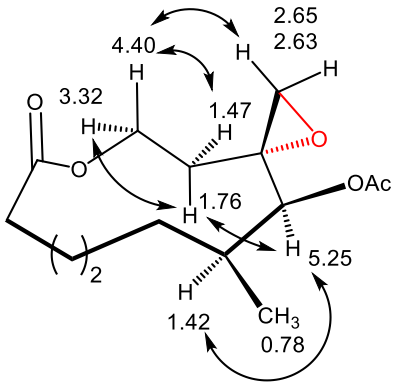

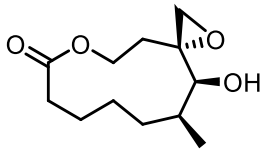

(3*R*,12*S*,13*S*)-13-Hydroxy-12-methyl-1,6-dioxaspiro[2.10]tridecan-7-one (43):

To an oven-dried flask equipped with stir bar was added 0.089 g (0.419 mmol) of (7*S*,8*S*)-8-hydroxy-7-methyl-9-methyleneoxacycloundecan-2-one and CH_2Cl_2 (10 mL). The reaction was stirred for 5 min before the addition of 0.165 g (0.671 mmol) of 70% w/w mCPBA. The reaction was stirred overnight. The following day, the reaction was quenched by diluting with 1M NaOH and transferred to a separatory funnel. The aqueous layer was extracted thrice with CH_2Cl_2, the organic layers combined, dried over Na_2SO_4,

filtered, and concentrated. The crude residue was purified by column chromatography (30% EtOAc/Hexanes) to yield 0.094 g (99%) of the desired product as a clear oil.

^{1}H NMR (401 MHz, $CDCl_3$) δ 4.72 (ddd, *J* = 12.7, 11.6, 2.5 Hz, 1H), 3.92 (ddd, *J* = 11.7, 4.1, 2.8 Hz, 1H), 3.75 (s, 1H), 3.06 – 2.97 (m, 2H), 2.53 (ddd, *J* = 15.4, 7.7, 2.1 Hz, 1H), 2.30 (ddd, *J* = 16.5, 12.8, 4.1 Hz, 1H), 2.17 (ddd, *J* = 15.4, 11.6, 2.0 Hz, 1H), 2.12 – 2.02 (m, 1H), 2.00 (s, 1H), 1.98 – 1.79 (m, 2H), 1.73 – 1.57 (m, 2H), 1.53 – 1.41 (m, 1H), 1.39 – 1.17 (m, 2H), 1.06 (d, *J* = 6.9 Hz, 3H).

^{13}C NMR (176 MHz, $CDCl_3$) δ 174.00, 75.37, 60.68, 59.75, 48.40, 35.26, 31.72, 29.47, 25.68, 24.96, 20.30, 17.14.

HRMS (ESI) *m/z* calculated for $[M+Na]^+$ 251.1254, found 251.1253.

Stereochemical Determination of (3*R*,12*S*,13*S*)-13-hydroxy-12-methyl-1,6-dioxaspiro[2.10]tridecan-7-one (43):

To an oven-dried vial equipped with stir bar was added 0.006 g (0.026 mmol) of (3*R*,12*S*,13*S*)-13-hydroxy-12-methyl-1,6-dioxaspiro[2.10]tridecan-7-one, 0.002 g (0.016 mmol) of DMAP and 1.0 mL of acetonitrile. The contents were stirred for for ~5 min before the sequential addition of 0.010 mL (0.130 mmol) of pyridine and 0.008 mL (0.078 mmol) of acetic anhydride. The reaction was stirred until all the starting material was consumed as judged by GCMS. Upon completion, the reaction was quenched with a solution of sat'd aqueous sodium bicarbonate. The aqueous layer was extracted thrice with CH_2Cl_2, the organic layers combined, dried over Na_2SO_4, filtered, and the solvent removed. The crude residue was purified by column chromatography (20% EtOAc/Hexanes) to give 5.8 mg (83%) of the acetylated product whose ^{1}H NMR matched that of the product obtained from the Fe(*S,S*-PDP) oxidation. See part 6 for the comparison of the ^{1}H NMRs.

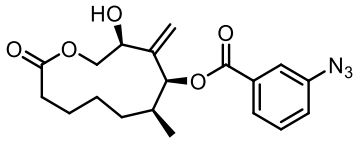

(3*S*,5*S*,6*S*)-3-Hydroxy-6-methyl-4-methylene-11-oxooxacycloundecan-5-yl-3-azidobenzoate (50):

An oven-dried vial equipped with stir bar was charged with 0.060 g (0.168 mmol) of (5*S*,6*S*)-6-methyl-4-methylene-11-oxooxacycloundecan-5-yl 3-azidobenzoate and 0.022 g (0.201 mmol) of selenium dioxide. The contents were suspended in 3.0 mL of dioxane and allowed to stir for 5 min before the addition of 0.064 g (0.671 mmol) of pyridine *N*-oxide. The vial was sealed, heated to 90 °C, and allowed to stir until all the starting material was consumed as judged by TLC. Upon completion, the reaction was quenched with a sat'd solution of sodium bicarbonate and the aqueous layer extracted three times with EtOAc. The organic layers were combined, dried over Na2SO4, filtered, and concentrated. The resulting residue was purified by chromatography (gradient 10% EtOAc/hexanes to 45% EtOAc/hexanes) to yield 0.030g (48%) of the desired compound. **^{1}H NMR (500 MHz, $CDCl_3$)** δ 7.82 (dt, *J* = 7.7, 1.2 Hz, 1H), 7.71 – 7.68 (m, 1H), 7.45 (t, *J* = 7.9 Hz, 1H), 7.24 (ddd, *J* = 8.1, 2.4, 1.0 Hz, 1H), 5.58 (d, *J* = 1.5 Hz, 1H), 5.50 (s, 1H), 5.23 (s, 1H), 4.84 (t, *J* = 10.6 Hz, 1H), 4.33 (dd, *J* = 10.8, 4.4 Hz, 1H), 3.99 (dd, *J* = 10.3, 4.7 Hz, 1H), 2.55 (ddd, *J* = 16.1, 7.5, 1.9 Hz, 1H), 2.27 (s, 1H), 2.15 (ddd, *J* = 16.1, 12.0, 1.8 Hz, 1H), 2.11 – 2.01 (m, 1H), 1.95 – 1.82 (m, 1H), 1.79 – 1.44 (m, 4H), 1.28 – 1.18 (m, 1H), 1.03 (d, *J* = 6.8 Hz, 3H).

^{13}C NMR (126 MHz, $CDCl_3$) δ 172.70, 164.90, 148.87, 140.76, 131.79, 129.98, 125.88, 123.58, 119.99, 113.84, 80.61, 66.96, 65.67, 34.94, 30.09, 25.65, 24.46, 19.97, 16.57.

HRMS (ESI) *m/z* calculated for $[M+NH_4]^+$ 391.1976, found 391.1977.

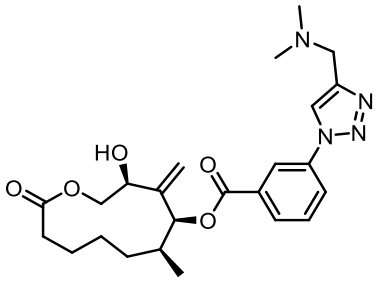

(3*S*,5*S*,6*S*)-3-Hydroxy-6-methyl-4-methylene-11-oxooxacycloundecan-5-yl 3-(4-((dimethylamino)methyl)-1H-1,2,3-triazol-1-yl)benzoate (39k):

Following the general CuAAC reaction procedure, the reaction of 0.005 g (0.013 mmol) of (3*S*,5*S*,6*S*)-3-Hydroxy-6-methyl-4-methylene-11-oxooxacycloundecan-5-yl 3-azidobenzoate, 0.003 mL (0.027 mmol) N,N-dimethylprop-2-yn-1-amine, $1.3x10^{-4}$ mmol $CuSO_4•5H_2O$, and $1.3x10^{-3}$ mmol of sodium ascorbate in 1.0 ml of H_2O/*t*-BuOH (1:1) afforded 0.005 g (85%) of the title compound after purification by column chromatography (gradient CH_2Cl_2 to 10% MeOH/CH_2Cl_2).

^{1}H NMR (500 MHz, $CDCl_3$) δ: 8.37 (s, 1H), 8.19 (s, 1H), 8.11 (d, *J* = 7.8 Hz, 1H), 8.02 (d, *J* = 8.0 Hz, 1H), 7.63 (t, *J* = 7.9 Hz, 1H), 5.60 (s, 1H), 5.54 (s, 1H), 5.25 (s, 1H), 4.84 (t, *J* = 10.6 Hz, 1H), 4.34 (dd, *J* = 10.9, 4.6 Hz, 1H), 4.00 (dd, *J* = 10.3, 4.6 Hz, 1H), 3.88 (s, 2H), 2.55 (dd, *J* = 15.9, 6.8 Hz 1H), 2.46 (s, 6H), 2.16 (dd, *J* = 15.0, 12.4 Hz 1H), 2.12 – 2.04 (m, 1H), 1.88 (q, *J* = 13.0 Hz, 1H), 1.74 – 1.56 (m, 3H), 1.56 – 1.46 (m, 1H), 1.33 – 1.17 (m, 1H), 1.04 (d, *J* = 6.7 Hz, 3H)

^{13}C NMR (176 MHz, $CDCl_3$) δ 172.71, 164.50, 148.88, 144.7, 137.33, 131.84, 130.19, 129.55, 125.00, 121.49, 121.20, 113.89, 80.90, 66.98, 65.69, 53.91, 44.69, 34.92, 30.15, 25.65, 24.49, 19.98, 16.60.

The fully substituted triazole carbon was detected at 144.7 ppm by HMBC.

HRMS (ESI) *m/z* calculated for $[M+H]^+$ 457.2445, found 457.2449.

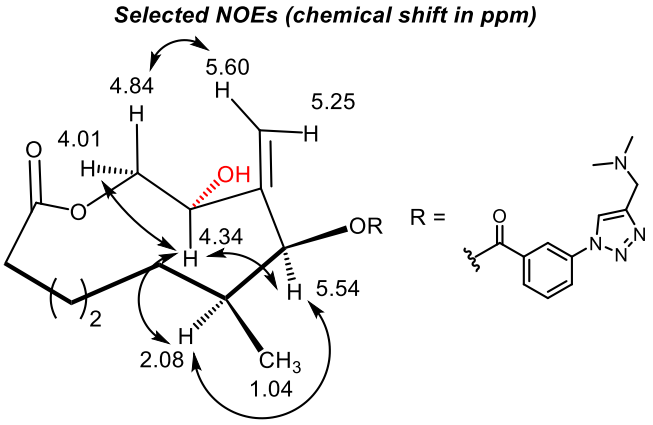

Chemical synthesis of (3*R*,8*S*,12*S*,13*S*)-8-hydroxy-12-methyl-7-oxo-1,6-dioxaspiro[2.10]tridecan-13-yl-4-(4-((dimethylamino)methyl)-1H-1,2,3-triazol-1-yl)benzoate:

An oven-dried vial equipped with stir bar was charged with 2.4 mg (0.0064 mmol) of (5*S*,6*S*,10*S*)-10-hydroxy-6-methyl-4-methylene-11-oxooxacycloundecan-5-yl 4-azidobenzoate and suspended in 1 mL of CH_2Cl_2. 0.007 g of 70% w/w mCPBA was then added in a single portion. After consumption of the starting material as judged by TLC, the reaction was quenched with 1M NaOH, and the aqueous layer extracted three times with CH_2Cl_2. The organic layers were combined, dried over Na_2SO_4, filtered, and concentrated. The 1H NMR revealed a 94:6 mixture of diastereomers. The crude material was carried on directly to the CuAAC cyclization.

Following the general CuAAC reaction procedure, the reaction of 0.0064 mmol of (8S,12S,13S)-8-hydroxy-12-methyl-7-oxo-1,6-dioxaspiro[2.10]tridecan-13-yl 4-azidobenzoate, 0.007 mL (0.064 mmol) N,N-diethylprop-2-yn-1-amine, 3.20×10^{-4} mmol $CuSO_4 \cdot 5H_2O$, and 3.20×10^{-3} mmol of sodium ascorbate in 1.0 mL of H_2O/*t*-BuOH (1:1) afforded 0.002 g (67% over two steps) of the title compound as a clear oil after purification by column chromatography (gradient CH_2Cl_2 to 10% MeOH/CH_2Cl_2)

The ^{1}H NMR of the chemically prepared standard (vide supra) matched that of the analogous product obtained through enzymatic oxidation.

5.3.6 Stereochemical Determination and Chemical Correlation

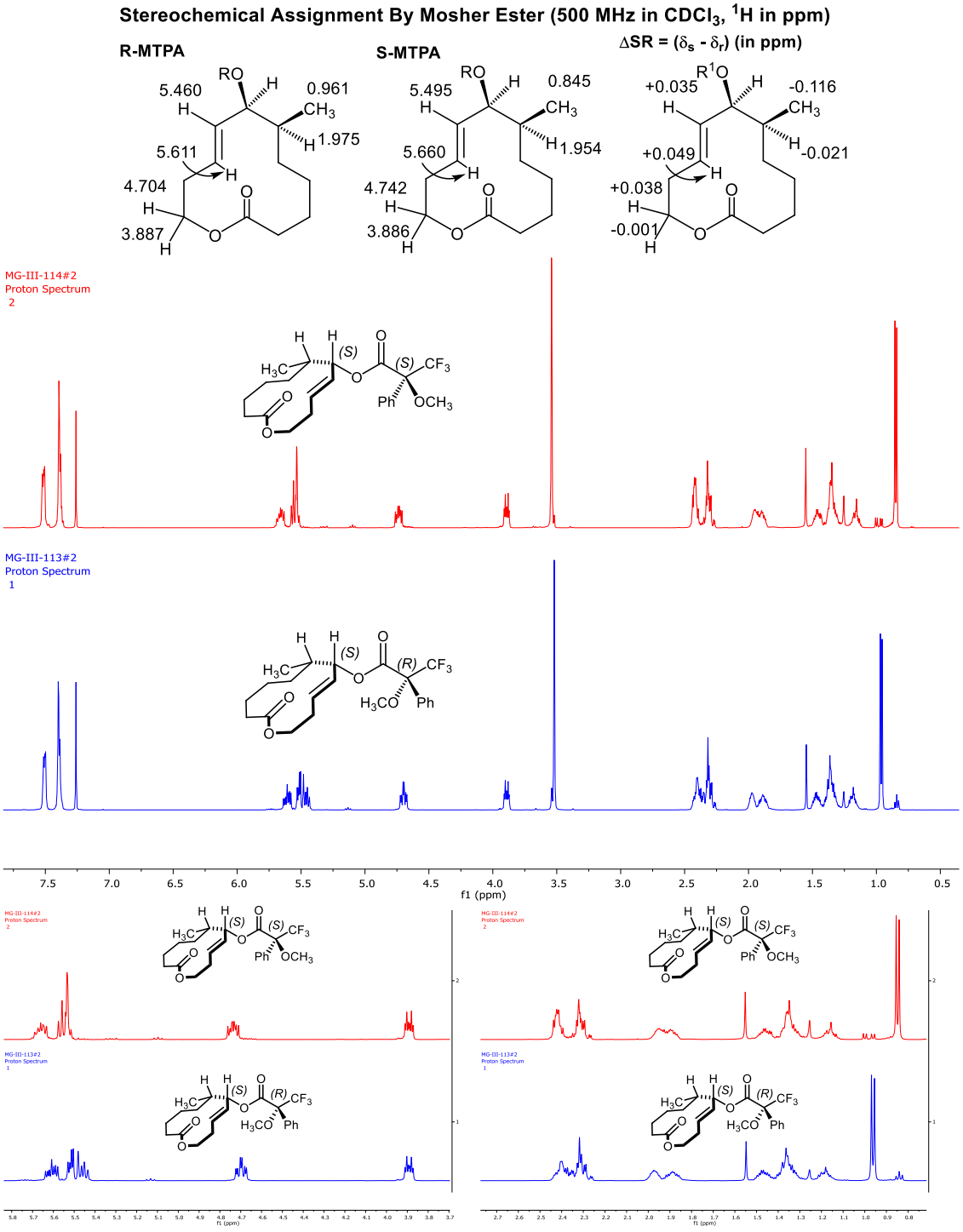

Figure 5.12: Stereochemical assignment of the hydroxyl group in **35B** by Mosher Ester derivatization. Assignments were made following the protocol established by Hoye et. al. where protons shielded by the phenyl group in the conformations shown are shifted upfield in the ^{1}H NMR.[133]

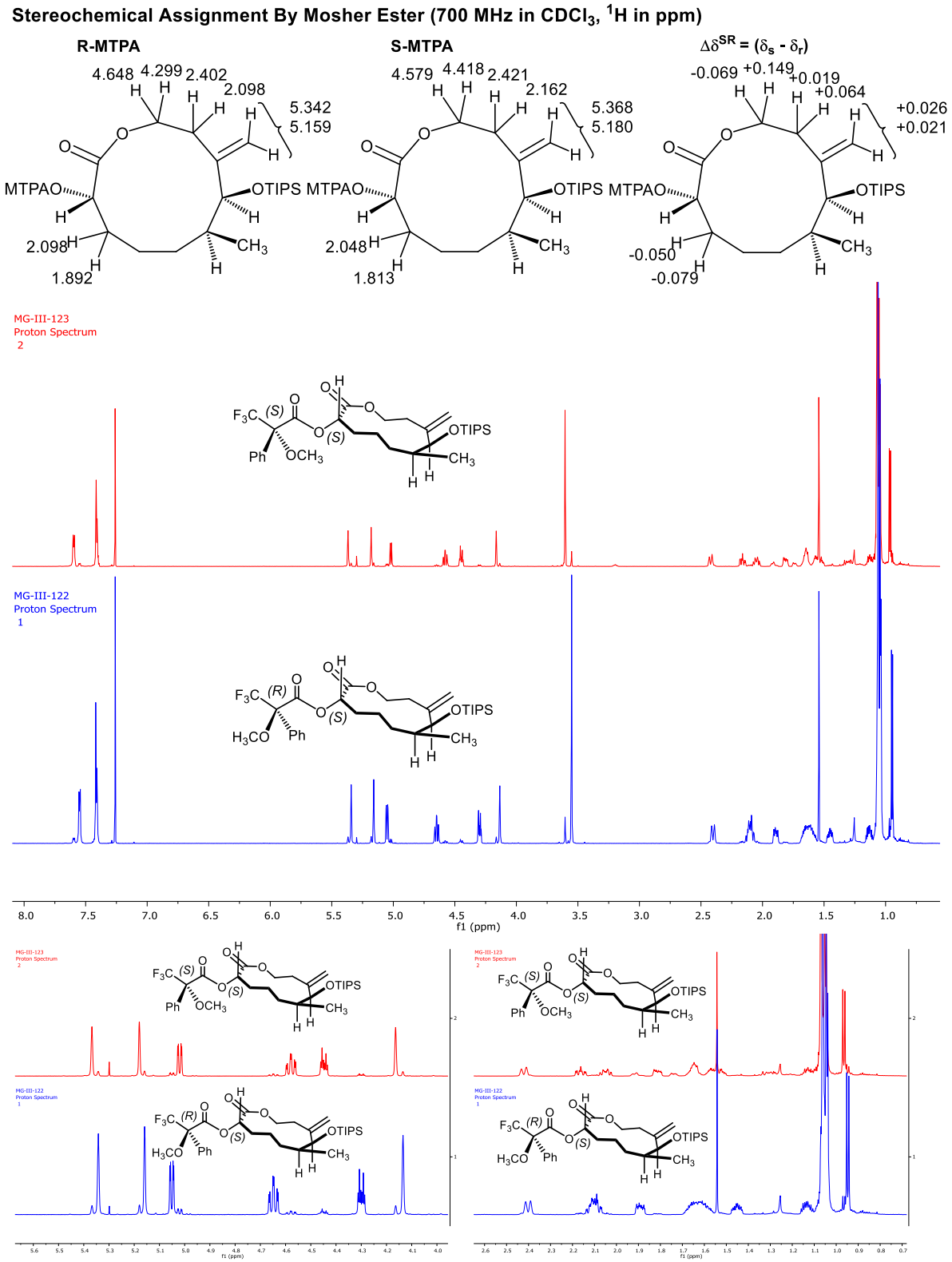

Figure 5.13: Stereochemical assignment of compound **45** by Mosher ester derivatization.

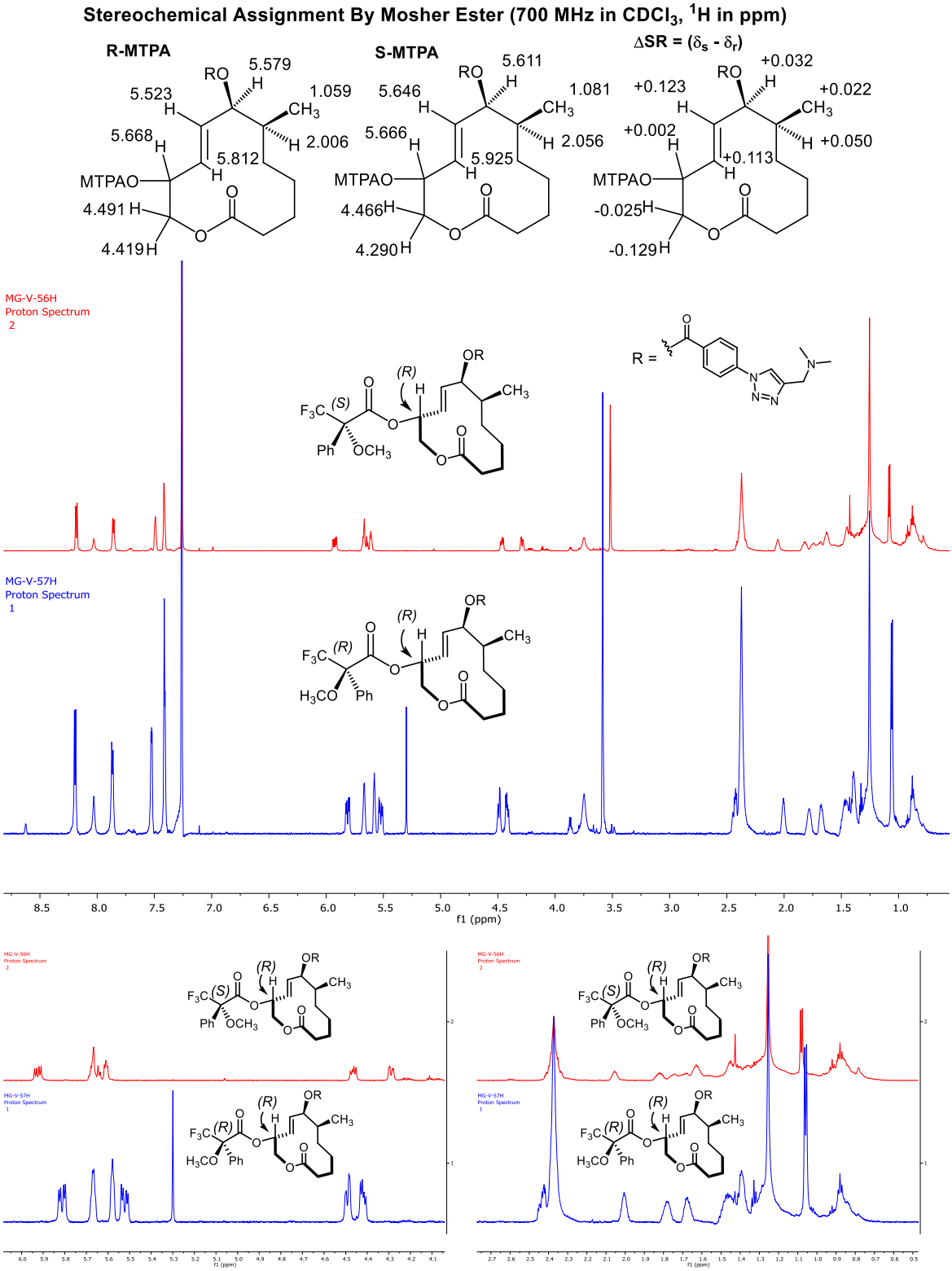

Figure 5.14: Stereochemical assignment of compound **56j** by Mosher ester derivatization.

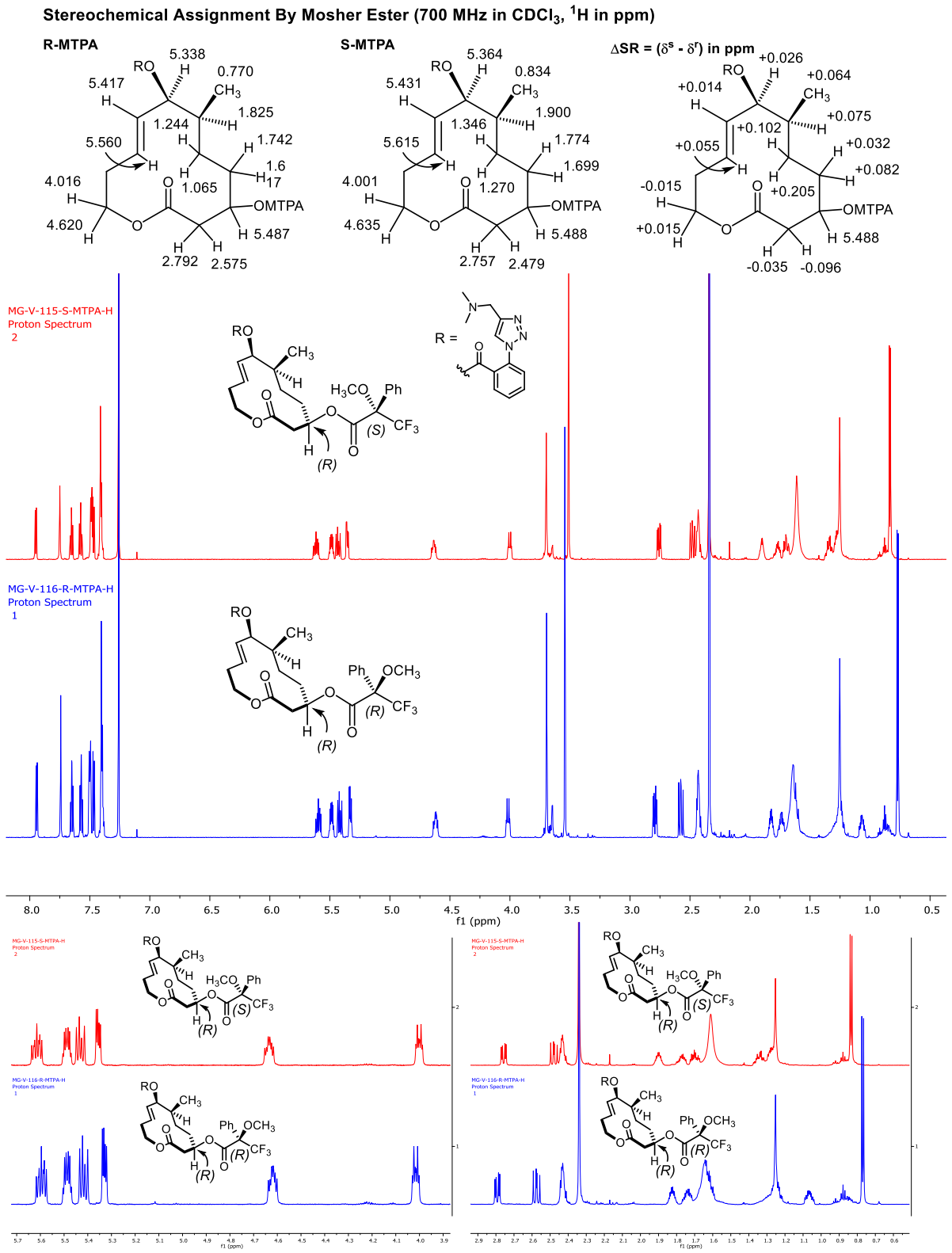

Figure 5.15: Stereochemical assignment of **57l** by Mosher ester derivatization.

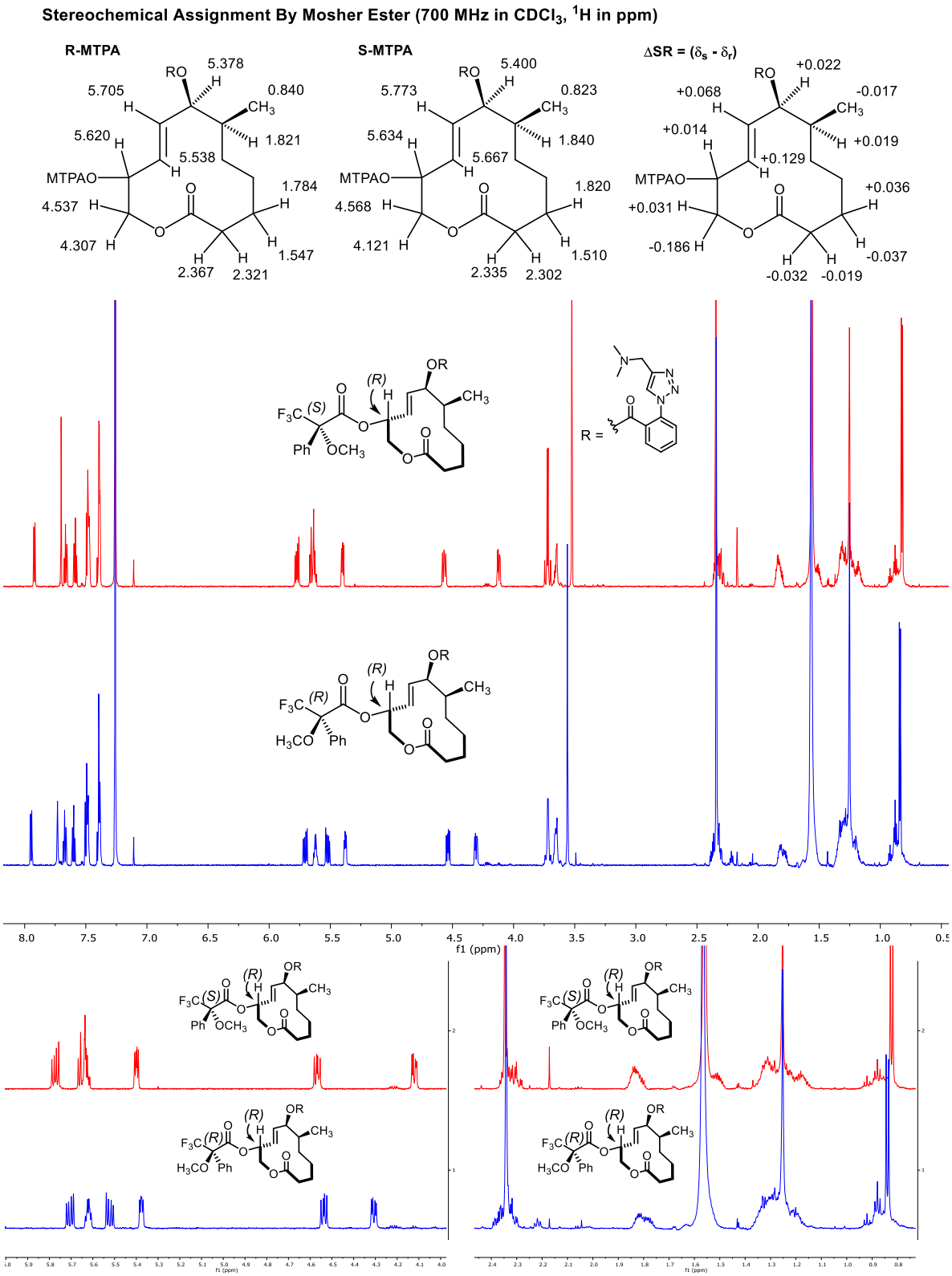

Figure 5.16: Stereochemical assignment of **56l** by Mosher ester derivatization.

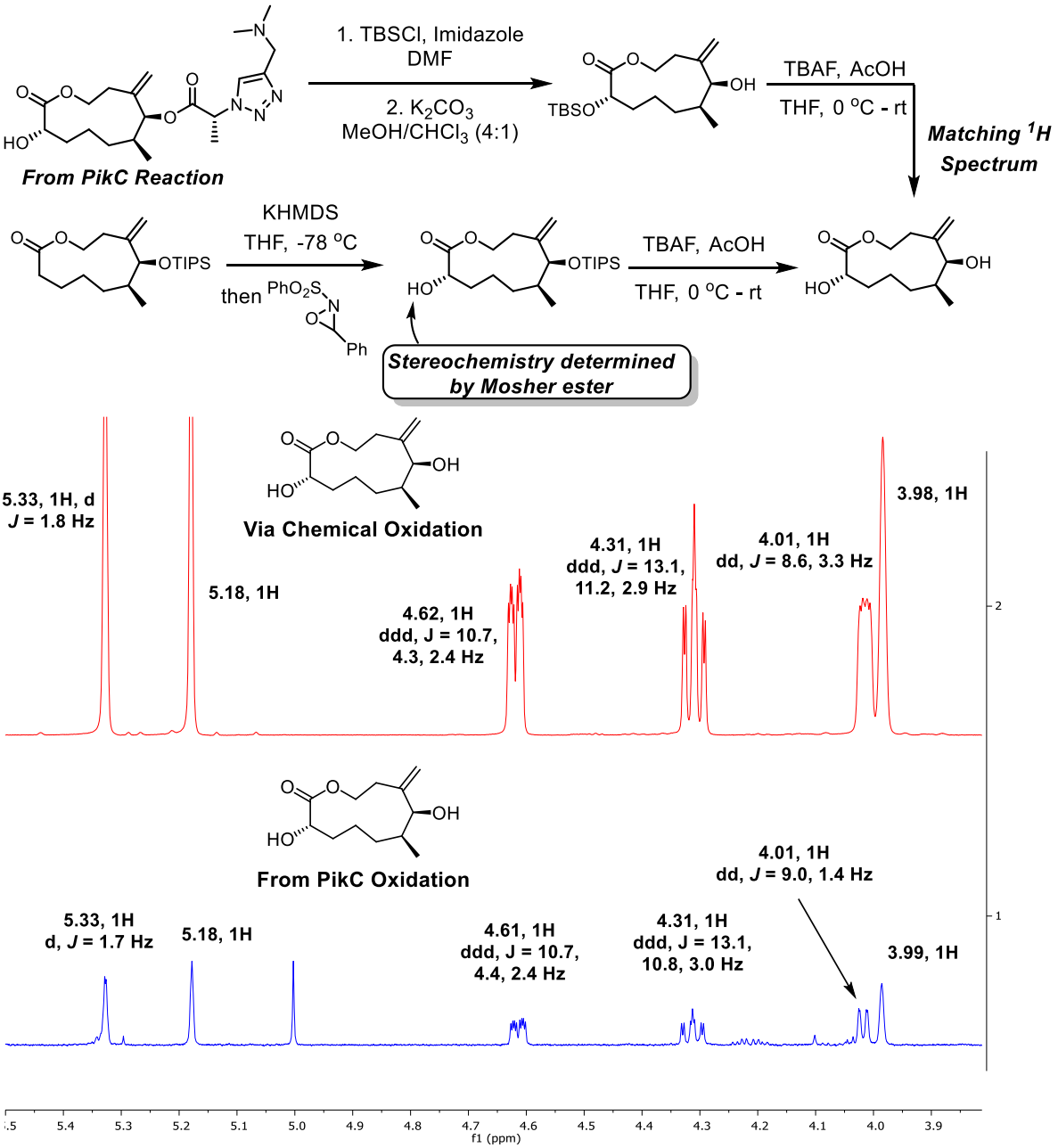

Figure 5.17: Comparison of the ^{1}H NMR spectra of **46** obtained through PikC oxidation and chemical oxidation.

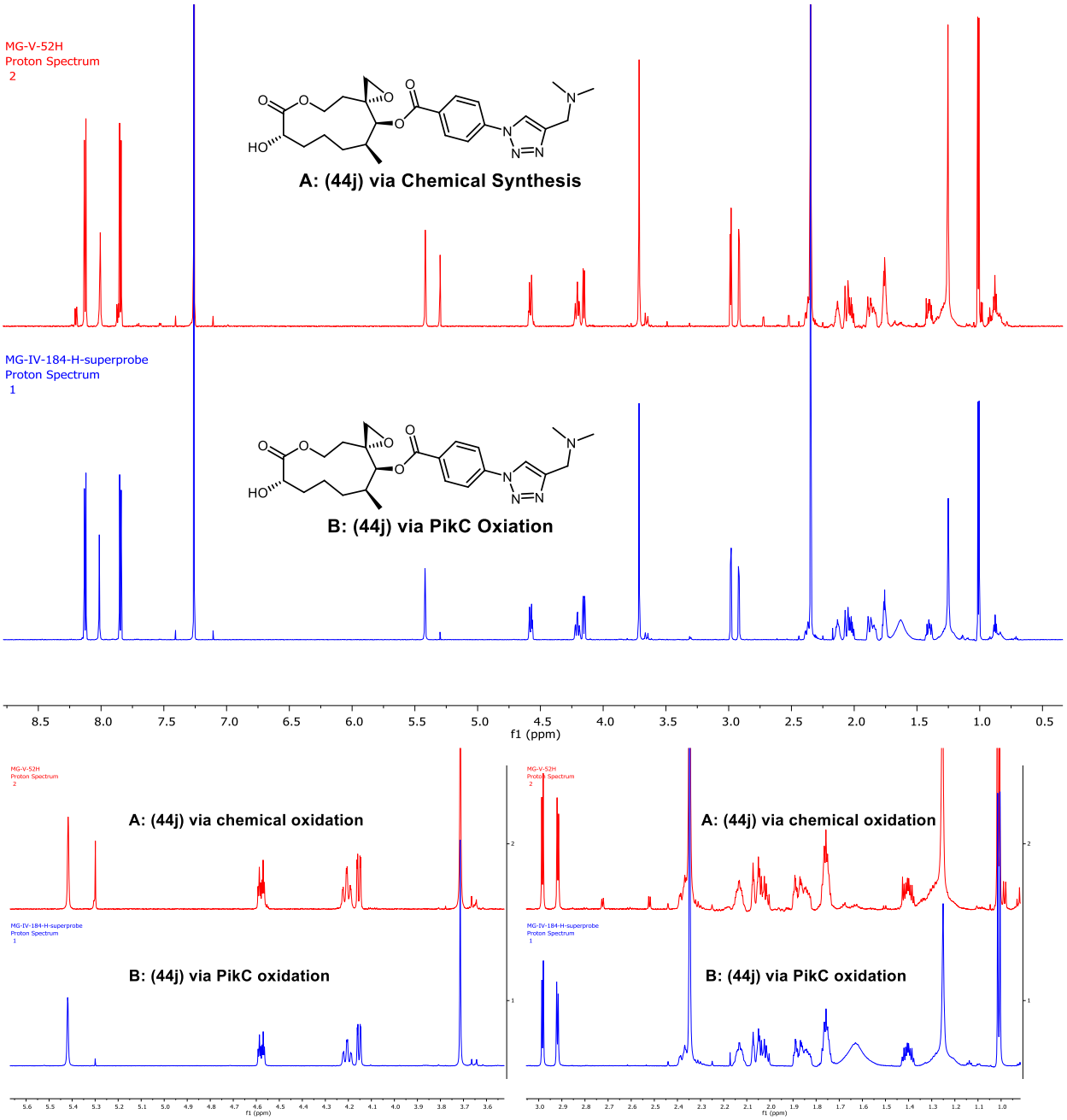

Figure 5.18: Comparison of the ^{1}H NMR spectra of **44j** obtained through PikC oxidation and chemical oxidation. **A**: ^{1}H NMR obtained through chemical synthesis. **B**: ^{1}H NMR obtained through PikC oxidation.

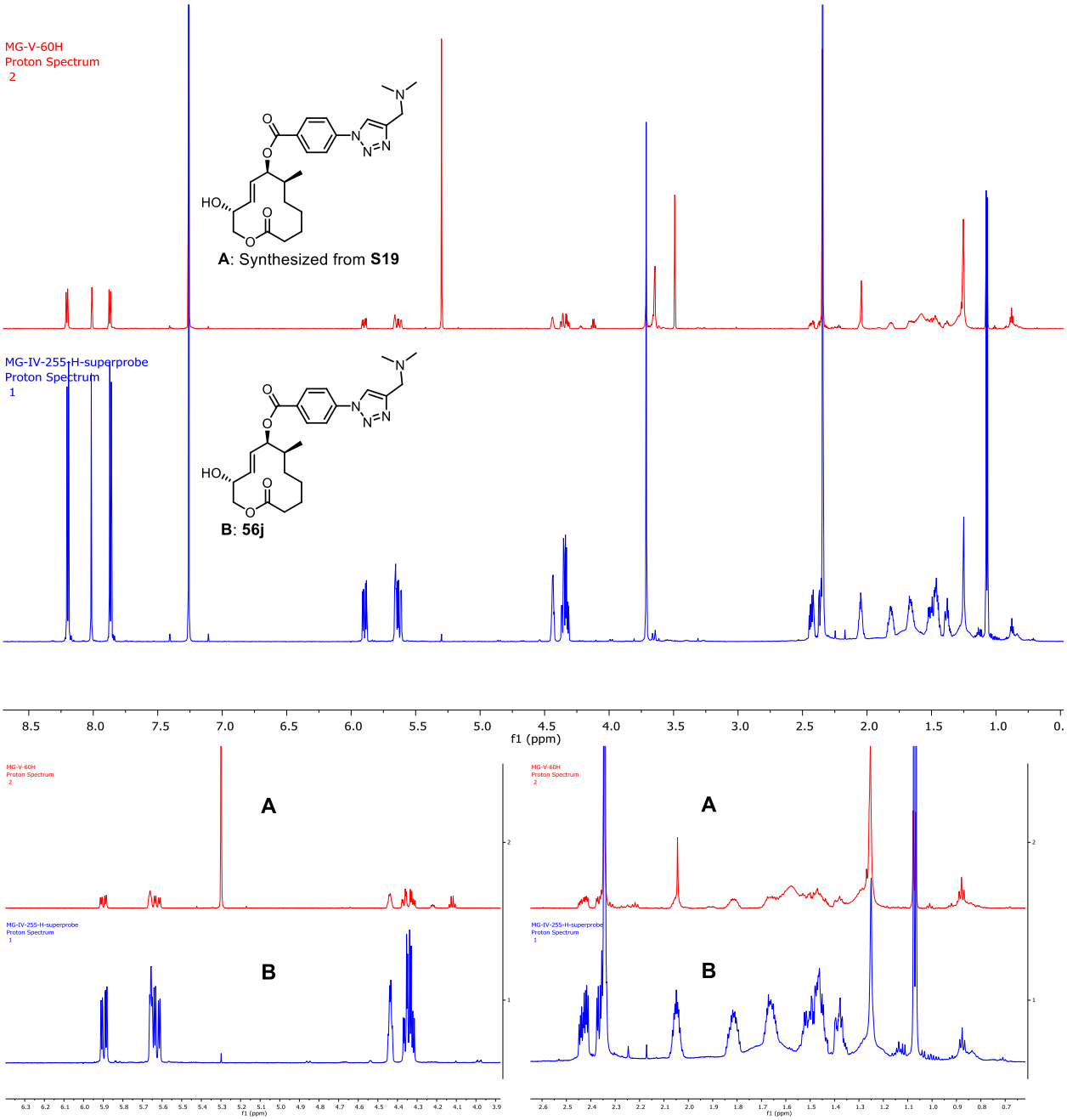

Figure 5.19: Comparison of the ^{1}H NMR of the 12-membered macrolactone allylic oxidation product. **A**: ^{1}H NMR of the allylic oxidation product from **S19.** **B**: ^{1}H NMR of **56j** from the PikC oxidation of **55j**.

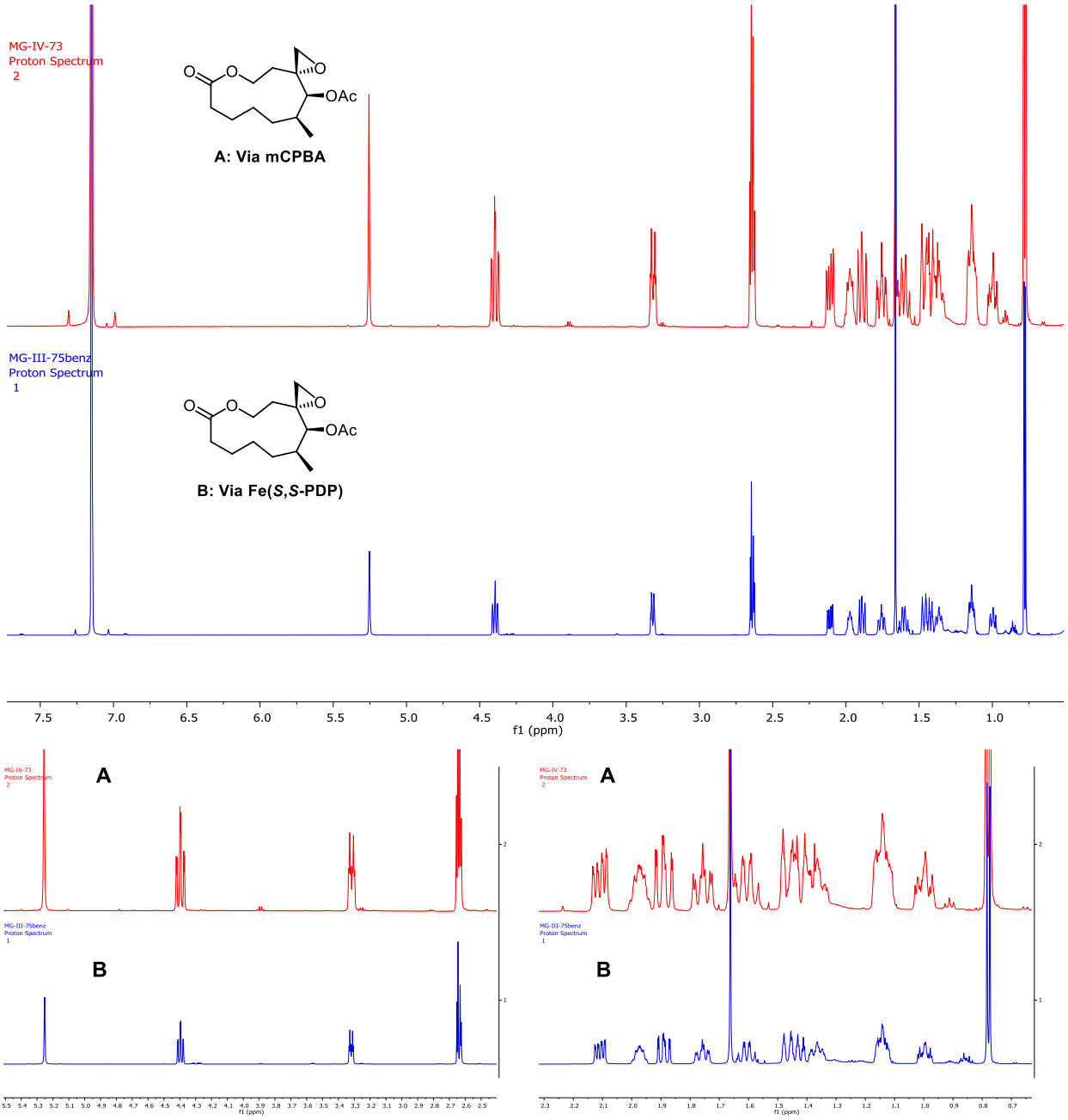

Figure 5.20: Comparison of the ^{1}H NMR of epoxidized macrocycles obtained through **A**: mCPBA and **B**: Fe(*S,S*-PDP) oxidation.

References

(1) Godula, K.; Sames, D. *Science* **2006**, *312*, 67–72.
(2) Nicolaou, K. C.; Yang, Z.; Liu, J. J.; Ueno, H.; Nantermet, P. G.; Guy, R. K.; Claiborne, C. F.; Renaud, J.; Couladouros, E. A.; Paulvannan, K.; Sorensen, E. J. *Nature* **1994**, *367*, 630–634.
(3) Nicolaou, K. C.; Ueno, H.; Liu, J.-J.; Nantermet, P. G.; Yang, Z.; Renaud, J.; Paulvannan, K.; Chadha, R. *J. Am. Chem. Soc.* **1995**, *117*, 653–659.
(4) Nicolaou, K. C.; Yang, Z.; Liu, J.-J.; Nantermet, P. G.; Claiborne, C. F.; Renaud, J.; Guy, R. K.; Shibayama, K. *J. Am. Chem. Soc.* **1995**, *117*, 645–652.
(5) Nicolaou, K. C.; Liu, J.-J.; Yang, Z.; Ueno, H.; Sorensen, E. J.; Claiborne, C. F.; Guy, R. K.; Hwang, C.-K.; Nakada, M.; Nantermet, P. G. *J. Am. Chem. Soc.* **1995**, *117*, 634–644.
(6) Nicolaou, K. C.; Nantermet, P. G.; Ueno, H.; Guy, R. K.; Couladouros, E. A.; Sorensen, E. J. *J. Am. Chem. Soc.* **1995**, *117*, 624–633.
(7) Croteau, R.; Ketchum, R. E. B.; Long, R. M.; Kaspera, R.; Wildung, M. R. *Phytochem. Rev.* **2006**, *5*, 75–97.
(8) Chau, M.; Jennewein, S.; Walker, K.; Croteau, R. *Chem. Biol.* **2004**, *11*, 663–672.
(9) Newhouse, T.; Baran, P. S. *Angew. Chem. Int. Ed.* **2011**, *50*, 3362–3374.
(10) Labinger, J.; Bercaw, J. E. *Nature* **2002**, *417*, 507–514.
(11) Mendoza, A.; Ishihara, Y.; Baran, P. S. *Nature* **2012**, *4*, 21–25.
(12) Wilde, N. C.; Isomura, M.; Mendoza, A.; Baran, P. S. *J . Am. Chem. Soc.* **2014**, *136*, 4909–4912.
(13) Cernak, T.; Dykstra, K. D.; Tyagarajan, S.; Vachal, P.; Krska, S. W. *Chem. Soc. Rev.* **2016**, *45*, 546–576.
(14) Lyons, T. W.; Sanford, M. S. *Chem. Rev.* **2010**, *110*, 1147–1169.
(15) Dangel, B. D.; Johnson, J. A.; Sames, D. *J . Am. Chem. Soc.* **2001**, *123*, 8149–8150.
(16) Desai, L. V; Hull, K. L.; Sanford, M. S. *J. Am. Chem. Soc.* **2004**, *126*, 9542–9543.
(17) Dick, A. R.; Hull, K. L.; Sanford, M. S. *J. Am. Chem. Soc.* **2004**, *126*, 2300–2301.
(18) Sharpe, R. J.; Johnson, J. S. *J . Am. Chem. Soc.* **2015**, *137*, 4968–4971.
(19) Hui, C.; Xu, J. *Tetrahedron Lett.* **2016**, *57*, 2692–2696.
(20) Siler, D. A.; Mighion, J. D.; Sorensen, E. J. *Angew. Chem. Int. Ed.* **2014**, *53*, 5332–5335.
(21) Ren, Z.; Mo, F.; Dong, G. *J . Am. Chem. Soc.* **2012**, *134*, 16991–16994.
(22) Thompson, S. J.; Thach, D. Q.; Dong, G. *J . Am. Chem. Soc.* **2015**, *137*, 11586–11589.
(23) Wang, D.-H.; Hao, X.-S.; Wu, D.-F.; Yu, J.-Q. *Org. Lett.* **2006**, *8*, 3387–3390.
(24) Giri, R.; Liang, J.; Lei, J.-G.; Li, J.-J.; Wang, D.-H.; Chen, X.; Naggar, I. C.; Guo, C.; Foxman, B. M.; Yu, J.-Q. *Angew. Chem. Int. Ed.* **2005**, *44*, 7420–7424.
(25) Simmons, E. M.; Hartwig, J. F. *Nature* **2012**, *482*, 70–73.
(26) Li, B.; Driess, M.; Hartwig, J. F. *J . Am. Chem. Soc.* **2014**, *136*, 6586–6589.
(27) Das, S.; Incarvito, C. D.; Crabtree, R. H.; Brudvig, G. W. *Science* **2006**, *312*, 1941–1943.
(28) Carney, J. R.; Dillon, B. R.; Thomas, S. P. *European J. Org. Chem.* **2016**, *2016*, 3912–3929.

(29) Nagataki, T.; Tachi, Y.; Itoh, S. *Chem. Commun.* **2006**, 4016–4018.
(30) Ishii, Y.; Iwahama, T.; Sakaguchi, S.; Nakayama, K.; Nishiyama, Y. *J. Org. Chem.* **1996**, *61*, 4520–4526.
(31) Qi, J.-Y.; Ma, H.-X.; Li, X.-J.; Zhou, Z.-Y.; Choi, M. C. K.; Chan, A. S. C.; Yang, Q.-Y. *Chem. Commun.* **2003**, 1294–1295.
(32) Muzart, J. *Chem. Rev.* **1992**, *92*, 113–140.
(33) Goez, L.; Canta, M.; Font, D.; Prat, I.; Ribas, X.; Costas, M. *J. Org. Chem.* **2013**, *78*, 1421–1433.
(34) Murray, R. W.; Iyanar, K.; Chen, J.; Wearing, J. T. *Tetrahedron Lett.* **1995**, *36*, 6415–6418.
(35) Puzari, A.; Baruah, J. B. *J. Mol. Catal. A Chem.* **2002**, *187*, 149–162.
(36) Lee, M.; Sanford, M. S. *J . Am. Chem. Soc.* **2015**, *137*, 12796–12799.
(37) Zhou, M.; Schley, N. D.; Crabtree, R. H. *J . Am. Chem. Soc.* **2010**, *132*, 12550–12551.
(38) Griffith, W. P. In *Ruthenium Oxidation Complexes*; 2011; pp 1–134.
(39) Oloo, W. N.; Que, L. *Acc. Chem. Res.* **2015**, *48*, 2612–2621.
(40) Chen, M. S.; White, M. C. *Science* **2007**, *318*, 783–787.
(41) Chen, M. S.; White, M. C. *Science* **2010**, *327*, 566–571.
(42) Gormisky, P. E.; White, M. C. *J . Am. Chem. Soc.* **2013**, *135*, 14052–14055.
(43) Howell, J. M.; Feng, K.; Clark, J. R.; Trzepkowski, L. J.; White, M. C. *J . Am. Chem. Soc.* **2015**, *137*, 14590–14593.
(44) Nanjo, T.; De Lucca, E. C.; White, M. C. *J . Am. Chem. Soc.* **2017**, *139*, 14586–14591.
(45) McNeill, E.; DuBois, J. *J . Am. Chem. Soc.* **2010**, *132*, 10202–10204.
(46) McNeill, E.; DuBois, J. *Chem. Sci.* **2012**, *3*, 1810–1813.
(47) Mack, J. B. C.; Gipson, J. D.; Bois, J. Du; Sigman, M. S. *J . Am. Chem. Soc.* **2017**, *139*, 9503–9506.
(48) Breslow, R.; Fang, Z. *Tetrahedron Lett.* **2002**, *43*, 5197–5200.
(49) Breslow, R.; Huang, Y.; Zhang, X.; Yang, J. *Chemistry (Easton).* **1997**, *94*, 11156–11158.
(50) Breslow, R.; Yang, J.; Yan, J. *Tetrahedron* **2002**, *58*, 653–659.
(51) Breslow, R.; Zhang, X.; Xu, R.; Maletic, M.; Merger, R. *J . Am. Chem. Soc.* **1991**, *7*, 39–53.
(52) Yang, J.; Breslow, R. *Angew. Chem. Int. Ed.* **2000**, *39*, 2692–2695.
(53) Yang, J.; Gabriele, B.; Belvedere, S.; Huang, Y.; Breslow, R. *J. Org. Chem.* **2002**, *67*, 5057–5067.
(54) Weber, L.; Hommel, R.; Behling, S. J.; Haufe, G.; Hennigg, H. *J. Am. Chem. Soc.* **1994**, *116*, 240–2408.
(55) Feiters, M. C.; Rowan, A. E.; Nolte, R. J. M. *Chem. Soc. Rev.* **2000**, *29*, 375–384.
(56) Kuroda, Y.; Sera, T.; Ogoshi, H. *J. Am. Chem. Soc.* **1991**, *113*, 2793–2794.
(57) Murray, R. W. . J. *J. Org. Chem* **1985**, *50*, 2847–2853.
(58) Curci, R.; D 'accolti, L.; Fusco, C. *Acc. Chem. Res.* **2006**, *39*, 1–9.
(59) Mello, R.; Fiorentino, M.; Fusco, C.; Curci, R. *J. Am. Chem. Soc.* **1989**, *111*, 6749–6757.
(60) Chen, K.; Baran, P. S. *Nature* **2009**, *459*, 824–828.
(61) Zou, L.; Paton, R. S.; Eschenmoser, A.; Newhouse, T. R.; Baran, P. S.; Houk, K.

N. *J. Org. Chem.* **2013**, *78*, 4037–4048.
(62) Wender, P. A.; Hilinski, M. K.; Mayweg, A. V. W. *Org. Lett.* **2005**, *7*, 79–82.
(63) Pierce, C. J.; Hilinski, M. K. *Org. Biomol. Chem.* **2014**, *16*, 6504–6507.
(64) Brodsky, B. H.; DuBois, J. *J . Am. Chem. Soc.* **2005**, *127*, 15391–15393.
(65) Kasuya, S.; Kamijo, S.; Inoue, M. *Org. Lett.* **2009**, *11*, 3630–3632.
(66) Denisov, I. G.; Makris, T. M.; Sligar, S. G.; Schlichting, I. *Chem. Rev.* **2005**, *105*, 2253–2277.
(67) Fasan, R. *ACS Catal.* **2012**, *2*, 647–666.
(68) Ortiz De Montellano, P. R. *Chem. Rev.* **2009**, *110*, 932–948.
(69) Paulo, J.; Zaragoza, T.; Yosca, T. H.; Siegler, M. A.; Moë Nne-Loccoz, P.; Green, M. T.; Goldberg, D. P. *J . Am. Chem. Soc.* **2017**, *139*, 13640–13643.
(70) Grogan, G. *Curr. Opin. Chem. Biol.* **2010**, *15*, 241–248.
(71) Romero, P. A.; Arnold, F. H. *Nat. Rev. Mol. Cell Biol.* **2009**, *10*, 866–876.
(72) Kawakami, N.; Shoji, O.; Watanabe, Y. *Angew. Chem. Int. Ed.* **2011**, *50*, 5315–5318.
(73) Shoji, O.; Fujishiro, T.; Nakajima, H.; Kim, M.; Nagano, S.; Shiro, Y.; Watanabe, Y. *Angew. Chem. Int. Ed.* **2007**, *46* (20), 3656–3659.
(74) Zilly, F. E.; Acevedo, J. P.; Augustyniak, W.; Deege, A.; Häusig, U. W.; Reetz, M. T. *Angew. Chem. Int. Ed.* **2011**, *50* (12), 2720–2724.
(75) Le-Huu, P.; Heidt, T.; Claasen, B.; Laschat, S.; Urlacher, V. B. *ACS Catal.* **2015**, *5*, 1772–1780.
(76) Rentmeister, A.; Arnold, F. H.; Fasan, R. *Nat. Chem. Biol.* **2009**, *5*, 26–28.
(77) Zhang, K.; Damaty, S. El; Fasan, R. *J. Am. Chem. Soc* **2011**, *133*, 3242–3245.
(78) Zhang, K.; Shafer, B. M.; Demars, M. D.; Stern, H. A.; Fasan, R. *J . Am. Chem. Soc.* **2012**, *134*, 18695–18704.
(79) Loskot, S. A.; Romney, D. K.; Arnold, F. H.; Stoltz, B. M. *J . Am. Chem. Soc.* **2017**, *139*, 10196–10199.
(80) Kittendorf, J. D.; Sherman, D. H. *Bioorg. Med. Chem.* **2009**, *17*, 2137–2146.
(81) Khosla, C. *Chem. Rev.* **1997**, *97*, 2577–2590.
(82) Katz, L. *Chem. Rev.* **1997**, *97*, 2557–2575.
(83) Xue, Y.; Zhao, L.; Liu, H.-W.; Sherman, D. H. *Biochemistry* **1998**, *95*, 12111–12116.
(84) Staunton, J.; Weissman, K. J. *Nat. Prod. Rep.* **2001**, *18*, 380–416.
(85) Khosla, C. *J. Org. Chem.* **2009**, *74*, 6416–6420.
(86) Xue, Y.; Wilson, D.; Zhao, L.; Liu, H.-W.; Sherman, D. H. *Chem. Biol.* **1998**, *5*, 661–667.
(87) Sherman, D. H.; Li, S.; Yermalitskaya, L. V; Kim, Y.; Smith, J. A.; Waterman, M. R.; Podust, L. M. *J. Biol. Chem.* **2006**, *281*, 26289–26297.
(88) Larsen, A. T.; May, E. M.; Auclair, K. *J. Am. Chem. Soc.* **2011**, *133*, 7853–7858.
(89) Shin, H. S.; Slattery, J. T. *J. Pharm. Sci.* **1998**, *87*, 390–393.
(90) Li, S.; Ouellet, H.; Sherman, D. H.; Podust, L. M. *J. Biol. Chem.* **2009**, *284*, 5723–5730.
(91) Ruettinger, R. T.; Fulco, A. J. *J. Biol. Chem.* **1981**, *256*, 5728–5734.
(92) Lambalot, R. H.; Crane, D. E. *Biochemistry* **1995**, *34*, 1858.
(93) Ogura, H.; Nishida, C. R.; Hoch, U. R.; Perera, R.; Dawson, J. H.; Ortiz De Montellano, P. R. *Biochemistry* **2004**, *43*, 14712–14721.

(94) Roberts, G. A.; Grogan, G.; Greter, A.; Flitsch, S. L.; Turner, N. J. *J. Bacteriol.* **2002**, *184*, 3898–3908.
(95) Li, S.; Podust, L. M.; Sherman, D. H. *J . Am. Chem. Soc.* **2007**, *129*, 12940–12941.
(96) Wong, C.-H.; Whitesides, G. M. *J . Am. Chem. Soc.* **1981**, *103*, 4890–4899.
(97) De Raadt, A.; Griengl, H. *Curr. Opin. Biotechnol.* **2002**, *13*, 537–542.
(98) Chen, H.; Yamase, H.; Murakami, K.; Chang, C.-W.; Zhao, L.; Zhao, Z.; Liu, H.-W. *Biochemistry* **2002**, *41*, 9165–9183.
(99) Anzai, Y.; Li, S.; Chaulagain, M. R.; Kinoshita, K.; Kato, F.; Montgomery, J.; Sherman, D. H. *Chem. Biol.* **2008**, *15*, 950–959.
(100) Li, S.; Chaulagain, M. R.; Knauff, A. R.; Podust, L. M.; Montgomery, J.; Sherman, D. H.; Walsh, C. T. *Proc. Natl. Acad. Sci. U. S. A.* **2009**, *106*, 18463–18468.
(101) Negretti, S.; H Narayan, A. R.; Chiou, K. C.; Kells, P. M.; Stachowski, J. L.; Hansen, D. A.; Podust, L. M.; Montgomery, J.; Sherman, D. H. *J . Am. Chem. Soc.* **2014**, *136*, 4901–4904.
(102) Lee, S.; Fuchs, P. L. *Org. Lett.* **2004**, *6*, 1437–1440.
(103) Yazerski, V. A.; Spannring, P.; Gatineau, D.; Woerde, C. H. M.; Wieclawska, S. M.; Lutz, M.; Kleijn, H.; Klein Gebbink, R. J. M. *Org. Biomol. Chem* **2014**, *12*, 2062–2070.
(104) Ottenbacher, R. V; Samsonenko, D. G.; Talsi, E. P.; Bryliakov, K. P. *Org. Lett.* **2012**, *14*, 4310–4313.
(105) Narayan, A. R. H.; Jiménez-Osés, G.; Liu, P.; Negretti, S.; Zhao, W.; Gilbert, M. M.; Ramabhadran, R. O.; Yang, Y.-F.; Furan, L. R.; Li, Z.; Podust, L. M.; Montgomery, J.; Houk, K. N.; Sherman, D. H. *Nat. Chem.* **2015**, *7*, 653–660.
(106) Montgomery, J. *Angew. Chem. Int. Ed.* **2004**, *43*, 3890–3908.
(107) Jackson, E. P.; Malik, H. A.; Sormunen, G. J.; Baxter, R. D.; Liu, P.; Wang, H.; Shareef, A.-R.; Montgomery, J. *Acc. Chem. Res.* **2015**, *48*, 1736–1745.
(108) Ogoshi, S.; Arai, T.; Ohashi, M.; Kurosawa, H. *Chem. Commun.* **2008**, *0*, 1347.
(109) Moslin, R. M.; Miller-Moslin, K.; Jamison, T. F. *Chem. Commun.* **2007**, *0*, 4441–4449.
(110) Malik, H. A.; Sormunen, G. J.; Montgomery, J. *J . Am. Chem. Soc.* **2010**, *132*, 6304–6305.
(111) Baxter, R. D.; Montgomery, J. *J. Am. Chem. Soc* **2011**, *133*, 5728–5731.
(112) Liu, P.; Montgomery, J.; Houk, K. N. *J. Am. Chem. Soc.* **2011**, *133*, 6956–6959.
(113) Jackson, E. P.; Montgomery, J. *J . Am. Chem. Soc.* **2015**, *137*, 958–963.
(114) Shareef, A.-R.; Sherman, D. H.; Montgomery, J. *Chem. Sci.* **2012**, *3*, 892–895.
(115) Wang, H.; Negretti, S.; Knauff, A. R.; Montgomery, J. *Org. Lett.* **2015**, *17*, 1493–1496.
(116) Chaulagain, M. R.; Sormunen, G. J.; Montgomery, J. *J. Am. Chem. Soc.* **2007**, *129*, 9568–9569.
(117) Wang, H.; Lu, G.; Sormunen, G. J.; Malik, H. A.; Liu, P.; Montgomery, J. *J . Am. Chem. Soc.* **2017**, *139*, 9317–9324.
(118) Hein, J. E.; Fokin, V. V.; Fokin, V. V.; Lercher, L.; Fokin, V. V.; Sharpless, K. B.; Chang, S.; Frechet, J. M. J.; Sharpless, K. B.; Fokin, V. V. *Chem. Soc. Rev.* **2010**, *39*, 1302.
(119) Rostovtsev, V. V.; Green, L. G.; Fokin, V. V.; Sharpless, K. B. *Angew. Chem. Int.*

Ed. **2002**, *41*, 2596–2599.
(120) Boren, B. C.; Narayan, S.; Rasmussen, L. K.; Zhang, L.; Zhao, H.; Lin, Z.; Jia, G.; Fokin, V. V. *J. Am. Chem. Soc.* **2008**, *130*, 8923–8930.
(121) Gilbert, M. M.; DeMars, M. D.; Yang, S.; Grandner, J. M.; Wang, S.; Wang, H.; H Narayan, A. R.; Sherman, D. H.; Houk, K. N.; Montgomery, J. *ACS Cent. Sci.* **2017**.
(122) Lowell, A. N.; Demars, M. D.; Slocum, S. T.; Yu, F.; Anand, K.; Chemler, J. A.; Korakavi, N.; Priessnitz, J. K.; Park, S. R.; Koch, A. A.; Schultz, P. J.; Sherman, D. H. *J. Am. Chem. Soc.* **2017**, *139*, 7913–7920.
(123) Arduengo, A. J.; Krafczyk, R.; Schmutzler, R.; Craig, H. A.; Goerlich, J. R.; Marshall, W. J.; Unverzagt, M. *Tetrahedron* **1999**, *55*, 14523–14534.
(124) Ye, H.; Liu, R.; Li, D.; Liu, Y.; Yuan, H.; Guo, W.; Zhou, L.; Cao, X.; Tian, H.; Shen, J.; Wang, P. G. *Org. Lett.* **2013**, *15*, 18–21.
(125) Yaqoob, M.; Farooq, A.; Anjum, S.; Asif, F.; Choudhary, M. I. *J. Nat. Prod.* **1998**, *61*, 1340–1342.
(126) Johns, B. A.; Grant, C. M.; Marshall, J. A. *Org. Synth.* **2002**, *79*, 59–71.
(127) El Zubir, O.; Barlow, I.; Ul-Haq, E.; Tajuddin, H. A.; Williams, N. H.; Leggett, G. J. *Langmuir* **2013**, *29*, 1083–1092.
(128) Zhu, W.; Ma, D. *Chem. Commun.* **2004**, *0*, 888.
(129) Bléger, D.; Schwarz, J.; Brouwer, A. M.; Hecht, S. *J. Am. Chem. Soc.* **2012**, *134*, 20597–20600.
(130) Dommerholt, J.; Van Rooijen, O.; Borrmann, A.; Guerra, C. F.; Bickelhaupt, F. M.; Van Delft, F. L. *Nat. Commun.* **2014**, *5*.
(131) Valverde, I. E.; Bauman, A.; Kluba, C. A.; Vomstein, S.; Walter, M. A.; Mindt, T. L. *Angew. Chem. Int. Ed.* **2013**, *52*, 8957–8960.
(132) Omura, T.; Sato, R. *J. Biol. Chem.* **1964**, *239*, 2370–2378.
(133) Hoye, T. R.; Jeffrey, C. S.; Shao, F. *Nat. Protoc.* **2007**, *2*, 2451–2458.